Separation of heavy metals from wastewater using liquid membrane based technique

Thesis

Submitted in partial fulfillment of the requirements for the degree of

DOCTOR OF PHILOSOPHY

by

Supriyo Kumar Mondal

Department of Chemical Engineering
Indian Institute of Technology Guwahati
Guwahati-781039

Department of Chemical Engineering
Indian Institute of Technology Guwahati
Guwahati – 781039 (India)

Certificate

It is certified that the work presented in the thesis entitled **"Separation of heavy metals from wastewater using liquid membrane based technique"**, is a bonafide work of **Mr. Supriyo Kumar Mondal**, carried out under my supervision and this work has not been submitted elsewhere for any other degree.

Date:

(Prabirkumar Saha, PhD)
Professor
Department of Chemical Engineering
Indian Institute of Technology Guwahati
Guwahati-781039, Assam, India

Acknowledgements

I would like to thank all the people who directly or indirectly have helped and inspired me during my doctoral study, without whom my doctoral work would not be completed. First of all, I would like to express my deep sense of gratitude to my supervisor **Professor Prabirkumar Saha** for giving me the opportunity to work with him. I am indebted to him for his inspiring guidance, invaluable suggestions and constant support throughout the entire course. His expertise in various theoretical and experimental aspects has helped a lot in improving the quality of this work. I respect him for his honesty and friendly nature. It has really been a great privilege to work with him.

I am thankful to my doctoral committee members **Professor Pranab K. Ghosh**, Department of Civil Engineering, **Professor Ramgopal Uppaluri** and **Dr. Prakash Kotecha**, Department of Chemical engineering for their valuable discussions on the subject of my research throughout my doctoral program and suggestions towards its completeness.

I must thank all the faculty members of the Department of Chemical Engineering for their co-operation and encouragement during my stay in this department. In particular, I thank to **Prof. Mihir Kumar Purkait, Prof. Animesh Kumar Golder, Prof. Bishnupada Mandal, Prof. Sasidhar Gumma** and **Prof. Chandan Das** for their help at various stages of work. I am thankful to the Central Instruments Facility for allowing me to utilize their experimental resources.

I express my thanks to all the technical staffs of the Department of Chemical Engineering for their timely assistance in my experimental works. I specially thank to Mr. P. Bhattacharjee, Mr. Dipak Barman, Dr. L. Borah, Mr. J. K. Mout, Mr. A. Hoque, Mr. B. C. Mahanta, Mr. D. J. Sinha, Mr. Sailen Das and Mr. Bhagya Boro for their support and help as and when I needed for. I am thankful to Mr. Harsaraj Biswanath, Scientific Officer of the Department of Chemical Engineering for his help to complete this work.

My heart felt thanks to Abhik, Kundu, Saty, Randeep, Sujoy for their constant co-operation, motivational talk and mental support in my research carrier. I sincerely acknowledge the cooperation and assistance of Ms. Soumi Sarkar PhD student of our research group. I express my thanks to Saptak, Ramteke, Sunny, Patwa, Rabari sir, Himadri, Raju, Piyal, Anwesan and Pradip for their encouragement and help in different forms during my research work. A big thank to all my laboratory associates in the department including past and present M. Tech students for their love and unconditional help.

My deepest gratitude goes to my family members for their unflagging support throughout my life. I would like to thank my parents and sister for their constant support and encouragement towards pursuing my passion with full dedication which kept me going in my hard times.

Last but not the least, I acknowledge my fellow research scholars, seniors and juniors for their kind help and cooperation towards the successful completion of my PhD program. I wish to thank to all well-wishers for being a constant support in my life.

I thank to Ministry of Human Resource Development (MHRD), Department of Science and Technology (DST) and IIT Guwahati for providing fellowship throughout the PhD program.

Finally, my greatest regards to the Almighty for bestowing upon me the courage and strength to overcome all the problems and complete this work successfully.

(Supriyo Kumar Mondal)

Abstract

This thesis aims at exploring the efficacy of liquid membrane (LM) based technology in order to separate Cr(VI), Ni(II) and Zn(II) from wastewater. A suitable LM that can extract the said solutes is identified through equilibrium study. Experimentations with various solvents and carrier agents reveal that the sunflower oil-N-methyl-N,N,N-trioctylammonium chloride (aliquat 336), sunflower oil-trioctylamine (TOA) and sunflower oil-di-(2-ethylhexyl)phosphoric acid (D2EHPA) are the favourable combinations for separation of the Cr(VI), Ni(II) and Zn(II) respectively. The performances of various LM based processes are investigated. The processes include the techniques based on bulk liquid membrane (BLM), flat sheet-supported liquid membrane (FS-SLM), FS-SLM assisted precipitation of Cr(VI) in stripping chamber and FS-SLM assisted electrodeposition of Ni(II) and Zn(II) on the cathode plate placed in the stripping chamber.

The components of LM *i.e.* the solvent and the carrier were selected through two-phase equilibrium studies. The stripping agents are selected based on their capacity for stripping the metals and recovery of metals in two different ways *i.e.* precipitation and electrodeposition. The various physico-chemical parameters such as pH of aqueous solutions, concentration of extractant in the organic solution, initial concentration of the feed solution, period of operation etc. were primarily evaluated in two-phase equilibrium studies. The optimum parameters obtained in two-phase equilibrium studies were later verified and improved in three-phase transportation studies. The three-phase transportation studies involve the diffusion step in between extraction and re-extraction or stripping of the heavy metals at the respective interfaces of the LM.

After the initial investigation on the merits of LM based techniques to separate the Cr(VI), Ni(II) and Zn(II) in two-phase equilibrium study and simplest BLM configuration (for Cr(VI)), further study was carried out in FS-SLM configuration. The possibility of using environmentally benign solvent in a LM setup in order to sepa-

rate Cr(VI) from wastewater has been explored. Vegetable oils have been used for this purpose as they have the capability of extracting heavy metals and they are well known for their biodegradability too. Additionally an extractant Aliquat 336 has been used to enhance the efficiency of separation as it showed very good carrier property for transport of Cr(VI). Di-sodium ethylene-di-amine-tetra-acetic acid (or Na_2-EDTA) was selected as stripping agent for its affinity towards metal. The efficiency is affected by various physico-chemical parameters which have been optimized for best transport of solute. An initial two-phase study followed by elaborate three-phase BLM study were confirmed by critically more industry-friendly supported liquid membrane study. In addition, new type of SLM setup has been developed which includes SLM technology with *in situ* electrochemical reactor in stripping section. SLM with *in situ* electrochemical reaction in stripping section helps to reduce hexavalent chromium to trivalent chromium by forming chromium-iron complex. Iron plate acts as anode in stripping section. The chromium-iron complex is an useful value added product and has immense commercial value that can be used for various purposes. Aliquat 336 has been used as carrier for transport of hexavalent chromium. Various physico-chemical parameters have been optimized to detect the condition of maximum transport and precipitation of chromium-iron complex in stripping phase. Further, a new type of design mechanism has been implemented for extraction and recovery with deposition/electroplating of Ni(II) and Zn(II). The setup consist of an *in situ* electrodeposition unit in strip phase which helps "stripped" Ni(II) and Zn(II) from synthetic wastewater get electrodeposited on the cathode surface. This type of separation technique not only helps to separate toxic heavy metals from wastewater but also yields an useful end product in the form of electroplated material. Two types of carrier, i.e., TOA and D2EHPA, have been used in the organic phase to separate Ni(II) and Zn(II). The separation has been done individually as well as in a condition of binary pollutant in the feed phase. Various physico-chemical parameters have been optimized to yield best transport and deposition of metals on the cathode sur-

face. The prime physico-chemical parameters affecting the system performance were identified for experimental optimization through response surface methodology using central composite design rule. A regression model along with analysis of variance evaluates whether the chosen parameters were of good agreement with experimental results.

Keywords: Bulk liquid membrane (BLM), Supported liquid membrane (SLM), Environmentally benign solvent, Chromium, Nickel, Zinc, Aliquat 336, TOA, D2EHPA, Chromium-iron complex, FESEM, TEM, FTIR, Electrochemical reaction, Electrodeposition, RSM, CCD, ANOVA.

Summary

The present research work provides a systematic approach to implement LM based technology for separation of heavy metals *viz.* Cr(VI), Ni(II) and Zn(II) form wastewater. Therefore, the overall aim of this thesis is to establish a LM based technique for extraction and recovery of Cr(VI), Ni(II) and Zn(II) from the industrial effluents in an environmentally and physiologically benign method which would minimize the production of secondary pollutant. To fulfil this overall aim, thesis finds the following measurable objectives:

- ✓ Identification of low cost, easily available and environmentally benign solvent.
- ✓ Identification of suitable solvent-carrier combination that enhances the extraction of solute from the aqueous phase.
- ✓ Identification of the best operating condition in respective configuration *i.e.* two-phase equilibrium study, BLM and FS-SLM.
- ✓ Development of efficient recovery strategies and stripping conditions so as to enhance the extraction and recovery of the selected metals and generate value added components out of them. This objective may further be achieved through the following two pathways:
  - Synthesis of useful nanoparticle from recovered heavy metal by electrochemical process.
  - Electrodeposition of metals in stripping solution by employing electric potential that can generate useful electroplated product.
- ✓ Perform experimental optimization of the LM process with the help of standard statistical methods that would ensure best operating condition of influential parameters affecting the LM process.

The thesis has been organized in six chapters that include

- ✓ **Chapter 1: Introduction and literature Review**
- ✓ **Chapter 2: Materials and methods**
- ✓ **Chapter 3: Separation of Cr(VI) through BLM and SLM**
- ✓ **Chapter 4: Electrochemical separation of Cr(VI) using flat sheet supported liquid membrane (FS-SLM)**
- ✓ **Chapter 5: FS-SLM based simultaneous separation and electrodeposition of Ni(II) and Zn(II)**
- ✓ **Chapter 6: Conclusion and future scope**

A brief description of each of the chapters is furnished below:

Chapter 1: Introduction and literature Review

This chapter defines the problem, discusses the state of the art solutions, gap areas in the published literature and finally defines the objective of the thesis. The merits of LM technology over the conventional process has been discussed. The problems associated with the conventional wastewater treatment process are also discussed. An elaborate literature study has been done to discuss about different sources of heavy metals *viz.* Cr(VI), Zn(II) and Ni(II) and their issues related to environment. Different types of liquid membrane and its application with merits and demerits are described in this chapter. The aim and objectives of this present work are also addressed in this chapter.

Chapter 2: Materials and methods

This chapter includes the details of various materials used in experimental purpose and different sources from where the materials were procured. The detailed description of analytical instruments and characterization techniques used in the experiments are discussed here. The two types of LM setup (BLM and FS-SLM) have been

used in this work. Elaborated study of experimental procedure of metal transport through both LM configurations are also discussed here.

Chapter 3: Separation of Cr(VI) through BLM and SLM

This chapter includes the theoretical background, results and discussion on transportation of Cr(VI) through BLM and SLM. One of the goals of this work is to explore the possibility of using environmentally benign solvent in a liquid membrane setup in order to separate Cr(VI) from industrial effluent and perform experimental optimization of its parameters for maximum performance. Vegetable oils have been used for this purpose as they have the capability of extracting heavy metals and they are well known for their biodegradability too. The prime physico-chemical parameters affecting the system performance were identified for experimental optimization through response surface methodology using central composite design rule. A regression model along with analysis of variance evaluates whether the chosen parameters were of good agreement with experimental results. Maximum extraction over 95% and maximum recovery over 45% of Cr(VI) were obtained in case of BLM, whereas SLM yielded 80% extraction and 73% recovery respectively. Combination of sunflower oil and aliquat 336 has been found to be the best solvent-carrier combination. The two-phase study reveals that the optimum process conditions are 100 mg L^{-1} Cr(VI) in aqueous solution, 1% (v/v) aliquat 336, 200 rpm stirring and 12 h of operation. Additional optimum process conditions for three-phase study are 0.03 M Na_2-EDTA and pH 6.5 in strip phase. Speed of stirring had to be increased to 400 rpm in case of BLM in order to reach effective recovery. On the other hand speed of stirring had to be reduced to 120 rpm in SLM in order to prevent premature destabilization of membrane support. The run time had to be increased to 48 h in order to compensate for the lower effect of stirring. The fed batch operations have also been successful which indicates that it is possible to design a continuous operation of LM based separation process. The most influential factors on transport

of Cr(VI) i.e. strip phase concentration, strip phase pH and carrier concentration are experimentally optimized through response surface methodology (RSM) following central composite design (CCD) rule. The comparison between experimentally observed data and those predicted by RSM model showed that all the values are in good agreement.

Chapter 4: Electrochemical separation of Cr(VI) using FS-SLM

This chapter presents separation of Cr(VI) using FS-SLM technology. SLM with *in situ* electrochemical reaction in stripping section helps to reduce hexavalent chromium (Cr(VI)) to trivalent chromium (Cr(III)) by forming chromium-iron complex. Iron plate acts as anode in stripping section. The chromium-iron complex is an useful value added product that can be used for various purposes. It is used as catalyst in water-gas shift (WGS) reaction. Aliquat 336 has been used as carrier for transport of Cr(VI). Various physico-chemical parameters have been optimized to detect the condition of maximum transport and precipitation of chromium-iron complex in stripping phase. The important physico-chemical parameters have been selected through response surface methodology to obtain optimum performance for %precipitation of chromium. SLM technology with *in situ* electrochemical reactor in stripping section has been successfully implemented for the production of chromium-iron hydroxide which may be calcinated to produce chromium-iron oxide. During production of chromium-iron complex the separation of Cr(VI) from feed phase and its reduction to Cr(III) is also performed simultaneously. For electrochemical reaction iron plate was used as an anode and graphite rod was used as cathode. Various parameters have been optimized to obtain maximum transport of chromium and its reduction to precipitate as chromium-iron complex. The optimum parameters found for SLM study are: concentration of Cr(VI) in feed phase 100 mg L^{-1}, pH of feed phase 4.5, concentration of NaCl in strip phase 0.15 M, pH of strip phase 8, concentration of

aliquat 336 as carrier in LM 1% (v/v), electric potential 2.5 V DC in strip phase, stirring speed 120 rpm in both aqueous phases, and 6 h of run time. The maximum %precipitation of chromium is ∼97%. The influential parameters such as strip phase concentration, strip phase pH and carrier concentration have been picked up for experimental optimization by RSM using CCD rule. The predicted output from RSM study is also shown in good agreement with experimental results.

Chapter 5: FS-SLM based simultaneous separation and electrodeposition of Ni(II) and Zn(II)

This chapter provides simultaneous separation and electrodeposition of Ni(II) and Zn(II). A new type of supported liquid membrane setup has been developed in this work. The setup consist of an *in-situ* electrodeposition unit in strip phase which helps "stripped" nickel and zinc from synthetic wastewater get electrodeposited on the cathode surface. The separation has been done individually as well as in a condition of binary pollutant in the feed phase. The Ni-Zn binary electroplated metal has immense commercial application. It is used as corrosion resistant coating to prevent oxidation of protected metal. Various physico-chemical parameters have been optimized to yield the best transport and deposition of metals on the cathode surface. Face-centered central composite designs in response to surface methodology have been performed on varied ratios of binary pollutant and their carriers in order to obtain optimum performance of the separation unit. The integration of the electrodeposition module in the strip phase of SLM not only helped to increase the separation efficiency but also proved to be a way to generate a value added product. In this regard, the copper plate was found to be an ideal cathode. Electrodeposition of metal in the strip phase maintains a high concentration gradient between feed and strip phases that helped better transport the metal across the SLM. The optimum parameters of the two phase studies are 100 mg L^{-1} of Ni(II) as the initial concentration, pH of 5 in aqueous solution, 5% (v/v) of TOA as the carrier/extractant in the organic

phase, stirring speed of 200 rpm, and run time of 12 h. The maximum extraction was noticed at $\sim$ 30%. On the other hand, the optimum parameters of the three phase SLM studies are 100 mg L^{-1} of Ni(II) in the feed phase, pH 5 in the feed phase, 0.15 M of NH_4Cl in the strip phase, 5% (v/v) of TOA in the sunflower oil, 3 V DC electric potential in the strip phase, stirring speed of 120 rpm in both phases, and 8 h of run time. The maximum deposition of Ni(II) was obtained at $\sim$ 93%. In the case of binary pollutants, the mixture, where Zn(II) and Ni(II) mixed with a 1:4 ratio, yields a maximum total deposition at 85% with TOA as the carrier, whereas the mixture where Zn(II) and Ni(II) were mixed with a 4:1 ratio yields a maximum total deposition at 75.98% with D2EHPA as the carrier. Experimental optimization with face centered CCD in RSM was done for the binary pollutants (i.e., Zn(II) and Ni(II)) with mixtures of binary carriers (i.e., TOA and D2EHPA) as parameters to optimize with a predicted output, *i.e.*, deposition of Zn(II) and Ni(II), which also showed good agreement with the experimental results.

Chapter 6: Conclusion and future scope

The overall conclusion and perspective of future work are discussed in this chapter.

Contents

List of Figures

List of Tables

Nomenclatures snd Abbreviations

η	Viscosity of organic phase
τ	Tortuosity of support membrane
ε	Porosity of support membrane
D	Diffusivity
J	Diffusional flux
k	Boltzmann constant
P	Permeability
r	Molecular radius
S	Effective surface area of strip-membrane interface
T	Absolute temperature
V	Volume of aqueous solution
V_p	Volume fraction of the polymeric framework
Aliquat 336	N-methyl-N,N,N-trioctylammonium chloride
ANOVA	Analysis of variance
BLM	Bulk liquid membrane

CCD	Central composite design
D2EHPA	Di-(2-ethylhexyl)phosphoric acid
DC	Distribution coefficient
EDX	Energy dispersive X-ray
ELM	Emulsion liquid membrane
FESEM	Field emission scanning electron microscopy
FS-HFM	Flat-sheet hollow fibre liquid membrane
FS-SLM	Flat-sheet supported liquid membrane
FTIR	Fourier-transform infrared spectroscopy
LM	Liquid membrane
PVDF	Polyvinylidene difluoride
RSM	Response surface methodology
SLM	Supported liquid membrane
TEM	Transmission electron microscopy
TOA	Trioctylamine
XRD	X-ray diffraction

Chapter 1

Introduction and Literature Review

This chapter includes the area as well as objective of the intended work. An elaborate literature study has been done to discuss about different sources of heavy metals viz. Cr(VI), Zn(II) and Ni(II) and their issues related to environment. The aim of this thesis is to explore the separation of these heavy metals from wastewater using liquid membrane (LM) based technology. In this regard the source of these heavy metals has been addressed. Different types of liquid membrane and its application with merits and demerits are described in this chapter. The relevant gap areas in the literature have been identified and the objectives have been formulated thereafter.

1.1 Introduction

Heavy metals such as Cr, Ni, Zn etc. are immensely carcinogenic and hence they are of huge ecological and physiological concern for human lives. Industrial effluents are the primary sources of heavy metal contamination in the environment. Heavy metals are not biodegradable either. It has also been seen that human exposure with these heavy metals have increased dramatically because of exponential increase in their use in several industrial, agricultural, domestic and technological applications [1]. Hex-

avalent chromium (Cr(VI)), nickel (Ni(II)) and zinc (Zn(II)) are found in the effluent emanating from different industries such as tanneries, electroplating, alloys, stainless steel, battery, metal plating etc. [2–5]. The adverse toxic effects of these metals are hemolysis, kidney and liver failure, diarrhoea, flu-like symptoms, etc. [6–10]. The concentration of Cr(VI), Ni(II) and Zn(II) ions in the industrial effluent vary from 0.5 to 270,000 mg L^{-1} [3, 11], from 3.4 to 900 mg L^{-1} [12, 13] and from 0.5 to 150000 mg L^{-1} [14–17], respectively. The permissible limits of chromium, nickel and zinc in drinking water are 0.05 mg L^{-1}, 0.02 mg L^{-1} and 3 mg L^{-1}, respectively as stated by World Health Organisation (WHO) [18]. It is very much essential to remove these heavy metals from industrial wastewater before discharging them into natural water body.

Several conventional processes such as adsorption, ion exchange, solvent extraction, reverse osmosis, ultrafiltration, nanofiltration, etc. are there for separation of heavy metals [19–23]. Each and every process has its inherent merits and demerits. Adsorption process can be economical provided adsorbents are of low cost. It has to be flexible and simple in terms of design. Adsorption process is simple to operate and effective to remove toxic pollutants [24, 25]. However, the process has many drawbacks such as loss of adsorbents, production of secondary pollutant, expensive regeneration process of adsorbent and problem with disposal of spent adsorbents etc. Ion exchange process is an old and proven technique that has been efficiently applied to various industrial processes to remove heavy metal [26, 27]. However, it suffers drawbacks such as high cost of resins, fouling problem, chlorine contamination etc. Solvent extraction process or liquid-liquid extraction process is also widely used as it is energy saving process and thus keeps production cost low. The major drawbacks of the solvent extraction process are utilization of large amount of solvent, loss of solvent and problem encountered during recovery of solvent.

Heavy metals separation using membrane based technology from industrial effluent have immense potential. Membrane technologies have several advantage over conven-

tional technologies such as low energy requirement, its ability to integrate with other processes, selective removal of pollutants, possibility for achieving "zero discharge" with reuse of product water and also its adjustable characteristics. Depending on the size and material to be separated they are classfied as microfiltration (MF), ultrafiltration (UF), nanofiltration (NF) etc. Other factors are also there on which membrane process may be classified such as affinity (*viz.* reverse osmosis, gas separation, pervaporation), charge (viz. dialysis, electrodialysis) and chemical nature [28, 29]. It can further be classified based on materials of the membrane such as solid membrane and liquid membrane [28, 29]. Solid membranes are in solid form (*viz.* organic, inorganic and polymeric) and liquid membranes (LM) are in the form of organic solvents. Though solid membranes are stable in nature, this generally suffer from the inherent drawbacks such as low trans-membrane flux, membrane fouling, and insufficient or low selectivity. LM is a thin homogeneous liquid film (membrane phase) which acts as diffusional barrier between other two phases, *viz.* feed (or source) phase and receiving (or strip) phase [30, 31]. Membrane phase is composed of solvent with/without extractant/carrier. The membrane phase should be immiscible with feed/receiving phase. The feed phase containing solute needs to be transported through the thin film LM to receiving phase. The transport of solute across the LM occurs due to the difference in chemical potential which is due to solubility and diffusivity in the liquid film as well as the concentration gradients in the phases. The advantages of this process are simultaneous extraction and stripping in a single step, high separation factor and selectivity. The LM based technique is very useful for wastewater treatment due to these inherent advantages. It is intended to perform further research with LM in this thesis. The configuration of LM *i.e.* source/membrane/strip phase depends on the type of application which can be either aqueous/organic/aqueous configuration or organic/aqueous/organic configuration [30–32]. As the central theme of thesis is treatment of wastewater, aqueous/organic/aqueous configuration have been used. The salient features of different LM have been elaborated in the subsequent sections.

1.1.1 Liquid membrane (LM)

The concept of LM was first introduced by Nernst and Riesenfeld at 1902, related to electrical properties of the interface between two immiscible liquid electrolyte phases [33]. In the sixties Norman Li developed large-scale desalination and hydrocarbon separation process using LM [34]. LM is basically two extraction processes in series where inorganic and/or organic solutes are transported selectively from feed phase to strip phase [30–32]. The transport of solute across the LM occurs due to the gradient in solubility and diffusivity in the liquid film as well as the concentration gradients in the phases and this type of mechanism is called solution-diffusion mechanism. Furthermore, diffusion coefficient of solute in liquid is higher than the solid which results in larger flux in LM [30]. The efficiency and selectivity of solute transport for LM may be enhanced by the presence of some carrier component. When appropriate carrier is added to the solvent, solubility of solute in membrane phase is increased due to formation of solute-carrier complex. In this case the membrane phase (*a.k.a* organic phase) is the combination of a solvent and a carrier. The increased solubility is manifested by the enhanced distribution coefficient (DC), defined as the ratio of solute in organic phase and the solute in feed phase after the equilibrium is reached. Carrier is not used solely as solvent because in general carrier has higher viscosity, high molecular weight and is more expensive. According to the Stokes-Einstein equation (Equation 1.1), transport mechanism in LM largely depends on the viscosity of membrane phase, as the diffusivity is directly inversely proportional to viscosity. If the viscosity of carrier is higher than the solvent, with increase in carrier concentration the viscosity is increased in LM, as a result diffusion coefficient and flux are reduced [29].

$$D = \frac{kT}{6\pi\eta r} \tag{1.1}$$

where, D is the diffusivity (cm^2/s), k is the Boltzmann constant (J/K), η is the vis-

cosity of the organic phase (cP), T is absolute temperature (K) and r is the molecular radius (cm). Therefore, the viscosity of membrane phase should be low for enabling higher transport. Further addition of carrier increases the distribution coefficient (DC), which yields to increase the overall transport efficiency as well [35]. Various transport mechanisms, involved in LM processes are briefly discussed below.

1.1.2 Mechanism of transport of solute in LM

Three different phases are involved in the system of LM. The solute of interest is transported from feed phase to other aqueous phase, *viz.* receiving or strip phase, via membrane phase. The transport of solute occurs through extraction from feed phase to recovery/re-extraction in strip phase due to feeble hydrogen bonding or by strong chemical reaction between solute and carrier. When solutes are transported by simple solution-diffusion mechanism due to different solubility or chemical potential between different phases, the transport is termed as passive transport. Passive transport is direct transport and it does not require any chemical energy to accomplish the solute movement. There are two basic types of principles involved in LM operation *viz.* passive transport and active transport.

Passive transport: In passive transport, ion/atom/molecule move from a zone of higher concentration to a zone of lower concentration across membrane driven by the growth of entropy of the system and does not require any chemical energy. Four different types of transport can be seen in passive transport such as solution diffusion, facilitated diffusion, filtration and osmosis. In case solution diffusion solute dissolves in membrane material and is transported through membrane due to concentration gradient. The process continues till the gradient is eliminated [32, 36]. Transport of solute A from feed phase to strip phase occurs due to concentration gradient from feed phase to strip phase as shown in Figure 1.1. In this case, the rate of diffusive transport can be low due to solubility of solute A in feed phase as well as strip phase.

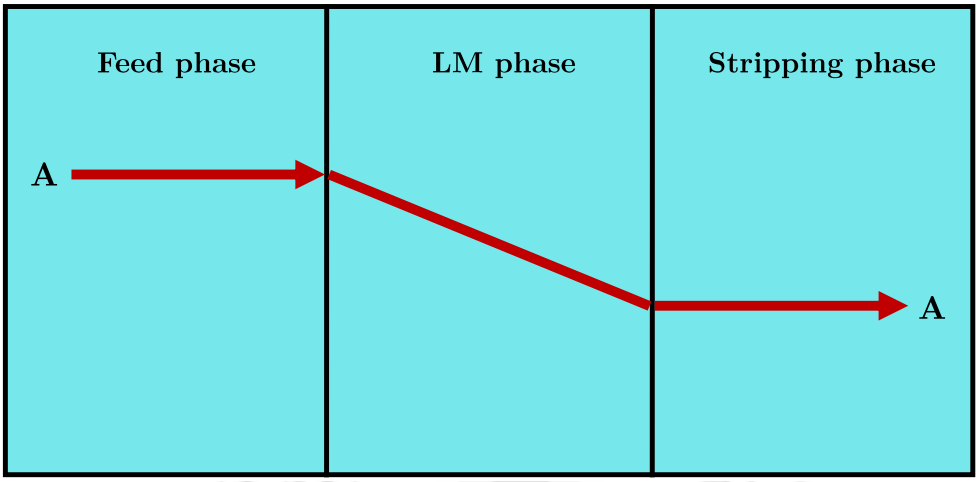

Figure 1.1: Ordinary diffusive transport of component, A through LM

In order to achieve high selectivity, a substrate specific carrier must be present in the LM. The type of molecular movement across membrane is called facilitated diffusion or carrier mediated diffusion. This type of solute transport is also called passive transport as there is no energy required for transporting solute. The carrier added in the membrane phase should be soluble only in the LM phase and must have the capability to form complex reversibly with specific solute. The mechanism is represented schematically in Figure 1.2. The transport mechanism is called as uniport, where only single component is transported through LM. The solute transport of feed phase component A is enhanced by the carrier C. The carrier C present in the LM forms complex AC at the feed-membrane interface. Complex AC diffuses through membrane from feed-membrane interface to strip-membrane interface due to concentration gradient and releases solute A at the strip-membrane interface. There after the carrier C again diffuses back to the feed-membrane interface and binds with A and cycle continues. There are two types of transport mechanism involved in the carrier mediated transport, (1) some portion of A transport freely due to concentration gradient which is called solution-diffusion mechanism and (2) A forms complex with carrier which enhances the solubility of A in membrane phase to boost transport rate of solute A. There are some important basic features that should be

present in the carrier mediated transport. One of the basic features is formation of solute-carrier complex should be reversible, *i.e.* the solute-carrier complex formed in feed-membrane interface should be easily separated at the strip-membrane interface, otherwise carrier present in the membrane phase will get saturated with solute-carrier complex which would limit the solute transport. Secondly, complex should not be very strong or very weak. Strong complex will create problem in releasing solute at strip-membrane interface whereas, very weak complex will not form solute-carrier complex very easily at feed membrane interface which eventually slows down the solute transport rate. There should be optimum bond energy in the reversible complex *i.e.* 10–50 kJ/mol [29].

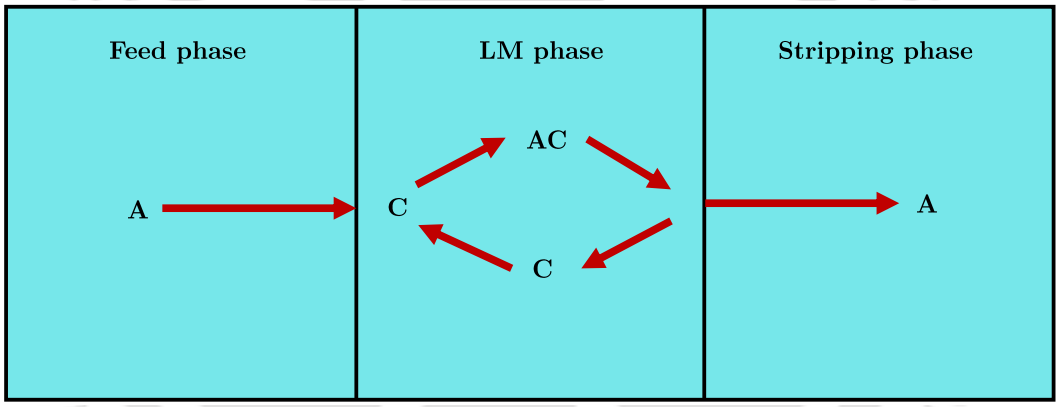

Figure 1.2: Mechanism of carrier mediated or facilitated transport in LM with mobile carrier

There are two types of carrier mediated coupled transport *viz.* co-transport and counter transport. The transport mechanism are shown in Figure 1.3. In co-transport carrier can form complex with two different species at the same time and transport in the same direction (refer Figure 1.3a). A and B form complex with C and gets transported at same direction. It is called as co-transport. In case of counter transport the carrier forms complex with two different species at the same time but gets transported in opposite direction (refer Figure 1.3b). A and B form complex with carrier C and gets transported in the opposite direction.

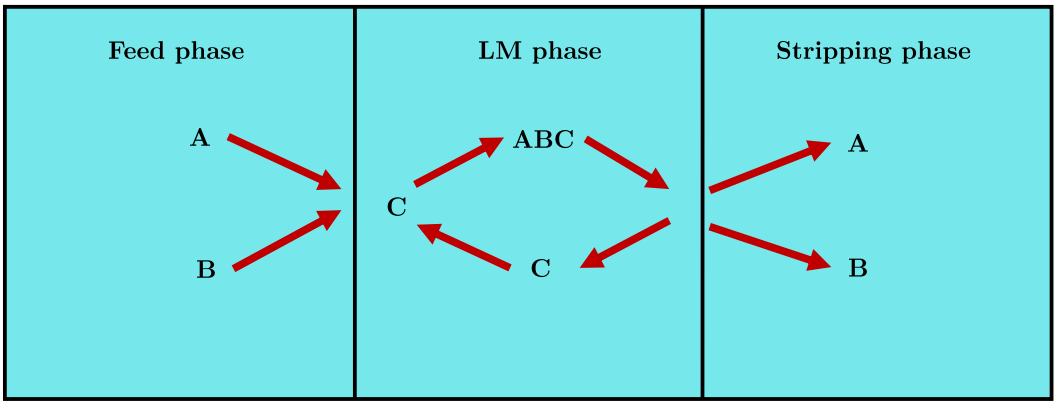

(a) Co-transport

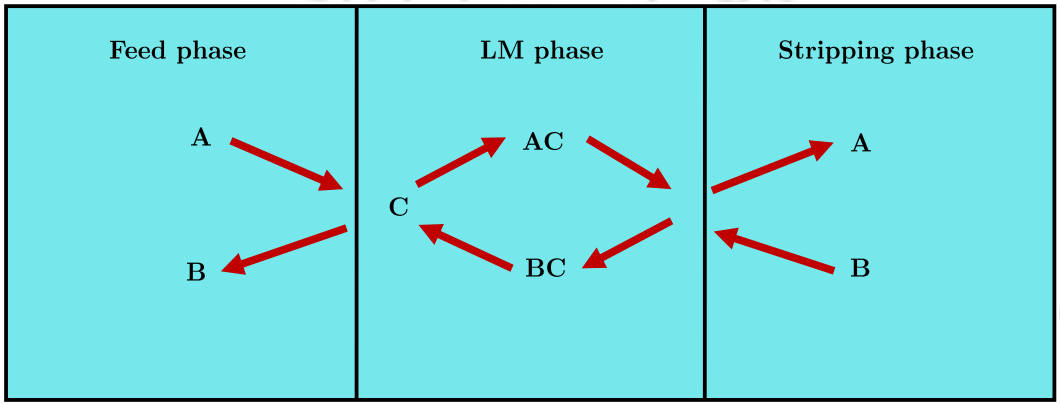

(b) Counter transport

Figure 1.3: Mechanism of coupled transport in LM

Active transport: Active transport, also known as uphill transport. This type transport occurs against the concentration gradient *i.e.* lower concentration to higher concentration. Active transport is mainly driven by oxidation-reduction, catalytic reactions, biochemical conversions on the membrane interfaces as shown in Figure 1.4. These reactions give energy to maintain a proper balance of ions and molecules. That is why active transport works against a concentration gradient. The active transport is very solute specific or highly selective and chemical reactions are irreversible [30, 37].

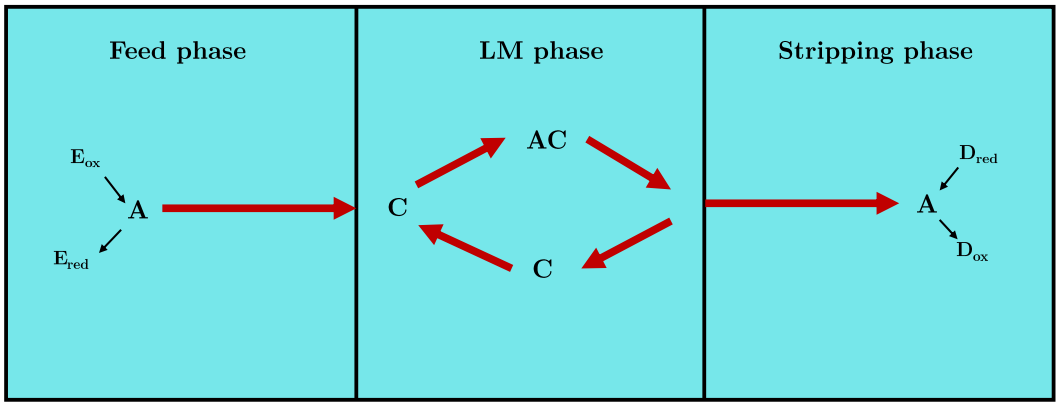

Figure 1.4: Mechanism of active transport in LM

1.1.3 Carrier

In LM, carrier is a type of reagent which act like a catalyst. Carrier enhances the selectivity and transport efficiency of the solute through organic phase. The carriers are mixed with solvent to prepare the LM. Amount of requirement of carrier is usually very small. High concentration of carrier increases viscosity of LM which slows down the diffusion rate. The carriers can be characterized by [38]:

- Ability to quick binding and release of specific substances
- Ability to selective and reversible binding of a component in the solution
- Non-binding with solvent
- Low viscosity
- Lack of ability to coalesce
- Less or non-toxicity

Carriers can be categorized as three main types depending on the functional groups of their molecules *viz.* acidic, basic and neutral (refer Table 1.1). The selection of carrier mainly depends on the nature of solute present in the aqueous phase. Acidic

carrier mainly contains COOH, P(OH), SO_3H groups which have affinity towards cations. Di(2-ethylhexyl)phosphoric acid (D2EHPA) is an ideal example for acidic carrier. Whereas, alkaline carriers are used to extract anionic solute. Amines (such as trioctylamine, aliquat 336) are ideal examples of alkaline carriers. Neutral carriers (such as tributyl phosphate) are generally used as cationic carrier for selective transport of different metal ions or they make hydrogen bonding with un-ionized solute to form the complex.

Table 1.1: List of carriers used in various LM processes

Type	Name of carrier agent	Application in the extraction of heavy metals	Ref.
Acidic	Di(2-ethylhexyl)phosphoric acid [D2EHPA] ($C_{16}H_{35}PO_4$ 322.4)	Ni, Ag, Cu, Pb, Cd and Hg	[35]
”	Trioctylphosphine oxide [TOPO] ($C_{24}H_{51}OP$ 386.63)	Cd, Cr and Pt	[39]
Basic	Trioctylamine [TOA [$(C_8H_{17})_3N$ 353.67]	Hg and Ni	[40, 41]
”	Trioctylmethylammonium chloride [Aliquat 336] ($C_{25}H_{54}ClN$ 404.16)	Cr	[42]
”	N,N-Dimethyloctylamine [DMOA] ($C_{10}H_{23}N$ 157.3)	Cd	[43]
Neutral	Di-benzo-18-crown-6 [DB18C6] ($C_{20}H_{24}O_6$ 360.4)	Hg	[44]
”	Tributyl phosphate [TBP] ($C_{12}H_{27}O_4P$ 266.31)	Rare earth U	[35]

1.1.4 Types of LM

LMs are broadly classified into three types according to their configuration *viz.* bulk liquid membrane (BLM), supported liquid membrane (SLM) and emulsion liquid membrane (ELM) [30]. As per the geometry of SLM, it is classified into three types

(Figure 1.5), *viz.* flat sheet supported liquid membrane (FS-SLM), hollow fibre supported liquid membrane (HF-SLM) and spiral wound supported liquid membrane (SW-SLM). Two other types of membrane are also there, electrostatic pseudo LM and contained liquid membrane. This research work is focussed on BLM and FS-SLM. BLM process is well suited for initial study about various parameters related to mass transfer and transport feasibility of solute, where as SLM process is most promising towards commercial application, it is studied in detail. The following sub-sections, BLM and SLM have been discussed in brief.

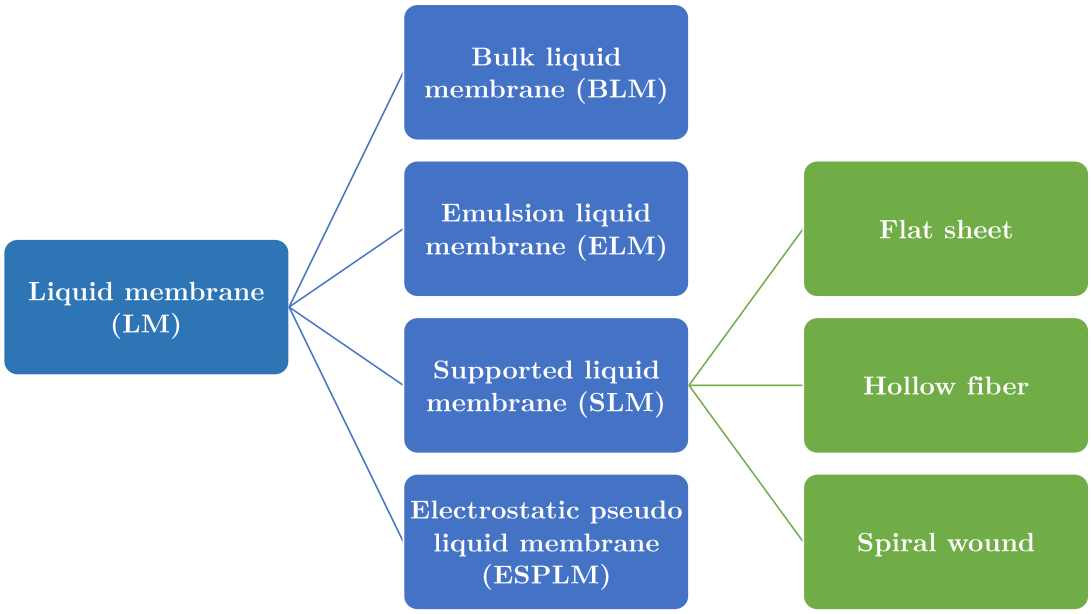

Figure 1.5: Family of liquid membranes

1.1.4.1 Bulk liquid membrane (BLM)

In BLM, the feed and strip phases are separated with a solid barrier (*e.g.* glass wall) and bulk amount of organic phase is placed in such a way that the liquid is in contact with both feed and strip solutions. A schematic diagram is in Figure 1.6. The difference in density between membrane and aqueous phases is the determining factor *i.e.* membrane phase density is lower than feed and strip phase (refer Figure 1.6a) and membrane phase density is heavier than feed and strip phase (refer Figure 1.6b).

The BLM is simplest among other LMs. BLM process is helpful to determining rate constants and distribution coefficients of novel carrier and it is suitable for selection of stripping solution. But BLM has comparably small surface area to volume ratio and longer diffusion path of the solute or solute-carrier complex which limits its industrial usefulness.

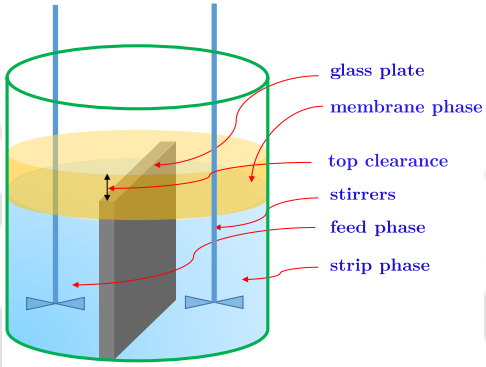

(a) Lighter LM

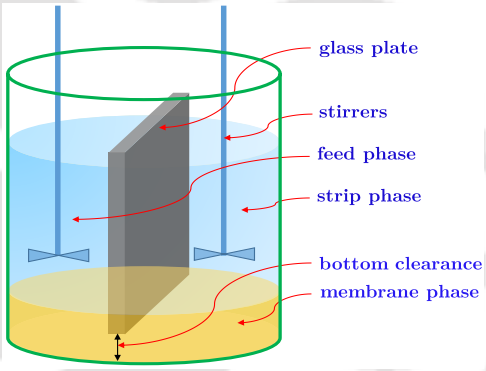

(b) Heavier LM

Figure 1.6: Schematic of BLM

1.1.4.2 Supported liquid membrane (SLM)

The SLM uses a thin micro-porous solid support where organic/membrane phase is immobilized within the pores by capillary forces. The solid support containing organic/membrane phase act as barrier between feed and strip phases. The porous support can be inorganic or organic (polymer) depending on the mechanical stability, chemical properties and application. In polymeric support, typical thickness varies in the range of 25-170 μm and the average diameters of the pores are in the range

of 0.075-0.45 μm [45]. The novelty of SLM lies in the diffusional path (L) of solute transport. The diffusional path can be designed very small provided the stability of membrane is not compromised. Fick's law of diffusion says the rate of diffusion of solute through medium (here liquid) is inversely proportional to the length of diffusional path. Hence, to increase the solute diffusion the length of diffusion path should be kept as small as possible. These factors are important to increase the solute flux. The success of SLM technique depends also on the judicious selection of support, proper selection of LM and the stripping agent for solute of interest. The stability of organic phase in SLM is also an important part for transporting any solute. The stability of LM or organic phase mainly depends on the viscosity of LM, interfacial tension between aqueous phases and organic phase, solubility of LM in aqueous phases *etc.* The compatibility between LM and solid support is also a key factor for stability of LM in SLM process. Mainly two types of compatibility are involved *i.e.* physical and chemical compatibility. Physical compatibility lies mainly in the support characteristics such as thickness, pore size, shape of the pores, tortuosity *etc.* Whereas, relative hydrophobicity of LM and the support material involves in chemical compatibility.

Ideally, the pores should be of identical in size and cylindrical in shape. But in real case support pores are neither identical nor regular in shape. The support should have higher porosity which would provide higher effective surface area for solute diffusion. The tortuosity (τ) of the solid support is an effective membrane characteristics which can be defined as the following equation [46]:

$$\tau = \frac{1 + V_p}{1 - V_p} \tag{1.2}$$

Where, $V_p = 1 - \varepsilon$, V_p is the volume fraction of the polymeric framework and ε is porosity of the support membrane.

Based on the geometry of the support and applications, SLM can be designed in a

variety of different configurations, namely, flat sheet-SLM (FS-SLM), hollow fiber-SLM (HF-SLM) and spiral wound-SLM. Simplest is the flat sheet configuration, where the membrane phase is held in a porous sheet separating the compartments of the feed and receiving phases (see Figure 1.7). This configuration is simple to construct but has a fairly low mass transfer area per unit volume.

The other advantages of using SLM are:

- ✓ It incurs less capital, operating, maintenance and energy costs
- ✓ Amount of LM consumption is very less
- ✓ Easy to operate and scale-up
- ✓ Can be used for high selective transport
- ✓ Operating procedure is simpler than other LM processes

However, the main problem of the SLM technology is the instability of the membrane phase *viz.* the chemical stability of the LM, the mechanical stability of the support pores and limited membrane life.

The reason behind the instability of SLM are [35]:

- ✓ Loss of membrane solution from the pores of the solid support due to wetting of the pores by aqueous phases
- ✓ Effect of trans-membrane and osmotic pressure
- ✓ Emulsion formation in the LM phase
- ✓ Blockage of membrane pores by contamination

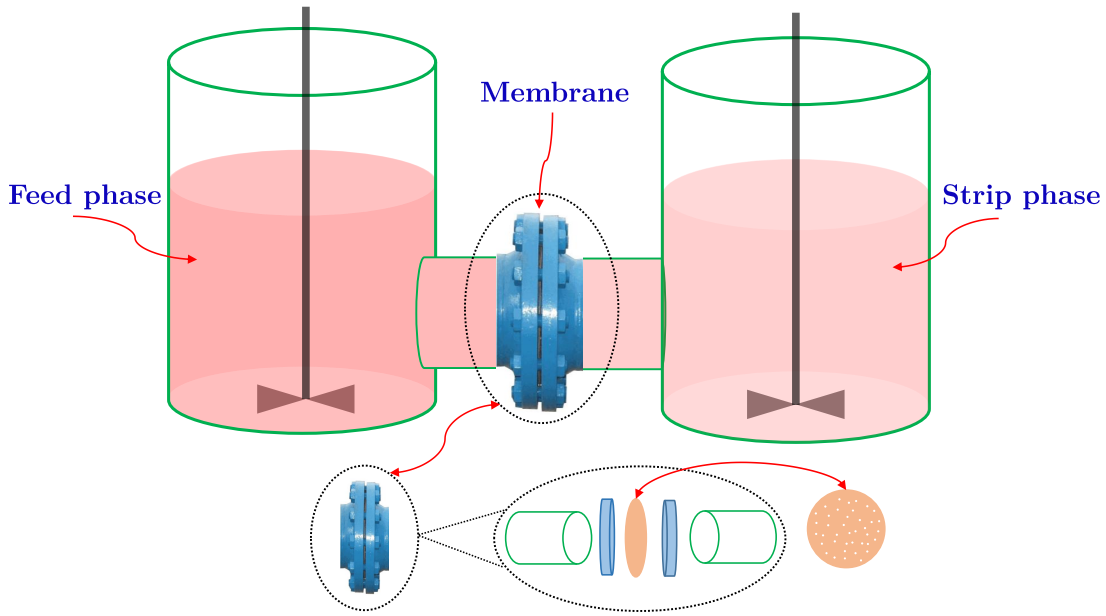

Figure 1.7: Schematic of flat sheet supported liquid membrane

1.1.5 Pollutant studied

Diffusion mechanism prevails in transportation of solute through LM. Various physical and chemical properties *viz.* size, affinity, charge and chemical nature of solute influence the transport process through LM. Three different and very common pollutants have been chosen for present study, *viz.* chromium (VI), nickel (II) and zinc (II). The pollutants are hazardous because of the their high solubility in aquatic environment. These pollutants co-exist in various industries such as leather, mining, electroplating, stainless steel, alloy, battery and paints [2–5]. The detailed discussion of these pollutants such as source of these pollutant, effects of these pollutants on environment as well as animal life have been done in following sub-sections.

1.1.5.1 Chromium (VI)

Chromium (Cr) can be found in most two stable oxidation states *i.e.* trivalent chromium, also written as Cr(III), and hexavalent chromium, also written as Cr(VI). Cr(VI) is more toxic and carcinogenic than Cr(III) [47, 48]. Cr(VI) is generally pro-

duced by industrial processes. The major industries *viz.* electroplating, stainless steel production, leather tanning, textile dyeing, industrial pigments and wood preservation are responsible for contaminating natural water body through Cr(VI) enriched effluent [48–51]. Cr(VI) has strong oxidizing potential and easily adsorbed by biological tissue. The adverse effects of Cr(VI) manifest through inhalation, respiratory and dermal irritation and ulceration. Cr(VI) results gastritis, nephrotoxicity, and hepatotoxicity. Workers of chromate production, pigment production, metal plating, and ferrometals industries are very much prone to lung cancer due to exposure of high concentration Cr(VI) [48, 52]. The international standard for maximum allowable limit of Cr(VI) in drinking water is 0.05 mg L^{-1} [18] whereas, in India, maximum allowable limit of Cr(VI) for inland surface water is 0.1 mg L^{-1}, public sewers is 2 mg L^{-1} and marine coastal areas is 2 mg L^{-1} [53].

1.1.5.2 Nickel (II)

Nickel (II) (also written as Ni(II)) and its compounds are found in both natural and anthropogenic sources. Ni(II) is an essential micro-nutrient for plant growth and can be found in food and water [54, 55]. Though Ni(II) is an essential element for plant, high consumption of Ni(II) leads to nickel-toxicity which is carcinogenic to human body [56]. Major source of Ni(II) exposure is due to oral consumption through food and water, also caused by air pollution. The environmental water body is contaminated with Ni(II) by effluents of industries such as stainless steel, alloy, battery, plating, paint and electronic [4, 57]. Excessive consumption of Ni(II) yields variety of adverse effects on human health varying from contact dermatitis to lung fibrosis, cardiovascular and kidney diseases, and even cancer [4, 58, 59]. The concentration of Ni(II) in a typical industrial effluent ranges from 3.4 to 900 mg L^{-1} [12, 13]. Considering its health hazard, the maximum permissible limit of Ni(II) in ground water range between 0.003 and 0.01 mg L^{-1}. In United States permssible range of Ni(II) in drinking water is between 0.002 and 0.04 mg L^{-1} [60, 61].

Permissible limit of Ni(II) in drinking water is 0.02 mg L^{-1} as stated by WHO [18]. In India, allowable limit of Ni(II) in inland surface water, public sewers and marine coastal areas are 3, 3 and 5 mg L^{-1} respectively [53].

1.1.5.3 Zinc (II)

Zinc (II) (also written as Zn(II)) and its compounds are used in different industries *viz.* alloy, electroplating, paint, rubber, battery, textile and steel [5]. Though Zn(II) is an essential mineral for humans, animals and plants, excess consumption of Zn(II) is harmful. Excessive consumption of Zn(II) suppresses copper and iron absorption. As a results it developes anemia, hypocupremia, leukopenia and neutropenia. Symptoms like headache, abdominal pain, nausea and vomiting are observed due to acute Zn(II) toxicity [62, 63]. The Zn(II) concentration in effluent of different industries varies from 0.5 to 150000 mg L^{-1} [14–17]. According to the WHO guideline permissible limit of Zn(II) in drinking water is 3 mg L^{-1}. In India, allowable limit of Zn(II) in inland surface water, public sewers and marine coastal areas are 5, 15 and 15 mg L^{-1} respectively [53]. Hence, It is very much essential to remove Zn(II) from industrial wastewater before discharging them into natural water body.

1.2 Literature review

LM based process has gained immense interest in recent times due to its application in various field. As the main theme of this thesis *viz.* separation of heavy metals from wastewater, this section presents a thorough review of literatures related to heavy metal separation.

1.2.1 LM for general application

The first LM (ELM) was invented by Norman Li in the sixties [34], since then LM based separation process has gain popularity for wide variety of applications. Since

then LM technology has been applied in diverse area from analytical and organic chemistry, to chemical, biochemical and biomedical engineering. In terms of particular activities within these areas *i.e.* gas separations, recovery of valued or toxic metals, removal of organic compounds *etc.*, summary of these works is discussed by Richard D. Noble and his co-workers [64]. In last two decades LM technology has been applied to separate metals including heavy metals *viz.* Cr, Fe, Co, Ni, Cu, Zn, As, Sr, Ag, Cd, Pt, Au, Hg, Pb, Mn, Li *etc.* [65–75]. Transport of alkaline metals, sodium and pottasium, have been performed by Dernini et al. [76] using BLM Lithium has been separated using SLM by Bansal et al. [77]. Mohapatra and his co-workers [78, 79] have separated cesium using HF-SLM and FS-SLM. Juang and Wang [80] have separated amino acid, a biomedical compound, using ELM technology whereas, transport of aspartic acid (also a biomedical compound) has been done by Lin et al. [81] using HF-SLM. Pharmaceutical products such as diclofenac, penicillin-G, cephalosporin-C *etc.* have been separated using LM technology, as discussed elesewhere [82–84]. Reis et al. [85] have experimented separation of phenol and its derivative *i.e.* tyrosol and p-coumaric acid. Park et al. [86] have also removed phenol and substituted phenols using ELM. Zidi et al. [87, 88] have removed phenol from wastewater using two different carriers *i.e.* tri-n-octyl phosphine oxide (TOPO) and tributyl phosphate in SLM. Aromatic hydrocarbons, *viz.* benzene, toluene and p-xylene, have been transported using SLM by Matsumoto et al. [89]. They have used imidazolium-based room temperature ionic liquid (IL) as a carrier in SLM. The selectivity of hydrocarbons is significantly improved using IL as carrier.

Major works on LM have been done using traditional organic solvent which are usually inflammable, toxic to human and environment, volatile in nature [90].

Permeation of copper using coconut oil as solvent and D2EHPA as carrier reported by Venkateswaran et al. [91]. They have used SLM technology for separation of copper ion and also used copper plating wastewater for this purpose. Almost 70% copper removal was achieved.

Muthuraman and Palanivelu [92] have separated textile dye using SLM. They have studied various vegetable oils as LM for separation of dye and palm oil, sunflower oil and coconut oil come out as suitable LM for dye separation. Among these vegetable oils palm oil was found to be the best solvent.

Removal of dye from textile wastewater has been done by Mahmoud et al. [93] using plant oil or vegetable oil. Using rotating discs contractor, Ehtash et al. [94] have removed phenol from wastewater by rapeseed oil. They have shown rapeseed oil has shown good extraction efficiency of phenol than conventionally used volatile organic solvents *i.e.* diisopropyl ether, kerosene etc.

Kazemi et al. [95] have used LM with combination of sesame oil and TBP for separation phenol from wastewater by SLM. Different factors affecting phenol transport were analysed by Taguchi method and optimal experimental conditions for transport of phenol were obtained by analysis of variance (ANOVA).

Chakrabarty et al. [96] have separated mercury (Hg) through SLM using coconut oil with TOA as LM and separation efficiency reported about 93%. They have reported SLM stability with coconut oil as solvent upto 98 h due to compatibility of coconut oil with PVDF membrane support.

BLM experiment was done by Manna et al. [97] to separate bioactive compound, catechin using sunflower oil as solvent and TBP as carrier. They have achieved 70% extraction and 40% recovery efficiency of catechin using BLM technology. The research works of Bhatluri et al. [43, 98–100] aimed at exploring LM based techniques for the separation of heavy metals *viz.* Cd(II) and Pb(II). They have used BLM and SLM technology with coconut oil as solvent for transporting Cd(II) and Pb(II) from wastewater.

In recent times, Kumar et al. [101] have separated a organic pollutant named lignosulfonate using sunflower oil as solvent with TOA as a carrier. The separation process has been done using BLM technology. The maximum extraction and recovery efficiency of lignosulfonate were 92.4% and 75.2 % respectively.

Dong et al. [102] have recovered copper and cyanide through ELM using quaternary amine salt as a mobile carrier. They have tried to form ideal ELM by optimizing different physical and chemical parameters.

Daraei et al. [103] have used ELM technology to separate dye for water decolorization. They have used sunflower oil as diluent with span 80 as surfactant. The influencing parameters for dye removal were determined by screening design of Plackett-Burman. The response surface methodology (RSM) with Box-Behnken design method were applied to determine optimum conditions for maximizing dye removal efficiency.

Mesli and Belkhouche [104] have used ELM technique to separate Pb(II) from nitrate medium. They have prepared ELM using n-heptane by mixing iso-octylphenoxypolyethoxyethanol as surfactant and aliquat336 as carrier. They have optimized different experimental parameters such as carrier concentration, surfactant concentration, run time, stirring speed, initial concentration and pH of feed phase. They have also studied RSM using Box-Benheken Design (BBD).

Using ELM technology Benderrag et al. [105] have separated Cd(II) from wastewater. They have used prepared ELM which consists of kerosene as organic solvents, Triton X-100 as biodegradable surfactant and D2EHPA as carrier. The process parameters was optimized using an empirical smoothing method. The results were represented on three-dimensional plots using RSM with Box-Behnken design.

Mokhtari and Pourabdollah [106] have separated bismuth (Bi(II)) using ELM technology. The different experimental parameters were evaluated and optimized for maximum yield of Bi(II). They have obtained maximum yield of Bi(II) using combination of D2EHPA, Triton X-100 and n-pentanol as carrier, surfactant and diluent respectively in ELM.

An innovative work has been developed by Zhao et al. [107] which includes production of nano-sized $CePO_4$ using ionic liquid-driven SLM system. They have shown how to control the morphology of the rare earth phosphate nanostructures by controlling the pH and the concentration of SO_4^{2-} in the feed phase of rare earth ions.

Lanthanum (La(III)) a rare earth metal has been separated using SLM technology by Ozevci et al. [108]. They have prepared LM using mixture of TBP and imidazolium-based IL ([C_4mim][Tf2N]). The transport efficiency of La(III) was optimized by two level three factor full factorial design.

Rare earth elements such as lanthanum (La(III)), cerium (Ce(III)), yttrium (Y(III)) and neodymium(III) (Nd(III)) have been recovered using ELM process by Zhang et al. [109]. They have prepared ELM using kerosene-D2EHPA with sorbitan monooleate (Span80) and polyisocrotyl succinimide was used as surfactants. The effects of the different parameters on rare earth elements extraction like type and concentration of carrier, type and concentration of surfactant, the concentration of the HCl as the internal aqueous phase, the volume ratio of the organic phase to internal phase, the volume ratio of the emulsion phase to the feed solution were studied.

Pavon ei al. [110] have separated yttrium and europium using SLM process. They have recovered rare earth elements from the leachate by FS-SLM using Cyanex 923 as carrier and Na_2EDTA as the receiving phase.

Mass transfer characteristics of Th(VI) have been investigated by Allahyari et al. [111] using hollow fiber renewal liquid membrane(HFRLM) containing kerosene-TBP and HNO_3 as LM and receiving phase respectively. They have developed mass transfer model to predict the individual and overall mass transfer coefficients of HFRLM process.

Removal of uranium from aqueous solution using ELM technique was done by Zaheri and Davarkhah [112]. The ELM has been made up of 2-thenoyltrifluoroacetone (HTTA) as a carrier, kerosene as an organic diluent, HCl as a stripping solution and sorbitan monooleate (Span-80) as a surfactant. They have used fractional factorial design to investigate most important parameters. Then, the effect of selected factors on the uranium transport was studied and the optimum operating conditions were obtained.

Mahanty et al. [113] have extracted americium (Am(III)) using SLM technology

from high level waste (HLW). They have used benzene-centered tripodal diglycolamide (Bz-T-DGA) (*i.e.* TPAMDGA and TPAEDGA) as carrier with isodecanol and n-dodecane for preparation of LM. The different parameters such as effective diffusion coefficient, permeability coefficient were evaluated for Am(III) by these extractants.

Gholap et al. [114] have reported the systematic studies on transport behaviour of Pu(IV) across a SLM using the novel ligand oxatricyclodiamide (OTDA). They have studied parameters controlling the transport behaviour of Pu(IV) *i.e.*, nature of feed acid concentration, concentration of OTDA and nature of diluents. Membrane diffusion co-efficient value have also been calculated using t_{lag} method as well as by varying membrane thickness.

1.2.2 LM based separation of Cr(VI), Ni(II) and Zn(II)

The separation of heavy metals such as Cr(VI), Ni(II) and Zn(II) using LM based technology have been done by various researchers. Kitagawa et al. [115] used isoparaffin as a solvent in ELM to remove NH_4^+, Cr^{6+}, Hg^{2+}, Cd^{2+} and Cu^{2+}. They have used different carriers such as Alamine 336 for removal Cr and Hg, Lix 64N for removal of Cu, and Aliquat 336 for removal of Cd.

Chakravarti et al. [116] used kerosene as solvent in ELM to study different types of strip phase reaction with Cr(VI). They have used Aliquat 336 and Alamine 336 as a carrier for removal of Cr(VI).

Chiha et al. [3] have used a combination of hexane (solvent)and tributyl phosphate (extractant) to develop the membrane phase in a liquid surfactant membrane (mentioned as LSM) and studied the strength of Span 80 as surfactant to know how much stability it can impart on the emulsion while they have also studied various physical and chemical parameters on extraction of Cr(VI).

Kumbasar and his research group [39, 117, 118] used various extractants and surfactants in ELM while the source was polluted with various other metal ions in addition

to Cr(VI). The interaction effects on various pollutants were easily understood from these experiments.

Bonam et al. [119] have used a combination of kerosene (solvent) and Aliquat 336 (extractant) and a rotating spray column to separate Cr(VI). They have also developed a mathematical model for estimating the effect of experimental parameters on mass transfer coefficient.

Huang et al. [120] have worked with SLM and tri-n-octylphosphine oxide (or abbreviated commonly as TOPO) as a carrier and kerosene as a diluent for separation of Cr(VI). They have also proposed a permeation transport model through SLM.

Djane et al. [121] have reported separation of total chromium (trivalent and hexavalent) using two serially connected SLM membrane units with kerosene as a solvent. Samples of effluent were collected from the drainage of tannery industry.

Venkateswaran et al. [122] have used tri-n-butyl phosphate (or TBP, as commonly abbreviated) as a carrier where polytetrafluoroethylene (hereafter abbreviated as PTFE) membrane was used as a membrane support in SLM. They have optimized parameters to maximize separation from synthesized effluent and tried the applicability of those parameters for treatment of real plating effluent.

Separation of trivalent chromium, i.e. Cr(III), through SLM have been reported by Chaudry et al. [123] where they have used triethanolamine-cyclohexanone-polypropylene film as the carrier-solvent-support combination.

Various physico-chemical parameters have been optimized by Ashraf and Mian [124] using alamine 336 as a carrier with toluene in SLM configuration. Separation through polymer inclusion membrane (hereafter referred to as PIM) and SLM has been carried out by Kozlowski and Walkowiak [125]. They have studied the effect of different tertiary amines across PIM. They have also done comparison of performances of BLM, SLM and PIM.

SLM study has been done by Nawaz et al. [126] to separate Cr(VI). Mixture of toluene and TOPO used as a LM. They have achieved 80% removal efficiency of

Cr(VI) with diphenylcarbazide (DPC) in sulfuric acid (H_2SO_4) as a stripping agent. A novel flat-type synergic SLM has been used by Jahanmahin et al. [127] for separation of Cr(VI) using Aliquat 336 and TBP as a carrier and kerosene as a diluent. RSM method has been applied for parameter optimization and achieved 94.3% of Cr(VI) removal efficiency.

Han et al. [128] have investigated removal of Cr(VI) using BLM where they have used mixture of sunflower oil and o-xylene as a solvent and various quaternary ammonium salts as a carrier. Among those carriers methyltrioctyl ammonium bromide is found to be best carrier. The removal efficiency of Cr(VI) was >98% over 4 h of operation.

SLM study has been done to separate Cr(VI) by Onac et al. [129]. They have used 2-nitrophenyl octyl ether dichloromethane as solvent and calix(4)arene as a carrier with celgard 2500 as a membrane support. They have calculated permeability coefficients for each studied parameter using Danesi mass transfer model.

Kumar and his research group [49] have extracted Cr(VI) using ELM. The ELM was prepared using mixture of rice brand oil (RBO) and hexane as a diluent with tridodecylamine (TDDA) as a carrier, and span 80 as emulsifying agent with sodium hydroxide (NaOH) as an internal agent, they achieved 97% extraction efficiency of Cr(VI).

Yesil and Tugtas [130] have investigated application of SLM technology for heavy metal removal (*i.e.* Cd, Cr, Cu, Ni, and Zn) from leaching effluents. They have used D2EHPA and aliquat 336 as carrier with kerosene as diluent. The parameters such as carrier type, carrier ratio, and concentration of strip solution have been optimized to get best separation yield of heavy metals.

Converting liquid waste to solid waste or value added product grossly reduces volume of the waste. Use of recovered heavy metals (Cr(VI), Ni(II) and Zn(II)) would be hugely beneficial for waste management program. However, industrial wastewater contain multiple heavy metals in various proportion. Researchers are now showing

interest to establish a technique for treating effluent containing various heavy metals. Parhi and Sarangi [131] have separated copper, zinc, cobalt, nickel with the help of different carriers such as LIX 841, TOPS-99 and Cyanex 272. They have done batch wise operation for selective transport of metals.

Duan et. al. [132] have used a new sandwich SLM (i.e. two-membrane-three-compartment cell) to separate copper, nickel and cobalt from its ammoniacal solution. They have used H_2SO_4 as stripping solution in two stripping compartments with different concentration and Acorga M5640 in kerosene as a LM. Separation efficiency of different metal in different compartment of SLM were 99.5% of cobalt, 98% of nickel, and 98.9% of copper.

In another study Duan et. al. [133] have used conventional SLM technology for separation of copper from nickel in ammoniacal solution. The organic phase of SLM was prepared by mixture of Acorga M5640 and trialkyphosphine oxide (abbreviated as TRPO) as carriers with kerosene as solvent. A number of influencing parameters on the Cu(II) transport and separation of Cu(II) from Ni(II) have been studied. The separation efficiency of Cu(II) was up to 98.4% under optimal conditions.

A comparative study of transport flux of cobalt and nickel cations through SLM and hybrid liquid membrane (HLM) have been experimented by Gega et. al. [134]. They have got best result in SLM. They have used di-2-ethylhexylphosphoric acid (D2EHPA) and Cyanex 272, 301, and 302 in kerosene as a LM. The separation efficiency of Co(II)/Ni(II) was higher in HLM than in SLM.

Yildiz et. al. [135] have separated cobalt and nickel from their acidic media by using SLM. They have used Alamine 308 as a carrier and tributylphosphate (TBP) as a modifier to improve the membrane performance.

Using SLM a comparative transport of cobalt and nickel with different ratio has been studied by Surucu et. al. [136]. They have calculated separation factor of equimolar and nonequimolar feed mixture (i.e. mixture of nickel and cobalt). They have used chloroform as a diluent and alamine as a carrier. Within 8 h of time they have

achieved 98.4% selective separation efficiency of cobalt.

Using bulk liquid membrane (BLM), Sing et. al. [137] have separated mixture of copper, nickel and zinc by varying feed metal ion concentration. They have used kerosene as a solvent with D2EHPA as a carrier. Mickler et. al. [138] have studied permeation of zinc, cadmium and nickel from its ammoniacal solution using 4-acyl-5-pyrazolones and β-diketones as a carrier. They have shown how permeation efficiency of solutes is affected by ammonia concentration.

Molinari et al. [139] have selectively removed copper from mixure of solute that contain copper, zinc, nickel and manganese using SLM. They have done comparative study of solute permeation efficiency with 2-hydroxy-5-dodecylbenzaldehyde (2H5DBA) and D2EHPA as carrier. They have also derived a transport model to calculate mass transfer co-efficient in the membrane.

Huang and Juang [140] have developed permeation rate mechanism of Zn(II) transport through diffusional mass transfer model using SLM technology. They have prepared LM by combination of D2EHPA and kerosene and H_2SO_4 as strip phase solution.

Separation of Zn(II) using SLM technology has been done by Takashi Saito [141]. Organic phase of SLM prepared by using 4,7-diphenyl-2,9-dimethyl-1,l0-phenanthroline (namely, bathocuproine) solution with dibenzyl ether as the carrier. The effects of the zinc ion concentration, anion, and carrier are determined, and a permeation velocity equation for the zinc ion through the membrane is proposed. The effects of types of carrier as well as of anions are also investigated.

In two separate work, Swain et al. [5, 142] have separated zinc with copper and cadmium using SLM process. LM was prepared by using TOPS-99 (D2EHPA) and kerosene. They have checked the effect of different anions *viz.* Cl^-, NO_3^-, SO_4^{2-}, CH_3COO^-, SCN^-, ClO_3^- on separation of zinc with copper and cadmium.

Hollow fiber membrane contractor is used by Urtiaga et al. [143] to separate Zn(II) and Fe(III) from Cr(III) spent passivation bath. LM consisting of Cyanex 272,

kerosene and 1-decanol are used in hollow fiber membrane contractor. Different proportion of HCl and H_2SO_4 are used as stripping agents. Different operational variables on kinetics of the separation of Zn(II) and Cr as well as on the enrichment of Zn(II) over iron and Cr in the stripping phase was investigated.

Winston et al. [144] have used three separate SLM technologies for separation of Cu, Zn and Ni. For Cu removal organic phase is prepared by LIX 973N, ketoxime, dodecanol, n-dodecane at different proportion and for removal of Zn organic phase prepared by Cyanex 301, dodecanol, n-dodecane with different percentage, whereas, for separation of Ni organic phase is prepared by di(2-butyloctyl) monothiophosphoric acid (C12 MTPA), dodecanol and n-dodecane. For all three cases they have used H_2SO_4 as stripping agent.

Selective transport of Zn(II) and Co(II) has been performed by Alguacil and Alonso [145] using SLM technology. They have used three different diluents such as Solvesso 100, Escaid 100, Iberfluid and toluene with DP-8R (also known as D2EHPA) as a carrier. They have also optimized different physico-chemical parameters form maximizing metal transport rate.

Marchese et al. [146, 147] have applied SLM technology for separation of Co(II), Ni(II) and Cu(II). They have used kerosene as solvent for its low solubility in water, high surface tension and low volatility. Two different carriers *viz.* D2EHPA and Alamine 336 have been used.

Kulkarni et al. [148] have studied stability of ELM *i.e.* swelling and breakage of the emulsion during transport of Ni(II) ion. The LM they have prepared using D2EHPA as a carrier with mixed xylene isomers, heptane, toluene and dodecane as a diluents.

Using SLM technology Ali et al. [149] have extracted and recovered Zn(II) simulated wastewater. They have used tri-ethanolamine (TEA) as a carrier with cyclohexanone as a solvent to prepare organic phase. They have studied different parameters affecting Zn(II) transport. The extraction efficiency of Zn(II) was found to be 87% in 120 min.

Stirred transfer cell-type ELM contactor has been used by Valenzuela et al. [150] for recovery of Zn(II) from an acidic mine drainage water. The have used D2EHPA, kerosene and H_2SO_4 as a carrier, solvent and internal phase respectively in ELM. Different parameters affecting transport of Zn(II) have been studied. Ma et al. [151] has selectively separated copper and nickel ions from calcium ions. They have used two stage ELM process to selectively separate copper and nickel ions. They have used Cyanex 301 carrier with LIX984N as a solvent.

Sulaiman et al. [152, 153] have removed nickel from industrial wastewater using SLM. They used D2EHPA, octanol and palm-oil as carrier, synergist and diluent respectively. The parameters have been optimized using Box-Behnken design (BBD). They have applied that optimized condition for further removal of nickel using palm oil as diluent.

Simultaneous extraction and separation of cobalt and nickel from chloride solution is studied by Hachemaoui and Belhamel [154] using ELM. They have first optimized different parameters such as effects of extractant and surfactant concentrations, mixing speed, concentration etc. to separate cobalt and using that optimum condition extraction of cobalt in competition with nickel has also been studied.

Using BLM Vergel et al. [155] have separated nickel from natural water. They have used 1,2-cyclohexanedione bis-benzoyl-hydrazone (1,2-CHBBH) as a carrier with toluene/dimethyl formamide. Also, they have optimized different chemical and hydrodynamic conditions for separation of nickel.

1.2.3 LM Based industrial applications

LM based technology has large scope of commercialization for separation of organic and inorganic solute with high treatment efficiencies. Some researchers have separated gases by using hollow-fiber-contained-liquid membrane (HFCLM) at large scale. HFCLM has been to used to separate CO_2 and CH_4 or N_2 from their mixture using diethanolamine (DEA) [156]. LM technology was first commercially developed

and implemented in 1986 in Austria. The application was to separate Zn(II) from textile plant effluent, that can treat up 75 m^3/h of zinc-bearing wastewater. The Zn(II) removal efficiency was greater than 99.5% [157, 158]. Three more ELM based industrial plant for recovery of Zn(II) located at (i) Glanzstoff, AG, Austria, with a capacity of 700 m^3/h; (ii) CFK Schwarza, Germany, with a capacity of 200 m^3/h; and (iii) AKZO Ede, the Netherlands, with a capacity of 200 m^3/h [30, 157–159]. Another industrial application of phenol removal using ELM technology has been successfully installed in China. The capacity of the plant treating 0.5 tons/h of a solution with a phenol content of 100 mg L^{-1}. The pH of wastewater was kept below 9 to get phenol in nondissociated form. Plant used NaOH as internal agent and phenol removal efficiency was 99.5% [90, 157]. Many other pilot plants are installed in metallurgical industries to treat effluent for recovery of metals, such as zinc, cadmium, lead, iron, copper, cobalt, nickel, manganese, magnesium, calcium and sodium [30, 160]. The U.S. Bureau of Mines was field tested to use of ELM technology for extraction of Cu from mine wastewater [161]. Alonso et al. [162] have performed experiment with two HFM modules in pilot plant to separate Cr(VI) from a galvanic process wastewater. The experimental results have been used as a case study for the simulation and experimental analysis of the nondispersive solvent extraction process. A commercial-scale hollow fiber extraction system has been develpoed by Seibert and Fair [163] to separate hexanol from water. A scale-up of hollow fiber reactor has been developed by Reiken and Briedis [164] for biomedical application. Hence, there is huge scope for LM technology to commercialize in different fields like wastewater treatment, biotechnological and biomedical applications, hydrometallurgy and separation of organic acids.

1.3 Gap areas

Extensive literature search on the field of LM based separation of heavy metals has been carried out prior to setting the objectives of the thesis. Few gap areas have been identified especially in the last ten years of published literature.

1. Organic solvents are most commonly used as solvents in the LM. Organic solvents are efficient but themselves are toxic in nature. They are potential to increase secondary pollutant in the already unhealthy effluent.

2. Most of the literature aims at purifying the water by removing the heavy metals, however they do not clearly identify what to do with the metal salts which are recovered in the stripping phase. Hence, the stripping phase again becomes full of pollutants no where to dispose.

3. In industrial effluent seldom more than one metals are present *viz.* Ni(II) and Zn(II) with varying ratios in effluent. Very few research works have been published with combinatorial separation of heavy metals from wastewater using conventional organic solvents [137, 165].

This thesis addresses the above issues at its core.

1.4 Importance and objective of the research work

Conversion of liquid waste to solid waste and/or as an useful end product is a hugely beneficial proposition for waste management. It can be a reasonable objective to precipitate heavy metals in strip phase towards useful end product. Synthesis of nanoparticle by converting heavy metal from wastewater in strip phase would be most sensible solution for mitigation of heavy metals.

The overall aim of this thesis is to establish a LM based technique for extraction

and recovery of Cr(VI), Ni(II) and Zn(II) from the industrial effluents in an environmentally and physiologically benign method which would minimize the production of secondary pollutant. To fulfil this overall aim, thesis finds the following measurable objectives:

- ✓ Identification of low cost, easily available and environmentally benign solvent that can extract solutes (heavy metals) from their aqueous solution by two phase equilibrium study. Potential candidate can be found among the vegetable oils such as coconut oil, mustard oil, sesame oil, soybean oil and sunflower oil.
- ✓ Identification of suitable carrier compounds (*i.e.* extractant) or more precisely a suitable solvent-carrier combination that enhances the extraction of solute from the aqueous phase.
- ✓ Identification of the best operating condition in terms of feed phase pH, initial concentration of feed phase and concentration of carrier which would yield best extraction of solute(s) in two phase extraction study.
- ✓ Identification of suitable stripping agent that ensures re-extraction of solute from the membrane phase to the aqueous strip phase through a three phase BLM study.
- ✓ Identification of the best operating condition in terms of feed phase pH, initial concentrations of feed phase, concentration of strip phase, pH of strip phase and concentration of carrier which would yield best separation of solute(s) in a BLM unit.
- ✓ Development of efficient recovery strategies and stripping conditions so as to enhance the extraction and recovery of the selected metals, so that some value added components may be produced out of the heavy metals in the stripping phase which would be useful for an end-user. This objective may further be achieved through the following two pathways:

- Synthesis of useful nanoparticle from recovered heavy metal by electro chemical process.
- Electrodeposition of metals in stripping solution by employing electric potential that can generate useful electroplated product.

✓ Perform experimental optimization of the LM process with the help of standard statistical methods that would ensure best operating condition of influential parameters affecting the LM process.

Chapter 2

Materials and Methods

This chapter includes the details of various materials used for experimental purpose and different sources from where the materials were procured. The detailed description of analytical instruments and characterization techniques used in the experiments are discussed here. The two types of LM setup (BLM and FS-SLM) have been used in this work. Elaborate study of experimental procedure of metal transport through both LM configuration are discussed here.

2.1 Chemicals and reagents

Different materials used for extraction and recovery of Cr(VI), Ni(II) and Zn(II) along with their sources are summarized in this section. All chemicals and reagents used for the experimentations were of Guranteed Reagents (a.k.a GR) grade. The stock solutions (aqueous) were prepared by using Milli-Q® deionized water (Millipore, USA). The wastewater was synthesized inside the lab using analytical grade potassium dichromate ($K_2Cr_2O_7$), nickel chloride hexahydrate ($NiCl_2$,$6H_2O$) and zinc sulfate heptahydrate ($ZnSO_4$,$7H_2O$). Analytical grade $NiCl_2.6H_2O$ and $ZnSO_4.7H_2O$, were purchased from Merck® India. Selection of strippant is an important factor, as it is directly related to the recovery of solute. Strippants, *viz.*, Na_2-EDTA, sodium chloride (NaCl), ammonium chloride (NH_4Cl), sodium hydroxide (NaOH), hydrochloric acid

(HCl, 37%) and sulphuric acid (H_2SO_4, 98%) were supplied by Merck® India. The extractants Aliquat 336, TOA and TBP were procured from Sigma Aldrich®(India) and D2EHPA was purchased from Merck® India. Standard AAS solution of 1000 mg L^{-1} (traceCERT®) of various metals *viz.* Cr(VI), Ni(II) and Zn(II) were purchased from Sigma Aldrich®(India). Refined vegetable oils, viz. mustard oil, coconut oil, soyabean oil and sunflower oil, of good quality (Fortune®, Adani Wilmer Limited India) were procured from local market. Polymeric support for SLM with support material polyvinylidene difluoride (PVDF) was procured from Merck® India. The physical properties and characteristics of PVDF membrane are tabulated in Table 2.1.

Table 2.1: Characteristics of membrane support.

Specification	Value
Support material	PVDF
Pore size, d(μm)	0.22
Thickness, L(μm)	88.5
Porosity, (ε)	0.30
Tortuosity, (τ)	5.6

2.1.1 Working solutions for pollutants

Stock solution (1000 mg L^{-1}) of pollutants were prepared by dissolving required amount of salt ($K_2Cr_2O_7$ for Cr(VI), $NiCl_2$,$6H_2O$ for Ni(II) and $ZnSO_4$,$7H_2O$ for Zn(II)) in Milli-Q® deionized water inside a 100 mL volumetric flask and then transferring it to a 1 L volumetric flask, filling it up to the 1 L mark with Milli-Q® deionized water and storing it for further use, as and when required. In a similar manner, the strip phase was prepared by dissolving the required amount stripping agent in Milli-Q® deionized water. The organic phases were prepared by mixing

appropriate amount of extractant (in % (v/v)), in 20 mL of various pure solvents (vegetable oils).

2.2 Analytical instruments

2.2.1 Atomic Absorption Spectroscopy (AAS)

Concentrations of Cr(VI), Ni(II) and Zn(II) in aqueous samples were measured by Atomic Absorption Spectroscopy (or AAS, in abbreviation)(Make: Varian Australia, Model:AA240FS) using hollow cathode lamp in flame mode with acetylene as fuel and air as support. The instrument is operated by Spectra AA software. The lamp specification of different metals are tabulated in Table 2.2. The calibration curve of standard sample with its equation for different metal from AAS are reported in Figure 2.1. The samples were collected directly from experimental runs and measured in AAS without any further processing. All the individual experiments were repeated thrice. Working principle and analysis procedure of standards and samples in AAS are incorporated in Appendix A.

Table 2.2: Working condition of different lamp.

Metal	Lamp current (mA)	Wave length (nm)	Slit width (nm)
Cr	7	357.9	0.2
Ni	4	232	0.2
Zn	5	213.9	1.0

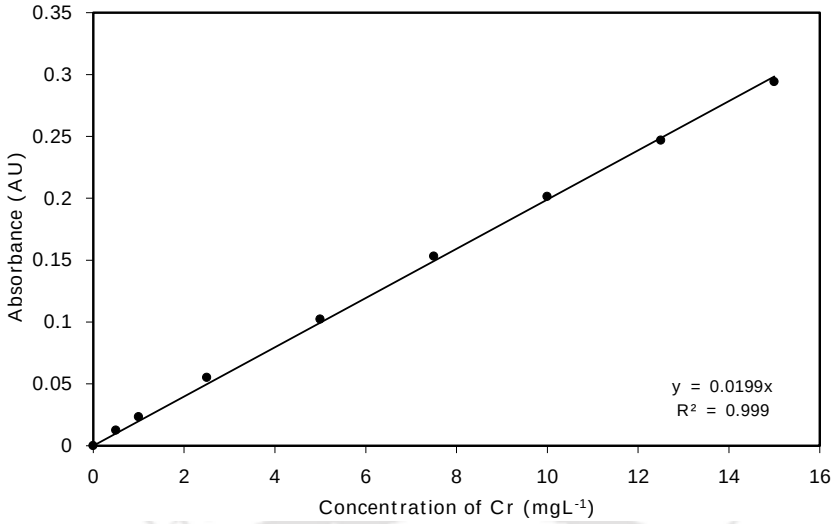

(a) Calibration curve of Cr(VI)

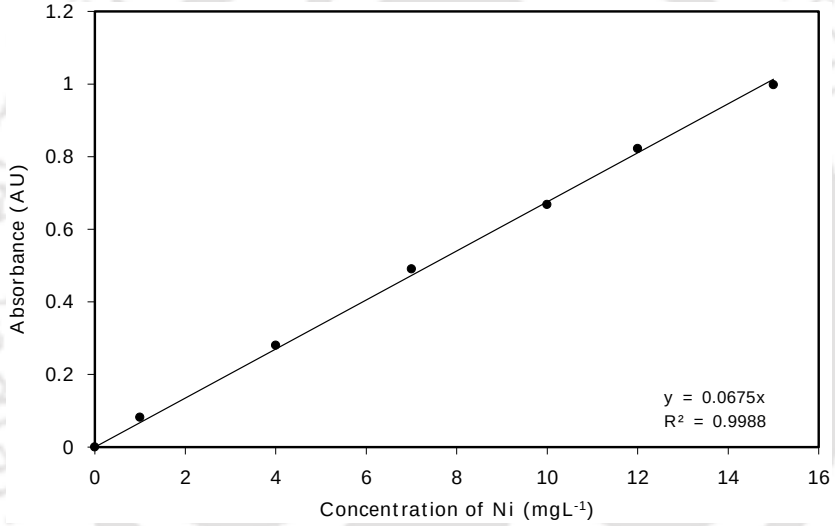

(b) Calibration curve of Ni(II)

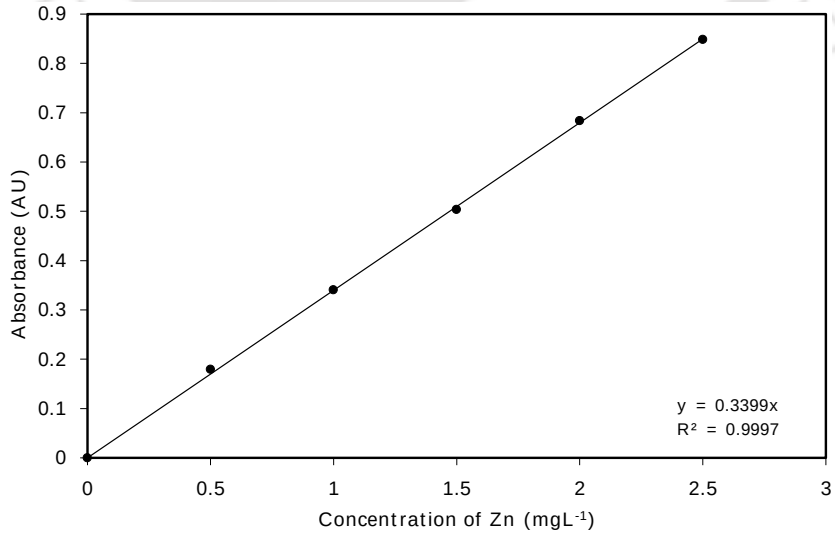

(c) Calibration curve Zn(II)

Figure 2.1: Calibration curves for analysis of different metal

2.2.2 Other analytical instruments

A digital pH meter (Make: Eutech Instruments, Model: EUTECH pH700) was used to measure pH of aqueous solutions. A shaking incubator (Make: Daihan Labtech Co. Ltd., Model: LSI 3016R) was used for enhancing mass-transfer between aqueous and organic phases during two phase equilibrium studies. For measurement of surface tension and interfacial tension of various vegetable oil, a tensiometer (Make: M/S Kwoya, Japan, Model No.: DY300) was used. Morphology of PVDF membrane support and synthesized nanoparticle were done using Field Emission Scanning Electron Microscope (FESEM) (Make: Zesis, Model: Sigma). For elemental analysis Energy-dispersive X-ray spectroscopy (EDX) in FESEM which confirmed the deposition of metal on cathode plate and EDX in transmission electron microscopy were used to confirm the Cr percentage in synthesized sample. TEM was used for particle size analysis of synthesized nanoparticle. X-ray diffraction (XRD) (Make: Rigaku, Model: SmartLab) was used to check crystallinity of particular complex with average particle size. The infrared spectra of synthesized nanoparticle was recorded by using an IR Affinity-1 (Shimadzu corp.) infrared spectrophotometer.

2.3 Physical properties of vegetable oils

As discussed in Section 1 viscosity of vegetable oil plays a major role in diffusional transport of solute through LM. All the experiments have been done at room temperature. The viscosity of various vegetable oils were checked at 25°C and tabulated in Table 2.3 which reveals that $\mu_{\text{Mustard}} > \mu_{\text{Soybean}} > \mu_{\text{Sesame}} > \mu_{\text{Sunflower}} > \mu_{\text{Coconut}}$. Surface tension and interfacial tension of vegetable oils with respect to Milli-Q® deionized water are tabulated in Table 2.4. These are important properties of LM to transport solutes. The surface tension and interfacial tension are measured by tensiometer at room temperature.

Table 2.3: Viscosity of various vegetable oil at 25°C.

Vegetable oil	Viscosity (Pa s)
Mustard oil	0.0583
Soybean oil	0.0418
Sesame oil	0.0392
Sunflower oil	0.0358
Coconut oil	0.0310

Table 2.4: Surface tension and interfacial tension of various vegetables oils.

Name of the sample	Surface tension at 25°C, mN m^{-1}	Interfacial tension (oil and water), mN m^{-1}
Water (Milli-Q® deionized water)	72.8	-
Mustard oil	35.7	24.8
Soybean oil	32.9	22.1
Sesame oil	33.58	17.7
Sunflower oil	33.89	16.2
Coconut oil	31.5	13.9

2.4 Two phase equilibrium set-up and procedure

Aqueous solutions for the two phase equilibrium studies were prepared by diluting the stock solutions appropriately and working with various concentrations of solute (*i.e.* Cr(VI), Ni(II) and Zn(II)). Equal volumes of aqueous and organic solutions (20 mL each) were taken inside a conical flask, placed on the shaking incubator, and mixed at high speed (in rpm) for sufficient period in order for it to reach equilibrium. The mixture was then kept undisturbed for 8 h so that the aqueous and organic phases could separate due to difference in their densities. The samples were carefully collected from aqueous phase. The concentration of solute in the aqueous sample was

measured in AAS. The quantity of metals transferred to the organic phase during the extraction was calculated by mass balance. All the experiments were carried out at room temperature (25°C).

2.5 Three phase experimental studies with BLM

The schematic of the BLM setup which consists of cubical shaped container with magnetic stirring facility is shown in Figure 2.2. The actual BLM setup used in this research work for the three phase experiments is shown in Figure 2.3. The container is divided into two equal volume leak proof compartments by fixing a thin glass plate in the middle of them. A leak test with coloured water was carried out in order to ensure that the compartments were truly leak proof. Feed and strip phases (65 mL each) were placed inside the two compartments leaving sufficient clearance up to the top edge of the glass barrier. The organic phase (30 mL), being lighter than aqueous phases, was then poured over both the aqueous phases with great care up to slightly above the top edge of the glass barrier so that the organic phase physically connects the two aqueous phases. A bridge is thus formed between the aqueous phases to transfer solute through diffusion via organic phase.

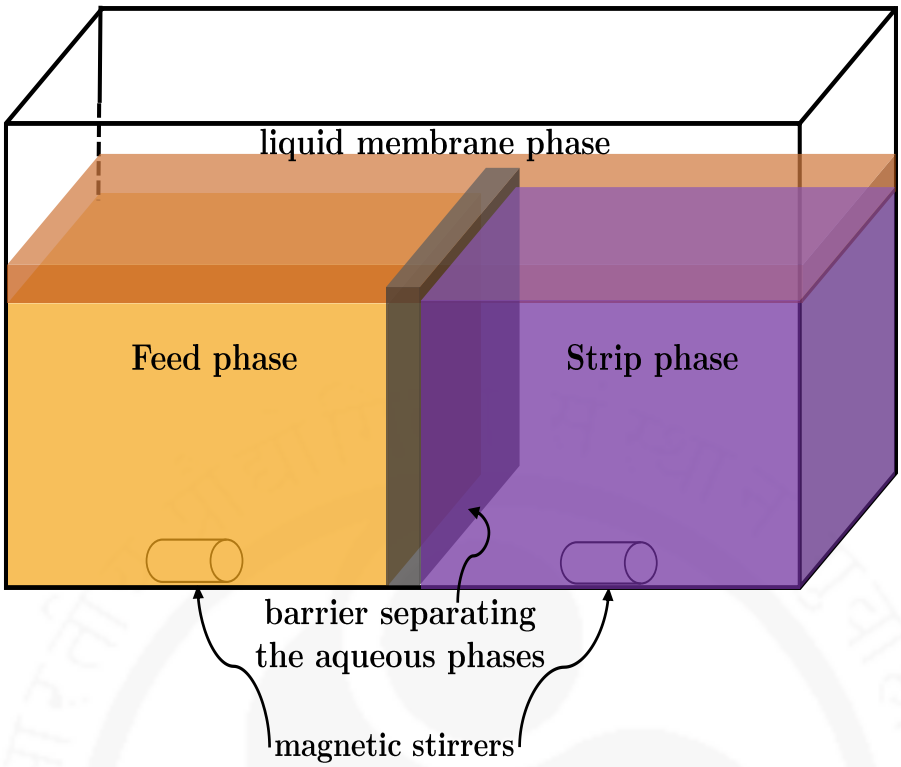

Figure 2.2: Schematic of BLM setup

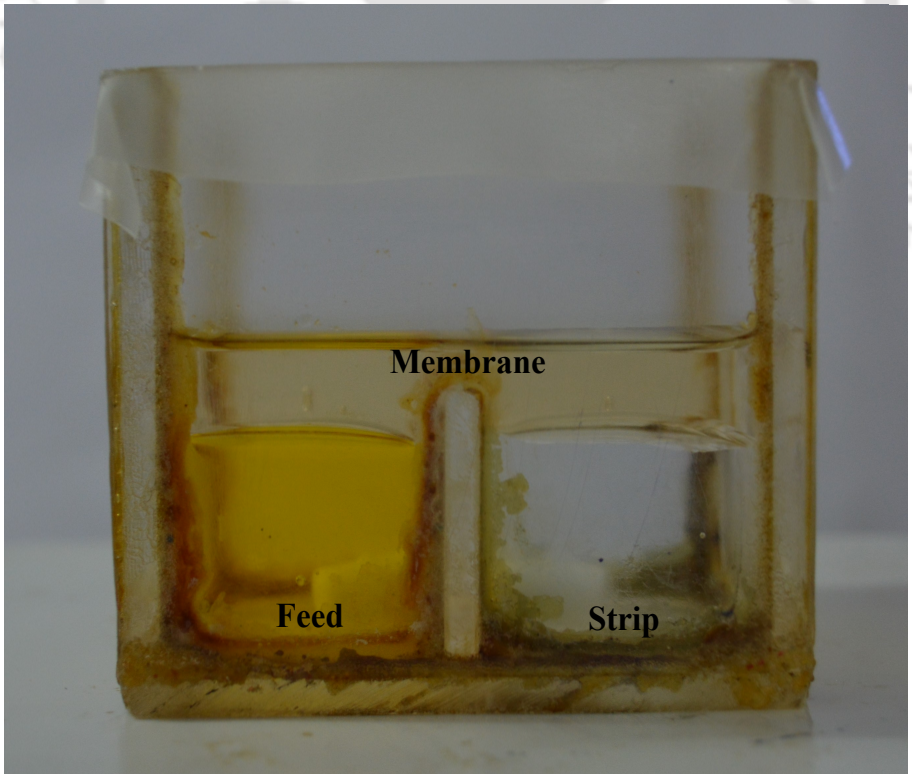

Figure 2.3: Three-phase BLM setup

2.6 Three phase experimental studies with FS-SLM

Different types of SLM configuration such as flat sheet, hollow fiber, spiral wound, etc. have been discussed in Section 1. Among these configurations, the simplest one is flat sheet supported liquid membrane (FS-SLM) which has been considered for this research work. The SLM setup along with its working procedure are described in the consecutive sections.

2.6.1 FS-SLM setup and experimental procedure

The experimental setup: The SLM setup consists of two cylindrical shaped containers (internal diameter 50 mm and height 90 mm) joined by flanges (vide the schematic in Figure 2.4). The actual SLM setup used in this research work for the three phase experiments is shown in Figure 2.5. The effective volume of either cylindrical vessel is 130 ml. Contents of the vessels were stirred by two mechanical stirrers (Make: Remi, Model: RGQ 121/D). The diameter of the membrane disc was 47 mm and the effective surface area of the membrane in contact with each aqueous phase was 11.3 cm^2.

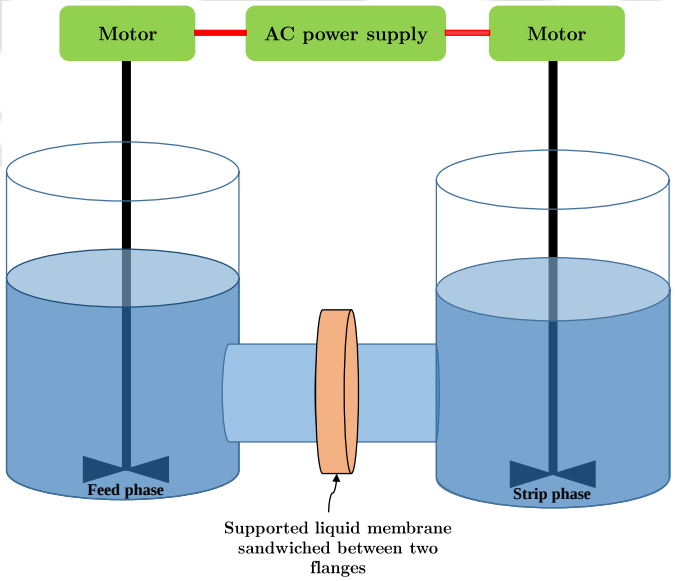

Figure 2.4: Schematic of SLM setup

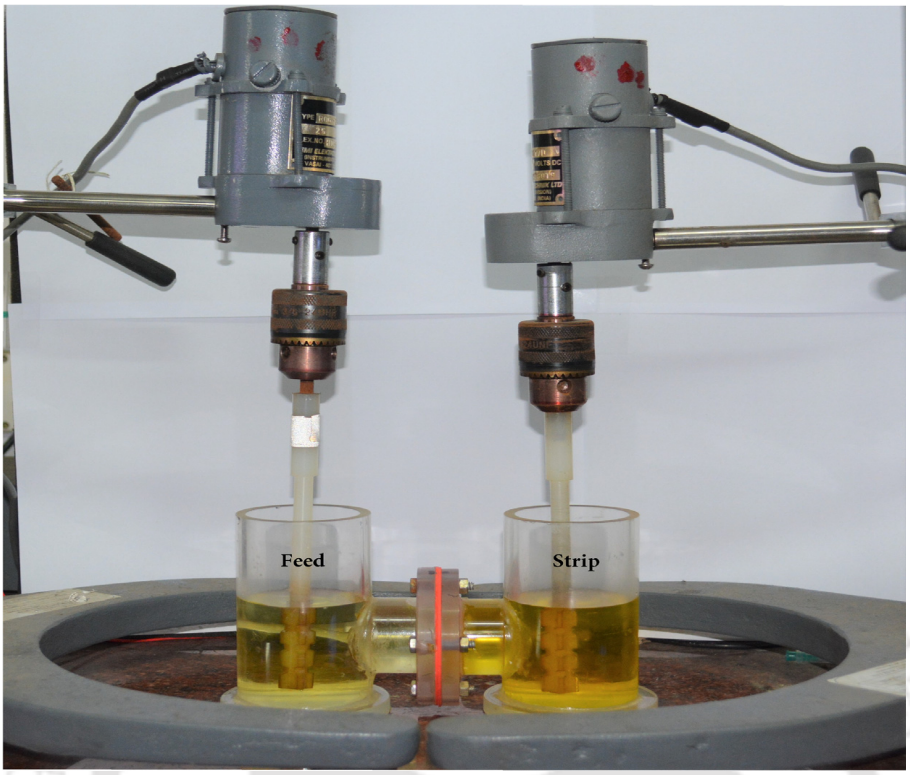

Figure 2.5: Three-phase SLM setup

Preparation of SLM: Pores of the solid polymeric support (PVDF membrane) were filled with organic phase by dipping the PVDF membrane in the organic phase for 24 h. The characteristics of PVDF membrane is already discussed in Table 2.1. The impregnated membrane was taken out of the organic phase and kept in a vacuum desiccator for 1 h. The excess amount of organic liquid on the surface of membrane was removed gently by a tissue.The prepared organic impregnated membrane support would act as the desired SLM. It was gently clamped between the two flanges of the cylindrical vessel. All the studies were conducted at room temperature. Figure 2.6 shows the field emission scanning electron microscopy (a.k.a FESEM) analyses of membrane support before and after the SLM experiment. Figure 2.6a shows the image of dry membrane support and Figure 2.6b shows impregnated membrane support. The empty pores are clearly visible in Figure 2.6a whereas pores are filled with solvent in Figure 2.6b. Figure 2.6c shows the same membrane support after

completion of 48 h experimental run and it reflects the loss of some solvent from the surface of the membrane support. Figure 2.6d shows the cross sectional view of membrane support after completion of 48 h experimental run.

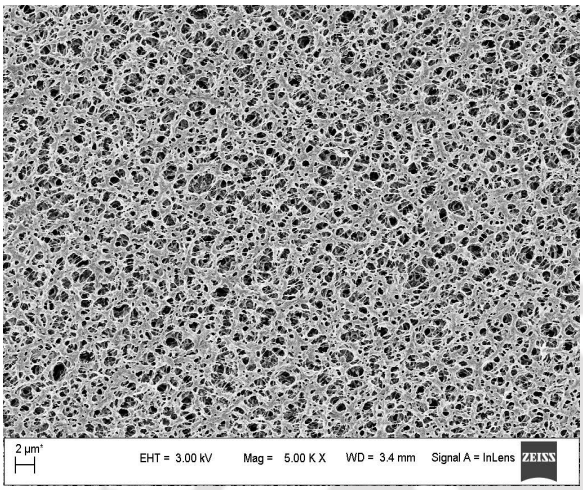

(a) Before LM impregnation on support

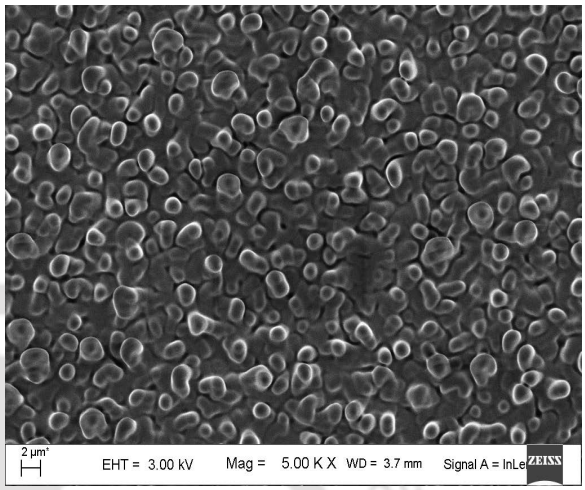

(b) After LM impregnation on support

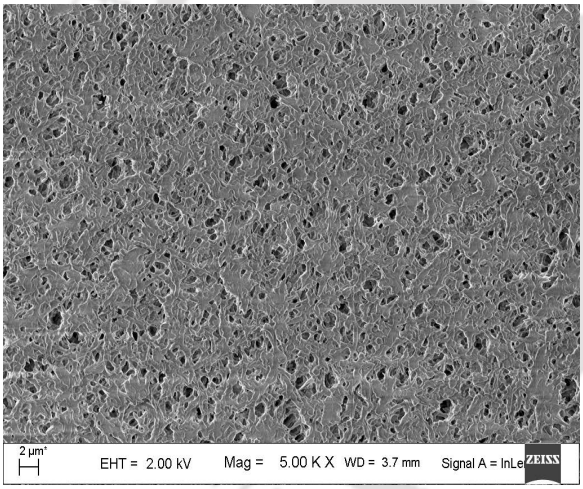

(c) Support with LM in the pores after 48h run

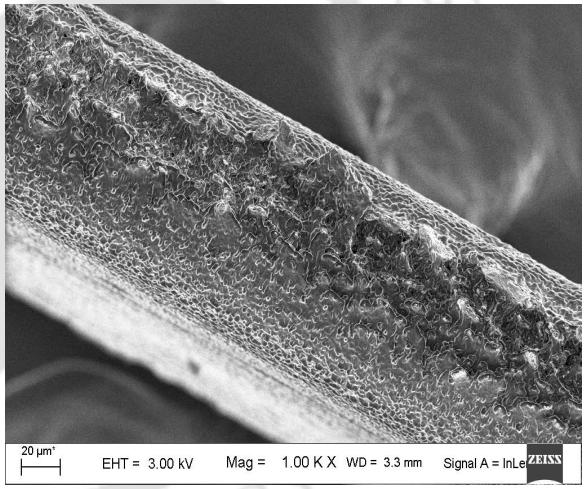

(d) Cross sectional view of the support with LM in the pores after 48h run

Figure 2.6: FESEM analysis of PVDF membrane support

2.6.2 FS-SLM setup with electrochemical and electrodeposition module

In order to augment the electrochemical/electrodeposition features in the SLM, a minor adjustment has been done in the SLM unit which has been shown through

schematic in Figure 2.7. Actual FS-SLM setup with *in situ* electrochemical reaction or electrodeposition module used in this research work for the three phase experiments is shown in Figure 2.8. Separate image of stripping sections of experimental setup has been shown in Figure 2.9. The effective membrane area is 706.85 mm^2. For electrochemical reaction two electrodes (one iron plate as anode another graphite rod as cathode) were kept inside strip phase solution. The distance between the electrodes was ∼4 cm. The electrodes were connected to a DC voltage source for supplying electric potential.

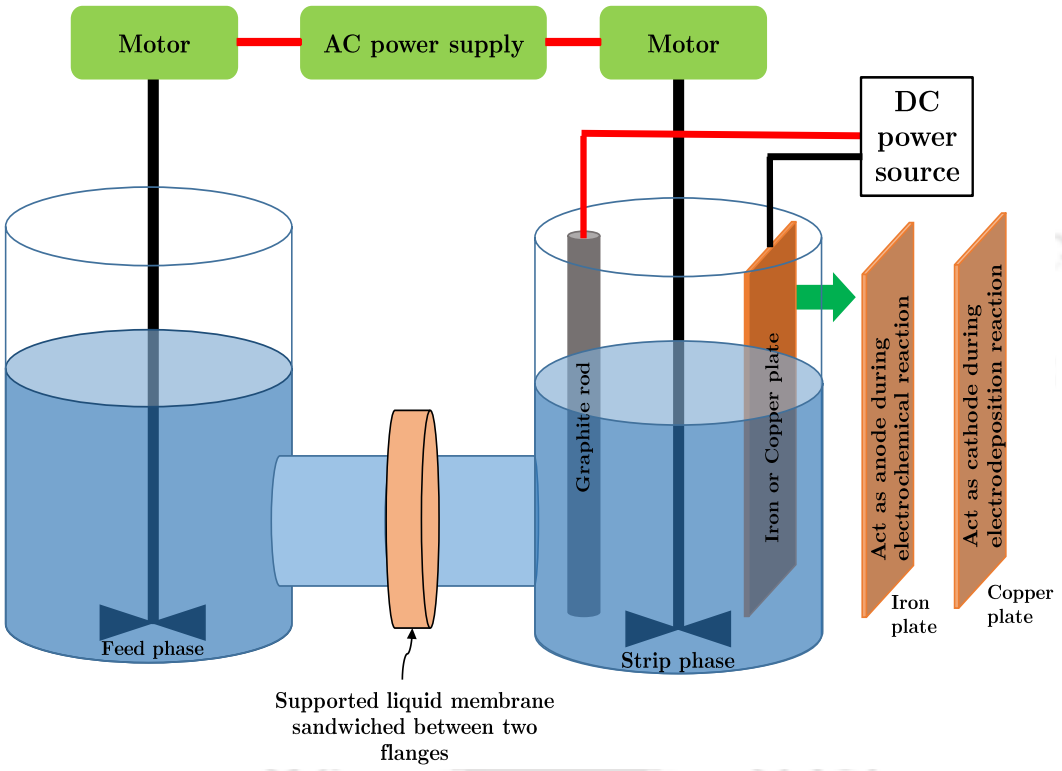

Figure 2.7: Schematic of FS-SLM setup with electrochemical or electrodeposition module

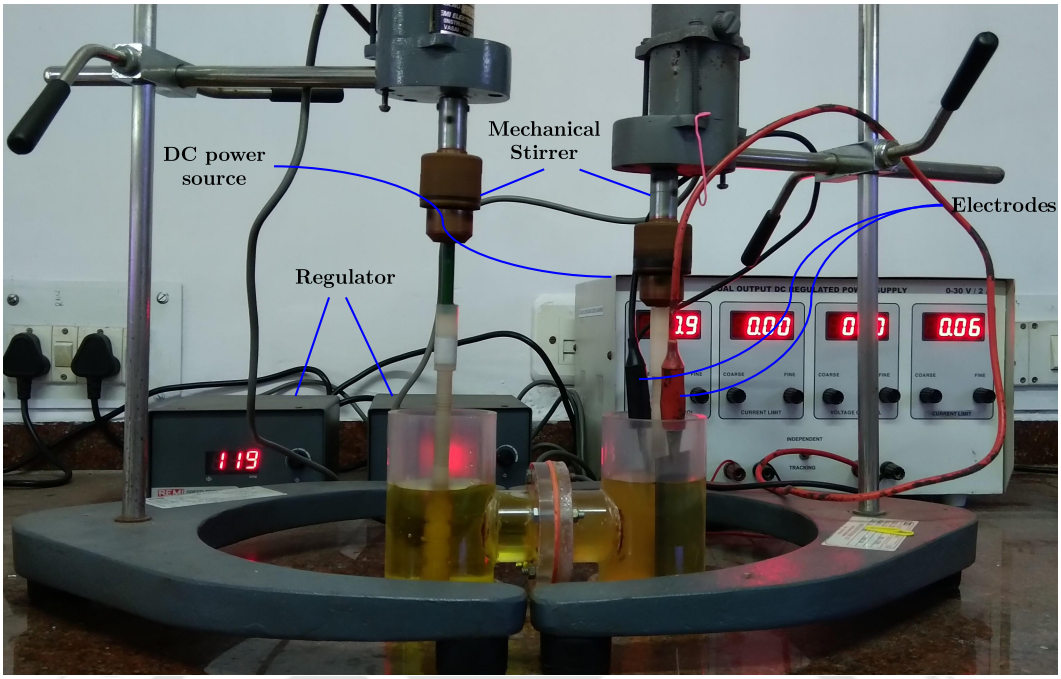

Figure 2.8: Experimental setup of FS-SLM with electrochemical or electrodeposition module

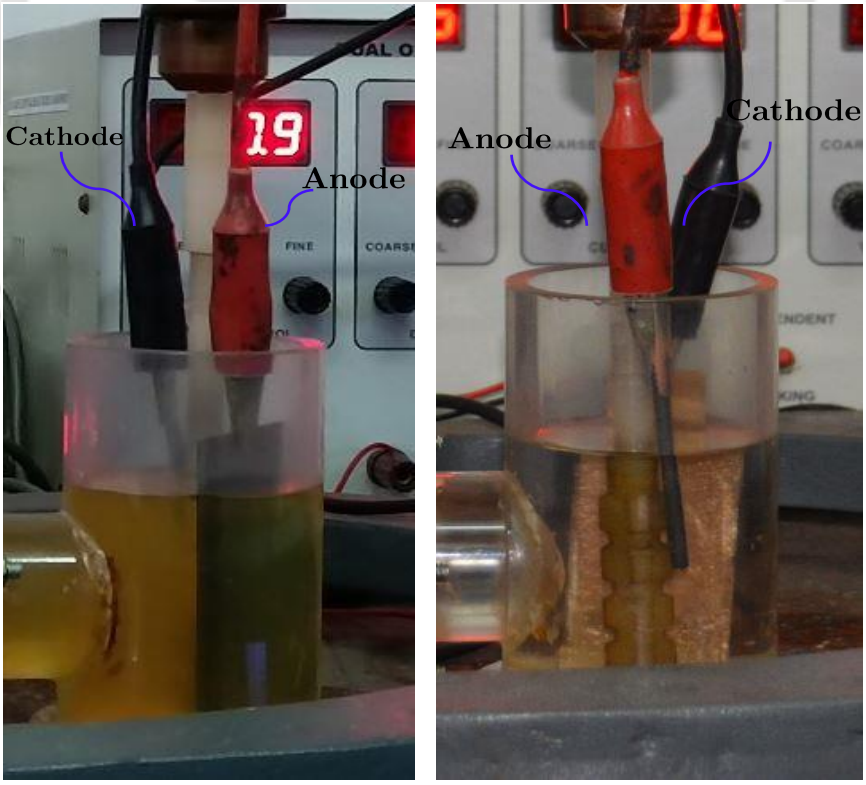

During electrochemical reaction **During electrodeposition reaction**

Figure 2.9: Arrangement of strippping section in FS-SLM setup

2.7 Model calculation

The following equations are used to calculate two phase equilibrium (2.1) and the three phase transport performance by measuring the feed and strip phase concentration of metal in terms of % extraction and % recovery:

$$\%\text{Extraction} = \frac{C_{f_{in}} - C_f}{C_{f_{in}}} \times 100 \tag{2.1}$$

$$\%\text{Recovery} = \frac{C_s - C_{s_{in}}}{C_{f_{in}}} \times 100 \tag{2.2}$$

where, $C_{f_{in}}$ and C_{sin} are the initial concentrations of solute in feed and strip phases respectively. C_f and C_s are the concentrations of solute in feed and strip phases respectively at any point of time of collecting the sample. The measurement of efficiency of solute precipitation/deposition in strip phase is difficult by weighing method. So, It was done indirectly from the feed phase and strip phase concentrations, taking the assumption that at the time of experiment no metal was trapped inside membrane phase. Following equation is used to calculate %precipitation or %deposition of heavy metal in strip phase.

$$\%\text{Precipitation/Deposition} = 100 \times \left\{ \frac{(C_{f_{in}} - C_f) - C_s}{C_{f_{in}}} \right\} \tag{2.3}$$

2.8 Experimental optimization through RSM

Nowadays statistical tools are frequently used for optimization techniques to reduce time and wastage of materials. Response surface methodology (RSM) is one such useful tool that is used for optimizing the operating parameters and to improve performance of processes. RSM mainly has three steps, *viz.* design of experiments, response surface modelling through regression and optimization. The objective of

RSM is to find out optimum response which is influenced by several independent variables (input variables) or region where it satisfies the operating conditions [166, 167]. Central composite design (CCD) rule has been used to design and evaluate the interactive effects of experimental variables. The total number of experiments N can be found through the following equation:

$$N = 2^k + 2k + n_c \tag{2.4}$$

where k is the number of variables and n_c is the number of central points. The statistical model helps to find out the important factors as well as most significant factor. It also helps to determine whether the experimental results are meaningful. The following quadratic model is used in this work [168–171].

$$y = \beta_0 + \sum_{i=1}^{k} \beta_i x_i + \sum_{i=1}^{k} \sum_{j=1}^{k} \beta_{ij} x_i x_j + \sum_{i=1}^{k} \beta_{ii} x_i^2 + \varepsilon \tag{2.5}$$

where β_0 is a constant, ε is error, x_i and x_j represents independent variable, and β_i, β_{ii} and β_{ij} are coefficients for linear, quadratic, and interaction effects respectively. Analysis of variance (or commonly abbreviated as ANOVA) is one of the most powerful statistical techniques that can be used to test the hypothesis that the means among two or more groups are equal, under the assumption that the sampled populations are normally distributed. ANOVA and residual analysis (abbreviated as RA) were used to verify the quadratic model. Comparing the respective co-efficient values of model variables it is possible to find out the interaction among the model variables. Positive coefficient symbolizes a synergistic effect and negative coefficient indicates an antagonistic effect [172]. A detailed account of the RSM procedure is given in the Appendix D. Design Expert software (Version 7.0) has been used for the above purpose.

Chapter 3

Separation of Cr(VI) through BLM and SLM

This chapter includes the theoretical background, results and discussion on transportation of Cr(VI) through BLM and SLM. The primary goal of this work is to explore the possibility of using environmentally benign solvent in a liquid membrane setup in order to separate hexavalent chromium from industrial effluent and perform experimental optimization of its parameters for maximum performance. Vegetable oils have been used for this purpose as they have the capability of extracting heavy metals and they are well known for their biodegradability too. Additionally an extractant N-methyl-N,N,N-trioctylammonium chloride (a.k.a. aliquat 336) has been used to enhance the efficiency of separation as it showed very good carrier property for transport of Cr(VI). Di-sodium ethylene-di-amine-tetra-acetic acid (or Na_2-EDTA) was selected as stripping agent for its affinity towards metal. The efficiency is affected by various physico-chemical parameters which have been optimized for best transport of solute.An initial two-phase study followed by elaborate three-phase bulk liquid membrane study were confirmed by critically more industry-friendly supported liquid membrane study. The prime physico-chemical parameters affecting the system performance were identified for experimental optimization through response surface

methodology using central composite design rule. A regression model along with analysis of variance evaluates whether the chosen parameters were of good agreement with experimental results.

3.1 Theoretical background

3.1.1 Reaction mechanism

In this work di-sodium ethylene-di-amine-tetraacetic acid(hereafter abbreviated as Na_2-EDTA) was selected as a stripping agent and N-methyl-N,N,N-trioctylammonium chloride(a.k.a aliquat 336) has been used as the extractant. Na_2-EDTA is known for its sequester behaviour with metal (tendency to bind with metal ions) i.e. EDTA inhibits normal behaviour of metallic ion in combination with added materials, especially the formation of coordination compounds or chelates of metallic ions. The chromate ion may exist in the aqueous phase in different ionic forms such as $HCrO_4^-$, CrO_4^{2-}, $Cr_2O_7^{2-}$ and $HCr_2O_7^{2-}$. It would later be revealed in Section 3.2.1.5 that optimum value of pH, for extraction operation with 100 mg L^{-1} Cr(VI) aqueous solution, is 4.5. Few researchers [117, 173, 174] suggested that $HCrO_4^-$ ion dominates in the aqueous solution of 100 mg L^{-1} Cr(VI). The following is the reaction mechanism [173, 174] for different Cr(VI) species:

$$H_2CrO_4 \rightleftharpoons H^+ + HCrO_4^- \tag{3.1}$$

$$HCrO_4^- \rightleftharpoons H^+ + CrO_4^- \tag{3.2}$$

$$2HCrO_4^- \rightleftharpoons Cr_2O_7^- + H_2O \tag{3.3}$$

The exchange reaction:

$$R_4N^+Cl^-_{(org)} + HCrO_4^- \rightleftharpoons (R_4N^+, HCrO_4^-)_{(org)} + Cl^- \tag{3.4}$$

Figure 3.1 shows the reaction mechanism of LM operation. Metal oxide ion ($HCrO_4^-$) binds with aliquat 336 (expressed as $R_4N^+Cl^-$) and form solute-carrier complex(R_4N^+,$HCrO_4^-$) at the interface of feed membrane side. Due to concentration gradient solute-carrier complex diffuses through the membrane and get re-extracted by the stripping agent (Na_2-EDTA) to form Cr-EDTA complex at the strip membrane interface. Cr-EDTA complex thereby diffuses back to the bulk of the strip phase.

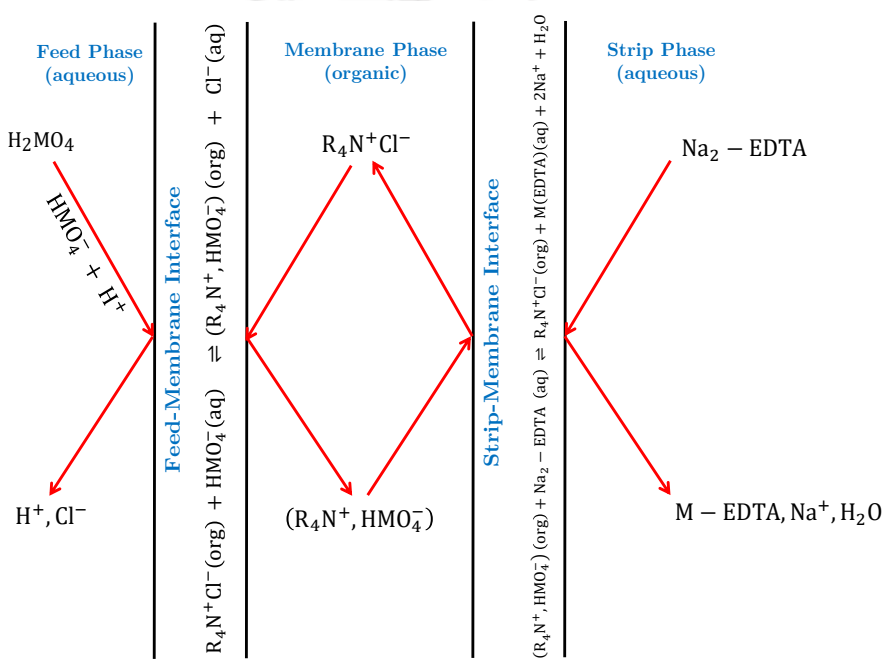

Figure 3.1: Reaction mechanism of three-phase BLM operation, M refers to metal (Cr in this study).

3.2 Results and discussion

3.2.1 Two-phase equilibrium study

As discussed in Section 2.4, the concentration of Cr(VI) varies in wide range depending upon the type of industries. For an example, tannery waste typically contains 80 mg L^{-1} of Cr(VI) in its effluent [175]. It is thus worth checking the concentration at which the efficiency of extraction of Cr(VI) is maximum. Hence the aqueous solution

for the two phase equilibrium study was prepared by diluting the stock solution appropriately and working with various concentration of Cr(VI) in the range of 50-400 mg L^{-1}. Two-phase extraction study has been performed as described in Section 2.4. For selection of suitable solvent with high efficiency of extraction (and/or separation factor). Dependency of efficiency upon various physical parameters were also examined. Effect of temperature on extraction of Cr(VI) had been studied at different temperature, *viz.* 25°C, 30°C, 35°C, 40°C, 45°C and 50°C. It is observed (refer Table 3.1) that effect of temperature on extraction is negligible in the above range of temperatures. Hence, all the experiments were performed at room temperature.

Table 3.1: Efficiency of extraction of Cr(VI) in two phase extraction process at various temperature

Temperature (°C)	Extraction of chromium (in %)
25	99.19
30	99.08
35	99.13
40	99.50
45	98.95
50	99.05

3.2.1.1 Selection of solvent

The criteria of ideal solvent are its immiscibility with aqueous phases, low viscosity, low volatility and high separation factor. Variety of vegetable oils, *viz.* coconut oil, mustard oil, sesame oil, soybean oil and sunflower oil, were tested for extraction purpose. Aliquat 336 [116, 176] had been added with these oils which would enhance the extraction. Results are shown in Table 3.2. All solvents yielded over 95% efficiency in extraction. However, viscosity plays an important role for diffusion too. Lower viscosity poses lower resistance to diffusion. The viscosity of vegetable oils, in

the decreasing order of their values, are mustard oil > soybean oil > sesame oil > sunflower oil > coconut oil. Hence coconut oil has lowest viscosity over other vegetable oils. Nevertheless, it has tendency to freeze at below 25°C. Thus the second best option, *i.e.* sunflower oil, along with aliquat 336 has been selected as the ideal solvent-carrier combination. Moreover efficiency of extraction of Cr(VI) is slightly better with sunflower oil than coconut oil. Cost of sunflower oil is lower than coconut oil but cost of soybean oil and sesame oil are almost same as sunflower oil.

Table 3.2: Efficiency of extraction of Cr(VI) in two phase extraction process using various vegetable oils.

Name of oil	Extraction of chromium (in %)
Coconut oil	95.91
Mustard oil	98.44
Sesame oil	99.72
Soybean oil	99.77
Sunflower oil	99.55

3.2.1.2 Effect of concentration of extractant

The experiments were carried out in absence of any extractant and it yielded only 20% efficiency in extraction. Hence presence of extractant is very much needed for extraction of Cr(VI). Extractant forms a solute-carrier complex which is more soluble and less viscous in the organic phase that eventually facilitates active transport of solute through LM in three phase operation. This is also known as carrier mediated transport. The subsequent experiments were carried out by varying the concentration of aliquat 336 in the range of 0-3% (vol/vol) with different initial feed concentration in the range of 50-400 mg L^{-1}. The results are shown in Figure 3.2. It is observed that increase in concentration of aliquat 336 (upto 1%) leads to an increment in efficiency of extraction and then it levels off (from 1% to 3%). Aliquat 336 reacts with Cr(VI) to form a Cr(VI)-aliquat 336 complex in the organic phase. Hence the

mass transfer across the aqueous-organic interface is enhanced by the complexation reaction. The efficiency attained an optimum at 1% (vol/vol) aliquat 336 which indicates that the complex had reached its saturation capacity. Further increase in concentration of extractant induces crowding effect [97, 98] in the solvent that reduces the complexation in the organic phase. It is further observed that the optimum extraction, at 1%(vol/vol) aliquat 336, for solution of initial feed concentration 50 mg L^{-1} is 99.5%. The optimum value is reduced to 99.08%, 98.32%, 97.94% and 96.26% for initial feed concentrations 100 mg L^{-1}, 150 mg L^{-1}, 200 mg L^{-1} and 400 mg L^{-1} respectively. Also it can be stated from the above observation that the rise in extractant concentration (from 1% to 3%) in organic phase can lead to enhancement of extraction efficiency for higher solute concentration (150-400 mg L^{-1}) due to availability of more solute for extraction at higher solute concentration. However in reality it did not happen (vide Figure 3.2) because increase in extractant concentration also increases viscosity of organic phase (vide Table 3.3).

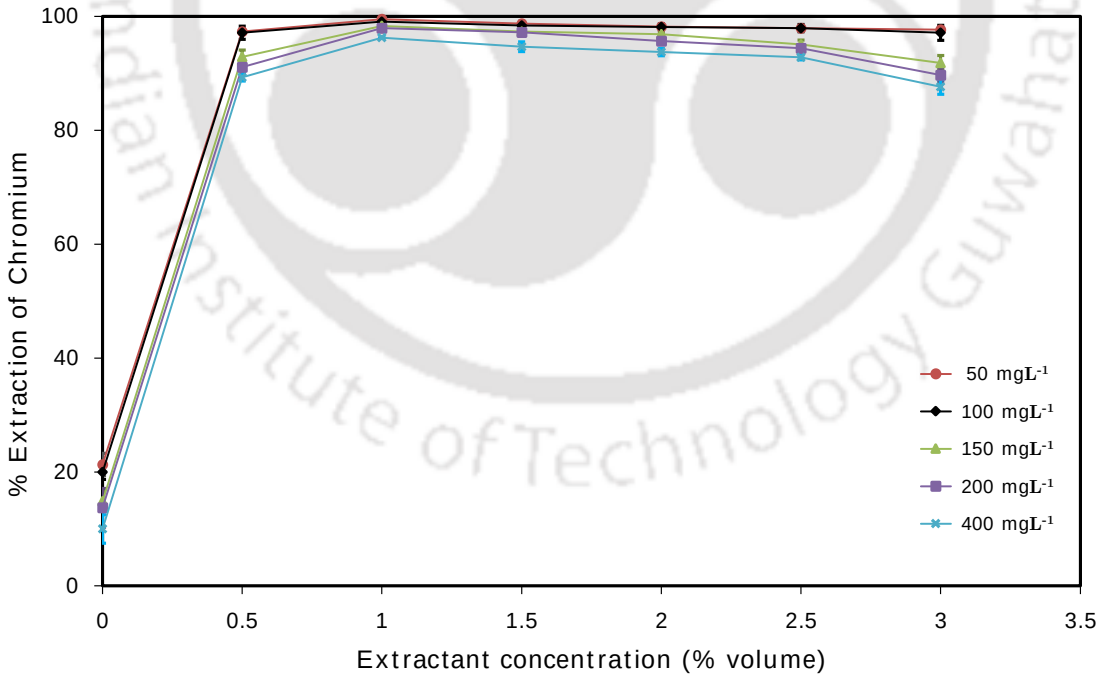

Figure 3.2: Efficiency of extraction of Cr(VI) in two phase extraction process at various concentrations of extractant in theorganic phase for various initial concentration of feed; solvent = sunflower oil.

Table 3.3: Viscosity of membrane phase with various concentrations of extractant in sunflower oil at 25°C.

Concentration of extractant (% volume)	Viscosity (Pa s)
1	0.0426
2	0.0481
3	0.0587

3.2.1.3 Effect of period of extraction

It is important to detect the period of completion of extraction and it is detected when the organic phase is completely saturated with Cr(VI) or its complex. The period of extraction indicates how much time one needs to allow for a batch of experimentations to reach its completion. It also indicates the residence time of material in a process vessel in industrial scenario where continuous operation is a norm. In this work a few experiments were initially performed for as long as 15-20 h. The results (vide Figure 3.3) indicate that the saturation point had been achieved much before 10 h. The duration of experiments were reduced gradually. It is observed that over 90% extraction had reached within one hour and over 99% at 10 h for upto 100 mg L^{-1} concentration of Cr(VI). In case of 150-400 mg L^{-1} of Cr(VI) over 80% extraction had reached within two hour and over 90% at 10 h. Therefore, the remaining two-phase studies are conducted for 12 h duration.

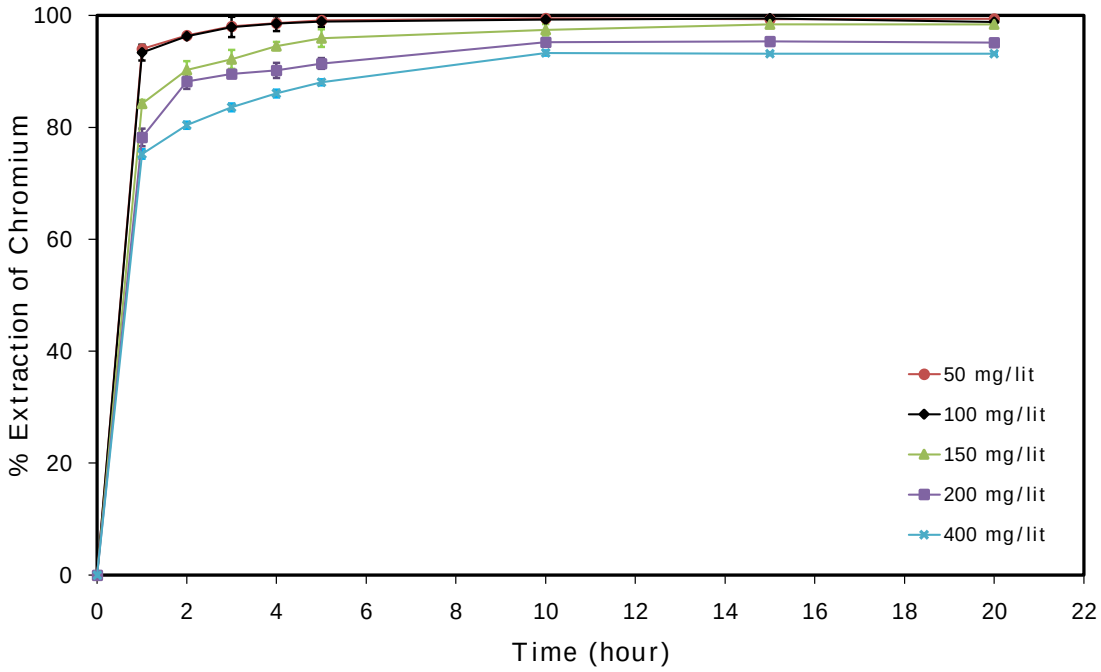

Figure 3.3: Efficiency of extraction of Cr(VI) in two phase extraction process at various periods of extraction for various initialconcentration of feed; solvent = sunflower oil, concentration of extractant = 1% (vol/vol).

3.2.1.4 Detection of appropriate stirring condition

Stirring is an important act in extraction operation as it induces sufficient turbulence in the liquid medium that enhances eddy diffusivity and directly influences extraction behaviour in positive direction. Various stirring conditions in the range of 50-250 rpm were induced in a series of experiments, each for 12 h duration with different initial concentrations of feed in the range of 50-400 mg L^{-1} and 1%(vol/vol) aliquat 336 in sunflower oil, while keeping all the other parameters constant. The results are shown in Figure 3.4. It reveals that for solutions with initial feed concentrations 100 mg L^{-1} or less the efficiency of extraction reaches almost its maximum value (over 99%) at 150 rpm and no appreciable increase in efficiency is observed beyond the speed of 200 rpm. For higher initial feed concentrations the maximum value is reduced to 97% or less at 150 rpm and no appreciable increase in efficiency is seen either for higher speed of stirring. Hence optimum speed of stirring is set at 200 rpm and no emulsion is formed at this stirring speed.

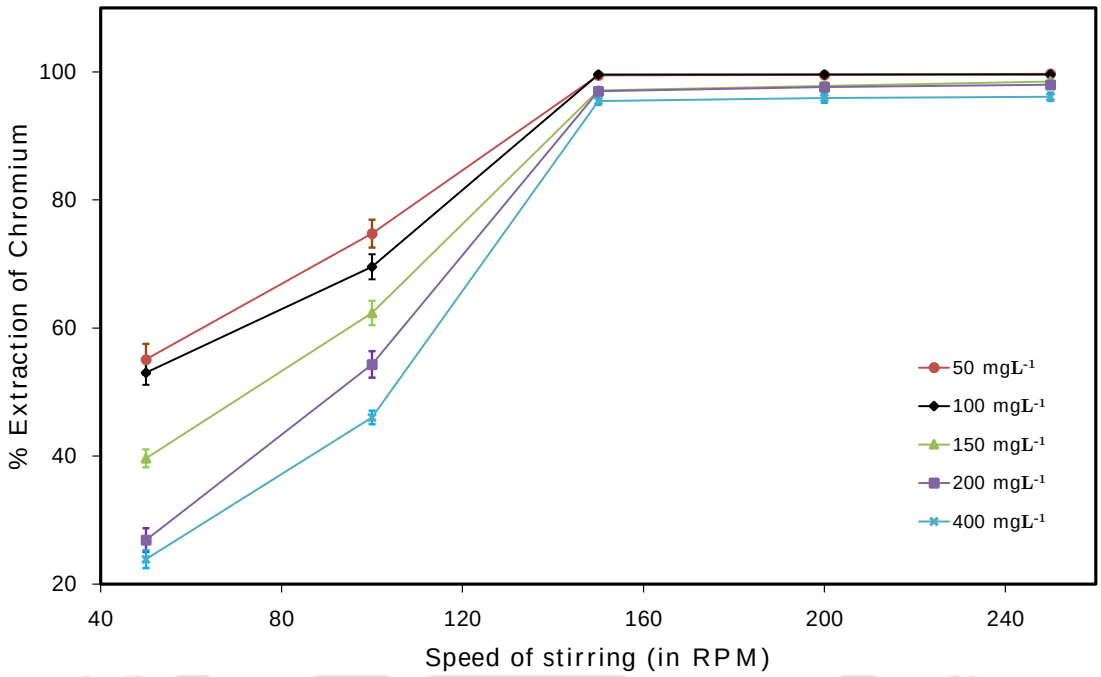

Figure 3.4: Efficiency of extraction of Cr(VI) in two phase extraction process at various stirring condition for various initialconcentration of feed: solvent = sunflower oil, concentration of extractant = 1% (vol/vol), period of extraction = 12 h.

3.2.1.5 Effect of pH of aqueous phase

The reaction mechanism, Equations (3.1)-(3.4), reveals that the role of proton is very important in the extraction process, and hence the efficiency of extraction hugely depends upon the pH of aqueous solution. It is observed that the nominal pH of a solution with concentration of 50 and 100 mg L^{-1} Cr(VI) are 4.73 and 4.56 respectively. A series of experiments, each for 12 h duration at 200 rpm with different initial concentrations of feed in the range of 50-400 mg L^{-1} and 1% (vol/vol) aliquat 336 in sunflower oil, were performed with variation of pH of aqueous solution in the range of 2-10 by adding HCl and NaOH. The results are shown in Figure 3.5. It is observed that the efficiency of extraction is significantly less at low pH. According to the chromate chemistry [173, 174] species such as $H_2Cr_2O_7$ dominates the reaction mechanism at low pH with concentration of Cr(VI) at 100 mg L^{-1}. As a result the solution might not ionise completely to form a complex with R_4N^+ cation. Efficiency

reaches its maximum value at pH ≈ 4.5 (over 99% for initial feed concentrations of 100 mg L^{-1}) which is very close to the nominal value of pH of 100 mg L^{-1} Cr(VI). The efficiency marginally decreases at higher pH condition due to decrease in proton concentration [43, 122].

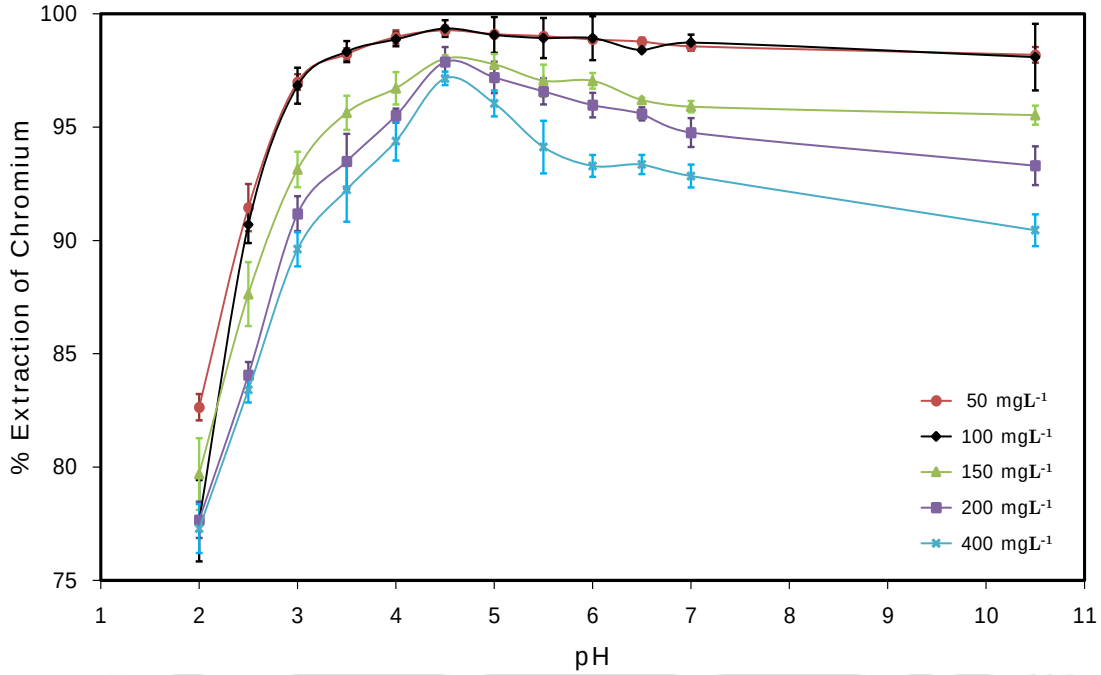

Figure 3.5: Efficiency of extraction of Cr(VI) in two phase extraction process at various pH of aqueous phase for various initialconcentrations of feed; solvent = sunflower oil, concentration of extractant = 1% (vol/vol), period of extraction = 12 h, speed of stirring = 200 rpm.

3.2.1.6 Effect of initial concentration of solute in aqueous phase

The influence of the initial concentration of Cr(VI) on the efficiency of its extraction had been studied in the range of 50-400 mg L^{-1} Cr(VI) in aqueous phase. The results are shown in Table 3.4. It is observed that efficiency of extraction is unchanged (98.7%) up to an initial concentration of 100 mg L^{-1} Cr(VI) in aqueous phase. The efficiency decreases thereafter with increase in initial concentration of Cr(VI) in aqueous phase. This is due to over crowding of solute in aqueous solution, as a result of which the availability of extractant is less for complexation reaction at the aqueous-organic interface. It also causes steric hindrance to extraction of Cr(VI)

at the aqueous-organic interface. It is thus customary to maintain the concentration of Cr(VI) in aqueous solution within the range of 50-100 mg L^{-1}.

Table 3.4: Efficiency of extraction of Cr(VI) in two phase extraction process at various initial concentrations of Cr(VI) in aqueous phase; solvent = sunflower oil, concentration of extractant = 1% (vol/vol), period of extraction = 12 h, pH = 4.5.

Feed concentration (in mg L^{-1})	Extraction of chromium (in %)
50	98.71
100	98.73
150	98.23
200	98.10
250	97.76
300	97.04
350	96.83
400	96.32

3.2.2 Three-phase BLM study

The configuration of BLM setup has already been discussed in Section 2.5. Effects of various physical parameters on three phase BLM operation has been described in the subsequent sections. As a starting point the relevant physical parameters were maintained in three phase study at values as they had been optimized in the two phase study. Samples were collected from both feed and strip phases at regular interval. The solute concentration of collected samples were measured by AAS.

3.2.2.1 Effect of concentration of strippant in strip phase

The effect of the concentration of Na_2-EDTA on the efficiency of extraction and/or recovery had been studied in the range of 0.005-0.04 M. The results are shown in Figure 3.6. Efficiencies of both extraction (95.45%) and recovery (26.47%) are maximum

at 0.03 M Na_2-EDTA and beyond this concentration both of them start declining. This is due to crowding effect of Na_2-EDTA at its higher concentration which inhibits the transport of Cr(VI) from strip-membrane interface to bulk of strip phase. For further experimentations the concentrations of strip phase was maintained at 0.03 M Na_2-EDTA.

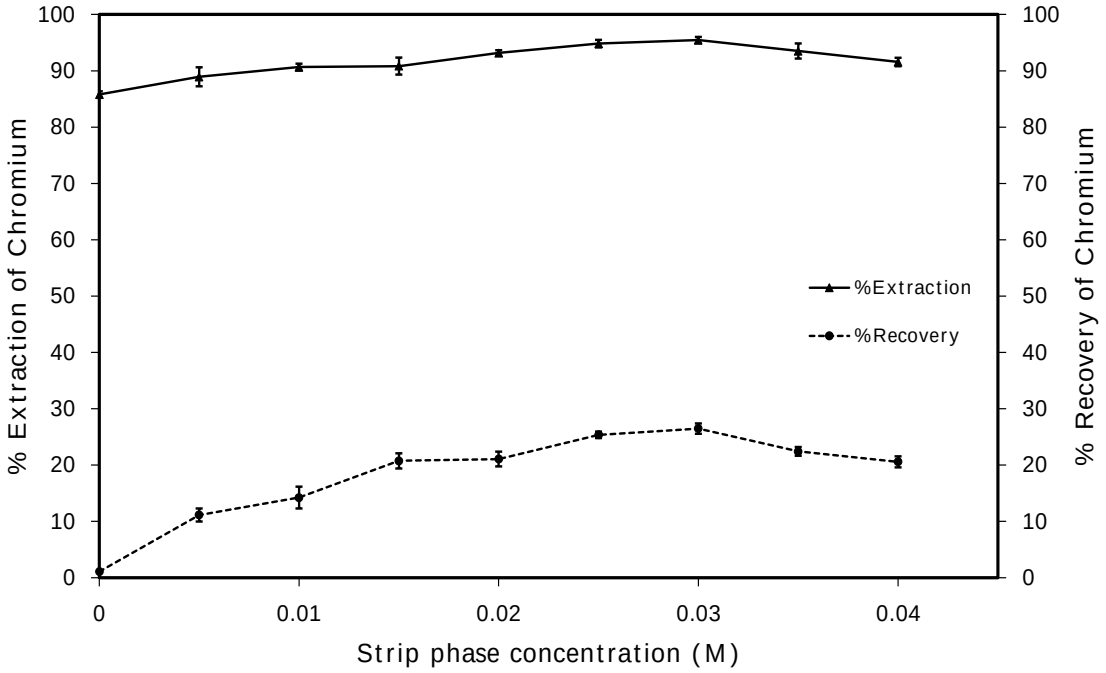

Figure 3.6: Efficiency of extraction and recovery of Cr(VI) in three phase LM based separation process at various concentrationsof strippant in strip phase; solvent = sunflower oil, concentration of extractant = 1% (vol/vol).

3.2.2.2 Effect of pH of strip phase

The effect of pH of strip phase (i.e. 0.03 M Na_2-EDTA solution) on extraction and recovery of Cr(VI) was examined by varying the pH within the range of 3-9. The results are reported in Figure 3.7. Recovery of Cr(VI) increased with increase in pH. The optimum value of pH was 6.5 where maximum recovery (34.5%) of Cr(VI) had been achieved. Recovery decreased very slowly beyond pH of 6.5. Normally Na_2-EDTA is stable at lower acidic condition but at very low pH, H^+ competes with metal ion M (i.e. chromium in this case) that creates problem in forming M-EDTA

complex. On the other hand, metal tends to form insoluble hydroxides at high pH condition and makes metal ions less accessible to EDTA.

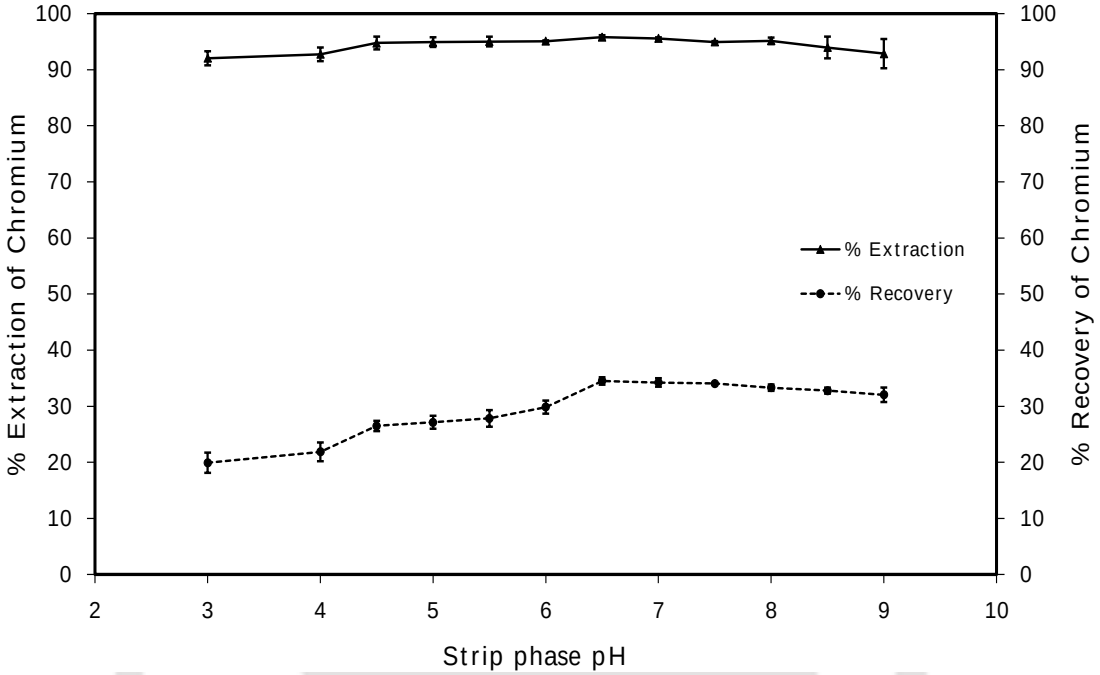

Figure 3.7: Efficiency of extraction and recovery of Cr(VI) in three phase LM based separation process at various pH of stripphase; solvent = sunflower oil, concentration of extractant = 1% (vol/vol), concentration of strippant = 0.03 M Na_2-EDTA.

3.2.2.3 Effect of speed of stirring

Effects of speed of stirring on transport of Cr(VI) needs to be re-evaluated in three phase operation. Unlike the two phase operation where intense turbulence would always benefit the operation, there are engineering problems associated with three phase operation against such high intensity agitation. In order to minimize resistance to mass transfer across the membrane phase, the thickness of the LM should be very less. On the other hand the upper edge of glass barrier that separates the compartments of BLM should lie between the levels of organic and aqueous phases. That would ensure that the aqueous solutions do not mix with each other and at the same time a bridge between two compartments can be established through the organic phase. An intense agitation would risk spoiling of such arrangement. Few

experiments were conducted by maintaining the speed of stirring between 60 and 500 rpm in both the compartments of the BLM. The results are shown in Figure 3.8. It is observed that over 93% of extraction was achieved when speed was maintained at 120 rpm. Beyond the speed of 120 rpm there is no substantial improvement of efficiency of extraction. On the other hand, recovery of Cr(VI) increased with increase in speed of stirring and over 45% recovery was obtained when the solutions were stirred at 500 rpm. However, at such high agitation, emulsion is formed due to minor mixing of either of the aqueous phases and its neighbouring membrane phase. Hence, a speed of 400 rpm was believed to be the optimum for extraction (95.87%) and recovery (42.64%) of Cr(VI) in three-phase study.

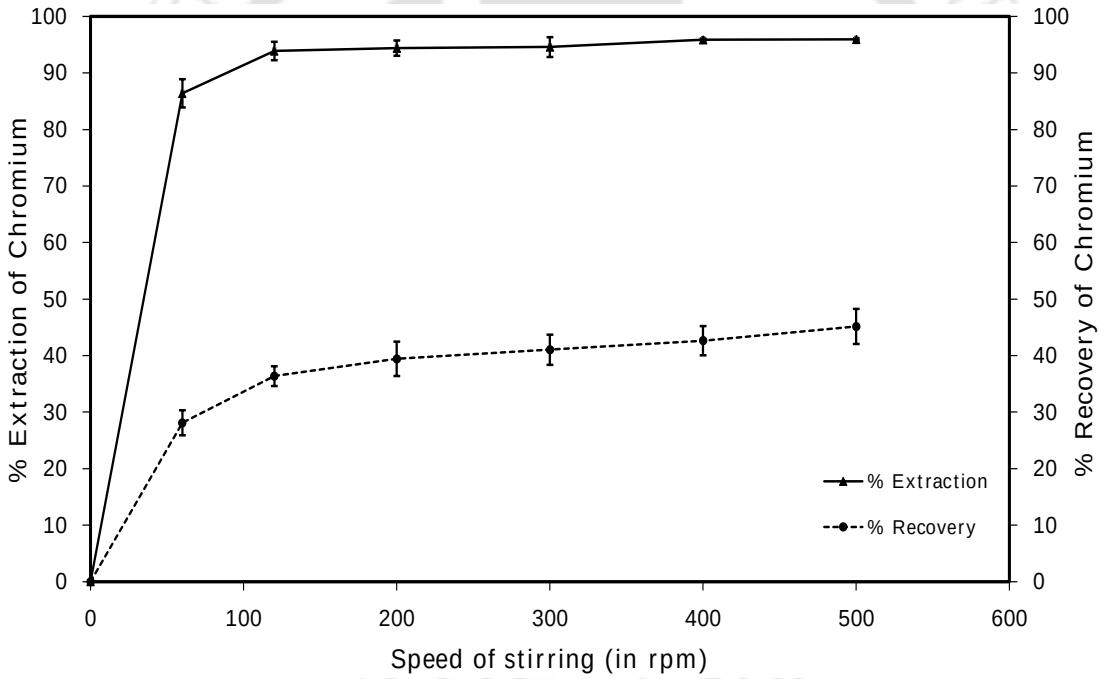

Figure 3.8: Efficiency of extraction and recovery of Cr(VI) in three phase LM based separation process at various speed ofstirring in aqueous phases; solvent = sunflower oil, concentration of extractant = 1% (vol/vol), concentration of strippant = 0.03 M Na_2-EDTA, pH = 6.5.

3.2.2.4 Effect of period of operation

Period of operation (i.e. extraction and/or recovery) is another important parameter whose optimum would differ from what was obtained during two phase study.

The two phase study could afford to bear intense agitation which yielded faster mass transfer. Three phase operation, being agitated with much lower speed of stirring, required more time for operation to be complete. Samples were however taken periodically and the results are shown in Figure 3.9 . Both the extraction and recovery achieved completeness after 48 h of operation at the values 95.86% and 35.67%, respectively.

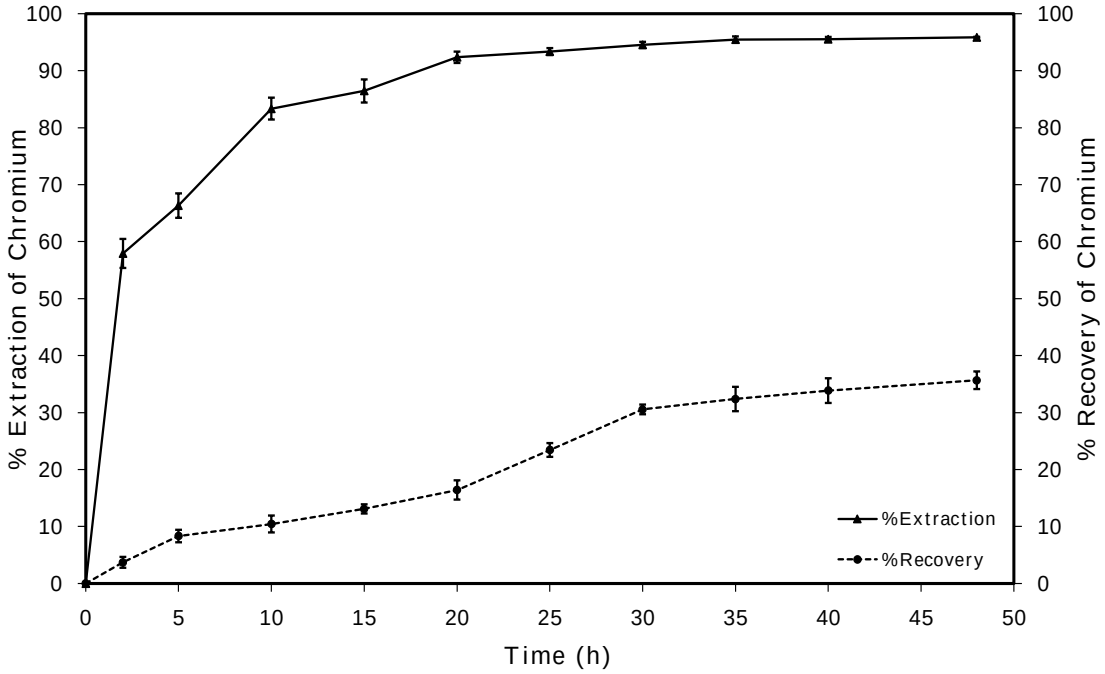

Figure 3.9: Efficiency of extraction and recovery of Cr(VI) in three phase LM based separation process at various periods ofoperation; solvent = sunflower oil, concentration of extractant = 1% (vol/vol), concentration of strippant = 0.03 M Na_2-EDTA, pH = 6.5, speed of stirring = 120 rpm.

3.2.2.5 Effect of concentration of carrier

The transport mechanism of BLM is quite complex and strongly dependant on concentration of extractant. Hence, the effects of concentration of carrier on simultaneous extraction and recovery of Cr(VI) are examined. The experimental results are shown in Figure 3.10. It is observed that extraction and recovery are quite low in absence of carrier. The extraction and recovery increased up to 1% (vol/vol) of aliquat 336. The maximum extraction (94.47%) and recovery (35.33%) can be seen

at the concentration of 1% (vol/vol) aliquat 336. Further increase in concentration of carrier does not help as extraction is decreased gradually. When carrier is added in the solvent to form Cr(VI)-aliquat 336 complex diffusive mass transfer through feed-membrane interface is increased. The solute is saturated at 1% (vol/vol) aliquat 336. Further increase in concentration of carrier increases the viscosity of solvent. On the other hand, recovery of Cr(VI) is almost constant beyond 1%(vol/vol) aliquat 336 due to the formation of stable solute-carrier complex. Thus the optimum concentration of carrier is 1% (vol/vol) aliquat 336. At higher concentration of carrier, the increased viscosity of the membrane phase hinders extraction and the recovery remains almost stagnant at that value. It can be concluded that Cr(VI)-aliquat 336 complex is formed till the saturation limit of the complex in the solvent. Further Figure 3.11 shows the ^{1}H nuclear magnetic resonance (a.k.a NMR) spectroscopy of sunflower oil and aliquat 336 mixture with deuterated chloroform ($CDCl_3$) as solvent. The NMR spectroscopy was performed before the start of BLM experiment and after the completion of BLM experiment. It is observed from NMR spectra that there has been no chemical shift in LM composition before and after the BLM experiment.

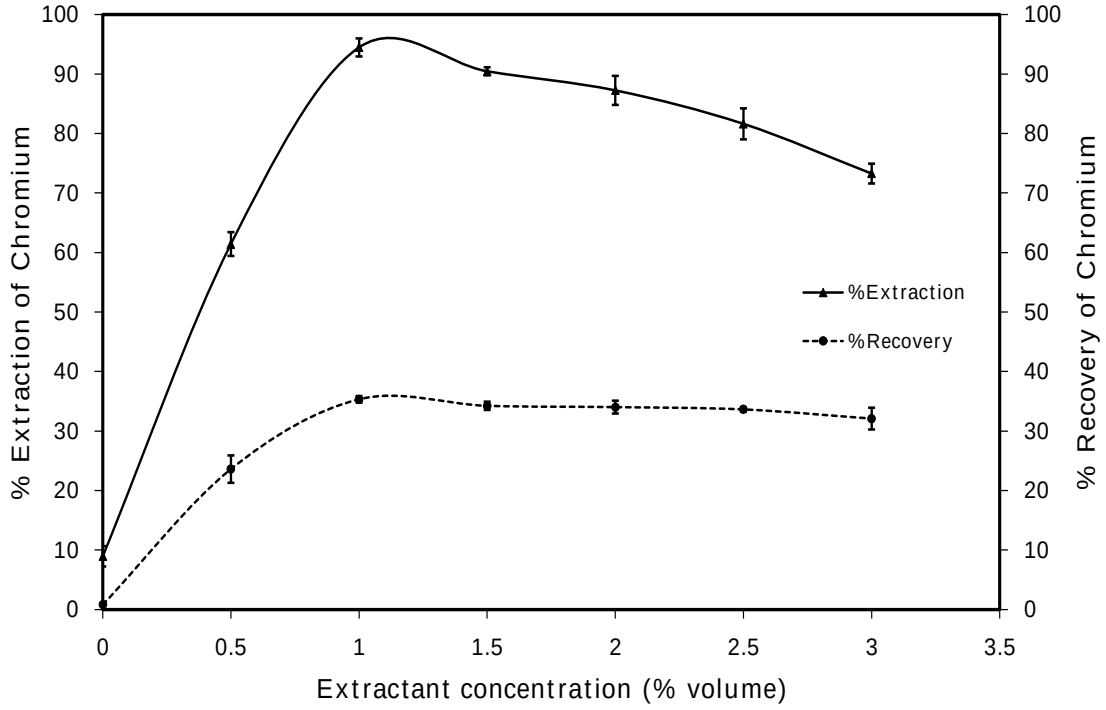

Figure 3.10: Efficiency of extraction and recovery of Cr(VI) in three phase LM based separation process at various concentrationsof extractant in the organic phase; solvent = sunflower oil, initial concentration of feed = 100 mg L^{-1}, concentration ofextractant = 1% (vol/vol), concentration of strippant = 0.03 M Na_2-EDTA, pH = 6.5, speed of stirring = 120 rpm, period of operation = 48 h.

3.2.2.6 Fed batch system

The study of fed batch operation in BLM is very useful in the context of industrial scenario. It is carried out to check whether the same LM and stripping solution have the capability to extract and recover more solute repeatedly in case feed phase is topped up with fresh solute in higher concentration. In this experiment samples were collected from feed phase once in every 24 h interval and make up solution was added to the feed phase in order to increase the concentration of Cr(VI) in feed solution up to 100 mg L^{-1}. The results are shown in Figure 3.12. At the end of 24 h, 48 h and 72 h (before replenishing with fresh feed) the concentrations of Cr(VI) in the feed phase became 6.58 mg L^{-1}, 19.7 mg L^{-1} and 25.96 mg L^{-1} respectively. The concentration of Cr(VI) in the strip phase increased from 25.52 mg L^{-1} (at the end of 24 h) to 43.38 mg L^{-1} at the end of 48 h. It did not show any more increase thereafter.

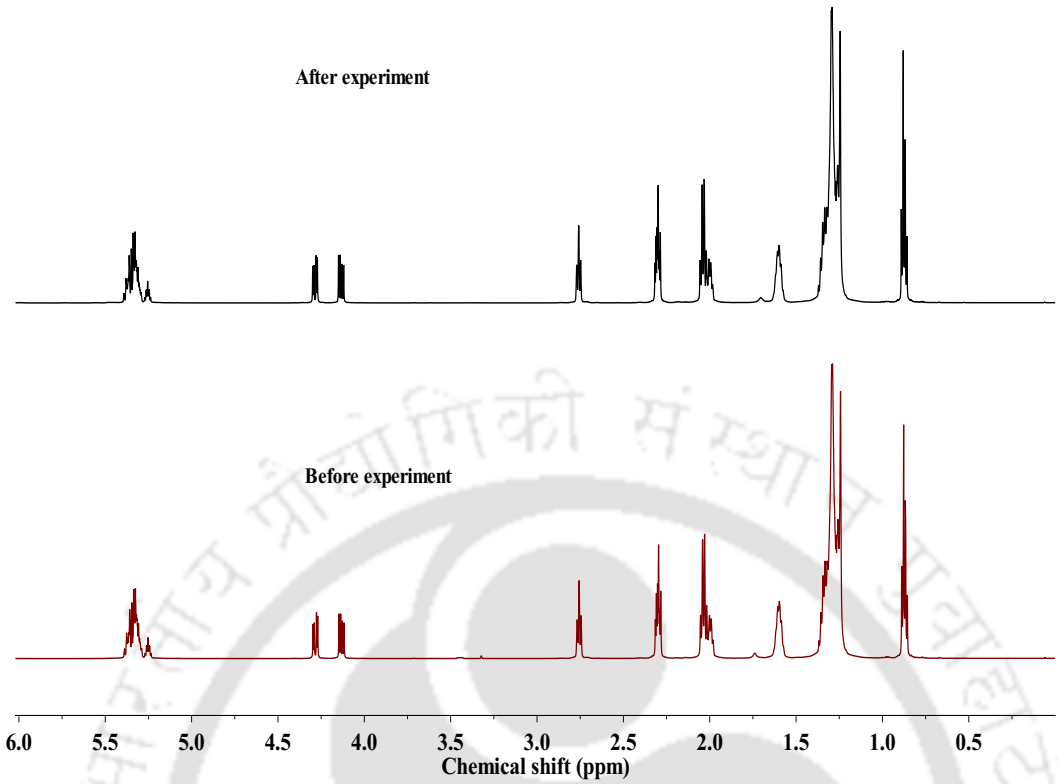

Figure 3.11: ^{1}H NMR spectra of organic phase containing sunflower oil and aliquat 336.

Marginal increase in the extraction may be explained by the quantity of organic phase that had the capacity to extract more Cr(VI) before saturation. After three cycles of *depletion* and *re-fill* of feed phase the efficiency of recovery in strip phase reached a saturation point. However, after every batch fed in the reaction chamber the extent of extraction was marginally decreased due to the enhanced viscosity of the solution and crowding effect of solute-carrier complex as stated earlier.

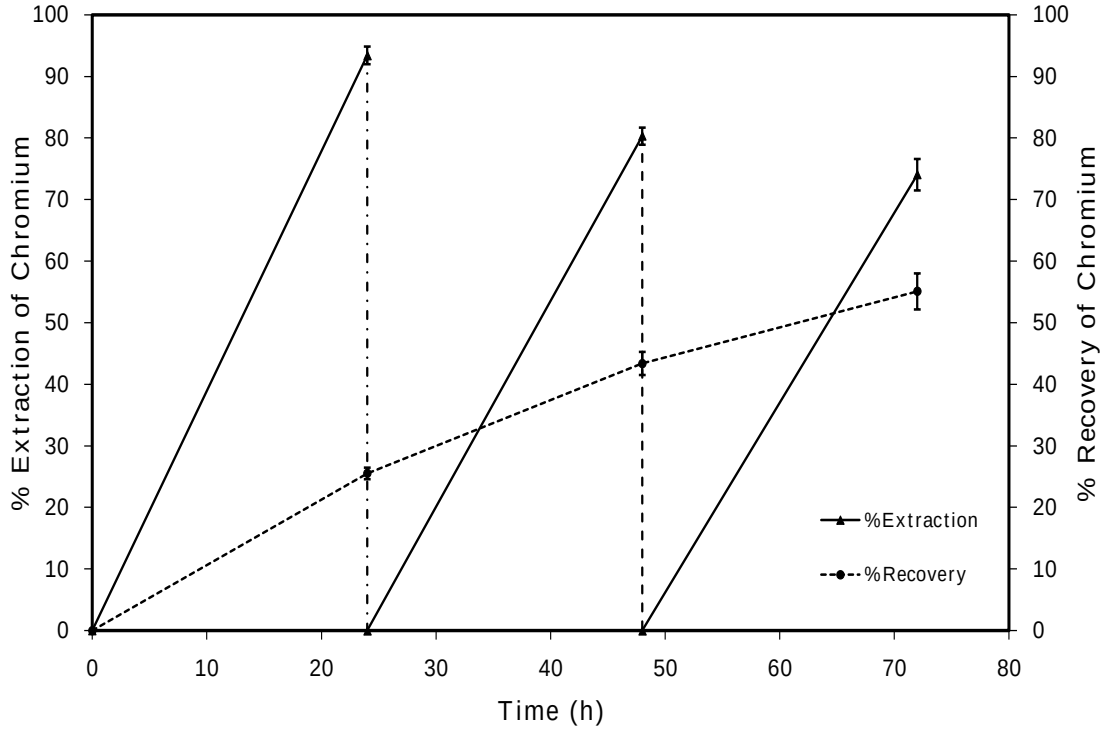

Figure 3.12: Efficiency of extraction and recovery of Cr(VI) in three phase LM based separation process during fed-batch operation.

3.2.3 Three-phase SLM study

The three-phase SLM studies had been performed as described in Section 2.6. The configuration of SLM setup has already been discussed in that Section 2.6. Effects of various physical parameters on three phase SLM operation has been described in the subsequent sections. As a starting point the relevant physical parameters were maintained in this study at values as they had been optimized in the three phase BLM study.

3.2.3.1 Effects of concentration of strippant and pH in strip phase

Various concentrations of Na_2-EDTA within the range 0.005-0.04 M and pH of strip phase within range of 4-9 had been experimented with to check their effects on the efficiency of recovery. The results are shown in Figures 3.13 and 3.14 respectively. It is clearly understood from the figures that both extraction and recovery are maximum

at 0.03 M Na_2-EDTA and at pH 6.5. Extraction and recovery were 67.78% and 58.25% respectively for 0.03 M Na_2-EDTA and 82.5% and 71.54% respectively at pH 6.5. However, the %recovery got enhanced as compared to that in BLM operation in both the cases. This was possible due to the structural advantage in SLM where the thickness of membrane is very small compared to that in BLM and hence the solute needs to diffuse through lesser distance across the two membrane interfaces. The amount of hold up of solute in the LM phase is also small as compared to that in BLM. Nevertheless the %extraction had been reduced in both the cases. It however is not a matter of concern as the final recovery in the strip phase is the factor which is of prime importance in case of three phase LM operation.

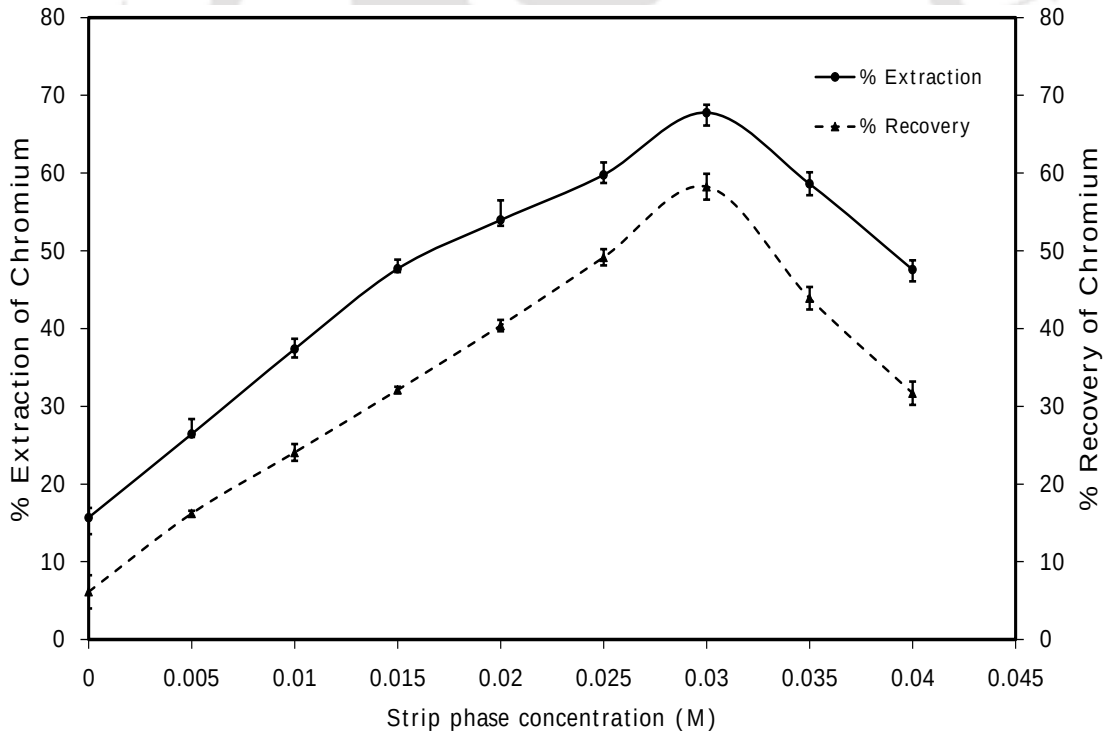

Figure 3.13: Efficiency of extraction and recovery of Cr(VI) in three phase SLM based separation process at various concentrations of strippant in strip phase; solvent = sunflower oil, concentration of extractant = 1% (vol/vol), stirring speed = 120 rpm, run time = 48 h.

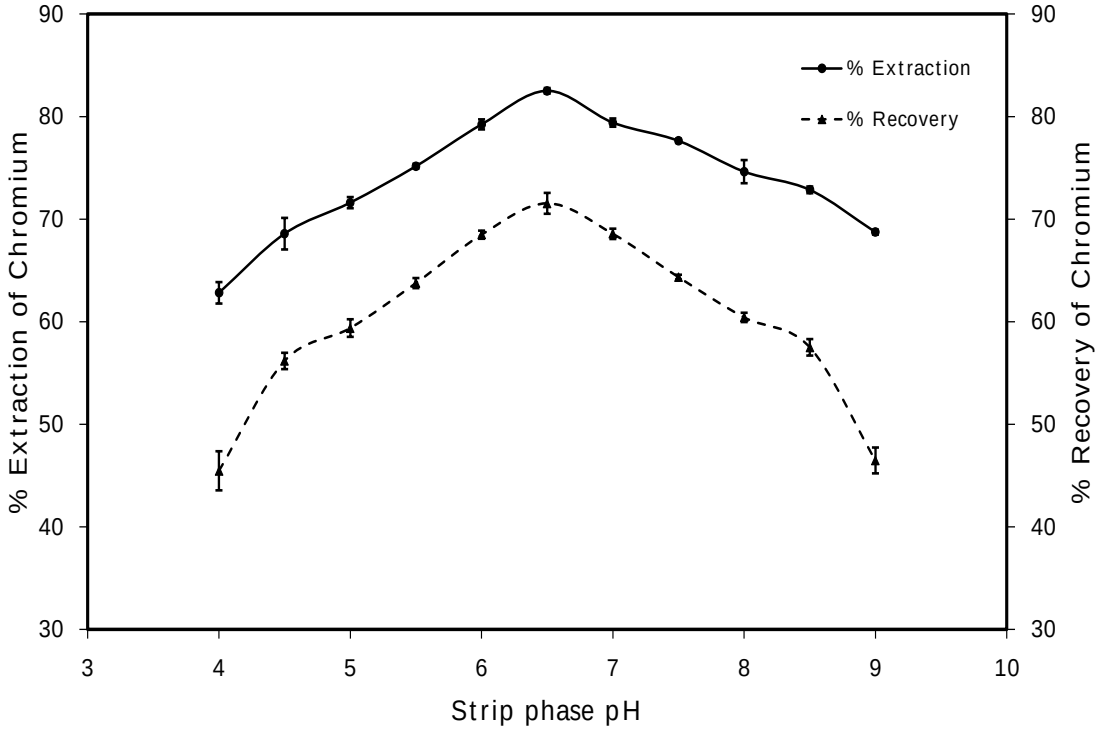

Figure 3.14: Efficiency of extraction and recovery of Cr(VI) in three phase SLM based separation process at various pH in strip phase; solvent = sunflower oil, strip phase conc. = 0.03 M, concentration of extractant = 1% (vol/vol), stirring speed = 120 rpm, run time = 48 h.

3.2.3.2 Effect of speed of stirring

Unlike in BLM the stirring speed could not be maintained at 400 rpm in the strip phase of SLM because higher turbulence disturbs the stability of SLM whereby the organic phase oozes out of the pores of PVDF membrane. The experiments were thus carried out with stirring speed in range of 60-200 rpm in both the compartments. The results are shown in Figure 3.15. As expected, the increase in stirring speed from 60 to 120 rpm manifest in higher %extraction and %recovery of Cr(VI) and reached over 80% extraction and over 70% recovery of Cr(VI), much higher recovery than in BLM. The speed of stirring was set at 120 rpm for all further experimentations.

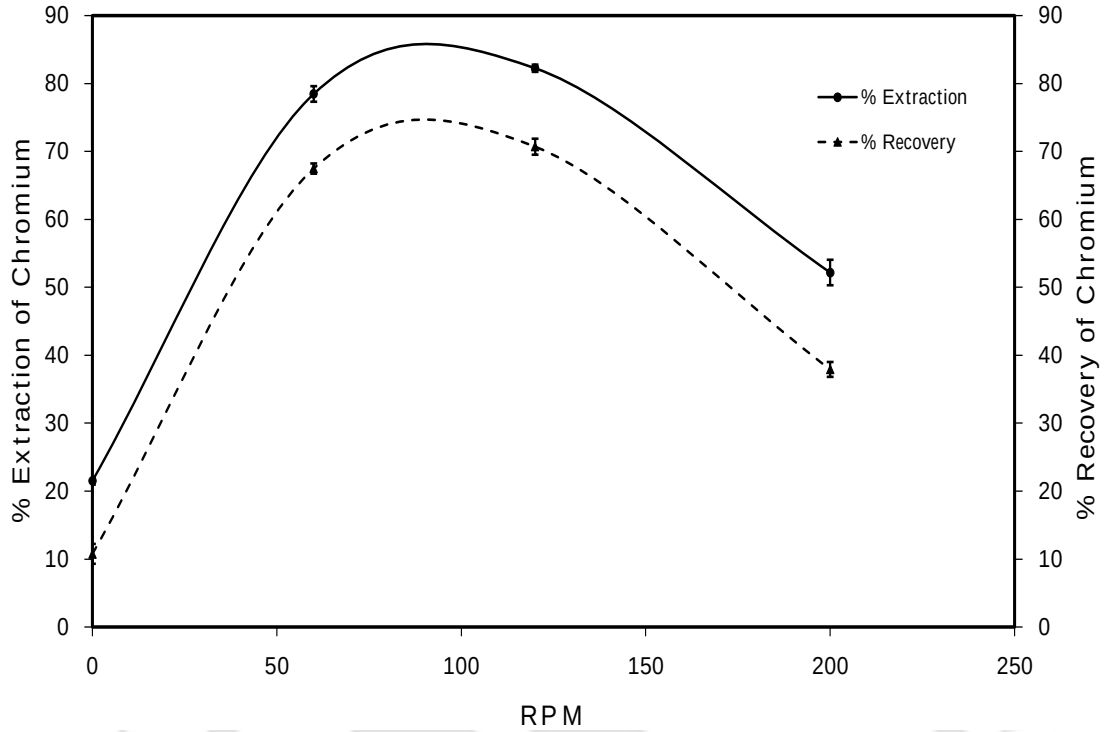

Figure 3.15: Efficiency of extraction and recovery of Cr(VI) in three phase SLM based separation process at various speed of stirring in strip phase; solvent = sunflower oil, strip phase conc. = 0.03 M, strip phase pH = 6.5, concentration of extractant = 1% (vol/vol), run time = 48 h.

3.2.3.3 Effect of period of operation

As the agitation (i.e. speed of stirring) in SLM operation is lower than that in BLM one requires higher period of operation in SLM if one desires to achieve the same level of performance. The experiment in SLM was thus performed for a duration of 78 h. The results are shown in Figure 3.16. Maximum extraction and recovery of Cr(VI) can be seen in between 48 h and 68 h respectively. The percent extraction and recovery reached over 80% and 70% respectively. Interestingly it is also observed that %extraction and %recovery show declining trend after 68 h of operation. This is due to the fact that SLM loses its stability after prolonged period of operation whereby the organic phase oozes out of the pores of PVDF membrane. This yields a direct channelling between two aqueous phases of feed and strip sides. It is also noticed that %extraction and %recovery of Cr(VI) do not significantly increase after

48 h. Hence the run time of 48 h was selected for rest of the study.

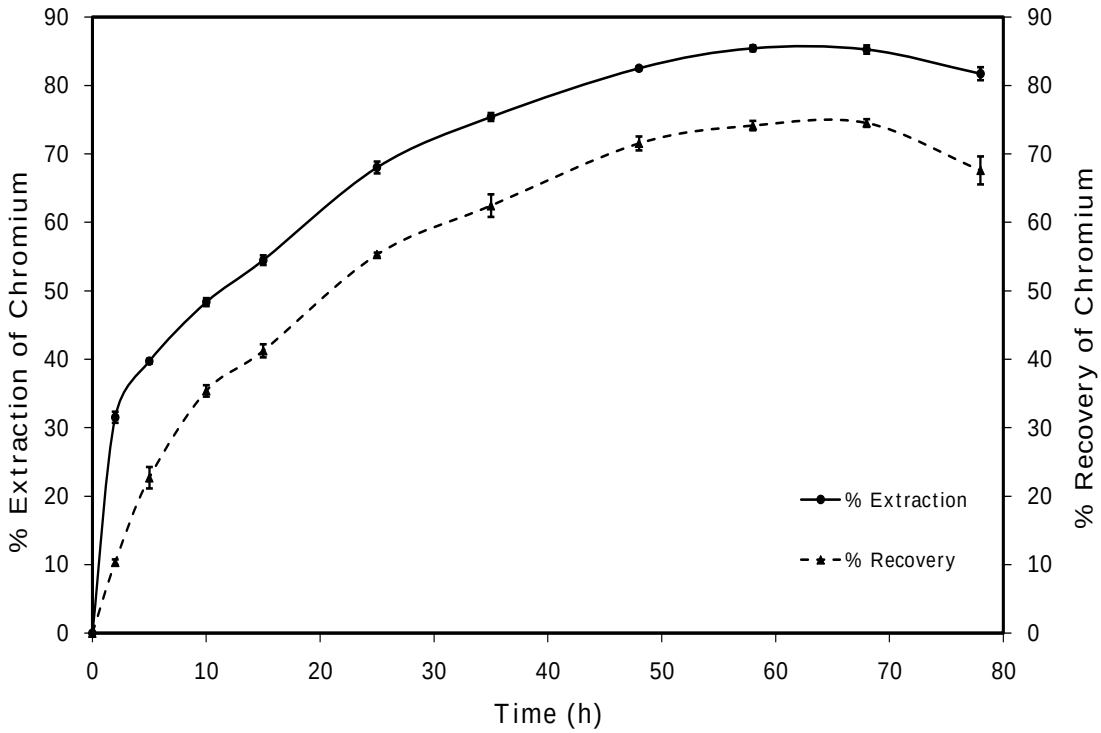

Figure 3.16: Efficiency of extraction and recovery of Cr(VI) in three phase SLM based separation process at various periods of operation; solvent = sunflower oil, strip phase conc. = 0.03 M, strip phase pH = 6.5, concentration of extractant = 1% (vol/vol), speed of stirring = 120 rpm.

3.2.3.4 Effect of concentration of carrier

The effect of concentration of aliquat 336 in organic phase on extraction and recovery were studied at concentration in the range of 0-3%. The results are presented in Figure 3.17. The trend of profile is similar to that observed in three phase BLM operation and the reasons are already stated in Section 3.2.2.5. However, the extent of recovery is nearly twice (71.54%) of that observed in BLM operation (35.33%) due to thinner membrane size.

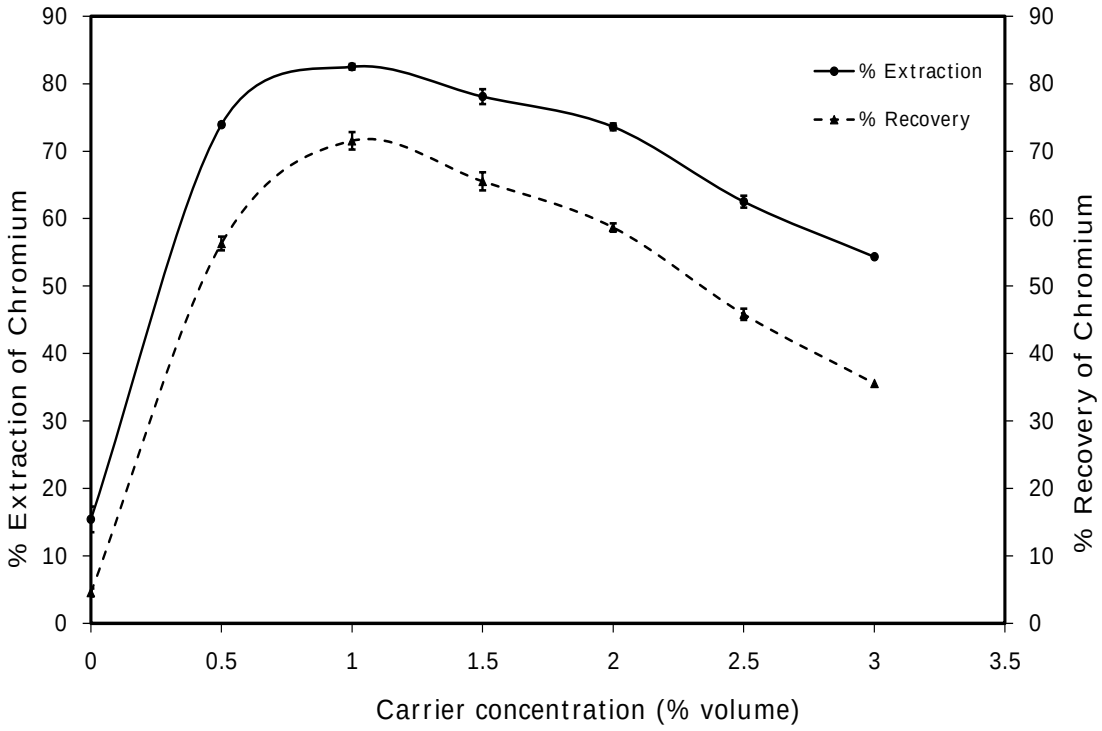

Figure 3.17: Efficiency of extraction and recovery of Cr(VI) in three phase SLM based separation process at variousconcentrations of aliquat 336; solvent = sunflower oil, strip phase conc. = 0.03 M, strip phase pH = 6.5, period ofoperation = 48 h, speed of stirring = 120 rpm.

3.2.3.5 Fed batch system

The fed batch runs were carried out in SLM in the same fashion as they were carried out in BLM. The results are shown in Figure 3.18. The trends of profile are similar in both BLM and SLM operations, however, the concentration of Cr(VI) in strip phase reaches 90.68 mg L^{-1} in case of SLM operation within 72 h period as compared to mere 43.3 mg L^{-1} in case of BLM operation in the same time duration. Unlike in BLM, it didn't reach any saturation point either.

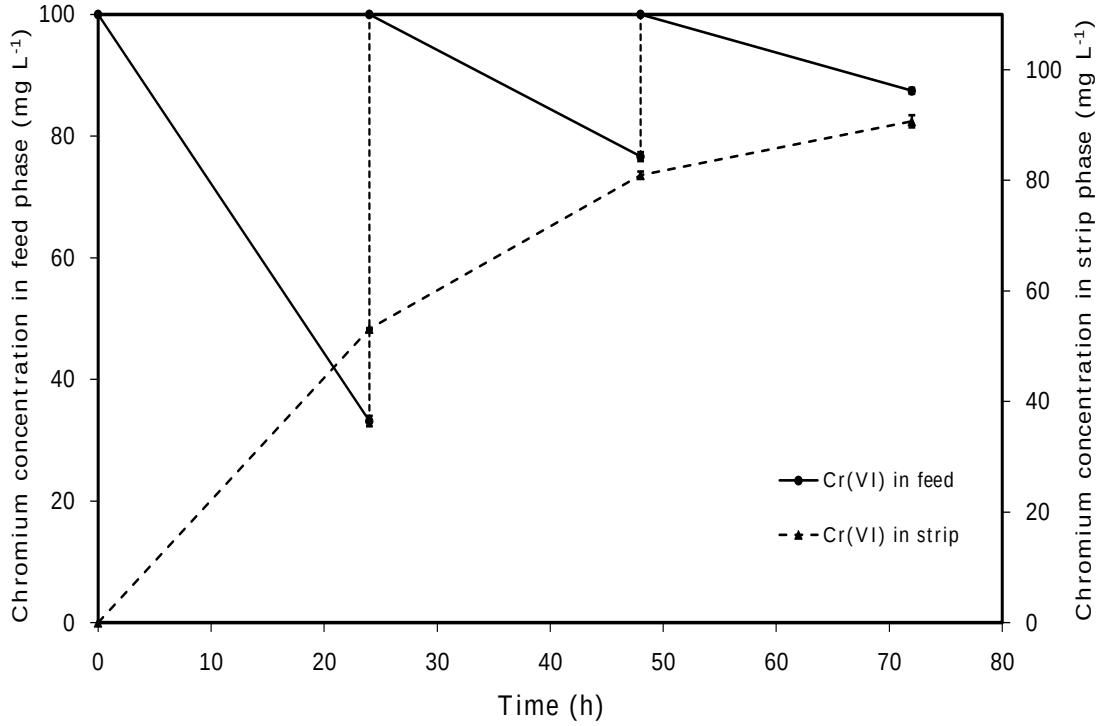

Figure 3.18: Efficiency of extraction and recovery of Cr(VI) in three phase SLM based separation process during fed-batch operation; solvent = sunflower oil, strip phase conc. = 0.03 M, strip phase pH = 6.5, concentration of extractant = 1% (vol/vol), speed of stirring = 120 rpm.

3.2.4 Experimental optimization of operating parameters in SLM

The procedure documented in Section 2.8 has been followed. It can be seen from the experimental studies that the most influential parameters for three-phase LM based separation of Cr(VI) are strip phase concentration, strip phase pH and concentration of carrier in LM. These three parameters are chosen for design plan as input parameters. The output parameters are %extraction and %recovery of Cr(VI). Design parameters and experimental results are tabulated in Table 3.5. The experiments were conducted with strip phase concentration (denoted with A) ranging from 0.005 to 0.04 M, strip phase pH (denoted with B) ranging from 4 to 9 and carrier concentration (denoted with C) ranging from 0.5% to 3% (v/v). The experimental

results of %extraction and %recovery were analyzed and fitted with quadratic model (Equation 2.5). The models of %extraction and %recovery are given by Equations (3.5) and (3.6) respectively.

$$\begin{aligned} \%Extraction =& 72.42 + 6.97 \times A + 3.93 \times B - 0.83 \times C - 2.83 \times A \times B \\ &+ 2.60 \times A \times C + 0.80 \times B \times C - 27.17 \times A^2 - 9.44 \times B^2 \\ &- 12.82 \times C^2 \end{aligned} \tag{3.5}$$

$$\begin{aligned} \%Recovery =& 58.93 + 2.62 \times A + 2.79 \times B - 1.01 \times C + 0.11 \times A \times B \\ &+ 1.33 \times A \times C + 0.50 \times B \times C - 32.89 \times A^2 - 4.29 \times B^2 \\ &- 12.01 \times C^2 \end{aligned} \tag{3.6}$$

The actual output parameters and their predicted ones against the input parameters through the quadratic model have been shown in Table 3.5. ANOVA study of %extraction and %recovery are shown in Table 3.6.

Fischer variation (F value), probability values (p value) and correlation coefficient (R^2) are used to check applicability of the proposed model. The p values < 0.05 confirm that model and variables are strongly significant on output responses. In both cases the quadratic models, F values are quite high and p values < 0.0001 (vide Table 3.6) indicate strong significance. It also signifies that there is only a 0.01% chance to not follow the model. The model-predicted R^2 values of 0.9882 and 0.9441 are very much comparable with adjusted R^2 of 0.9951 and 0.9748 for %extraction and %recovery respectively. The adequate precision value of the model indicates the signal to noise ratio, whereas linear and quadratic model terms are compared to explain their relative effects on output parameters. Desirable value of precision is greater than 4. It can be seen from Table 3.6 that adequate precision value for both models are quite high. It is also observed linear terms A, B and quadratic terms

AB,AC, A^2, B^2, C^2 with p value < 0.005 have significant impact on %extraction, whereas linear terms A, B and A^2, C^2 with p value < 0.005 have significant impact on %recovery.

Table 3.5: Design Arrangement and Experimental Responses for CCD.

Run	factor 1:A, strip phase conc.(M)	factor 2:B, strip phase pH	factor 3:C, carrier conc.(%vol.)	response 1: R1, %extraction		response 2: R2, %recovery	
				Actual	Perd	Actual	Pred
1	0.04	9.0	3.00	33.91	33.63	16.76	16.08
2	0.04	4.0	0.50	28.22	27.89	10.36	09.63
3	0.02	6.5	1.75	73.57	72.41	61.97	58.92
4	0.005	9.0	0.50	25.47	25.39	12.60	11.64
5	0.02	6.5	0.50	58.65	60.42	43.81	47.92
6	0.02	6.5	1.75	73.87	72.41	61.07	58.92
7	0.005	9.0	3.00	20.64	20.14	09.13	07.96
8	0.04	6.5	1.75	50.05	52.21	25.10	28.65
9	0.04	4.0	3.00	30.56	29.82	10.21	09.28
10	0.005	4.0	3.00	05.02	05.03	2.29	01.60
11	0.005	6.5	1.75	37.16	38.27	19.38	23.42
12	0.02	6.5	3.00	57.27	58.77	42.43	45.90
13	0.02	6.5	1.75	73.57	72.41	61.57	58.92
14	0.02	6.5	1.75	73.77	72.41	61.27	58.92
15	0.04	9.0	0.50	29.31	28.49	15.64	14.43
16	0.02	4.0	1.75	57.46	59.04	48.28	51.85
17	0.02	9.0	1.75	65.22	66.90	53.41	57.43
18	0.02	6.5	1.75	73.17	72.41	61.17	58.92
19	0.02	6.5	1.75	73.07	72.41	61.67	58.92
20	0.005	4.0	0.50	14.03	13.49	08.49	07.28

Figure 3.19a and 3.19b present the residuals versus predicted response for the %extraction and %recovery for Cr(VI) respectively. The scattering of all experimental data points across the horizontal line of residual reveals that the suggested models are well fitted. The comparison between actual values and predicted values of %extraction and %recovery are shown in Figure 3.20a and 3.20b respectively. The predicted values obtained from the regression model are compared with the actual ones from experimental studies to confirm the consistency and acceptability of empirical models from individual response(Figure 3.20a and 3.20b). All design points

are distributed along the diagonal line where over-estimated data are above the diagonal line and under-estimated data are under the diagonal line. The over-estimated and under-estimated values are with in the range of ±3%. This comparative study indicates a negligible experimental error as the responses from the empirical model are well-fitted in acceptable variance range. According to this results, the empirical model obtained from CCD (Table 3.5) can be used as an analyst for the optimization of the selected variables.

Based on analysis of the experimental data, the relation between the process factors (i.e. strip phase concentration, strip phase pH and concentration) and desired responses (i.e.%extraction and %recovery of Cr(VI)) are plotted graphically in Figure 3.21.

The optimization study of all input variables was performed through desirability function in Design Expert 7.0 software. The desirability value varies in a range of 0.0 (undesirable) to 1.0 (desirable), where a value between 0.5 and 1.0 is expected for feasibility. The numerical optimization was performed with in specific ranges of input variables Table 3.7. The outcome of the optimization result is tabulated in Table 3.8. It can be observed from Table 3.7 that desirability value is 0.973. The obtained optimum conditions were analysed experimentally and error percentage were calculated as tabulated in Table 3.8.

Table 3.6: ANOVA for respective response surface quadratic models.

Source	Sum of squares (SS)	Degree of freedom (DF)	Mean square (MS)	F-value	p value Prob>F	Remarks
%Extraction of Cr(VI)						
Model	10082.31	9	1120.26	428.38	<0.0001	
A	486.37	1	486.37	185.98	<0.0001	
B	154.28	1	154.28	58.99	<0.0001	In this
C	6.86	1	6.86	2.62	0.1364	case A, B,
AB	63.88	1	63.88	24.43	0.0006	AB, AC,
AC	53.98	1	53.98	20.64	0.0011	A^2, B^2, C^2
BC	5.16	1	5.16	1.97	0.1905	are
A^2	2030.26	1	2030.26	776.36	<0.0001	significant
B^2	244.97	1	244.97	93.68	<0.0001	model
C^2	451.67	1	451.67	172.72	<0.0001	
Residual	26.15	10	2.62			
Lack of fit	25.64	5	5.13	49.94	0.0003	
Pure error	0.51	5	0.10			
R^2=0.9974, R^2_{adj}=0.9951, R^2_{pred}=0.9882, Adequate precision=58.927						
%Recovery of Cr(VI)						
Model	9919.45	9	1102.16	82.75	<0.0001	
A	68.51	1	68.51	5.14	0.0467	
B	77.90	1	77.90	5.85	0.0362	
C	10.16	1	10.16	0.76	0.4030	In this
AB	0.094	1	0.094	0.007071	0.9346	case A, B,
AC	14.19	1	14.19	1.07	0.3263	A^2, C^2 is
BC	2.00	1	2.00	0.15	0.7064	significant
A^2	2974.72	1	2974.72	223.33	<0.0001	model
B^2	50.52	1	50.52	3.79	0.0801	
C^2	396.72	1	396.72	29.78	0.0003	
Residual	133.20	10	13.32			
Lack of fit	132.61	5	26.52	225.40	<0.0001	
Pure error	0.59	5	0.12			
R^2=0.9868, R^2_{adj}=0.9748, R^2_{pred}=0.9441, Adequate precision=22.214						

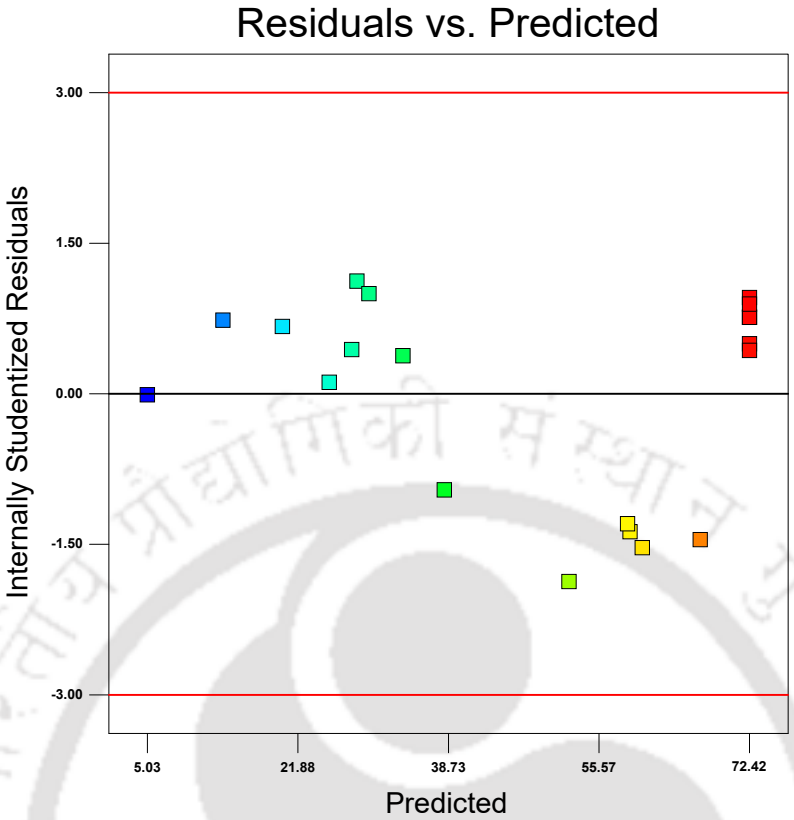

(a) %Extraction of Cr(VI)

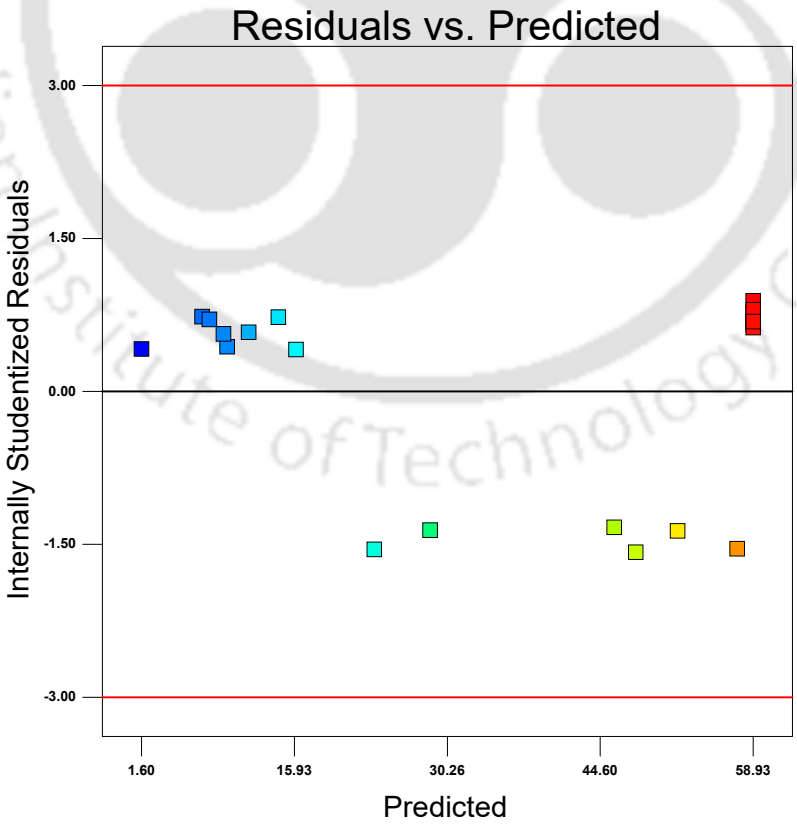

(b) %Recovery of Cr(VI)

Figure 3.19: Residual versus predicted graphs.

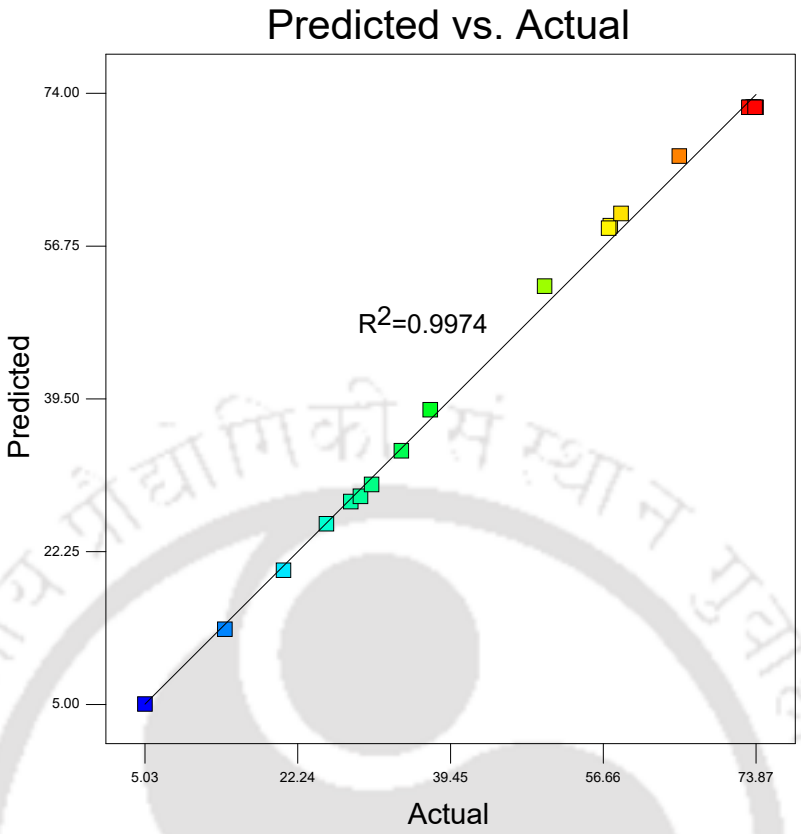

(a) %Extraction of Cr(VI)

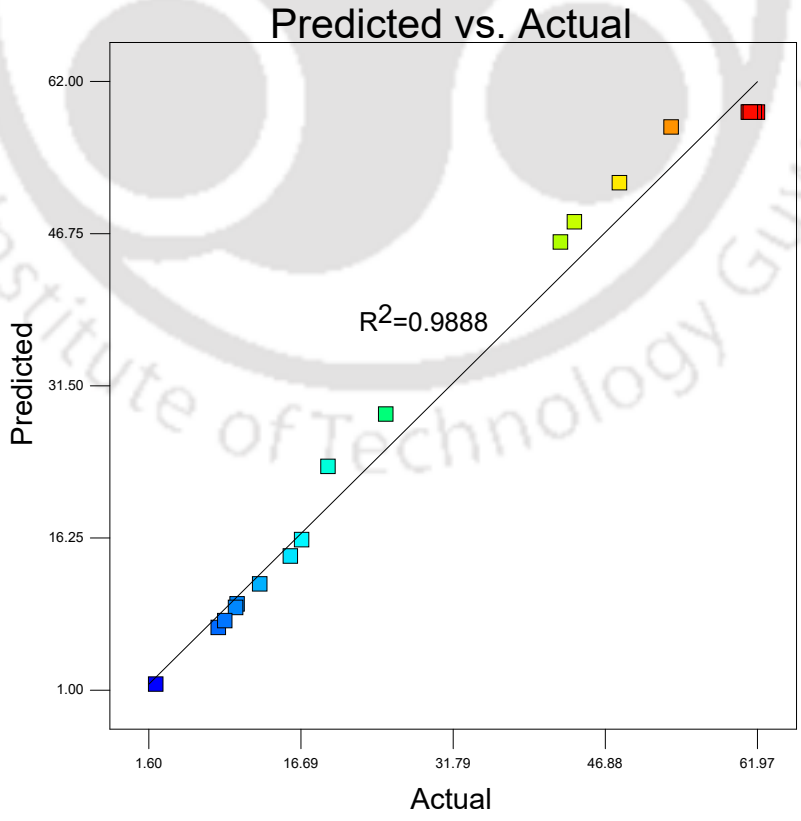

(b) %Recovery of Cr(VI)

Figure 3.20: Predicted versus actual graphs.

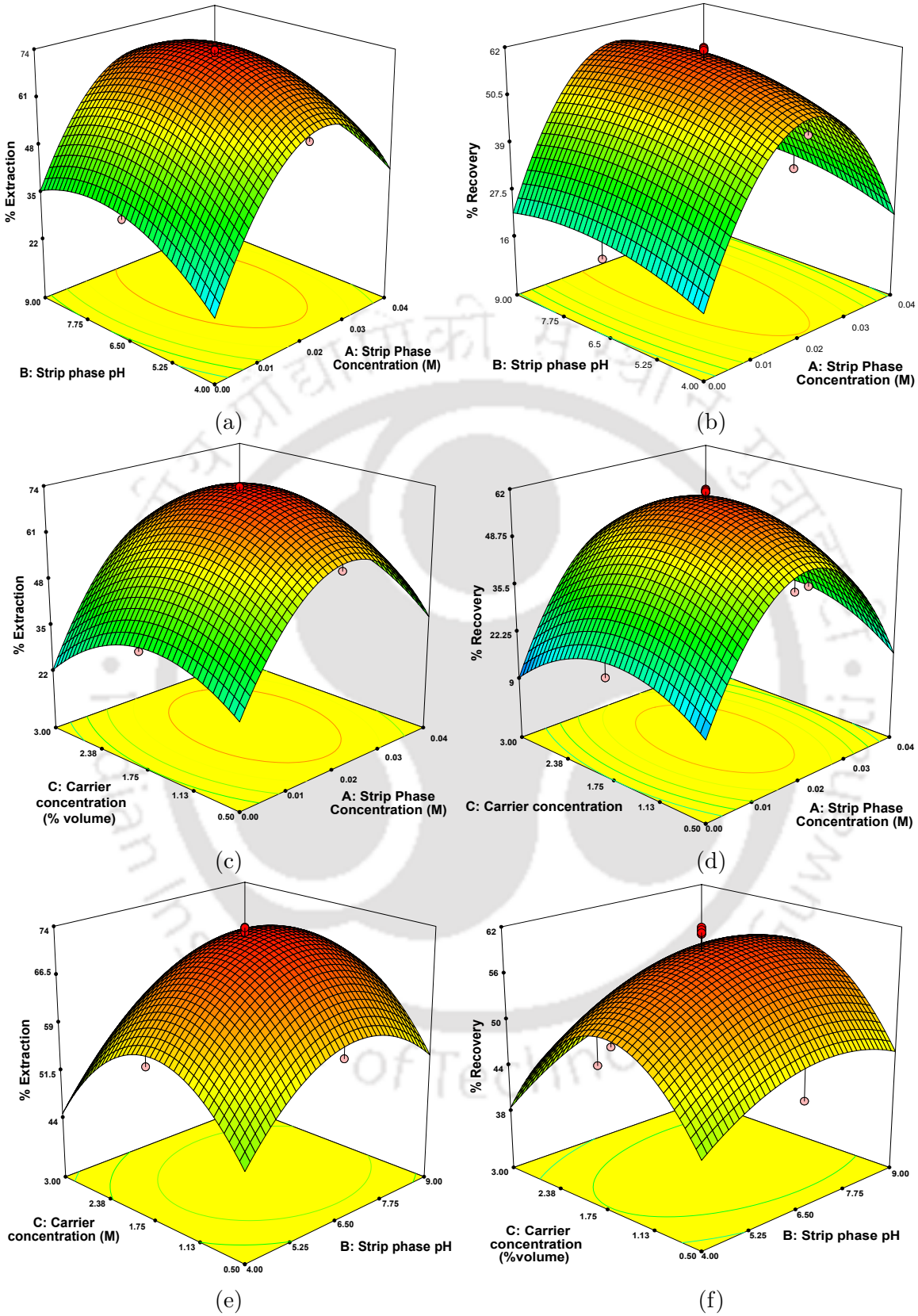

Figure 3.21: Response surface plot of (3.21a) strip phase concentration and strip phase pH, (3.21c) strip phase concentration and carrier concentration, (3.21e) strip phase pH and carrier concentration for %extraction of Cr(VI) and (3.21b) strip phase concentration and strip phase pH, (3.21d) strip phase concentration and carrier concentration, (3.21f) strip phase pH and carrier concentration for %recovery of Cr(VI).

Table 3.7: Optimization constraints for %extraction and %recovery of Cr(VI).

Name	Goal	Lower limit	Upper limit	Lower weight	Upper weight	Importance
Strip phase concentration	in range	0.005	0.04	1	1	3
Strip phase pH	in range	4	9	1	1	3
Carrier concentration	in range	0.5	3	1	1	3
%Extraction	in range	5.028	73.871	1	1	3
%Recovery	in range	2.29	61.972	1	1	3

Table 3.8: Optimization results for %extraction and %recovery of Cr(VI).

Strip phase concentration (M)	Strip phase pH	Carrier concentration (% volume)	%Extraction	%Recovery	Desirability
0.02	7.10	1.72	73.1263	59.3862	0.973

Table 3.9: Error analysis between predicted and experimental results.

Responses	Predicted value	Experimental value	Error (%)
%Extraction	73.1263	70.524	3.5
%recovery	59.3862	57.847	2.5

3.3 Summary of studies on the separation of Cr(VI) through BLM and SLM

- ✓ Sunflower oil is found to be an ideal green solvent.
- ✓ Maximum extraction over 95% and maximum recovery over 45% were obtained in case of BLM.
- ✓ In case of SLM extraction and recovery were over 80% and 73% respectively.
- ✓ Combination of sunflower oil and aliquat 336 has been found to be the best solvent-carrier combination.
- ✓ The two-phase study reveals that the optimum process conditions are 100 mg L^{-1} Cr(VI) in aqueous solution, 1% (v/v) aliquat 336, 200 rpm stirring and 12 h of operation.
- ✓ Optimum process conditions for three-phase study are 0.03 M Na_2-EDTA and pH 6.5 in strip phase.
- ✓ The fed batch operations have also been successful which indicates that it is possible to design a continuous operation of LM based separation process.
- ✓ The most influential factors on transport of Cr(VI) i.e. strip phase concentration, strip phase pH and carrier concentration are experimentally optimized by RSM following CCD rule.
- ✓ The comparison between experimentally observed data and those predicted by RSM model showed that all the values are in good agreement.

Chapter 4

Electrochemical separation of Cr(VI) using FS-SLM

This chapter presents separation of Cr(VI) using FS-SLM technology. A new type of supported liquid membrane (SLM) has been used where stripping chamber has been used as an electrochemical reactor. SLM set up with in situ electrochemical reactor in stripping section is used to reduce hexavalent chromium (Cr(VI)) to trivalent chromium (Cr(III)) by forming chromium-iron complex with the help of iron plate which acts as anode in stripping section. The wastewater containing Cr(VI) has been targeted for separation and reduction to precipitate in stripping phase which helps easy removal of chromium (Cr), and also yield useful end product. Aliquat 336 has been used as carrier for separation of Cr(VI). Various physico-chemical parameters have been optimized to maximize transport and precipitation of chromium-iron complex in stripping phase. The important physico-chemical parameters have been selected for response surface methodology to get optimum performance for %precipitation of Cr.

4.1 Theoretical background

4.1.1 Reaction mechanism and transport methodology

The chemistry of chromate ion was elaborately discussed in previous work [177]. However, in this work NaCl is used as stripping agent in place Na_2-EDTA because presence of electrolyte is necessary in electrochemical reaction. Nevertheless, aliquat 336 has been used as a carrier and the exchange reaction is as follows:

$$R_4N^+Cl^-_{(org)} + HCrO_4^- \rightleftharpoons (R_4N^+, HCrO_4^-)_{(org)} + Cl^- \tag{4.1}$$

The reaction mechanism is shown in Figure 4.1. The metal oxide $HCrO_4^-$ form complex (R_4N^+,$HCrO_4^-$) with carrier aliquat 336 at the feed-membrane interface [177]. The solute-carrier complex diffuses from feed membrane to strip membrane interface due to concentration gradient. The solute is re-extracted from solute carrier complex by stripping agent (NaCl) and binds with sodium ion to form $HCrO_4^-Na^+$ at strip membrane interface and diffuses back to bulk strip phase.

When electric field is applied to the strip phase, Fe^{2+} ion is released from the anode and water splits into H^+ and OH^- ion at the cathode.

In anode:

$$Fe_{(s)} \rightleftharpoons Fe^{2+}_{(aq)} + 2e^- \tag{4.2}$$

In cathode:

$$2H_2O + 2e^- \rightleftharpoons H_2 + 2OH^- \tag{4.3}$$

Under basic condition:

$$3Fe^{2+}_{(aq)} + Cr_2O^-_{4\,(aq)} + 4H_2O_{(l)} + 4OH^+_{(aq)} \rightleftharpoons 3Fe(OH)_3\downarrow + Cr(OH)_3\downarrow \tag{4.4}$$

As the Fe^{2+} ion is unstable, it tends to oxidize by reducing the Cr^{6+} to Cr^{3+} (refer

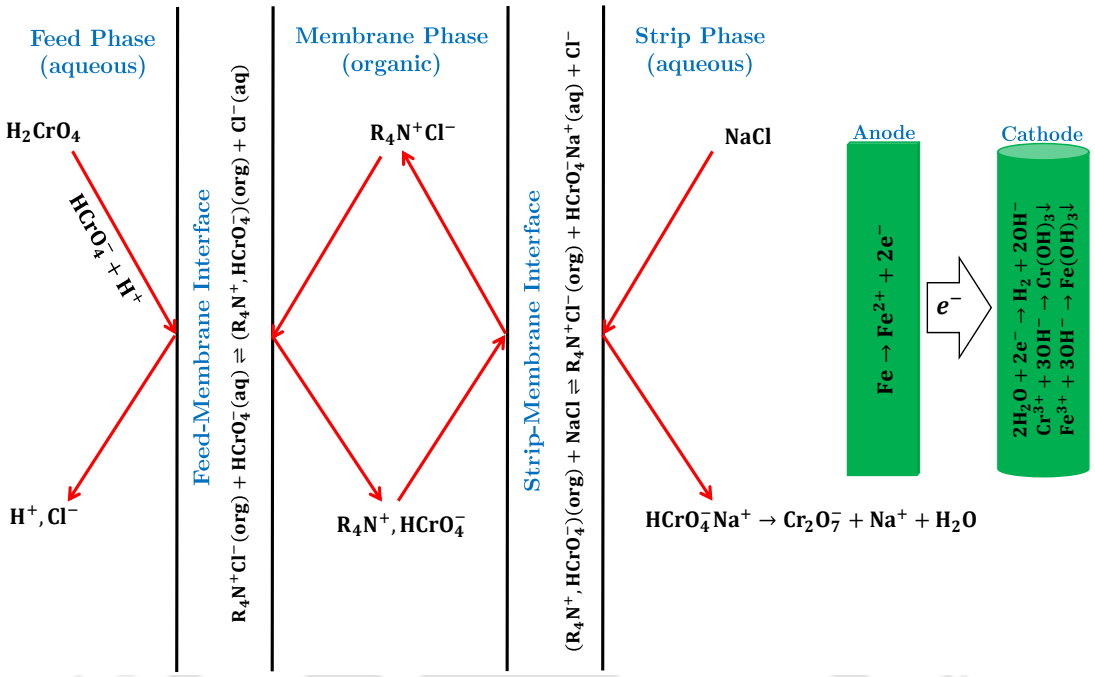

Figure 4.1: Reaction mechanism

Equation 4.2 and 4.5) [178–181].

Under acidic condition:

$$6Fe^{2+}_{(aq)} + Cr_2O^-_{7\,(aq)} + 14H^+_{(aq)} \rightleftharpoons Fe^{3+}_{(aq)} + 2Cr^{3+}_{(aq)} + 7H_2O_{(l)} \tag{4.5}$$

OH^- ion binds with Cr^{3+} and Fe^{3+} to form insoluble chromium-iron hydroxide [178, 179].

Co-precipitation:

$$Cr^{3+} + 3OH^- \rightleftharpoons Cr(OH)_3 \downarrow \tag{4.6}$$

$$Fe^{3+} + 3OH^- \rightleftharpoons Fe(OH)_3 \downarrow \tag{4.7}$$

4.1.2 Model calculation

It is assumed that only diffusional transfer of chromium occurs across the membrane. Due to fast chemical reaction, interfacial flux is neglected. As a result the metal concentration at the interfaces will be equal to equilibrium concentrations [182]. The

overall flux across the membrane can be described using the Fick's first law of diffusion (refer Equation 4.8):

$$J_{org} = \Delta_{org}^{-1}([R_4N^+, HCrO_4^-]_{i,f} - [R_4N^+, HCrO_4^-]_{i,s}) \tag{4.8}$$

where, $[R_4N^+, HCrO_4^-]_{i,f}$ and $[R_4N^+, HCrO_4^-]_{i,s}$ are the concentrations of Cr-aliquat 336 complex at feed-membrane and strip-membrane interfaces respectively. Δ_{org} is the diffusional resistance of the complex in membrane phase.

Solution of Cr(VI) with concentration 100 mg L^{-1} predominantly contains $HCrO_4^{-1}$ ion whose permeability can be written as:

$$P = \frac{J}{[HCrO_4^{-1}]_f} \tag{4.9}$$

where $[HCrO_4^-]_f$ is the concentration of $[HCrO_4^-]$ in the feed phase (mg L^{-1}) which is not constant. Then the total flux J (mg cm^{-2} s^{-1}) can be calculated according to the following equation:

$$J = \left(\frac{V}{S}\right)\left(\frac{d[HCrO_4^-]_f}{dt}\right) \tag{4.10}$$

where V is the volume of aqueous solution and S is the effective surface area of strip-membrane interface (cm^2). Combining Eqs. 4.9 and 4.10, and integrating with following boundary conditions:

$[HCrO_4^-]_f = [HCrO_4^-]_{f,0}$ at t=0

$[HCrO_4^-]_f = [HCrO_4^-]_{f,t}$ at t=t

The final equation may be expressed as follows:

$$\ln\left(\frac{[HCrO_4^-]_{f,t}}{[HCrO_4^-]_{f,0}}\right) = -\frac{V}{S}Pt \tag{4.11}$$

4.2 Results and discussion

4.2.1 Three-phase SLM study

In this section three-phase SLM study has been performed to extract and recover Cr(VI). Previous study [177] of three phase SLM shows optimum concentration of Cr(VI) in feed section was 100 mg L^{-1} Cr(VI). As observed by Bera et al. [175] tannery wastewater contains 80 mg L^{-1} of Cr(VI). Hence the concentration of Cr(VI) in feed phase was maintained at 100 mg L^{-1} while other parameters have been re-optimized for the best precipitation of chromium in strip phase.

4.2.1.1 Selection of strippant

It is necessary that strip phase should have electrolytic property in an electrochemical process. Di-sodium ethylenediaminetetra acetic acid (a.k.a Na_2-EDTA), used in the previously (Chapter 3 [177]), does not have electrolytic property. Hence, four types of strip phase solutions such as H_2SO_4 [123, 183], NH_4Cl [184, 185], NaCl [185, 186], and NaOH [3, 122, 187–189] have been investigated to find the better one suited for the said purpose. The concentration of strip solution in each case was maintained at 0.1 M. The experimental results are plotted in Figure 4.2. The reduction of Cr(VI) to Cr(III) and subsequent precipitation as chromium-iron hydroxide were possible in case of NH_4Cl and NaCl with 14.53% and 21.17% efficiency respectively. However in case of H_2SO_4 and NaOH as a strip solution no such precipitation was observed. At high concentration of acid or alkaline solution, oxide or hydroxide layer is formed on iron anode plate which inhibits iron plate for further formation of iron-hydroxide complex [181, 190–193]. The percent recovery of Cr(VI) in strip phase for H_2SO_4 and NaOH are 2.58% and 32.90% respectively. NaCl, being a common edible salt, is both physiologically as well as environmentally benign. Hence, NaCl was selected as a stripping agent for further study.

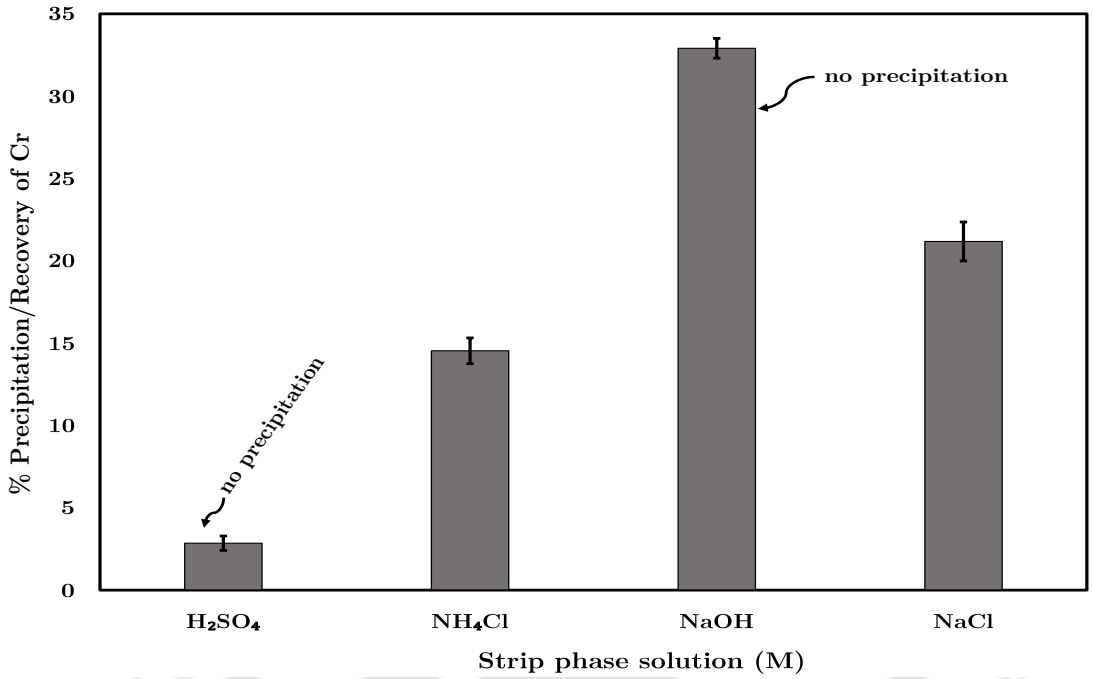

Figure 4.2: % Precipitation/Recovery of Cr with various strip phase solution; solvent = sunflower oil, feed phase concentration of Cr(VI)=100 mg L^{-1}.

4.2.1.2 Effect of pH of feed phase

The reaction mechanism (vide Figure 4.1) reveals that role of proton is very significant in case of extraction process. The pH of aqueous solution plays an important role towards extraction of chromium. The experimental results are demonstrated in Figure 4.3. The experiment was done in the range of 2-8 pH by appropriately adding HCl and NaOH. At low pH the efficiency of extraction is significantly less as a result the precipitation of chromium in strip phase is also less. This is due to the dimerization reaction of $HCrO_4^-$ at acidic pH where $Cr_2O_7^{2-}$ predominates [173, 174]. As a result the complexation with R_4N^+ ion is not proper. The maximum extraction and precipitation efficiency are 32% and 20.6% respectively at pH 4.5. Again the separation efficiency of chromium marginally decreased with increase in pH of aqueous solution due decrease in proton concentration [43, 122]. At higher pH, CrO_4^{2-} dominates in the solution [174] which is less accessible than $HCrO_4^-$ for complexation reaction with R_4N^+ ion [122, 194].

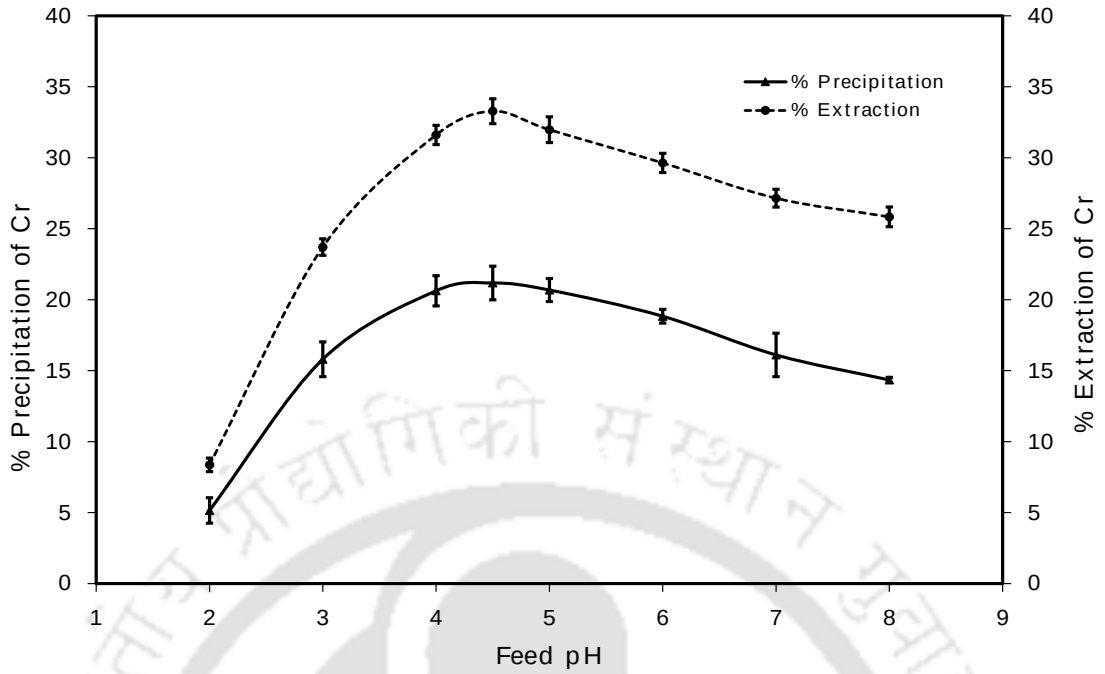

Figure 4.3: % Precipitation of Cr with different feed phase pH; solvent = sunflower oil, feed phase concentration of Cr(VI)=100 mg L^{-1}.

4.2.1.3 Effect of concentration of strip phase

The reaction mechanism discussed in Section 4.1.1 (vide Figure 4.4) reveals that Na^+ plays an important role in stripping process as it forms $HCrO_4^-Na^+$ salt which aids re-extraction of chromium at strip-membrane interface and subsequent diffusion to the bulk of strip phase [189]. Hence, concentration of Na^+ ion in strip phase solution affects the rate of transport of chromium. The concentration of NaCl in strip phase is varied from 0.05 M to 0.3 M. The results are shown in Figure 4.4. It is observed that the extraction and precipitation of chromium increases with increase in concentration of NaCl up to 0.15 M where the %extraction and %precipitation of chromium reach 42.1% and 34.5% respectively. Further increase in concentration of NaCl does not help as the efficiency appears to hit a saturation level. This happens due to generation of high osmotic pressure in the SLM which causes leaching out of aliquat 336 with sodium ions [186].

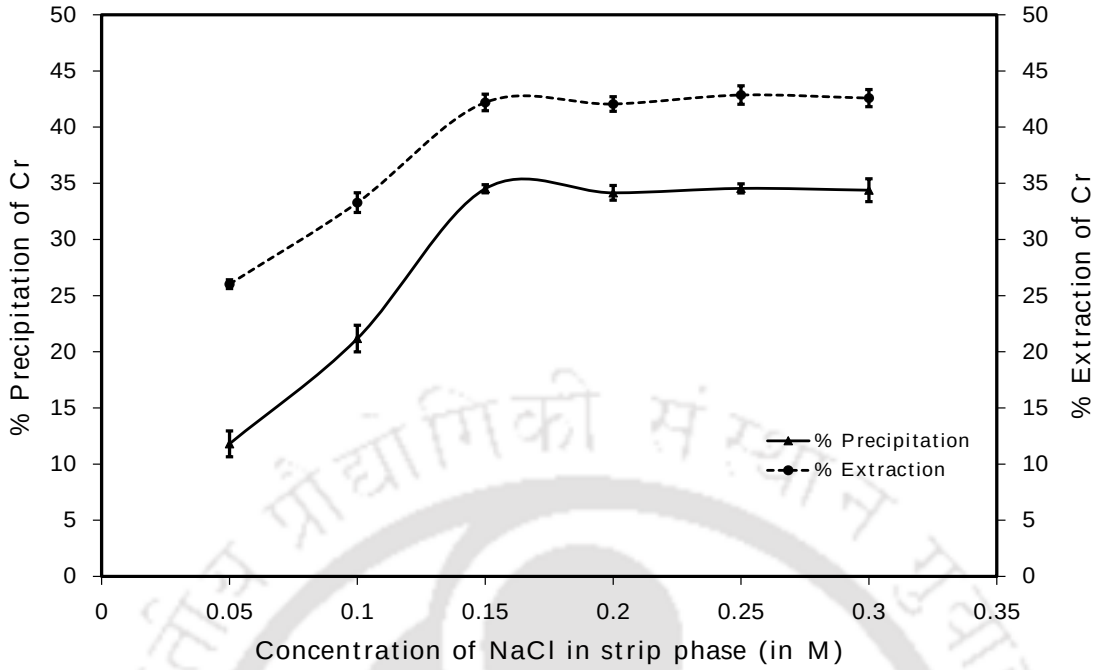

Figure 4.4: Effect of concentration of NaCl in stripping solution on % extraction/precipitation of Cr; solvent = sunflower oil, feed phase concentration of Cr(VI)=100 mg L^{-1}.

4.2.1.4 Effect of pH in strip phase

Study reveals that OH^- also takes part in forming metal-carrier complex with aliquat 336 which helps metal ion to be extracted from strip-membrane interface to bulk strip phase [176, 195–197] (refer Equations. 4.12 and 4.12).

$$R_4N^+OH^-_{(org)} + HCrO_4^- \rightleftharpoons (R_4N^+, HCrO_4^-)_{(org)} + OH^- \tag{4.12}$$

$$R_4N^+Cl^-_{(org)} + HCrO_4^- \rightleftharpoons (R_4N^+, HCrO_4^-)_{(org)} + Cl^- \tag{4.13}$$

Hence the pH of strip phase was varied by adding NaOH to measure its effect on the transport of chromium ions as well as its precipitation efficiency. The results are shown in Figure 4.5. It appears that with increase in strip phase pH the efficiencies of extraction and precipitation are increased and reached over 95% at pH 8. Further increase of pH does not help as the transport of chromium reaches its saturation limit

due to low concentration of chromium in the feed phase. At lower pH, the reactions Eqs.(4.5) and (4.6) explain the limitation in formation of chromium-iron complex as discussed earlier [180, 181].

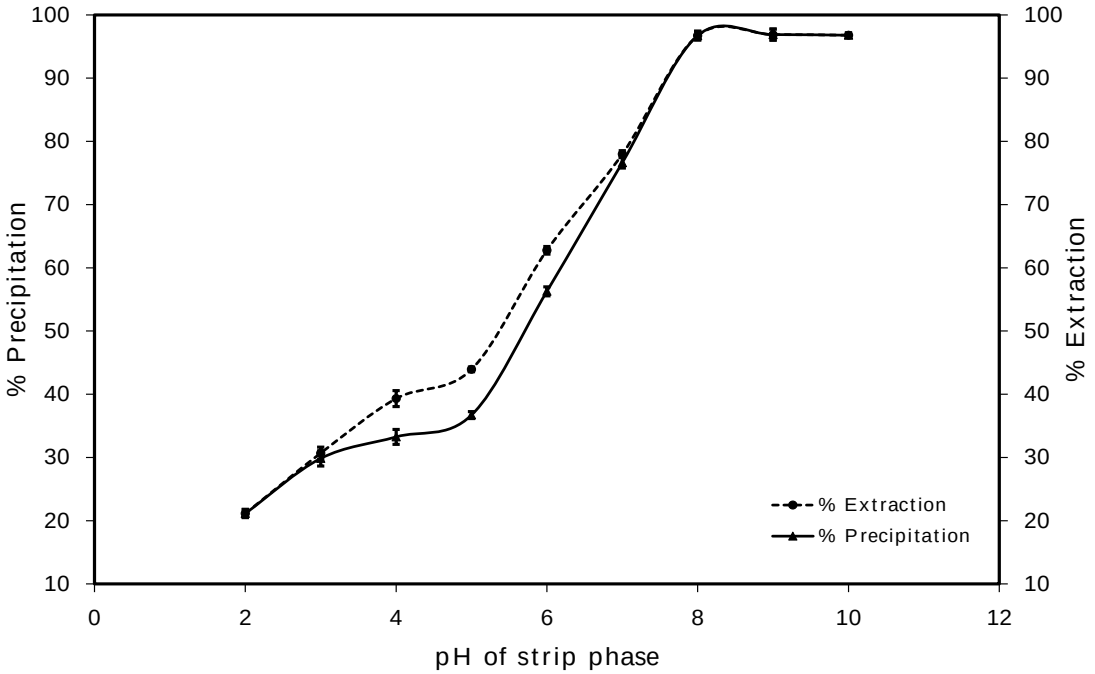

Figure 4.5: Effect of pH of strip phase on % extraction/precipitation of Cr; solvent = sunflower oil, feed phase concentration of Cr(VI)=100 mg L^{-1}, strip phase conc.= 0.15M.

4.2.1.5 Effect of concentration of carrier

In this study, concentration of carrier is varied from 0 to 3% (v/v) and the experimental results are shown in Figure 4.6. Without the presence of any carrier the separation efficiency of chromium is very low. As the concentration increases upto 1% (v/v) efficiency of extraction increases too, which eventually helps to increase the precipitation efficiency. However further increase in carrier concentration does not help. The viscosity (at room temperature) of carrier aliquat 336 (1.048 Pa s) is much higher than viscosity of sunflower oil (0.036 Pa s). Hence at increased carrier concentration viscosity of LM increases. Higher viscosity of LM reduces the diffusional rate of chromium due to increase of mass transfer resistance in the LM [177, 188].

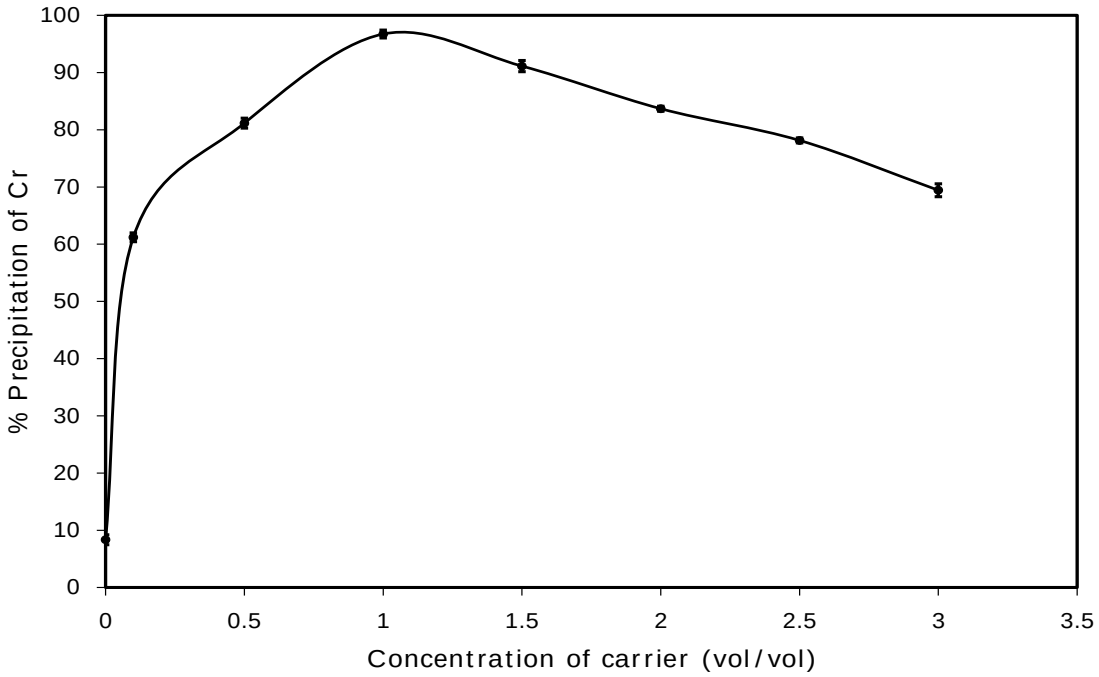

Figure 4.6: Effect of concentration of carrier on % precipitation of Cr; solvent = sunflower oil, feed phase concentration of Cr(VI)=100 mg L^{-1}, strip phase conc.= 0.15M, strip phse pH=8.

4.2.1.6 Role of electric field for transportation of metal ion

The importance of electric field for the separation/transport of chromium ion has been studied/ compared with the case when no electric field was used in strip phase solution. The profile of concentration of chromium against time in the feed and strip phases have been plotted in Figure 4.7. The concentration of chromium in feed and strip phases reached ∼51 mg L^{-1} and ∼45 mg L^{-1} respectively after 8 h of run when no electric field was applied. Whereas, the concentration of chromium in feed phase decreased rapidly when electric field was applied and it reached ∼ 3 mg L^{-1} after 8 h. Concentration of chromium in strip phase never rose above 2.5 mg L^{-1} on application of electric field and finally reached below detection limit. The confirmation of presence of chromium in the precipitates in strip phase has been discussed in Section 4.2.2.3.

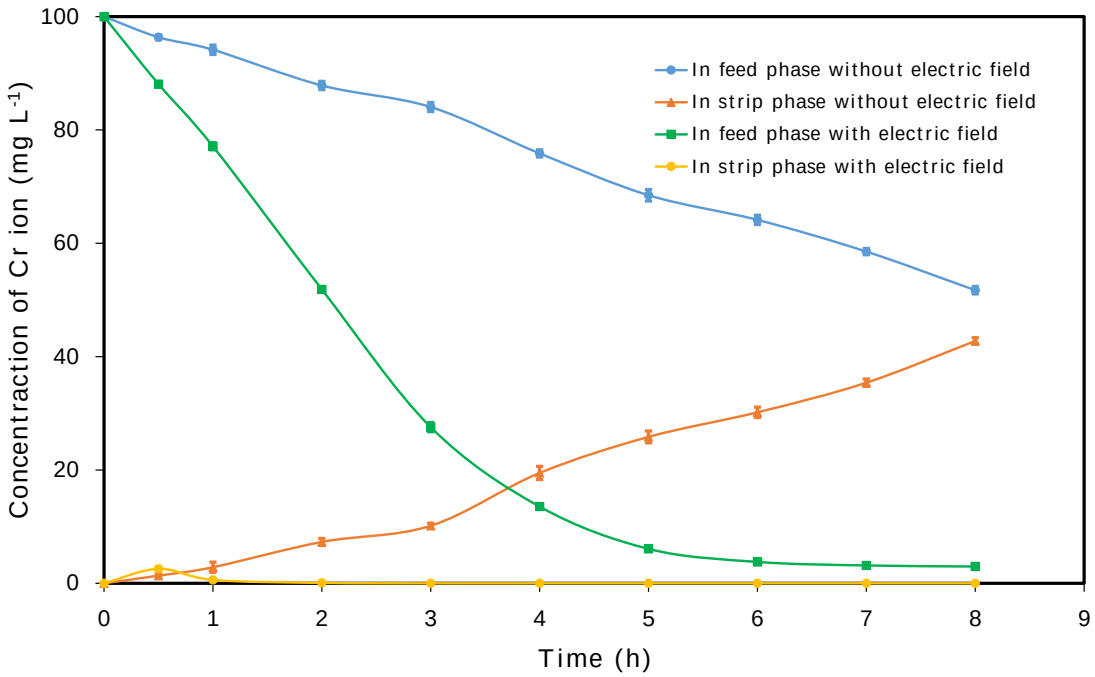

Figure 4.7: Three phase SLM with and without electric field; solvent = sunflower oil, feed phase concentration of Cr(VI)=100 mg L^{-1}, strip phase conc.= 0.15M, strip phse pH=8, concentration of carrier = Aliquat 1% (vol/vol).

4.2.1.7 Effect of electric potential across the electrodes

In electrochemical process electric potential is the parameter which controls the rate of electrochemical reaction inside the reactor [190, 198–201]. The %extraction and %precipitation of chromium were measured by varying electric potential within the range of 0.5 to 4 V DC inside the strip phase. The transport of chromium reached its saturation limit of ∼97% at around 2.5 V DC (refer Figure 4.8). Further increase of electric potential does not help.

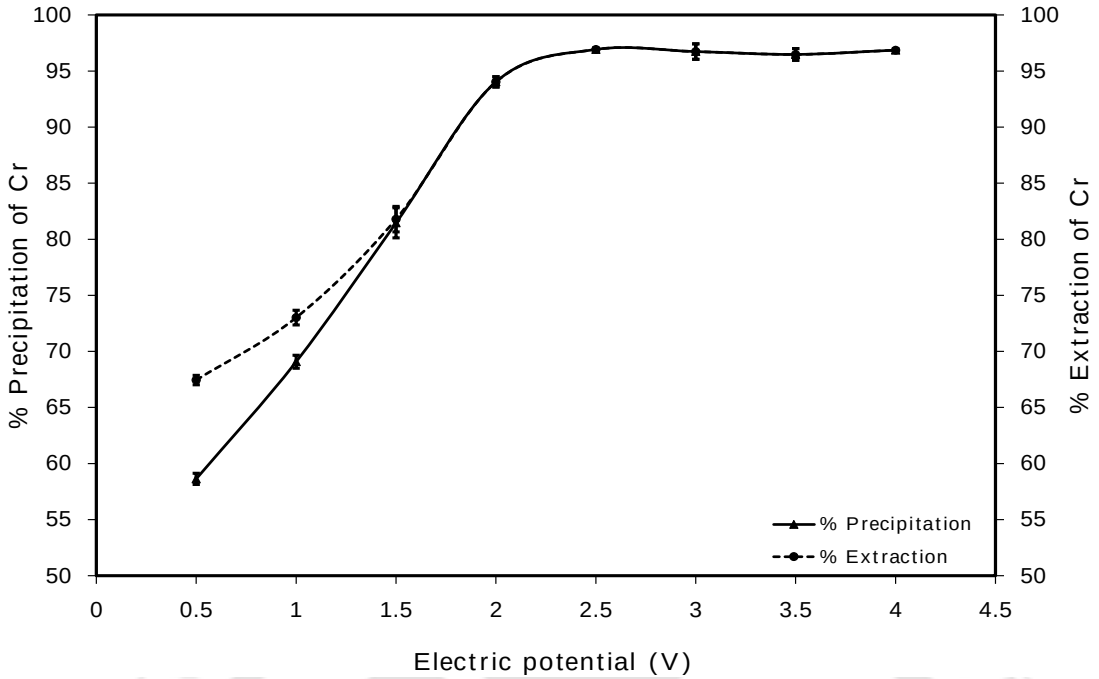

Figure 4.8: Effect of electric potential on % extraction/precipitation of Cr; solvent = sunflower oil, feed phase concentration of Cr(VI)=100 mg L^{-1}, strip phase conc.= 0.15M, strip phse pH=8, concentration of carrier = Aliquat 1% (vol/vol).

4.2.1.8 Required period of operation

The required period of SLM operation was identified through experimentation in order to know how much time would be ideal to reach the saturation limit of extraction/recovery and/or precipitation. Some reliable information on this issue is already available in Figure 4.7 which indicates that the saturation point is reached after 8 h of operation. Hence further experiment was carried out for 8 h and samples were collected at fixed time interval of 1 h. The results are plotted in Figure 4.9. It is observed that precipitation of chromium reached over 85% within 4 h and saturation point of ∼96% is reached by 6 h time. Increase in %precipitation is not significant beyond 6 h and it settles at ∼97% at 8 h time. The permeability value is obtained from experimental results and concentration profiles of Cr(VI) at feed phase have been used to fit the model equation (Equation 4.11). Both the experimental as well as model values are plotted in Figure 4.9. The model is found to be in good agreement

with experimental values.

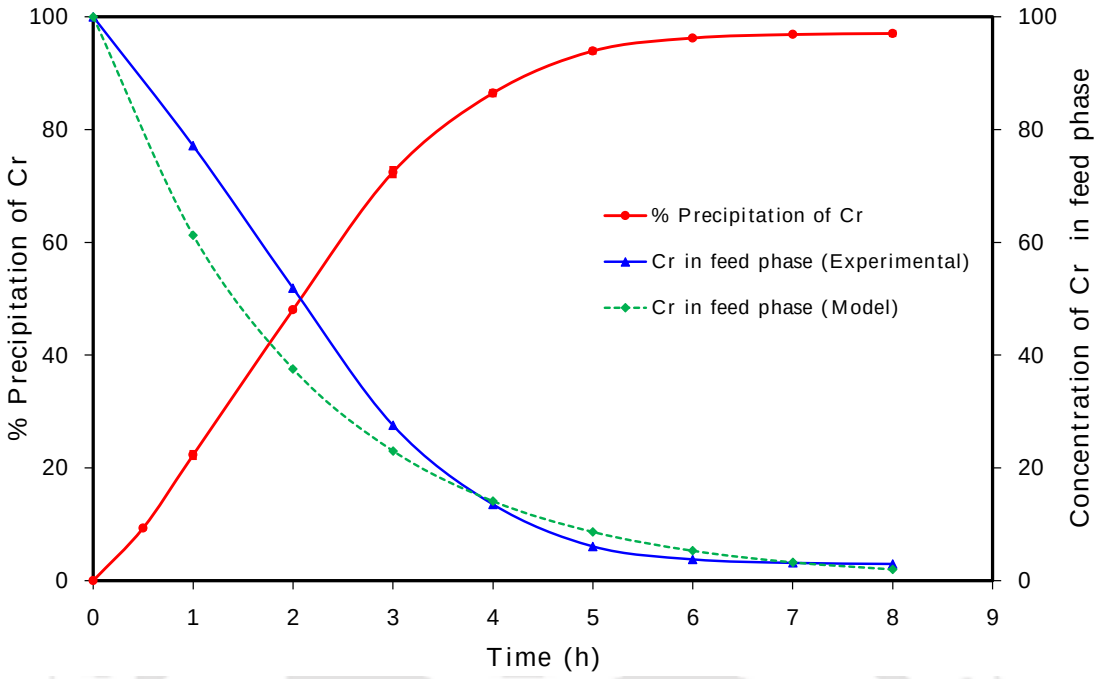

Figure 4.9: Saturation period of transport of Cr; solvent = sunflower oil, feed phase concentration of Cr(VI)=100 mg L^{-1}, strip phase conc.= 0.15M, strip phse pH=8, concentration of carrier = Aliquat 1% (vol/vol), voltage = 2.5 V DC.

4.2.1.9 Effect of stirring in aqueous phase

A minimum degree of stirring is required for effective and efficient transport of chromium. The effect of stirring was studied by varying the speed of stirring within the range of 0-250 rpm. The results are shown in Table 4.1. It is observed that precipitation of chromium reaches almost ∼97% when stirring speed is 120 rpm. Further increase in stirring speed does not help in significant improvement of %precipitation of chromium. Hence, the ideal stirring speed of 120 rpm is maintained in all successive experimentations.

Table 4.1: Effect of stirring condition of aqueous phases on transport of Cr; solvent = sunflower oil, feed phase concentration of Cr(VI)=100 mg L^{-1}, strip phase conc.= 0.15M, strip phse pH=8, concentration of carrier = Aliquat 1% (vol/vol), voltage = 2.5 V DC, period of operation = 6 h

Stirring speed (RPM)	% Precipitation of Cr
0	17.89
60	88.09
120	96.73
200	96.40
250	96.94

4.2.1.10 Fed batch system

In fed batch process, feed phase is topped up periodically with fresh solution of high solute concentration to bring the feed phase to initial concentration level, i.e. 100 mg L^{-1} in the present case. This top-up is done whenever the concentration of solute in feed phase is found to be depleted below a certain level. This study is very important to know whether the LM is able to bear the "shock loading" and how many such top-up cycles can be treated by the same strip solution over and again. Samples (i.e both feed and strip phase) are periodically collected and analyzed throughout the experimentation cycles. The results are shown in Figure 4.10. After every 4 h, make up feed was added to increase the Cr(VI) concentration to 100 mg L^{-1}. The "shock loading" is handled by the system however the efficiency decreases marginally as the residual solute concentrations in feed and strip phases at the end of feed cycles increased over the runs. The solute concentrations at the feed phase after 4 h, 8 h and 12 h were 13.3 mg L^{-1}, 18.5 mg L^{-1} and 33.2 mg L^{-1} respectively. Whereas, solute concentrations of strip phase (which is not precipitated) increased from 0 mg L^{-1} (after 4 h) to 12.24 mg L^{-1} (after 12 h). As a result the %precipitation of chromium slowly decreased too. With increase in concentration of chromium in the strip phase,

corrosion of iron is lowered that eventually increases iron surface passivation. As a result it increases the corrosion potential of iron and lower the corrosion current [202].

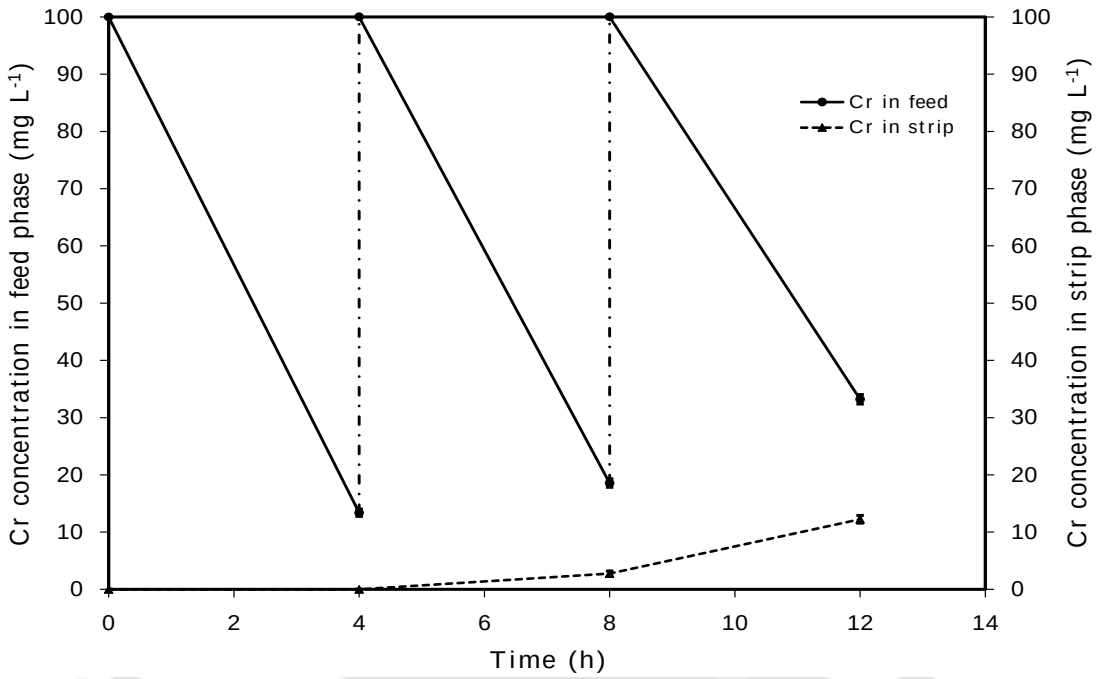

Figure 4.10: Effect of stirring condition of aqueous phases on transport of Cr; solvent = sunflower oil, feed phase concentration of Cr(VI)=100 mg L^{-1}, strip phase conc.= 0.15M, strip phse pH=8, concentration of carrier = Aliquat 1% (vol/vol), voltage = 2.5 V DC, period of operation = 12 h, speed of stirring = 120 rpm.

4.2.2 Synthesis and characterization of chromium-iron oxide

The reaction mechanism discussed in Sec. 4.1.1 describes that insoluble chromium-iron hydroxide forms at strip phase and the said insolubility property leads to precipitation of chromium-iron hydroxide. The precipitated complex was washed by deionized water and oven-dried at 80°C for 12h. The dried sample was further calcined at 500°C for 3h.

4.2.2.1 X-ray diffraction (XRD) spectroscopy

Powder X-ray diffraction (PXRD) pattern of Cr_2O_3−Fe_2O_3 was obtained in air at room temperature on a Rigaku (Model: SmartLab) XRD analyzer operating at 45

kV and 112 mA using Cu Kα (λ = 1.5406 $\AA$) radiation. The XRD results (vide Figure 4.11) show that chromium oxide forms solid solution with Fe_2O_3 as discussed elsewhere [203]. The chromium-iron complex is formed in the strip phase solution as indicated by the slight shift in major peak of XRD (vide Figure 4.12) at 34.5-37.5 degree. The characteristic peaks (vide Figure 4.11) at 2θ exactly matches the crystalline plane which is reported elsewhere [204].

The average crystal size is found to be 31 nm which was calculated from the peak of XRD using Scherrer's formula d=Kλ/B cos θ, where d is the diameter in angstrom, K is the constant (shape factor), B is the half maximum linewidth, and λ is the wavelength [205].

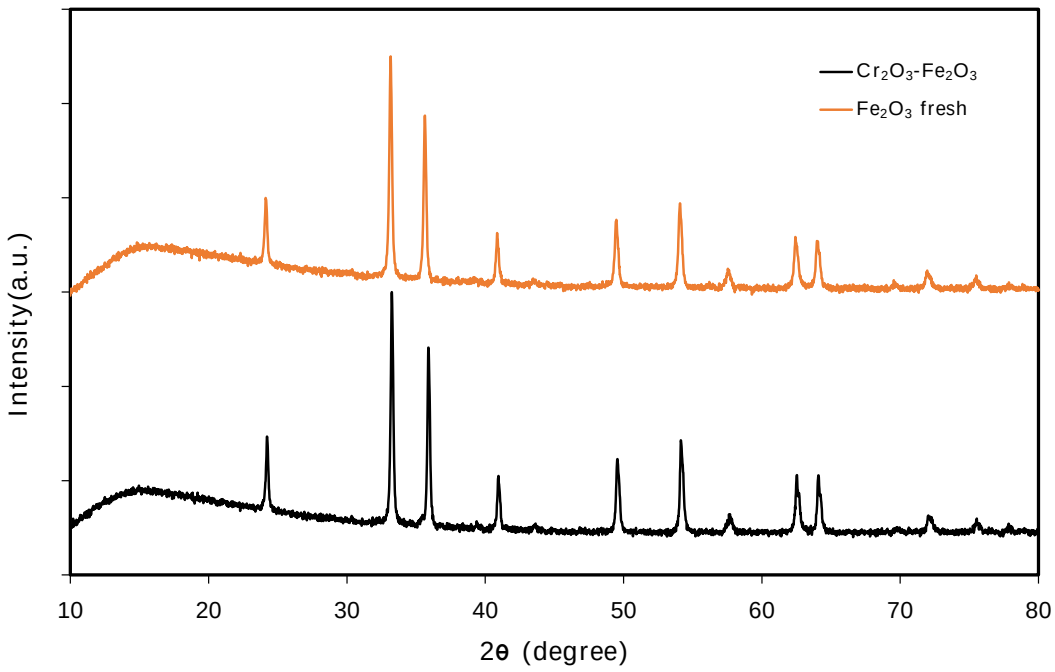

Figure 4.11: X-Ray diffraction data of chromium-iron oxide

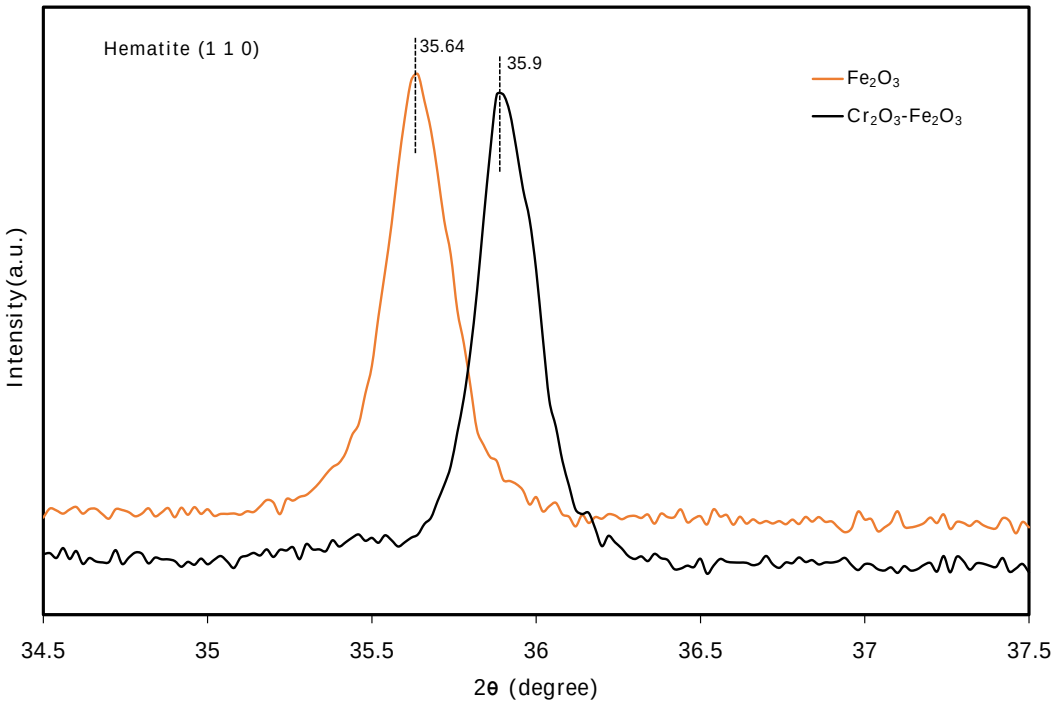

Figure 4.12: X-Ray diffraction of main peak spectra of hematite (1 1 0) of the Fe_2O_3 and Cr_2O_3-Fe_2O_3

4.2.2.2 FESEM

Tests on Field emission scanning electron microscope (FESEM) (vide Figure 4.13) was performed by Zeiss (Model: Sigma 300) with an accelerating voltage of 5 kV. The samples were drop cast on aluminium and placed on a stub containing carbon tape. The stub containing samples was coated with conducting gold layer using a sputtering unit for 120 s before the analysis.

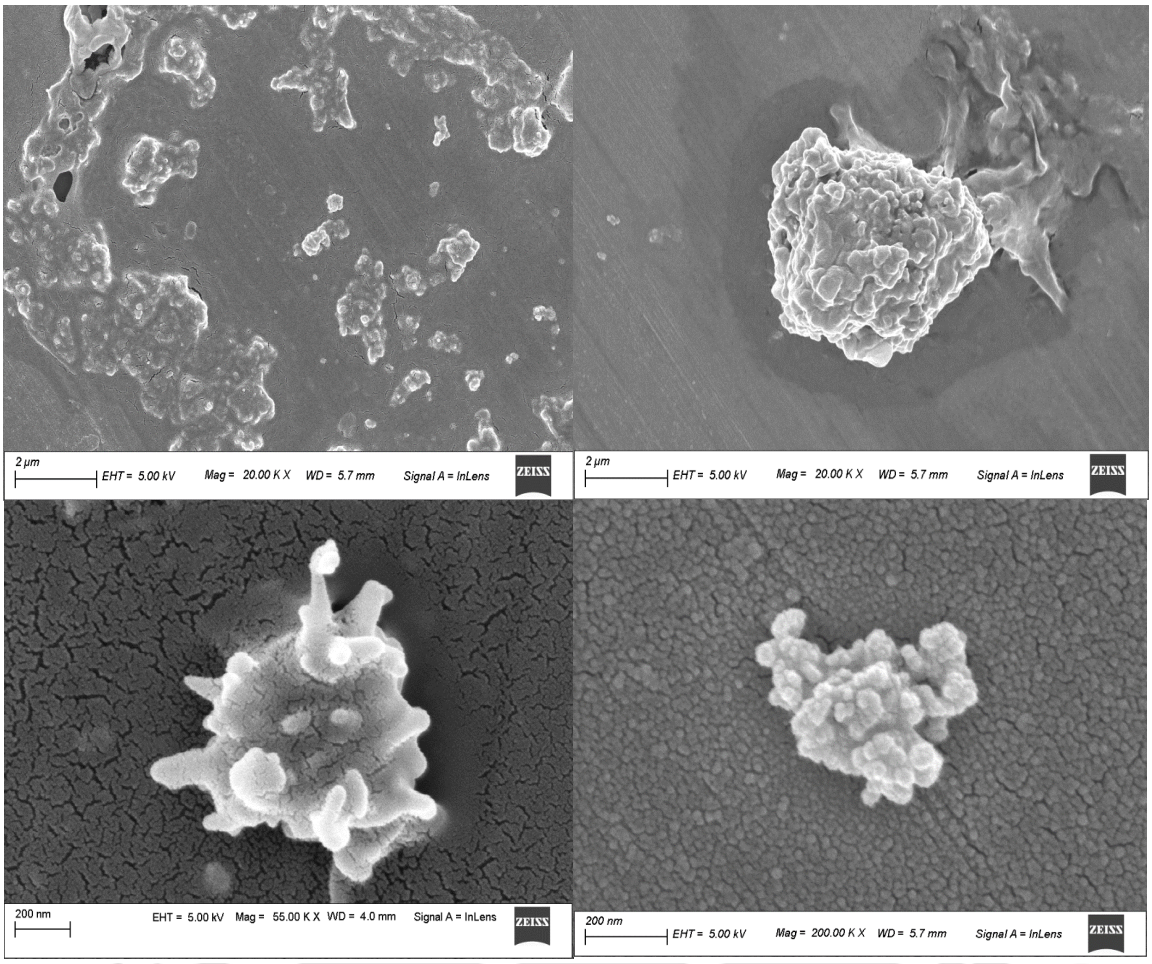

Figure 4.13: FESEM image of chromium-iron oxide

4.2.2.3 TEM

Transmission electron microscopy (TEM) was also performed by JEOL (Model: 2100F) using carbon coated Cu TEM grid. The micrograph of synthesized particle are shown in Figure 4.14. The TEM image in Figure 4.14 shows that the range of particle size is within 100 nm. An energy dispersive X-ray (EDX) in TEM (refer Figure 4.15) was also done for elemental analysis. The sample was grinded, dispersed in ethanol solvent and placed on carbon coated Cu TEM grid. The TEM-EDX analysis confirms the presence of oxygen, chromium, and iron with 25.90, 7.75 and 42.49 weight percent. Also copper has been detected due to use of Cu TEM grid.

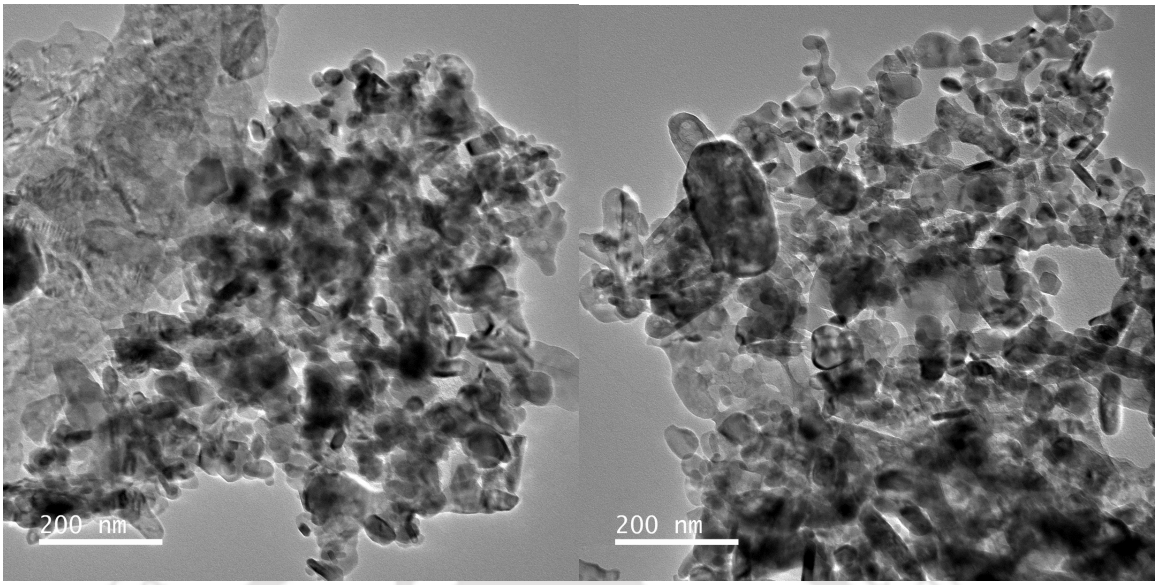

Figure 4.14: TEM image of chromium-iron oxide

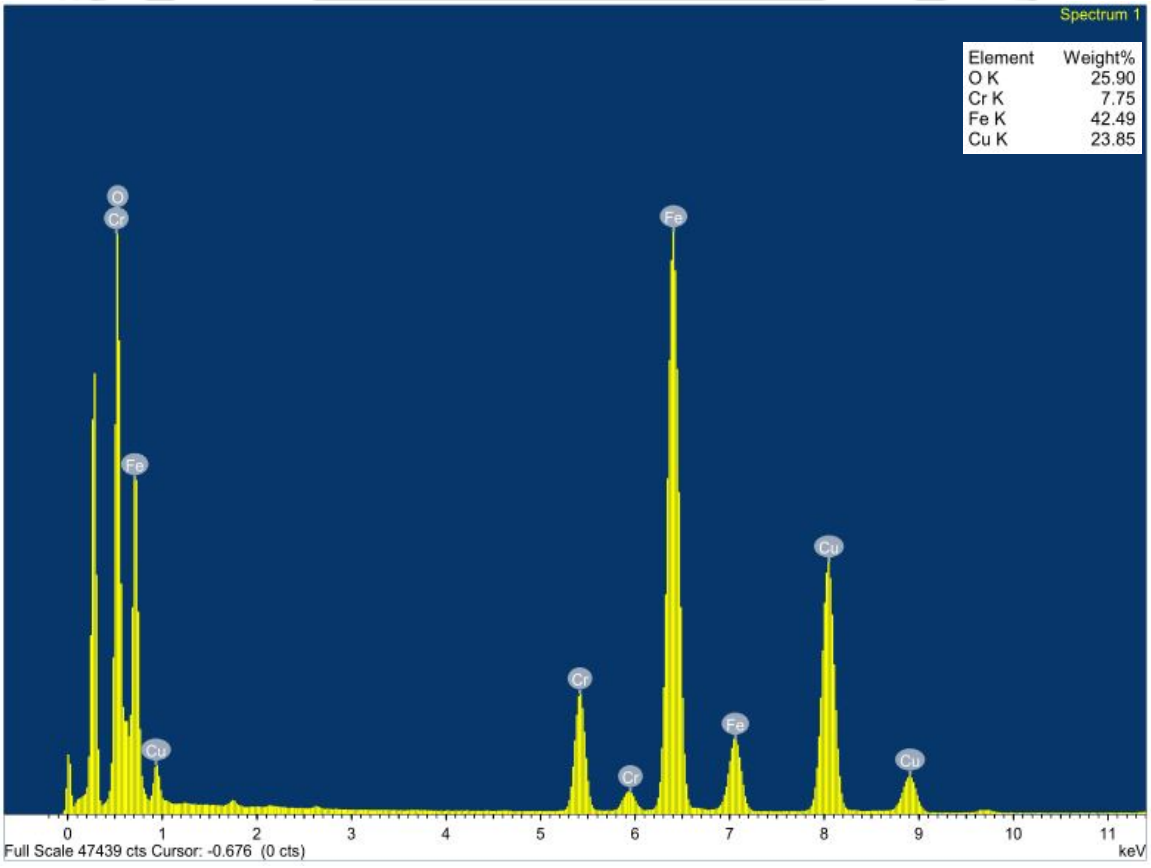

Figure 4.15: TEM-EDX spectra of chromium-iron oxide

4.2.2.4 FTIR

Fourier-transform infrared spectroscopy (FTIR) (make: Shimadzu, model: IRAffinity-1) of chromium-iron oxide (refer Figure 4.16) was done by mixing calcinated complex with excess amount of dried potassium bromide (KBr). In general the metal oxide symbolizes the peaks below 1000 cm^{-1} due to inter-atomic vibrations [206]. The transmission was recorded within the range of 400 cm^{-1} to 1000 cm^{-1}. The IR bands near 418 cm^{-1}, 457 cm^{-1}, 472 cm^{-1} and 547 cm^{-1} corresponds to the Cr-O bond stretching vibration [206, 207]. A peak near 472 cm^{-1} and 550 cm^{-1} corresponds to metal-oxygen stretching vibration [208–210]. All the observed peaks are well in agreement with referred literatures.

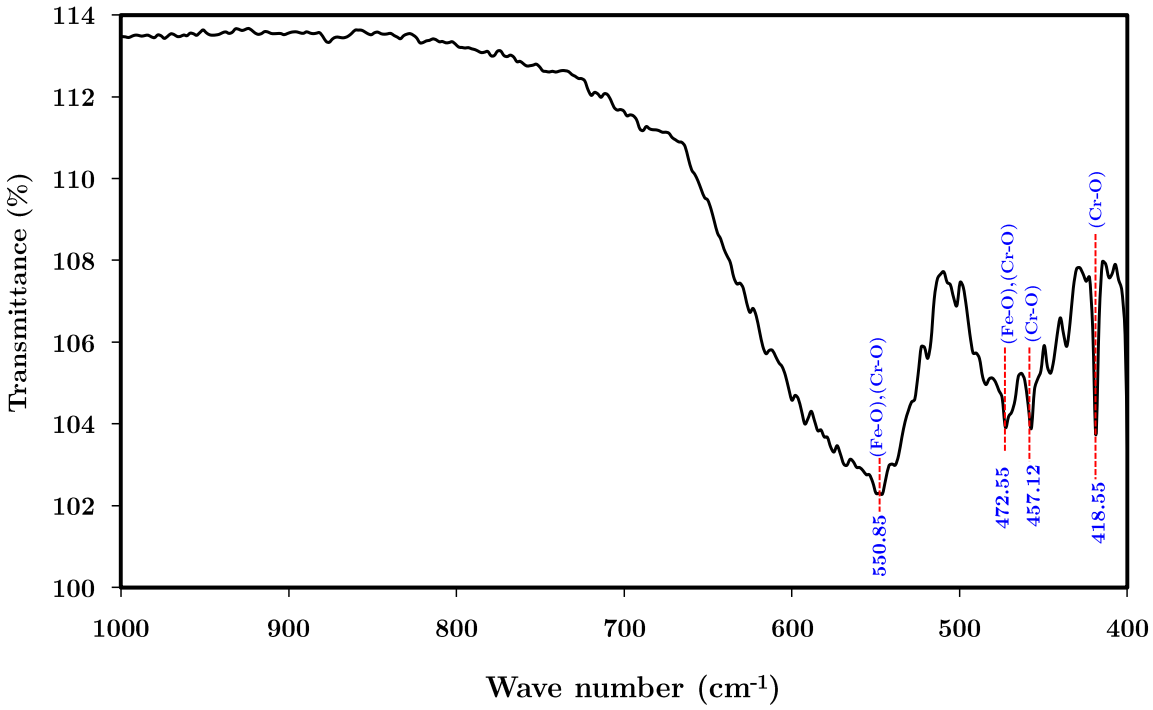

Figure 4.16: FTIR spectra of chromium-iron oxide

4.2.3 Experimental optimization of operating parameters in SLM

From experimental data, it is observed that the most influencial parameters for transport of chromium are strip phase concentration (in M), strip phase pH and concentration of carrier (% v/v) in LM. Hence, these three parameters have been chosen as input factors with %precipitation of chromium as output parameter (R1). The different ranges of input parameters are as follows: concentration of strip phase (denoted by A) with range of 0.05 to 0.3 M, strip phase pH (denoted with B) with range of 2 to 10, concentration of aliquat 336(denoted with C) with range 0.1% to 3% (v/v). Other parameters are kept constant such as solute concentration in feed phase at 100 mg L^{-1}, electric potential at 2.5 V DC, speed of stirring at 120 rpm, and run time at 8 h. Table 4.2 shows the experimental output with predicted ones which were calculated from input parameters through the quadratic model. Table 4.3 shows ANOVA study of %precipitation of chromium. The regression model equation for %precipitation of chromium is given by Equation 4.14.

$$\begin{aligned}\%\text{Precipitation of Cr} =& 51.81 + 11.04 \times A + 21.45 \times B - 4.36 \times C \\ &+ 10.59 \times A \times B + 6.41 \times A \times C - 5.24 \times B \times C \\ &- 20.97 \times A^2 + 5.58 \times B^2 - 5.89 \times C^2\end{aligned} \tag{4.14}$$

To check the applicability of model, fischer variation (F value), probability values (p value) and correlation coefficient (R^2) are used. As evident from the calculated model F-values (i.e. 16.07) and very low p values < 0.0001 (vide Table 4.3), model is highly significant (for model significance p-value should be < 0.05). Whereas, the predicted R^2 of 0.8344 is in reasonable agreement with the adjusted R^2 of 0.8771 for precipitation of chromium. The signal to noise ratio *a.k.a* adequate precision value greater than 4 is desirable. The adequate precision for precipitation of chromium is

13.14 which is quite high against minimum desirable value of 4. The scattering points of predicted values across the horizontal line of residuals (vide Figure 4.17a) are in the range of ±3% which suggests that model is well fitted. Figure 4.17b presents the correlation between predicted values and actual or experimental values of %precipitation of chromium. Experimental results are found in actual values whereas, predicted values are evaluated from model. This predicted values were compared with experimental results to verify consistency and acceptability of empirical model (vide Figure 4.17b). The scattered points over and under the diagonal line reflects the overestimation and underestimation of design points. ANOVA (vide Table 4.3) is used to check significance and fitness of model.

In order to understand the interaction between parameters or the relation between input factors (i.e. concentration of NaCl in strip phase, pH of strip phase and concentration of aliquat in sunflower oil) required for optimum condition for %precipitation of chromium is illustrated in Figure 4.18.

The statistical optimization study of all three parameters with specific ranges (see Table 4.4) is done by design of experiments with the help of Design Expert 7.0 software. The calculated optimum parameters with predicted results are as follows: concentration of strip phase should be 0.23 M, pH of strip phase should be 10, and the concentration of carrier should be 0.75% (v/v). The resulting precipitation of chromium is expected at 86.22%. The desirability value of optimized outcome is 1.00. The desirability value ranges between 0.0 (undesirable) and 1.0 (desirable). The experiment was done as per the optimized parameters and the precipitation of chromium was found to be 88.48%. The error is only 2.55%.

Table 4.2: Design Arrangement and Experimental Responses for Central Composite Design (CCD)

Run	factor 1:A, strip phase conc.(M)	factor 2:B, strip phase pH	factor 3:C, carrier conc.(%vol.)	response 1: R1, %extraction	
				Actual	Perd
1	0.17	6.00	1.55	51.24	51.81
2	0.17	2.00	1.55	24.29	35.94
3	0.05	10.00	0.10	49.84	46.36
4	0.05	2.00	3.00	11.34	3.10
5	0.30	10.00	3.00	68.26	70.42
6	0.17	6.00	1.55	51.97	51.81
7	0.30	10.00	0.10	68.42	76.79
8	0.17	6.00	0.10	48.14	50.28
9	0.30	2.00	0.10	7.27	2.24
10	0.30	2.00	3.00	13.2	16.82
11	0.05	6.00	1.55	11.24	19.80
12	0.17	6.00	3.00	44.29	41.56
13	0.17	6.00	1.55	51.57	51.81
14	0.17	0.00	1.55	91.07	78.83
15	0.17	6.00	1.55	51.86	51.81
16	0.05	10.00	3.00	9.17	14.33
17	0.17	6.00	1.55	51.39	51.81
18	0.05	2.00	0.10	16.21	14.18
19	0.30	6.00	1.55	51.03	41.88
20	0.17	6.00	1.55	51.68	51.81

Table 4.3: Analysis of variance (ANOVA) for respective response surface quadratic models

Source	Sum of squares (SS)	Degree of freedom (DF)	Mean square (MS)	F-value	p value Prob>F	Remarks
%Precipitation of Cr						
Model	9822.34	9	1091.37	16.07	<0.0001	
A	1218.31	1	1218.31	17.94	0.0017	
B	4598.88	1	4598.88	67.72	<0.0001	
C	190.27	1	190.27	2.80	0.1251	In this
AB	897.82	1	897.82	13.22	0.0046	case A, B,
AC	329.09	1	329.09	4.85	0.0523	AB, A^2 are
BC	219.35	1	219.35	3.23	0.0125	significant
A^2	1208.81	1	1208.81	17.80	0.0018	model
B^2	85.55	1	85.55	1.26	0.2879	
C^2	95.32	1	95.32	1.40	0.2635	
Residual	679.11	10	67.91			
Lack of fit	678.73	5	135.75	1769.90	<0.0001	
Pure error	0.38	5	0.077			
R^2=0.9353, R^2_{adj}=0.8771, R^2_{pred}=0.8344, Adequate precision=13.143						

Table 4.4: Optimization constraints for %precipitaion of Cr

Name	Goal	Lower limit	Upper limit	Lower weight	Upper weight	Importance
Concentration of Nacl in strip phase (M)	in range	0.05	0.3	1	1	3
pH of strip phase	in range	2	10	1	1	3
Concentration of carrier (volume%)	in range	0.1	3	1	1	3
%precipitation of Cr	maximize	7.27	91.07	1	1	3

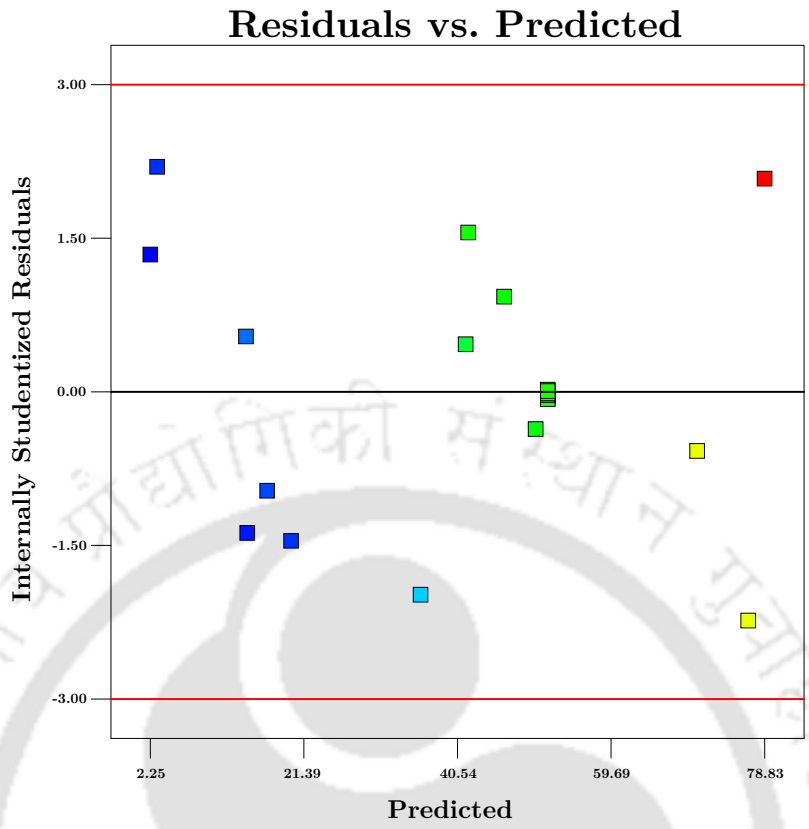

(a)

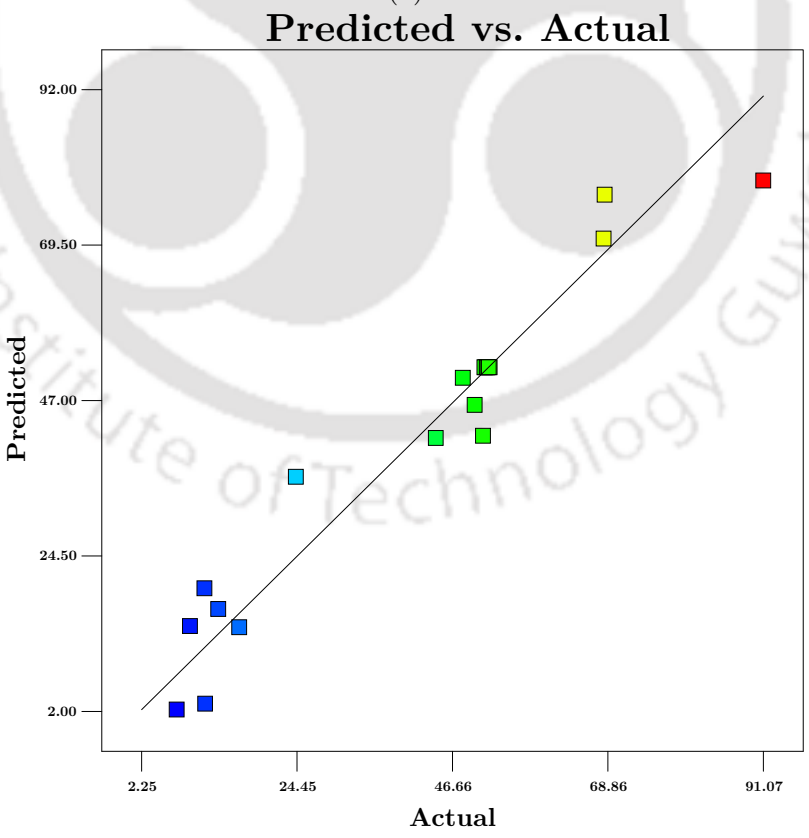

(b)

Figure 4.17: Residual versus pericted graphs 4.17a and predicted versus actual graphs 4.17b for %precipitation of Cr.

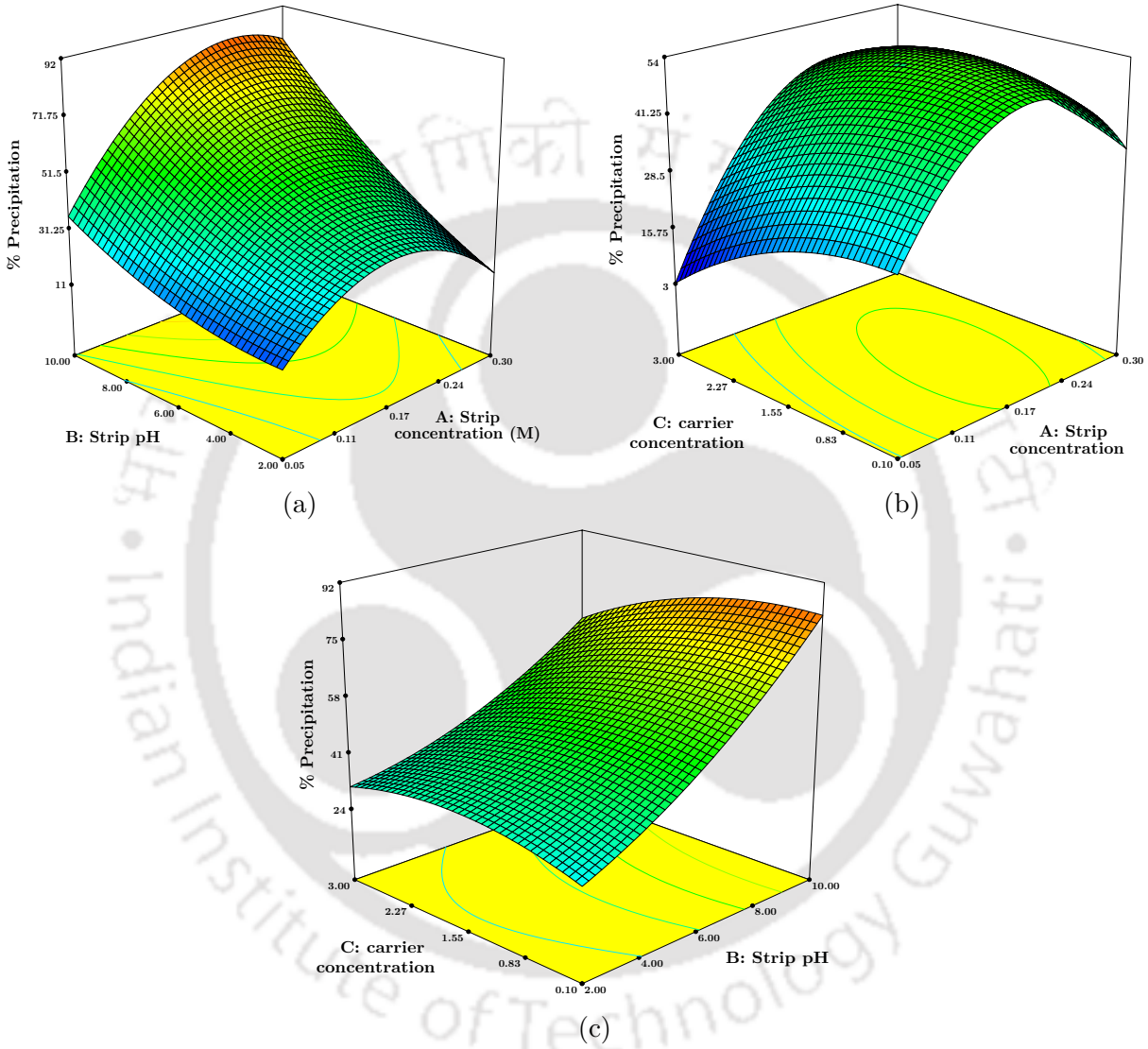

Figure 4.18: Response surface plot of (4.18a) strip concentration and strip pH, (4.18b) strip concentration and carrier concentration, (4.18c) strip pH and carrier concentration for %precipitation of Cr.

4.3 Summary of studies on electrochemical separation of Cr(VI)

- ✓ SLM technology with *in situ* electrochemical reactor in stripping section has been successfully implemented for the production of chromium-iron hydroxide which may be calcinated to produce chromium-iron oxide.
- ✓ During production of chromium-iron complex the separation of Cr(VI) from feed phase and its reduction to Cr(III) is also performed simultaneously.
- ✓ For electrochemical reaction iron plate was used as an anode and graphite rod was used as cathode.
- ✓ The optimum parameters found for SLM study are: Concentration of Cr(VI) in feed phase 100 mg L^{-1}, pH of feed phase 4.5, concentration of NaCl in strip phase 0.15 M, pH of strip phase 8, concentration of aliquat 336 as carrier in LM 1% (v/v), electric potential 2.5 V DC in strip phase, stirring speed 120 rpm in both aqueous phases, and 6 h of run time.
- ✓ The maximum %precipitation of chromium is ∼97%.
- ✓ The influential parameters such as strip phase concentration, strip phase pH and carrier concentration have been picked up for experimental optimization by RSM using CCD rule.
- ✓ The predicted output from RSM study is shown in good agreement with experimental results.

Chapter 5

FS-SLM based simultaneous separation and electrodeposition of Ni(II) and Zn(II)

This chapter provides simultaneous separation and deposition of Ni(II) and Zn(II). A new type of supported liquid membrane setup has been developed in this work. The setup consist of an in-situ electrodeposition unit in strip phase which helps "stripped" nickel and zinc from synthetic wastewater get electrodeposited on the cathode surface. This type of separation technique not only helps to separate toxic heavy metals from wastewater but also yields an useful end product in the form of electroplated material. Two types of carrier, i.e., trioctyl amine and di-(2-ethyhexyl)phosphoric acid, have been used in the organic phase to separate zinc and nickel. The separation has been done individually as well as in a condition of binary pollutant in the feed phase. Various physicochemical parameters have been optimized to maximize the transport and deposition of metals on the cathode surface. Face-centered central composite designs in response surface methodology have been performed on varied ratios of binary pollutant and their carriers in order to obtain optimum performance of the separation unit.

5.1 Theoretical background

5.1.1 Reaction mechanism and transport methodology

Reaction mechanism will differ with different extractants. However, the reaction mechanism as discussed below is applicable for trioctyl amine (TOA) as extractant. The medium with hydrochloric acid helps metal ion to form MCl_4^{2-} in feed solution and binds with carrier R_3N to form $R_3NH^+Cl^-$ complex in the organic phase, where M represents the metal (nickel or zinc) and R represents the octyl group of TOA, i.e., R≡CH_3. The complex of metal ion binds with carrier to form a metal-carrier complex ($R_3NH^+MCl_4^{2-}$), which diffuses across the organic phase up to the strip-membrane interface due to a concentration gradient. The metal-carrier complex releases metal ion that binds with ammonium chloride in the strip phase to form a metal-ammonium complex, viz., $M(NH_3)_2Cl_2$. The carrier diffuses back to the feed-membrane interface and again binds with another metal ion. This process continues until the strip phase solution gets saturated with metal ion. When an electric potential is applied to the strip phase, the metal ions present in the strip phase get deposited on the cathode surface. The reaction mechanism [211–220] is as follows:

$$M^{++} + 4Cl^- \rightleftharpoons MCl_4^{2-} \tag{5.1}$$

$$2R_3NH^+Cl^- + MCl_4^{2-} \rightleftharpoons (R_3NH^+)_2MCl_4^{2-} + 2Cl^- \tag{5.2}$$

$$(R_3NH^+)_2MCl_4^{2-} + 2NH_4Cl \rightleftharpoons 2R_3NH^+Cl^- + M(NH_3)_2Cl_2 + 2HCl \tag{5.3}$$

$$2H_2O \rightarrow 4H^+ + O_2(g) \uparrow + 4e^- \text{ (anode)} \tag{5.4}$$

$$M(NH_3)_2Cl_2 + 2e^- \rightarrow M \text{ (electrodeposition on cathode)} + 2NH_3 + 2Cl^- \tag{5.5}$$

The reaction mechanism is pictorially represented in Figure 5.1.

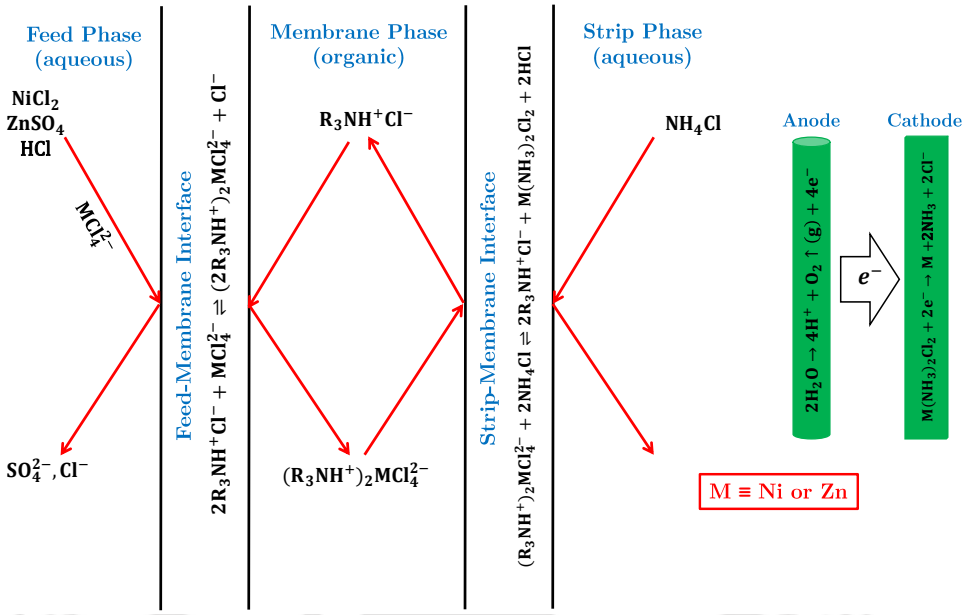

Figure 5.1: Reaction mechanism.

5.2 Results and discussion

5.2.1 Two-phase equilibrium study

The two-phase equilibrium study was carried out at room temperature with the method described in Section 2.4.

5.2.1.1 Selection of solvent-extractant combination

The selection of carrier is a crucial task in any liquid membrane based separation process as it enhances the capability of solvent in transporting the solute. Hence, various extractants have been added in sunflower oil to study their capacity to extract metal from the two phase liquid mixture. The results are tabulated in Table 5.1. It is observed that D2EHPA enables 97.42% extraction of Zn(II) while TOA yields a maximum efficiency of extraction of Ni(II) with a mere 16.05%. At the same time, D2EHPA yields very low efficiency (9%) for Ni(II) extraction. The performance of TOA is comparable with both the solutes, viz., 16.05% with Ni(II) and 22.78% with Zn(II).

Table 5.1: Two phase equilibrium study: Efficiency of various extractants in extracting metal ions using sunflower oil as solvent.

Carrier	Extraction of Ni(II) using 1% (v/v) extractant	Extraction of Zn(II) using 5% (v/v) extractant
TOA	16.05	22.78
D2EHPA	9.00	97.42
Aliquat 336	10.74	50.11
TBP	8.14	11.44

5.2.1.2 Effect of initial concentration of solute in aqueous phase

The relevant experiments were carried out with initial concentrations of solute in the aqueous phase in the range of 50-500 mg L^{-1}. The extraction of both the metals are highest at low initial concentration (see Table 5.2). About 30.52% Ni(II) and 98.13% Zn(II) were extracted in the organic phase at the lowest initial concentrations ($\leq$ 100 mg L^{-1}). As the concentration of solute increases in the aqueous phase, the availability of extractant to form a solute-carrier complex in the organic phase depletes due to over crowding of the solute. It is thus fair to maintain 50-100 mg L^{-1} of initial concentration of the solute in the aqueous phase.

The extractant D2EHPA is highly efficient on extraction of Zn(II), and the prevalent operating conditions yield above 97%. It is not worth devoting any further effort to optimize operating parameters in search of any higher value of efficiency of extraction of Zn(II). It is rather beneficial to dedicate the rest of the studies to optimize two phase operating parameters for Ni(II) extraction.

Table 5.2: Two-phase equilibrium study at various initial concentrations of metals in aqueous phase: Extraction of metal ions in organic phase composed of 5% Extractant (v/v) in sunflower oil.

Feed concentration(in mg L^{-1})	Extraction of nickel (in %) using TOA as extractant	Extraction extraction of zinc (in %) using D2EHPA as extractant
50	30.52	98.13
100	29.95	97.42
200	29.14	95.13
300	27.92	92.73
400	26.83	89.13
500		86.55

5.2.1.3 Effect of pH of aqueous phase

The reaction mechanism (Equations 5.1-5.5) reveals that the metal ion required excess chloride ion to form the metal-chloride complex. The presence of HCl in the aqueous phase helps the metal ion to form a metal-chloride complex. Hence, the pH of the aqueous solution is an important parameter to increase the efficiency of the extraction of Ni(II). The pH has been studied in the range of 2-8 by adding HCl and/or NaOH. The results are plotted in Figure 5.2. At lower pH, the extraction of Ni(II) is less. The maximum extraction of Ni(II) is achieved at pH 5. The maximum extraction of Ni(II) for initial concentrations of 50 and 100 mg L^{-1} are 16% and 15%, respectively. With further increase in pH (> 5), extraction of Ni(II) decreases. In the case of lower pH, excess Cl^- ion hinders the metal ion to bind with the carrier to form a metal-carrier complex; whereas at higher pH, NaOH reacts with metal ion to form insoluble metal hydroxide that results in metal ion being less accessible to the carrier.

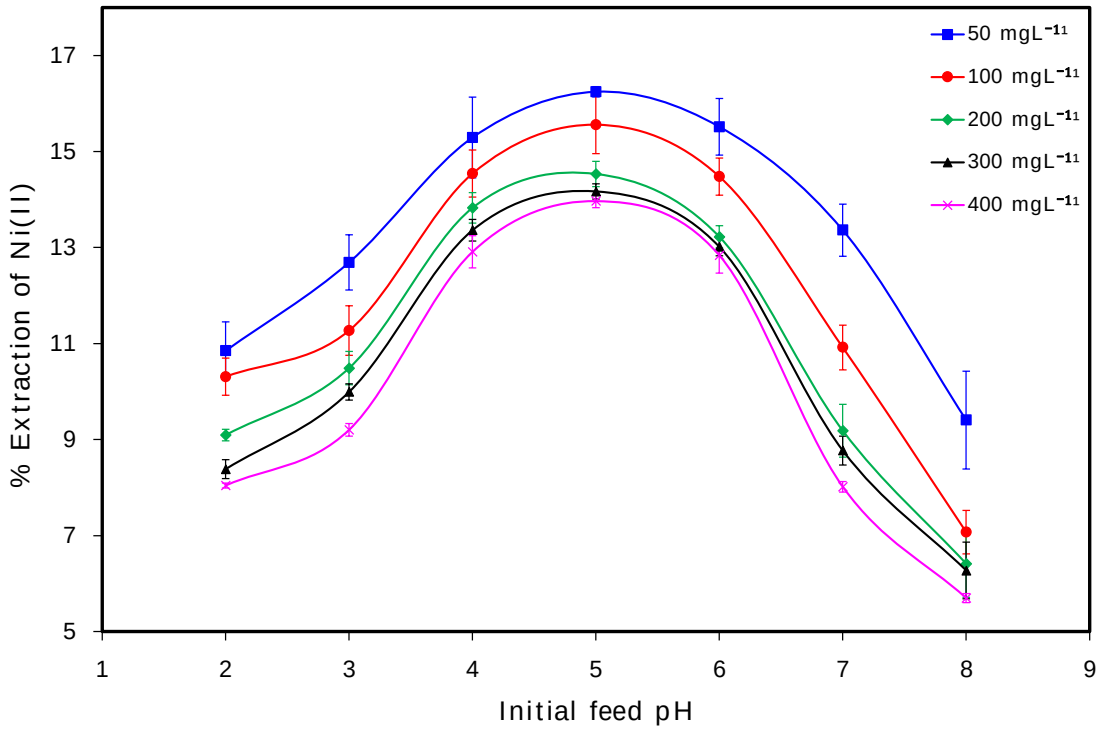

Figure 5.2: Two phase equilibrium study at various initial concentrations of Ni(II) in the aqueous phase: effect of pH of the aqueous phase on extraction of Ni(II) in the organic phase.

5.2.1.4 Effect of concentration of extractant

Extractant forms a complex with a solute that facilitates the transport of solute across the SLM. An increase in concentration of the extractant leads to formation of more solute-carrier complex that results in an increase in the extraction efficiency. The results of the study of extraction at various initial concentrations of solute are plotted in Figure 5.3. The concentration of extractant was within the range of 1-8% (v/v). It is observed in Figure 5.3 that 30% extraction is achieved at 5 vol% TOA at a lower initial concentration of solute (50-100 mg L^{-1}), whereas a higher concentration of TOA (6-8 vol%) is needed in the organic phase to achieve the highest extraction efficiency in the case of a higher initial concentration of solute (200-400 mg L^{-1}). At a higher solute concentration, the availability of solute is more, and hence it requires more extractant to form the solute-carrier complex.

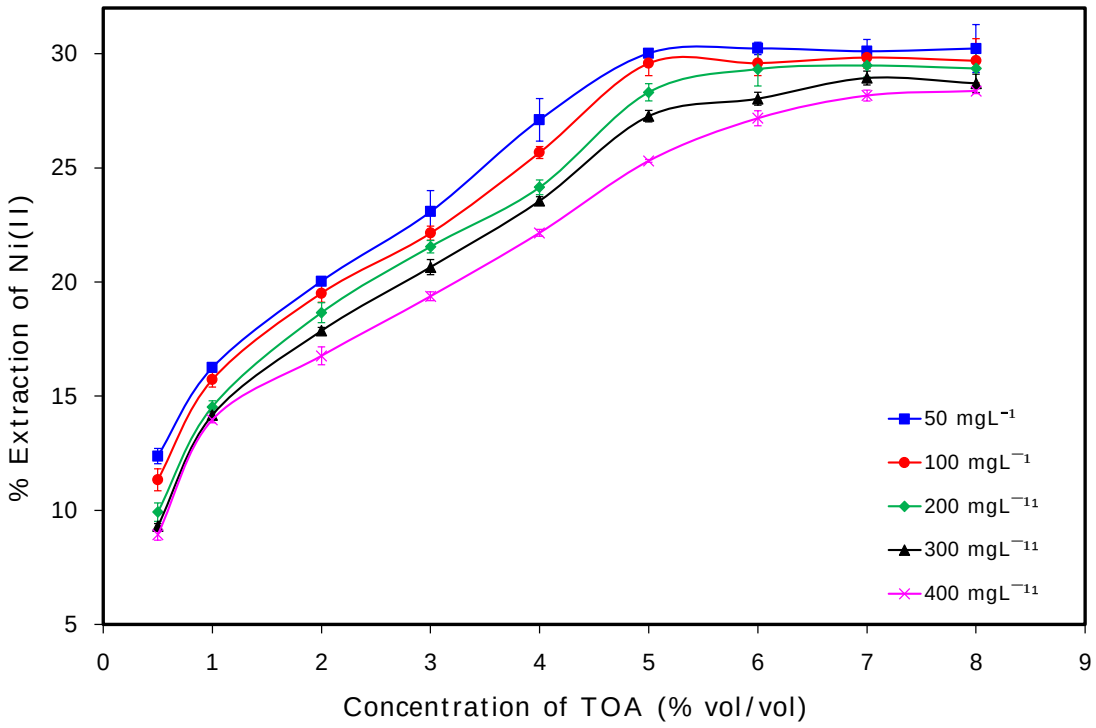

Figure 5.3: Two phase equilibrium study at various initial concentrations of Ni(II) in the aqueous phase: effect of concentration of TOA in sunflower oil on the extraction of Ni(II) in the organic phase.

5.2.1.5 Effect of period of extraction

The study of the period of extraction helps to detect the time required for the process to reach its maximum extraction efficiency also known as its saturation point. The experiments were carried out for 15 h, and samples were taken periodically. The results are shown in Figure 5.4. It is observed that extraction of Ni(II) is increased up to 12 h and thereby reaches its saturation limit. The saturation limit of extraction is higher at lower initial concentrations of the feed.

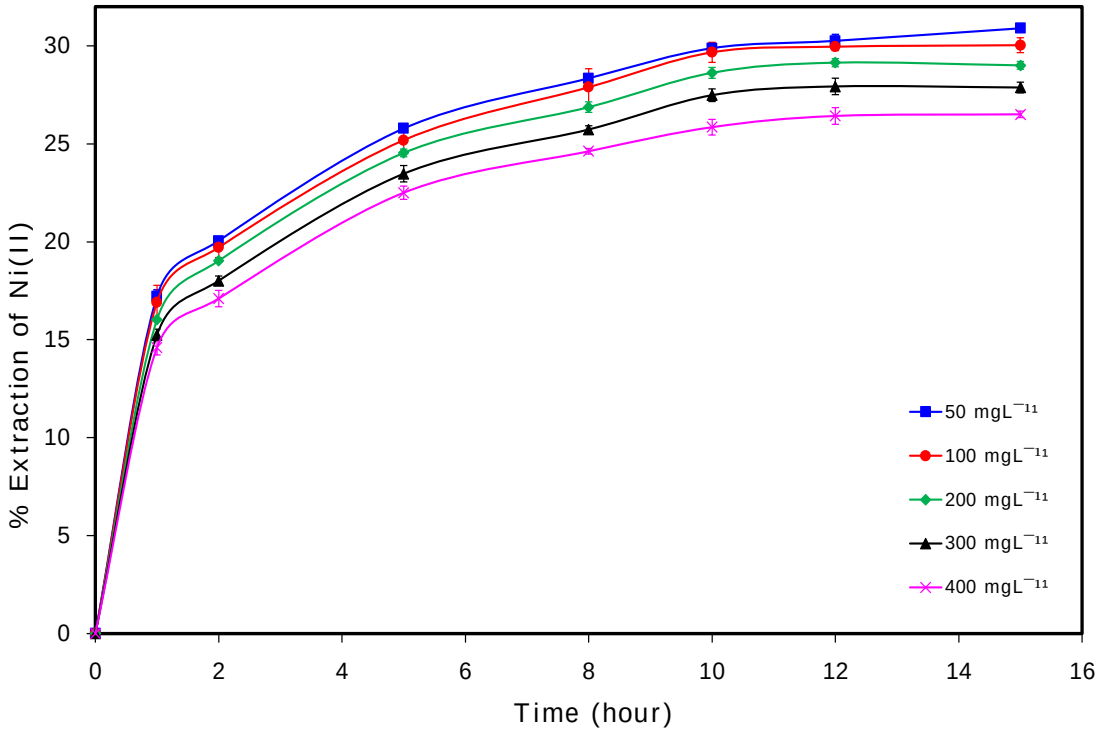

Figure 5.4: Two phase equilibrium study at various initial concentrations of Ni(II) in the aqueous phase: saturation period of extraction of Ni(II) in the organic phase.

5.2.1.6 Detection of appropriate stirring conditions

Stirring creates turbulence in the liquid content, which results in enhancement of diffusivity and increased extraction rate. The range of stirring speed was 50-250 rpm in the experimental runs. The results are demonstrated in Figure 5.5. An increase in the stirring rate increases the extraction of Ni(II) up to 200 rpm. A further increase in stirring speed does not help. The saturation limit is set at 200 rpm.

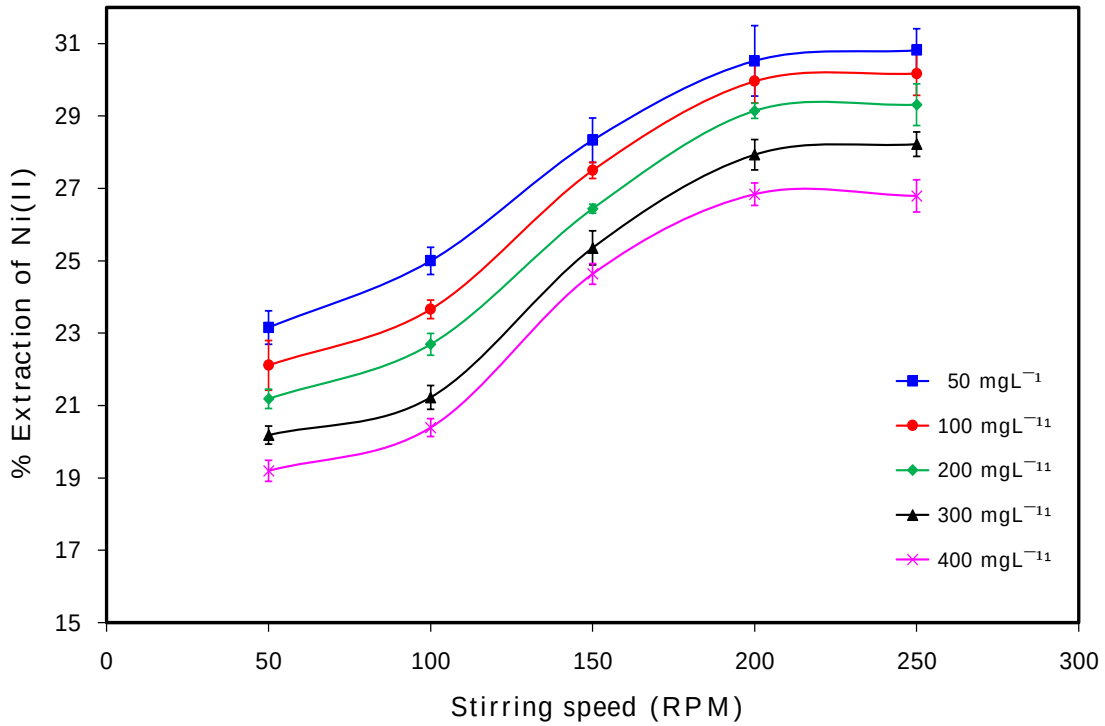

Figure 5.5: Two phase equilibrium study at various initial concentrations of Ni(II) in the aqueous phase: saturation stirring conditions for the extraction of Ni(II) in the organic phase.

5.2.2 Three-Phase SLM Study

5.2.2.1 Selection of strippant

Selection of the strippant is an important factor, as it is directly related to the recovery of solute. As the aim of the study is to electroplate/deposit the recovered solute in the strip phase, the strippant solution should have electrolytic properties. Hence, three types of strippants, *viz.*, H_2SO_4 [150, 221, 222], NH_4Cl [184, 185] and NaCl[185] have been tested for recovery as well as deposition of metals. The concentration of the strip phase was 0.1 M with either electrolyte. The results are tabulated in Table 5.3. It is observed from the figure that the % deposition of Zn(II) in H_2SO_4, NH_4Cl, and NaCl solutions are 26.71%, 76.98%, and 62.19%, respectively, while the same for Ni(II) are 23.51%, 83.68%, and 67.68%, respectively. The maximum deposition of

both the metals on the cathode plate is observed for NH_4Cl as a strippant. Hence, further studies have been done using NH_4Cl as a stripping solution.

Table 5.3: Three Phase SLM-EP Study: % Deposition of Metal on Cathode Plate Using Various Strippants.

Strippant solution	Deposition of nickel (in %) using TOA as carrier	Deposition of zinc (in %) using D2EHPA as carrier
H_2SO_4	23.51	26.71
NH_4Cl	83.68	76.99
NaCl	67.68	62.20

5.2.2.2 Selection of suitable cathode

Graphite has been used as an anode for this study. The deposition of metal/solute on the cathode plate depends on the characteristics of the cathode plate. The complex of extracted metal ion and carrier at the strip-membrane interface releases metal ion in the bulk strip phase as an ammonium-metal complex (refer to section 5.1.1). When the electric potential is applied in the strip phase, metal is deposited on the cathode plate. As a result, the concentration of metal ion in the strip phase remains very low. Two types of metals, *viz.*, copper and stainless steel, have been used as the cathode plate to check the deposition efficiency of metals. The results are shown in Figure 5.6. It is observed that the deposition of Ni(II) on copper and stainless steel plates are almost 85% and 62%, respectively, after 12 h of run time, of which 76% (on copper plate) and 54% (on stainless steel plate) deposition were over within the initial 6 h. On the other hand, deposition of Zn(II) on copper and stainless steel plates are almost 77.9% and 53.3%, respectively, after 12 h of run time, of which 72.3% (on copper plate) and 48.4% (on stainless steel plate) deposition were over within initial 6 h. A higher deposition rate on the copper plate is due to the electrical conductivity of copper (5.96×10^7 S m^{-1}), which is higher than that of stainless steel (1.45×10^6 S m^{-1}). Hence, the copper plate has been selected as a

cathode. It is well-known that the electrodeposition/electroplating process is a very fast process; hence, The SLM augmented with an electroplating feature (henceforth referred to as the SLM-EP method) technology is the rate determining step.

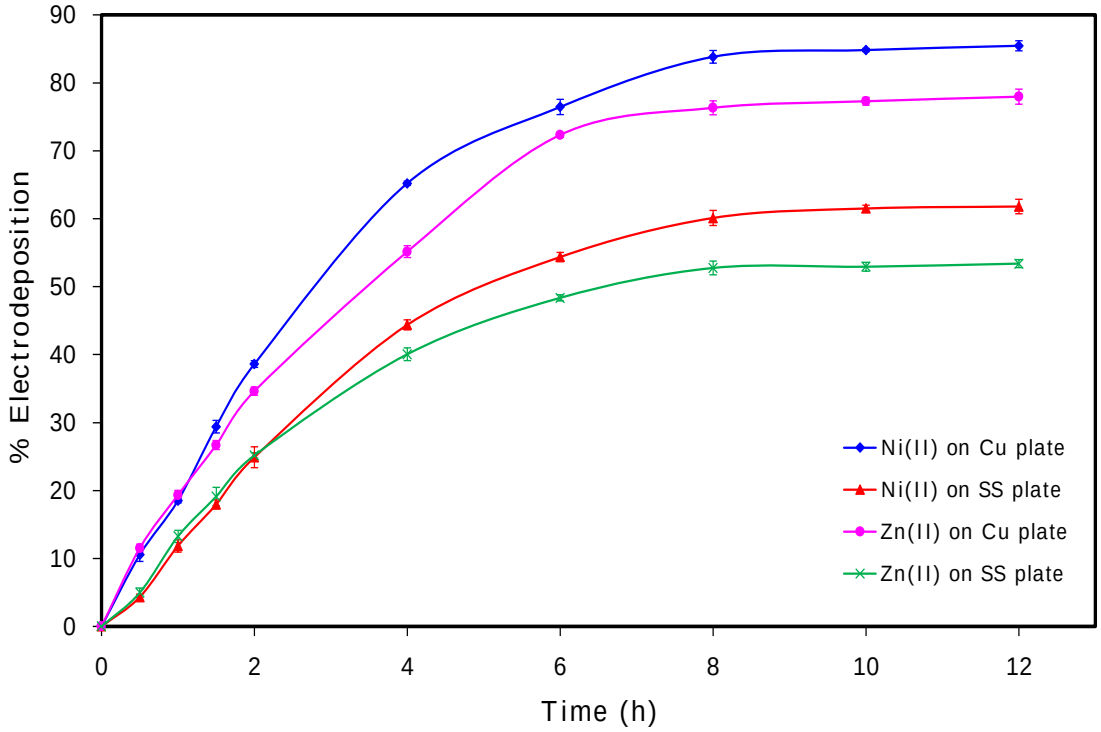

Figure 5.6: Three phase SLM-EP study: % electrodeposition of metals on two different materials of the cathode at the following operating conditions: concentration of metal in feed phase = 100 mg L^{-1}, pH of feed phase = 5.

5.2.2.3 Importance of surface area of cathode

It is also understandable that the surface area on the cathode should play an important role of the deposition of metal on it; and a higher surface area should lead to higher deposition. In order to obtain a quantitative analysis of such deposition of metal, cathode plates of three different sizes, *viz.*, 13 cm^2, 26 cm^2, and 52 cm^2 , have been used for the experiments. Moreover, the SLM study was conducted with consecutive fed-batch runs where electroplating was repeated on the same plate. The results are tabulated in Table 5.4. Deposition of Ni(II) on Plate I (13 cm^2) is 33.01% after the second run, on Plate II (26 cm^2) is 28.09% after the third run, and on Plate III (52 cm^2) is 27.09% after the fifth run. The accumulated metal on cathode plates

I, II, and III are 16.80 mg, 24.20 mg, and 43.60 mg, respectively. On the other hand, deposition of Zn(II) on Plate I (13 cm^2) is 39.39% after the second run, on Plate II (26 cm^2) is 34.55% after the third run, and on Plate III (52 cm^2) is 30.68% after the fifth run. The accumulated metal on cathode plates I, II, and III are 17.10 mg, 24.40 mg, and 41.10 mg, respectively. The results are comparative with zinc and nickel.

Table 5.4: Three Phase SLM-EP Study: % Electrodeposition on cathodes of different values of effective surface area.

Metal	Plates	Effective surface of copper plate (in cm^2)	Deposition of metal (in %)					Total deposition (in mg)
			Run 1	Run 2	Run 3	Run 4	Run 5	
Ni	I	13	91.12	33.01				16.80
	II	26	93.28	56.13	28.09			24.20
	III	52	94.63	86.18	70.63	44.77	27.09	43.60
Zn	I	13	89.97	39.39				17.10
	II	26	92.32	55.20	34.55			24.40
	III	52	95.34	80.66	67.36	41.31	30.68	41.10

5.2.2.4 Saturation point in period of operation

It was desired to measure the period of SLM operation in order for it to reach its saturation point. The experiment was carried out for 12 h, and samples were collected periodically to check the concentration of metal. The results are shown in Figure 5.7. It is observed that over 88% of Ni(II) and $\sim$ 80% Zn(II) were deposited on the cathode within initial 6 h of operation, and the deposition approaches its saturation limit between 6 and 8 h with $\sim$ 92% deposition. Deposition does not increase significantly thereafter and reaches saturation of $\sim$ 93% at 12 h.

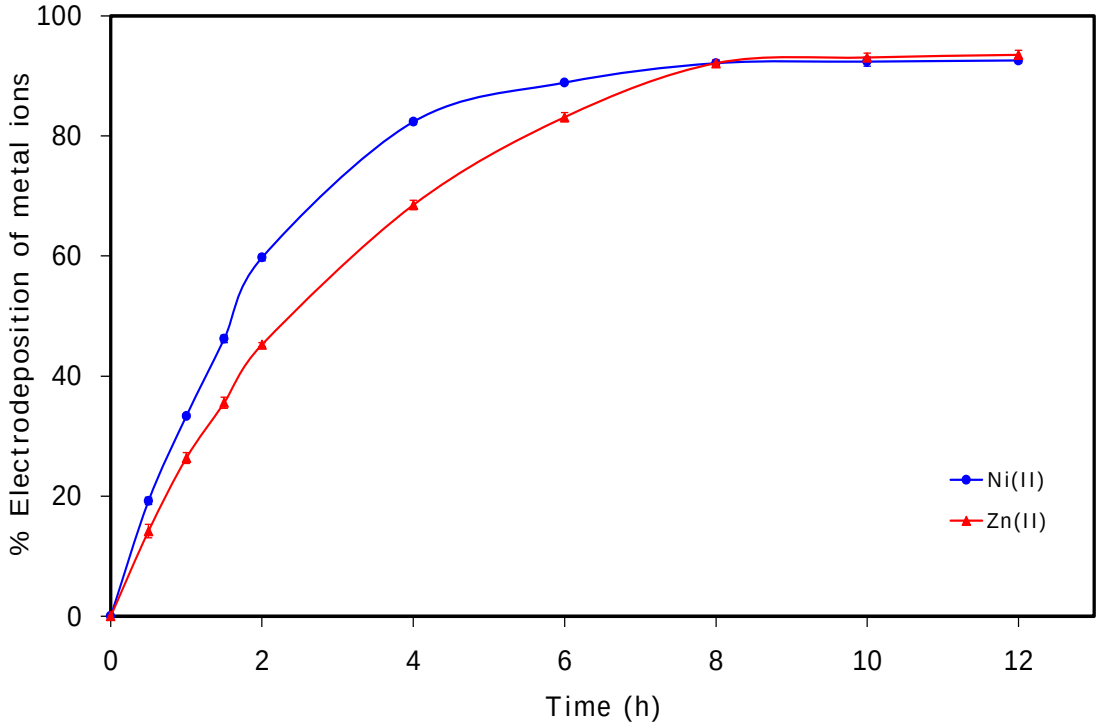

Figure 5.7: Three phase SLM-EP study: saturation period of %electrodeposition of metals on the copper cathode plate.

5.2.2.5 Effect of pH in feed phase

As observed in section 5.2.1.3, the pH of feed phase is an important parameter for improving the separation efficiency of metal from the feed phase to the membrane phase. The reaction mechanism suggests that an acidic environment (i.e., pH < 7) is required in order to maximize extraction of metal ions from the feed phase to the strip phase. The results are reflected in Figure 5.8, which is similar to Figure 5.2. The experiment was carried out in the pH range of 2-8. It is observed that deposition of metals is increased with an increase in pH from 2 to 5. Whereas, a further increase in pH (i.e., from 5 to 8) decreases the metal deposition. The reasons are already explained in section 5.2.1.3. The maximum deposition of Ni(II) and Zn(II), *viz.*, almost 84% and 76%, respectively, were observed at pH 5.

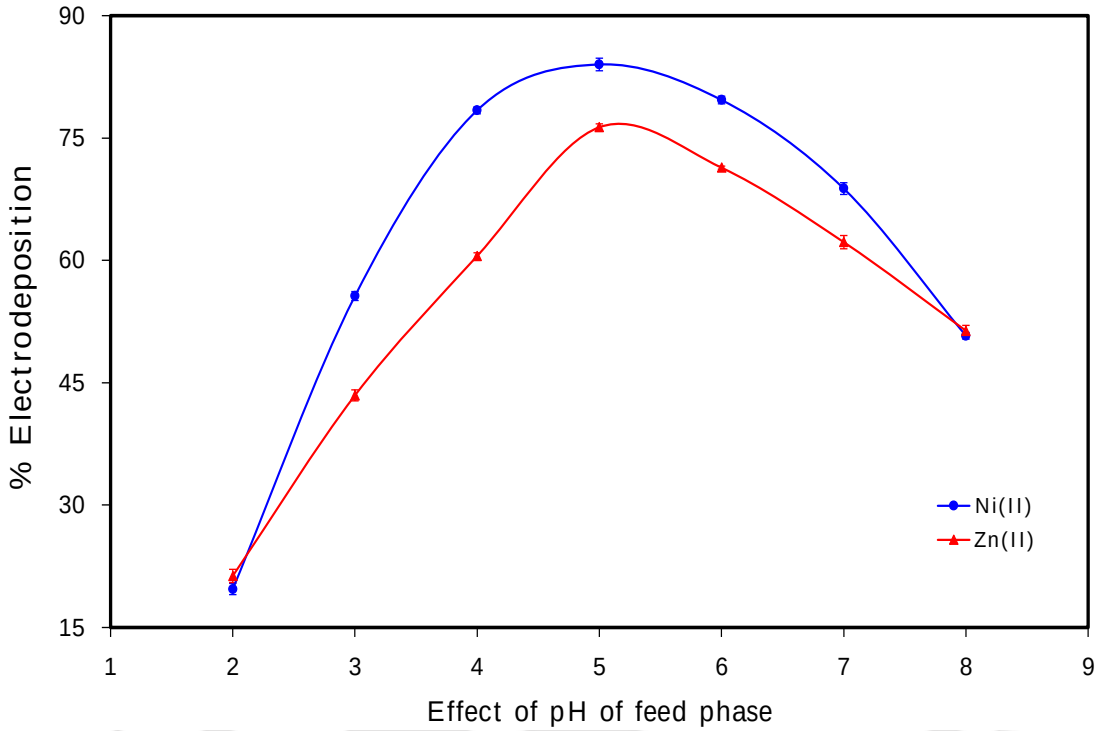

Figure 5.8: Effect of pH of feed phase

5.2.2.6 Effect of pH in strip phase

The pH of a metal deposition electrolyte is crucial because it can influence the conductivity of the solution and the metal deposition rate [223]. The nominal pH of 0.15 and 0.2 M NH_4Cl solution are $\sim$ 5.3 and $\sim$ 5.8, respectively. Electrodeposition of metal operates in a relatively narrow pH window [223] as confirmed in Figure 5.9. The metal deposition is almost invariably accompanied by ammonia evolution and its loss, as this will drive the solution toward a more acidic zone since hydrogen ions are left in the system in excess. In some cases, the redox values of the metal ion (or complex holding it) can be affected by a change in pH and it influences the overall process. Olper and Maccagni [211, 212] argued that the pH of the electrolyte has to be maintained in the range of 5.8-6.5 to avoid formation of chloroamine. In the present study, the effect of pH was studied in the range of 2-9 by adding NaOH.

$$NH_4Cl + NaOH = NH_3 \uparrow + NaCl + H_2O \tag{5.6}$$

It is observed that the deposition of Ni(II) and Zn(II) are maximum at pH $\sim$ 5.3-5.8, *i.e.*, at the nominal conditions of the strip phase. At low pH, the concentration of NH_3 in the strip phase is also low. As a result, M^{++} tends to form complexes with Cl ions. As the pH increases, NH_4^+ begins to dissociate and more NH_3 becomes available in the system [220]. As a weak acid, NH_4Cl acts as a pH buffer on its own.

$$NH_4^+ \rightleftharpoons NH_3 \uparrow + H^+ \tag{5.7}$$

The reactions stated in Equations 5.6 and 5.7 act as a proton source while keeping the concentration of free NH_3 relatively low. The maximum percentage of metal deposition was found to be almost $\sim$ 92-93% at 0.15-0.2 M NH_4Cl in the strip phase.

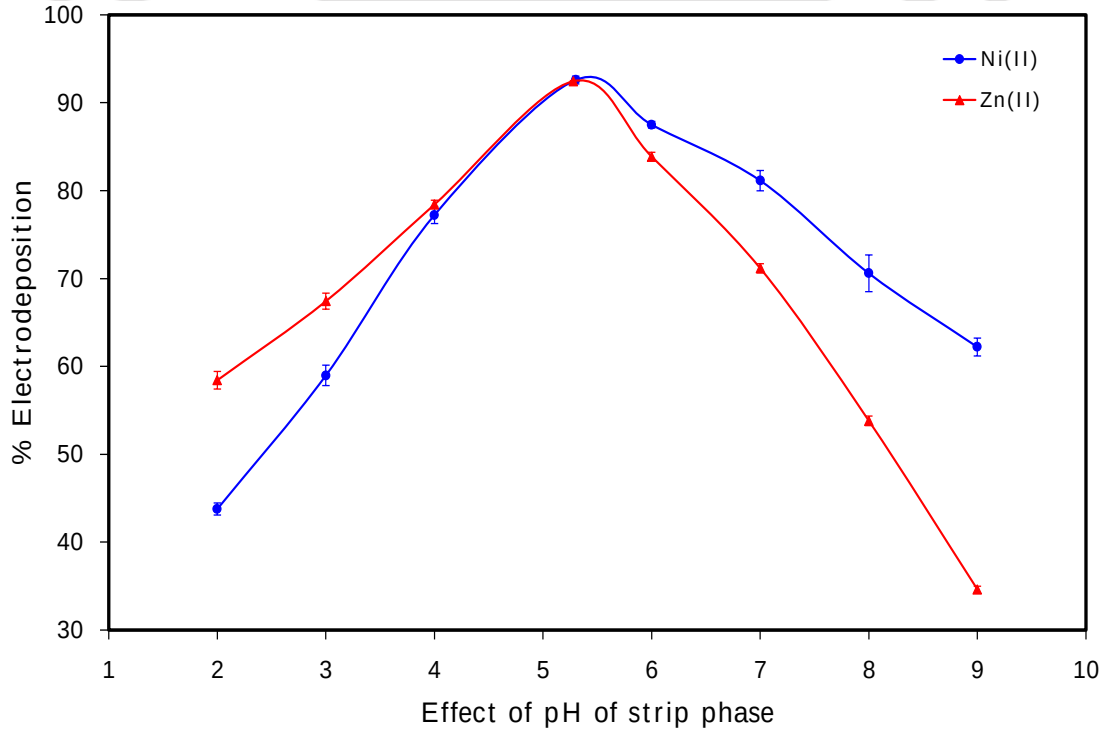

Figure 5.9: Effect of pH of strip phase

5.2.2.7 Effect of concentration of carrier

Carrier plays an important role in the overall transport of solute from the feed phase to the strip phase. To study this effect, the carrier concentration in SLM was varied from 0-8 vol % in the case of transport of Ni(II) using TOA and from 0-5 vol % in case of transport of Zn(II) using D2EHPA. It is observed from Figure 5.10 that deposition of metal increases with an increase in carrier concentration. Deposition of Ni(II) reaches $\sim$ 93% at 5 vol % of TOA, whereas deposition of Zn(II) reaches $\sim$ 93% at 3 vol % of D2EHPA. A further increase in carrier concentration does not aid in any significant increase in deposition of either metal. This observation is similar to the two phase study in Section 5.2.1.4.

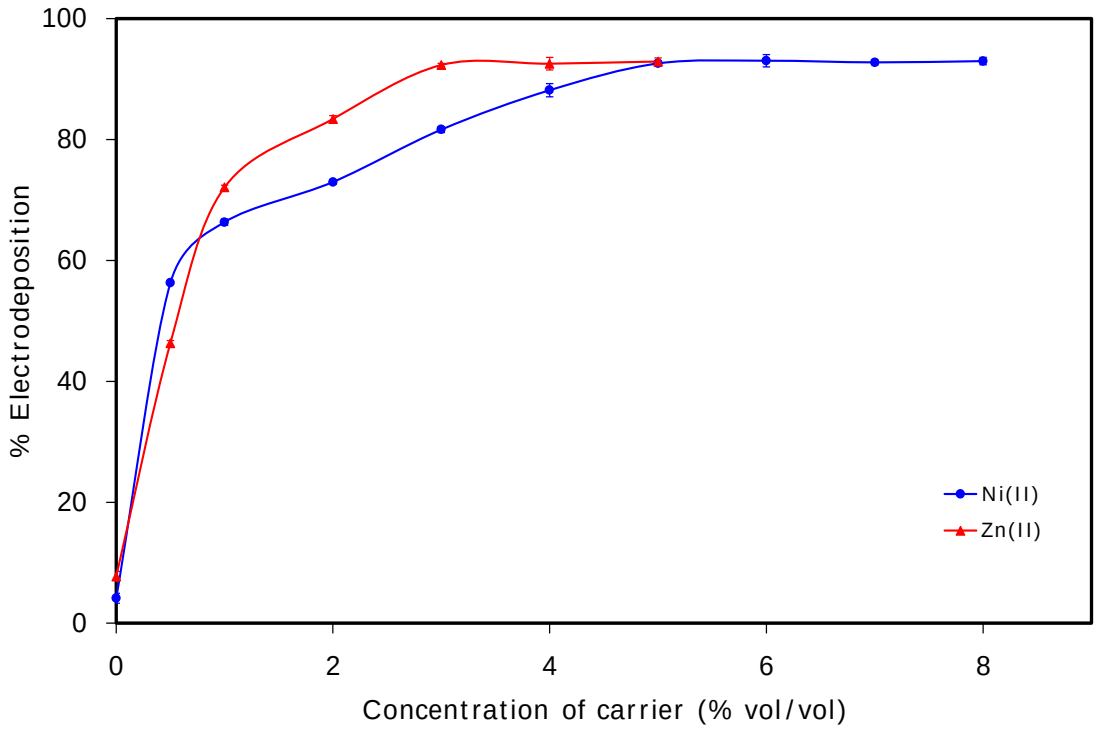

Figure 5.10: Effect of concenration of carrier (%vol/vol)

5.2.2.8 Effect of concentration of strip phase

The reaction mechanism in Section 5.1.1 suggests that the transport mechanism is coupled counter transport where the metal binds with the ammonium ion in the strip

phase to form the ammonium-metal complex. The concentration of NH_4Cl in the strip phase solution will affect the transport of the metal ion. The results are shown in Figure 5.11. An increase in the strip phase concentration leads to an increase in deposition of metal ion on the cathode plate. The maximum deposition of both the metals are almost same, *viz.*, 93% at 0.15 M NH_4Cl for Ni(II) and 92% at 0.2 M NH_4Cl for Zn(II). A further increase in the strip phase concentration does not help. It may be noted that after 94% of deposition of metal, the concentration of metal in the feed phase in very low ($\sim$ 5 mg L^{-1}). Hence the metal ion does not get enough driving force to bind with the carrier for complexation and transport.

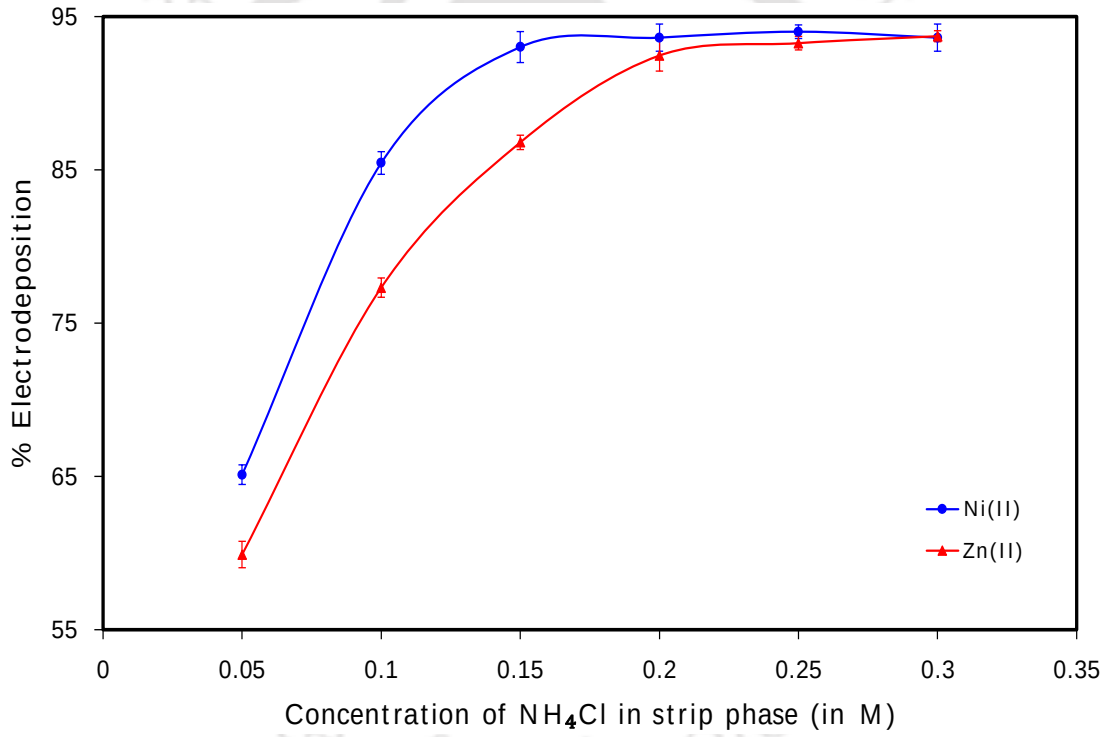

Figure 5.11: Effect of concentration of NH_4Cl in strip phase

5.2.2.9 Role of electric field for transportation of metal ion

The importance of the electric field in the strip phase solution for deposition of metal on the cathode plate has been studied and compared with the case when no electric field was used in the strip phase solution. The change of concentration of the metal ion in the feed and strip phases with and without an electric field in the strip phase has been shown in Figure 5.12. It may be observed that the concentration of Ni(II) in the feed phase decreases to $\sim$ 43 mg L^{-1}, while that of strip phase increases to $\sim$ 48 mg L^{-1} in 12 h time when no electrical field has been applied. On the other hand, when the electric field is applied in the strip phase, the concentration of Ni(II) drops to $\sim$ 6 mg L^{-1} in the feed phase in 12 h time while it remains very low (at $\sim$ 1.5 mg L^{-1}) in the strip phase throughout the operation. A similar phenomenon has been observed in the case of Zn(II) electroplating too. The concentration of Zn(II) in the feed phase decreases to $\sim$ 41 mg L^{-1}, while that of the strip phase increases to $\sim$ 51 mg L^{-1} in 12 h time when no electrical field has been applied. On the other hand, when the electric field is applied in the strip phase, the concentration of Zn(II) drops to $\sim$ 7 mg L^{-1} in the feed phase in 12 h time while it remains very low (at $\sim$ 0.6 mg L^{-1}) in the strip phase throughout the operation. The confirmation of metal deposition on the copper cathode plate has been confirmed through energy-dispersive X-ray spectroscopy (EDX) in field emission scanning electron microscopy (FESEM), *viz.*, FESEM-EDX (see Figure 5.13).

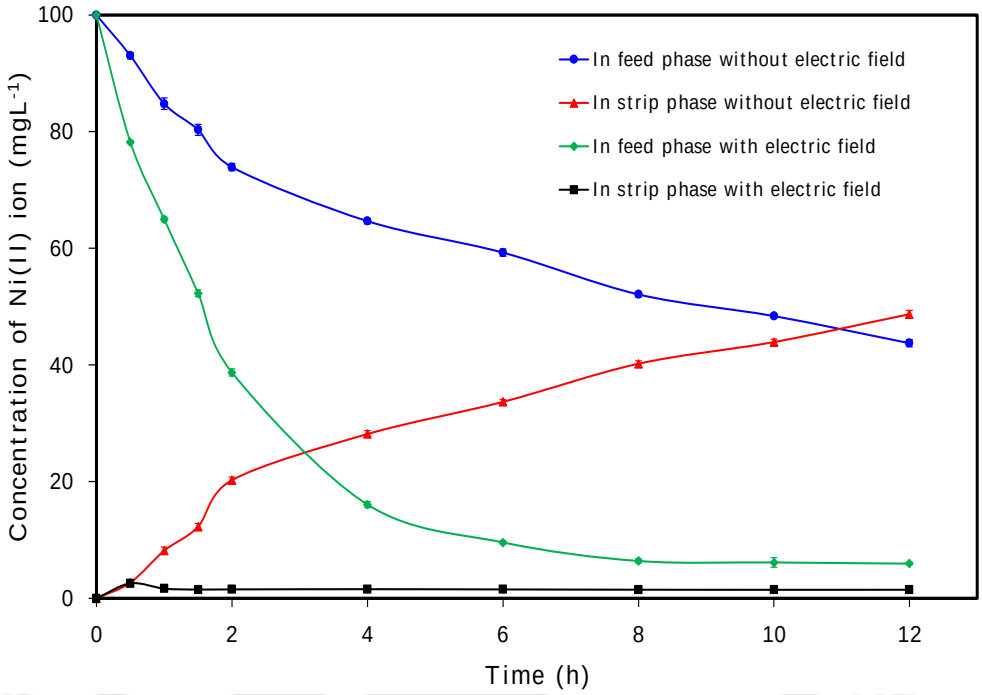

(a) Concentration of nickel

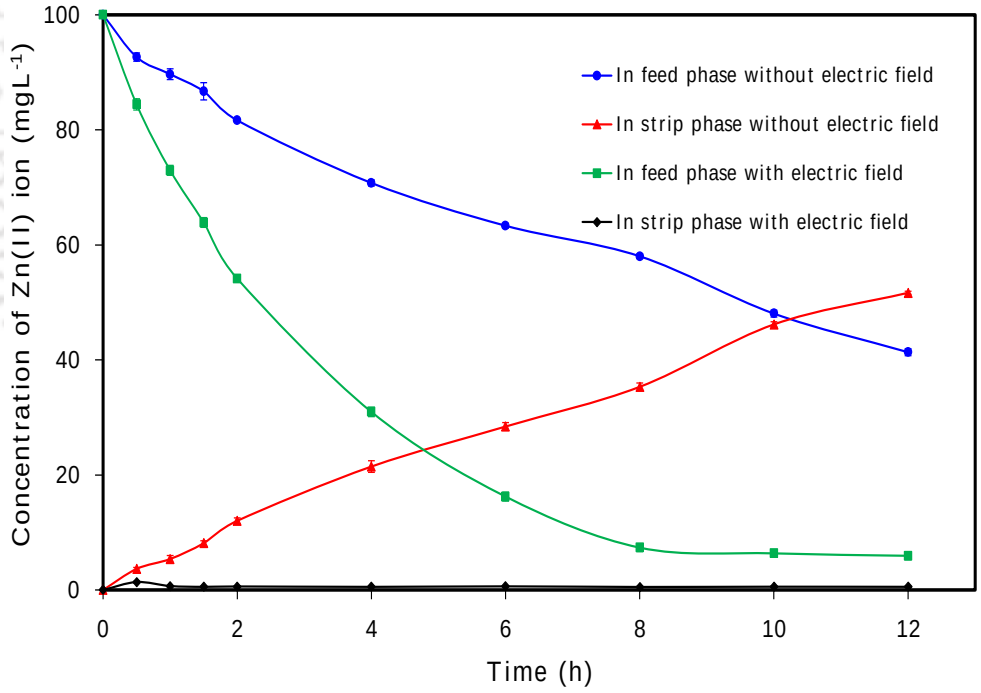

(b) Concentration of zinc

Figure 5.12: Three phase SLM-EP study with and without an electric field.

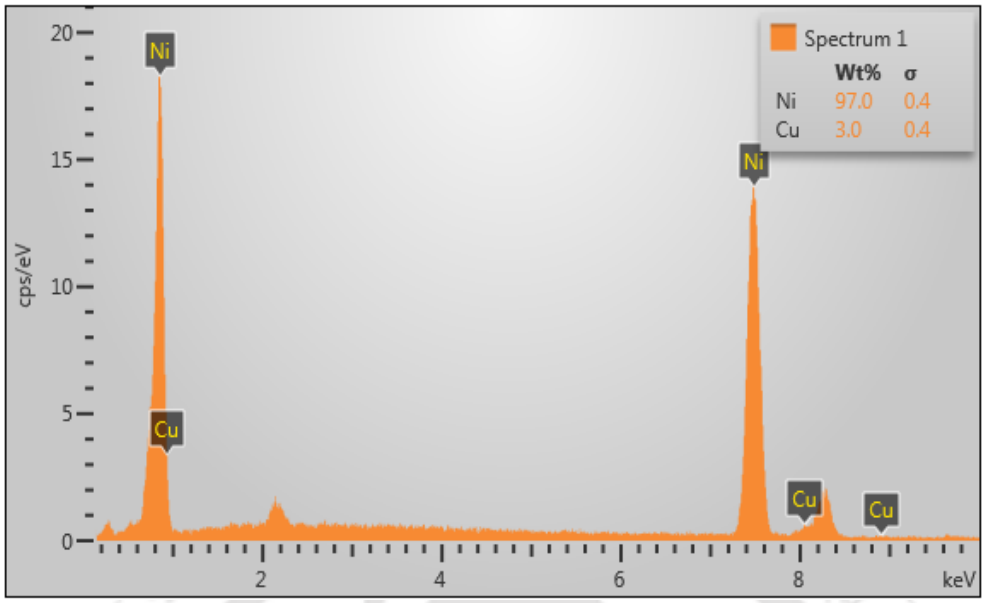

(a) Spectra of nickel

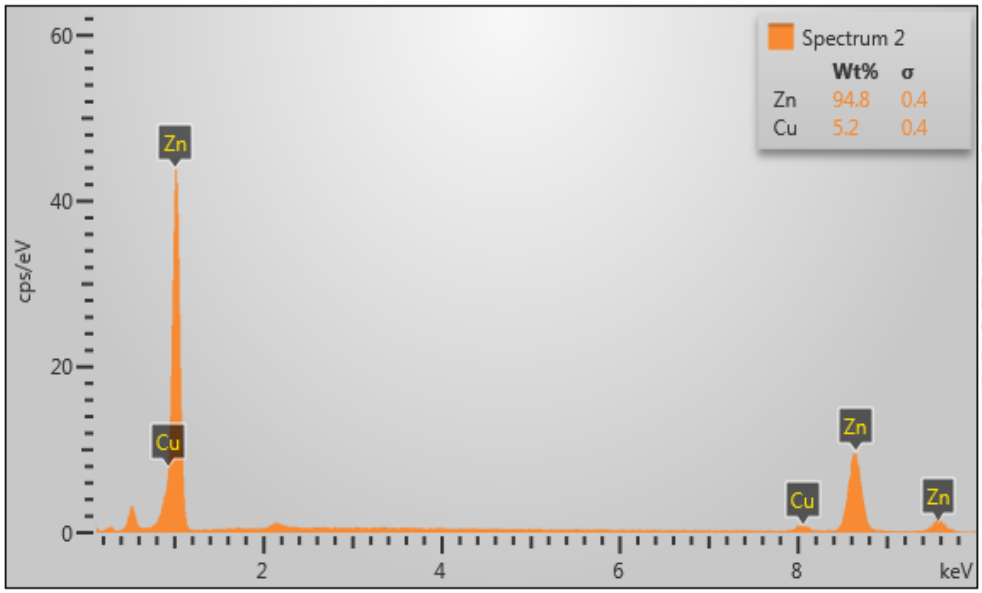

(b) Spectra of zinc

Figure 5.13: FESEM-EDX spectra of metal on a copper plate.

5.2.2.10 Effect of electric potential across the electrodes

It is quite natural that electrodeposition of metals on the cathode should have a direct relation with the electric potential applied across the electrodes. Cyclic voltammetry (CV) (potentiostat, Autolab, PGSTAT 302N) was carried out in a three electrode cell where the Ag/AgCl electrode was the reference electrode, platinum was the counter electrode, and the copper plate was the working electrode and ammonium chloride was the supporting electrolyte. The results are plotted in Figure 5.14. The main aim is to find out the metal deposition voltage on the copper plate. The negative scan shows the cathodic reduction. The deposition voltage of Ni is observed from the deflection of the curve in the region -0.75 to -0.9 V [224, 225] whereas the deposition voltage of zinc is detected from the deflection of the curve in the region -0.65 to -0.8 V [226]. In both cases, the CV diagram shows a broad peak due to the low metal concentration in the electrolyte solution. A further increase in voltage in both of the cases were associated with evolution of hydrogen due to decomposition of water [227]. Necessary experiments were carried out by varying the electric potential in the range of 0.5 to 4 V DC. The results are shown in Figure 5.15. With an increase in electric potential, the percentage deposition of metals increases and ultimately reaches a saturation limit of $\sim 93\%$ at 3 V DC. Hence, 3 V DC has been selected as the optimum parameter.

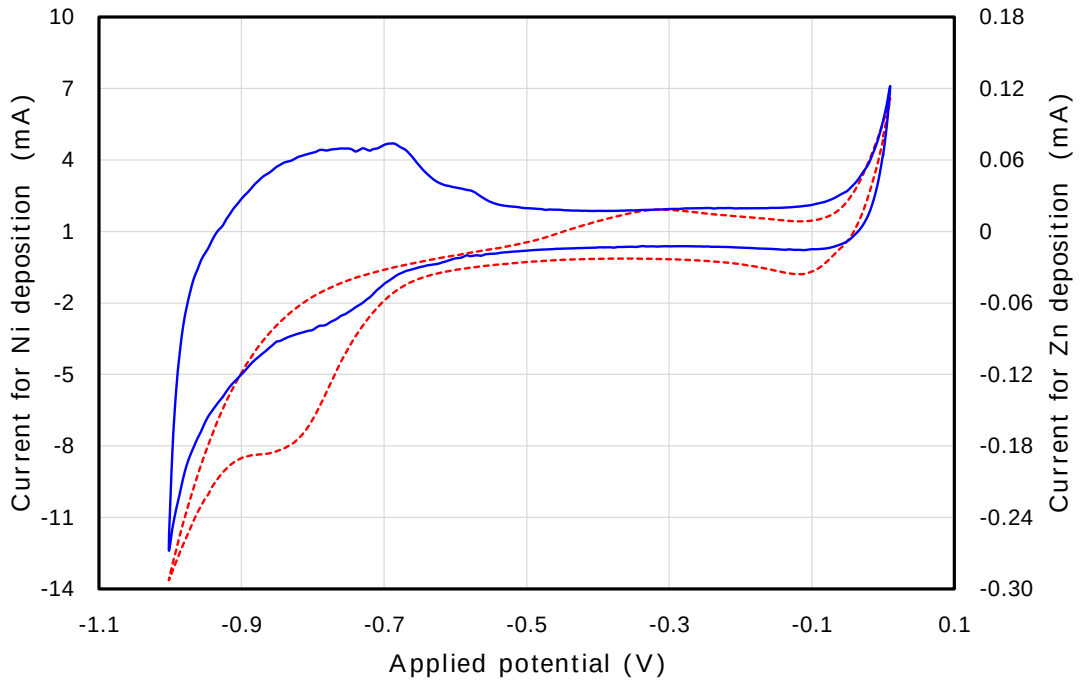

Figure 5.14: Cyclic voltammogram recorded with a copper electrode for deposition of Ni (red dashed line) and Zn (blue solid line).

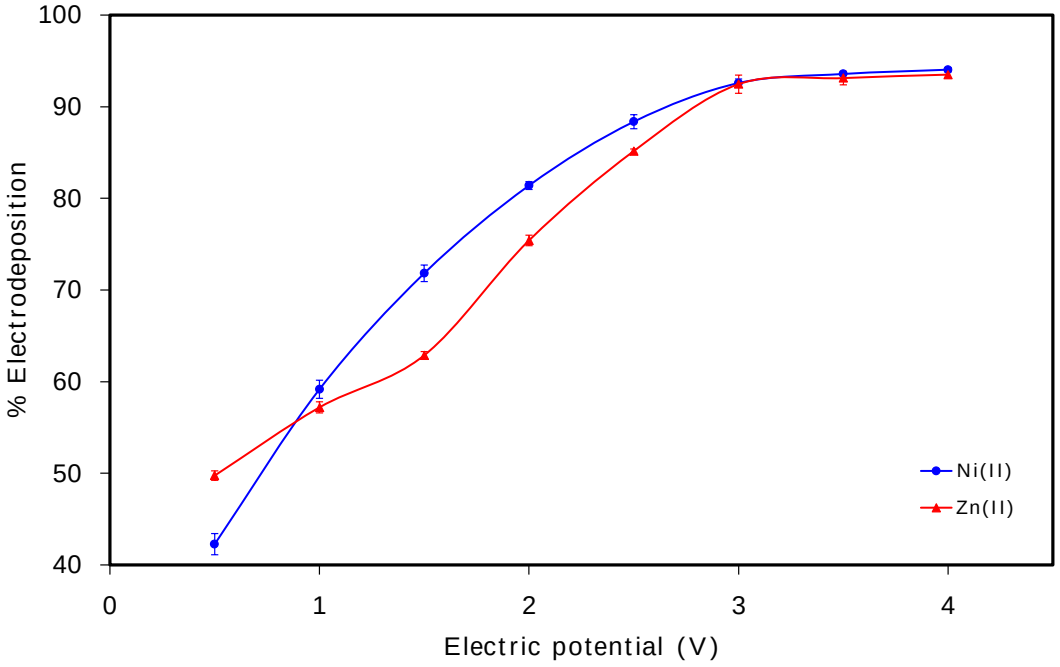

Figure 5.15: Effect of electric potential.

5.2.2.11 Effect of stirring in aqueous phase

Effective and efficient transport of the metal requires some agitation in the aqueous phases whereby the diffusion is enhanced in the bulk. The effect of speed of stirring of the aqueous phases has been studied in the range of 0-250 rpm. The results are shown in Figure 5.16. It is observed that deposition of metal on the cathode reaches $\sim$ 93% when the stirring speed is 120 rpm. A further increase in stirring speed does not yield any significant improvement on deposition. Hence, 120 rpm has been selected as the optimum stirring speed.

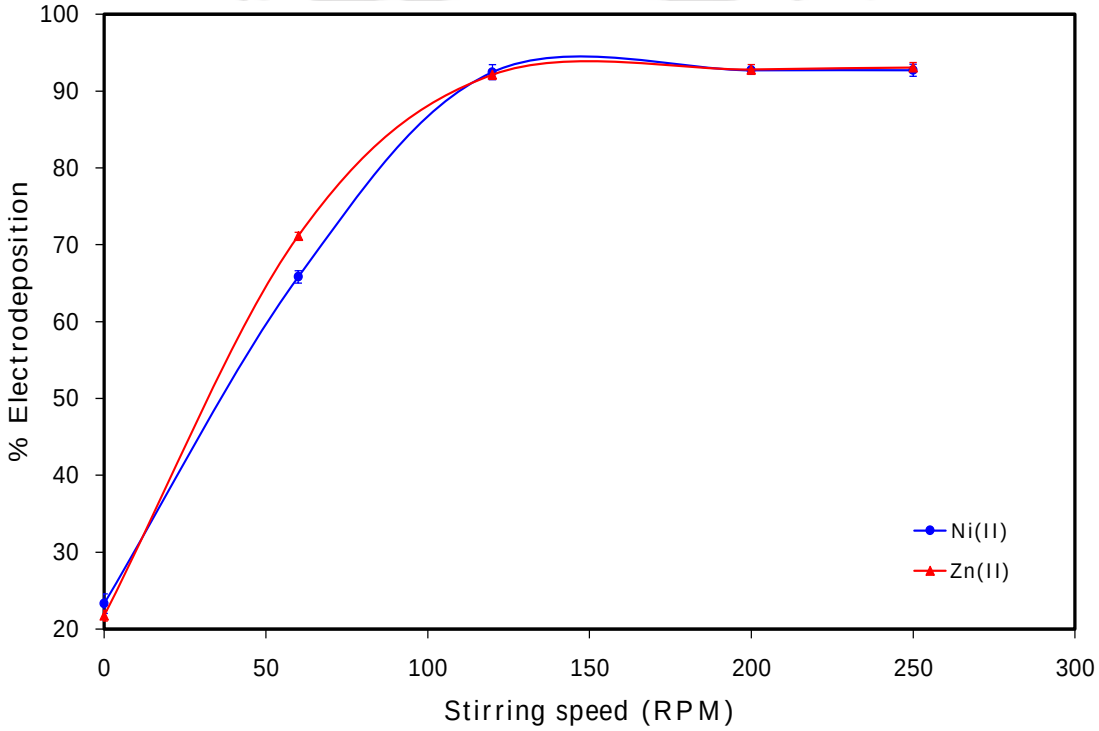

Figure 5.16: Effect of stirring condition of aqueous phases

5.2.3 Simultaneous separation of metals

Based on the studies on single heavy metal pollutants and their experimental results thereof, we are able to zero in on a set of optimum operating conditions. Hereafter it is worth studying the efficacy of the operating conditions on simultaneous extraction and electrodeposition of the binary pollutant at various ratios of Zn(II) and Ni(II)

in the feed. However, unfortunately, the best extractants for two heavy metal pollutants are different, *viz.*, D2EHPA is best for Zn(II), while TOA is best for Ni(II). It is thereby desired to test the individual efficiency of the extractants TOA and D2EHPA in transporting the metals Zn(II) and Ni(II) from a binary component mixture at varied ratios of metals. The extractants have also been employed with varying proportions to detect the ideal ratio of pollutant(s) and carrier(s) for the best transport and recovery. Other parameters were maintained as optimized before.

5.2.3.1 Simultaneous transportation and electrodeposition of metals using TOA as carrier

In this study, binary pollutant conditions have been set with varied ratios of Zn(II) and Ni(II) in the feed phase. The results of simultaneous extraction and deposition of metals are tabulated in Table 5.5. The transport and deposition of Ni(II) is preferential over Zn(II). The higher the ratio of Ni(II)/Zn(II), the higher would be the preference of Ni(II) over Zn(II). The kinetics of the transport and deposition of metals at a solute ratio of Zn(II)/Ni(II) = 1:4 have been measured. The results are reported in Figure 5.17. The trends of % deposition of Ni(II) and Zn(II) are as expected. Most of the metals were deposited on the cathode plate within 6 h as the concentration of metals at the beginning was very high. The concentration gradient reduces with time, and the deposition rates are reduced. The metal deposition reached 93% and 49% for Ni(II) and Zn(II), respectively, after a 12 h run.

5.2.3.2 Simultaneous transportation and electrodeposition of metals using D2EHPA as carrier

The set of experimentations, as described in section 5.2.3.1 has been repeated with D2EHPA as the carrier. The results of simultaneous extraction and deposition of metals are tabulated in Table 5.5. The transport and deposition of Zn(II) is preferential over Ni(II). The higher the ratio of Zn(II)/Ni(II), the higher would be the preference of Zn(II) over Ni(II). The kinetics of transport and deposition of metals at

solute ratio of Zn(II)/Ni(II) = 4:1 have been measured. The results are reported in Figure 5.18. The trends of % deposition of Ni(II) and Zn(II) are as expected. Most of the metals were deposited on the cathode plate within 6 h as the concentration of metals at the beginning is very high. The concentration gradient reduces with time, and the deposition rates are reduced. The metal deposition reached 21.87% and 89.5% for Ni(II) and Zn(II), respectively, after a 12 h run.

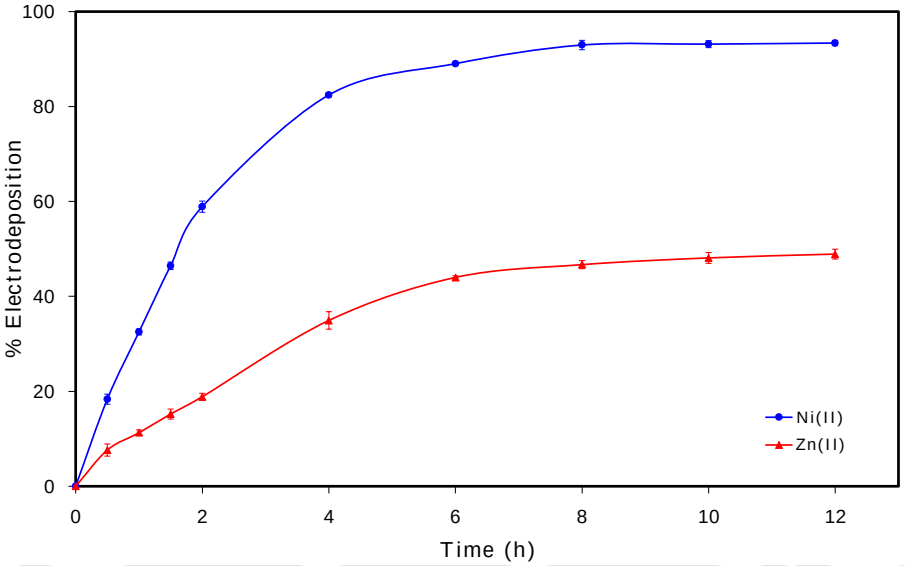

Figure 5.17: Saturation period with TOA

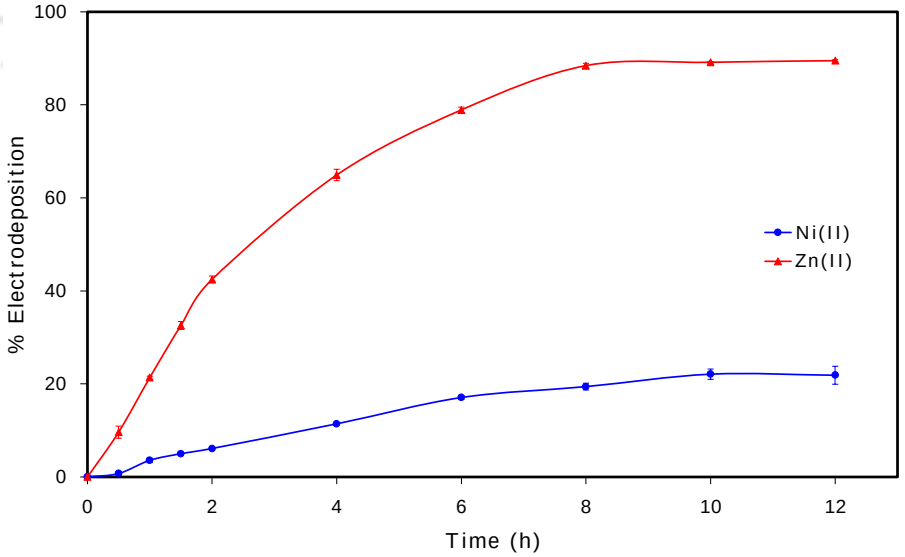

Figure 5.18: Saturation period with D2EHPA

Table 5.5: Three phase SLM-EP study: % extraction and %electrodepositon of Zn(II) and Ni(II) from their mixed feed in various ratios using 5% (v/v) TOA and 3% (v/v) D2EHPA as carriers.

Zn(II)(in mg L^{-1})	Ni(II)(in mg L^{-1})	Zn(II)/Ni(II)	extraction of Zn(II) (in %)		extraction of Ni(II) (in %)		total extraction of metals (in %)		total deposition of metals (in %)	
			using TOA	using D2EHPA	using TOA	using D2EHPA	using TOA	using D2EHPA	using TOA	using D2EHPA
100			73.81	93.64			73.81	93.64	73.21	93.07
	100				93.84	52.84	93.84	52.84	92.30	51.40
50	50	1:1	66.20	77.81	80.32	32.50	73.26	55.15	71.49	53.48
40	60	2:3	53.40	71.68	89.16	37.50	74.85	51.17	73.11	49.55
20	80	1:4	50.96	55.78	95.86	41.71	86.88	44.53	85.08	82.84
60	40	3:2	65.71	87.39	85.28	27.00	73.54	63.23	71.73	61.85
80	20	4:1	70.18	90.20	64.70	23.46	69.08	76.85	67.27	75.98

5.2.3.3 Experimental optimization of proportions of solute and carriers in SLM-EP

It is further desired to study whether a mixture of carriers is more useful in efficient transportation and electrodeposition of a mixture of metal ions. A series of experiments were carried out with various ratios of metal ions in the feed with various ratios of carriers in the sunflower oil in order to find out the best combinatorial proportions of compositions in the feed and organic phases. Face centered CCD in RSM has been employed to design the experiments and to optimize the ratios of carriers, i.e., D2EHPA and TOA, and metals (*i.e.*, Zn(II) and Ni(II)). Other parameters such as pH of aqueous solutions (*i.e.*, feed and strip), concentration of strip solution, stirring speed, and run time are already optimized from previous studies. The design input parameters are concentration of D2EHPA (referred to as A) with range of 1-5% (v/v), concentration of TOA (referred to as B) with a range of 1-8% (v/v), concentration of Zn(II) (referred to as C) with a range from 20-100 mg L^{-1} in the feed phase, and concentration of Ni(II) (referred to as D) with a range from 20-100 mg L^{-1} in the feed phase. Other parameters remained unchanged, such as pH of the feed phase at 5, concentration of the strip phase (NH_4Cl) at 0.2 M, speed of stirring at 120 rpm, and run time of 12 h. The actual output parameters from the experiments and their predicted ones against the input parameters through the quadratic model are shown in Table 5.6. Table 5.7 shows the ANOVA study of %deposition of Zn(II) and % deposition of Ni(II). The regression model equation for %deposition of Zn(II) and %deposition of Ni(II) are given by Equations 5.8 and 5.9, respectively.

The Fischer variation (F value), probability values (p value), and correlation coefficient (R^2) are examined in order to verify the significance of model. The p-value should be <0.05 for the model to be significant. The F-values were calculated from a quotient of coefficient mean square and residual mean square. As evident from the calculated model, F-values (*i.e.*, 87.96 for %deposition of Zn(II) and 29.01 for %deposition of Ni(II)) and very low p-values <0.0001 (see Table 5.7), the model is

highly significant. Further, the predicted R^2 of 0.9056 is in reasonable agreement with the adjusted R^2 of 0.9767 for deposition of Zn(II), and in case of deposition of Ni(II), a predicted R^2 of 0.8436 is also very much reasonable to the adjusted R^2 of 0.9311. The signal to noise ratio (called as adequate precision value) >4 is desirable. The adequate precision for deposition of Zn(II) and deposition Ni(II) are 29.20 and 15.80, respectively, which are quite high against the minimum desirable value of 4. Residuals versus predicted graphs for %deposition of Zn(II) and Ni(II) are plotted in Figure 5.19a and 5.19b. Scattering points of predicted values within the range of ±3% across the horizontal line of residuals suggest that models are well fitted. Figure 5.20a and 5.20b presents the correlation between the predicted values and the actual or experimental values of %deposition of Zn(II) and Ni(II). Actual values are experimental data obtained from a particular run, whereas predicted values are evaluated from the model. This predicted values were compared with the experimental results to verify consistency and acceptability of the empirical model (refer to Figure 5.20a and 5.20b). The scattered points over and under the diagonal line reflects the overestimation and underestimation of design points. ANOVA (see Table 5.7) is used to check the significance and fitness of the model.

In order to understand the interaction between parameters or the relation between input factors (*i.e.*, concentrations of D2EHPA and TOA in sunflower oil and concentration of Zn(II) and Ni(II) in the feed phase) required for optimum conditions for %deposition of Zn(II) and Ni(II) are illustrated in Figures 5.21 and 5.22, respectively.

The statistical optimization study of all four parameters with specific ranges (see Table 5.8) is done by design of experiments with the help of Design Expert 7.0 software. The calculated optimum parameters with a predicted result is tabulated in Table 5.9. The desirability value of the optimized outcome is 1.00. The desirability value ranges between 0.0 (undesirable) to 1.0 (desirable). The predicted results of %deposition of Zn(II) and Ni(II) are compared with the experimental results with

the error percentages tabulated in Table 5.10.

$$\begin{aligned}\%\text{Deposition of Zn(II)} =& 75.32 + 13.84 \times A - 1.50 \times B + 13.87 \times C - 0.64 \times D \\ &+ 1.57 \times A \times B + 1.36 \times A \times C - 0.99 \times A \times D \\ &- 0.76 \times B \times C - 0.64 \times B \times D + 1.39 \times C \times D \\ &- 16.34 \times A^2 + 0.85 \times B^2 - 8.21 \times C^2 + 0.44 \times D^2\end{aligned} \tag{5.8}$$

$$\begin{aligned}\%\text{Deposition of Ni(II)} =& 64.22 - 0.17 \times A + 11.99 \times B - 0.35 \times C + 17.76 \times D \\ &+ 0.43 \times A \times B + 0.45 \times A \times C + 0.85 \times A \times D \\ &+ 0.12 \times B \times C + 3.11 \times B \times D - 0.11 \times C \times D \\ &+ 4.04 \times A^2 - 19.20 \times B^2 + 4.98 \times C^2 - 13.74 \times D^2\end{aligned} \tag{5.9}$$

Table 5.6: Design Arrangement and Experimental Responses for CCD

Run	Input A: D2EHPA (%volume)	Input B: TOA (%volume)	Input C: Concentration of Zn(II)(mg L^{-1})	Input D: Concentration of Ni(II)(mg L^{-1})	response 1: R1, %deposition of Zn(II)		response 2: R2, %deposition of Ni(II)	
					Actual	Perd	Actual	Perd
1	3	4.5	60	60	75.66	75.32	66.43	64.22
2	3	4.5	20	60	52.69	53.24	65.89	69.55
3	3	4.5	60	60	75.91	75.32	66.52	64.22
4	5	8	20	20	50.33	53.88	31.42	30.50
5	5	8	100	20	81.31	80.06	31.12	31.18
6	1	8	100	20	45.53	44.54	28.28	31.46
7	3	4.5	60	60	75.52	75.32	66.41	64.22
8	3	1	60	60	76.27	77.67	18.56	33.03
9	1	8	20	100	24.76	23.00	71.93	72.84
10	5	1	20	100	50.31	48.73	46.31	43.35
11	1	1	20	20	30.26	27.16	18.26	15.93
12	1	1	100	20	47.37	50.91	18.67	14.32

Continued ....

Table 5.6–*Continued from previous page....*

Run	Input A: D2EHPA (%volume)	Input B: TOA (%volume)	Input C: Concentration of Zn(II)(mg L^{-1})	Input D: Concentration of Ni(II)(mg L^{-1})	response 1: R1, %deposition of Zn(II)		response 2: R2, %deposition of Ni(II)	
					Actual	Perd	Actual	Perd
13	3	4.5	60	20	75.81	75.12	27.63	32.72
14	5	1	20	20	50.76	50.93	13.44	12.11
15	3	8	60	60	75.51	74.68	67.16	57.01
16	3	4.5	60	60	75.66	75.32	66.57	64.22
17	3	4.5	60	100	75.15	76.40	69.01	68.24
18	3	4.5	60	60	75.52	75.32	66.29	64.22
19	1	1	100	100	64.34	58.22	40.55	41.69
20	5	8	100	100	80.33	80.86	71.84	74.39
21	1	8	20	20	24.22	23.82	31.29	32.58
22	5	8	20	100	50.22	49.12	71.11	74.16
23	5	1	100	20	80.95	80.14	13.00	12.31
24	1	1	20	100	25.22	28.90	45.11	43.75
25	1	8	100	100	47.03	49.29	71.23	71.26

Continued ....

Table 5.6–*Continued from previous page....*

Run	Input A: D2EHPA (%volume)	Input B: TOA (%volume)	Input C: Concentration of Zn(II)(mg L^{-1})	Input D: Concentration of Ni(II)(mg L^{-1})	response 1: R1, %deposition of Zn(II)		response 2: R2, %deposition of Ni(II)	
					Actual	Perd	Actual	Perd
26	5	4.5	60	60	75.15	72.82	65.26	68.09
27	3	4.5	60	60	75.34	75.32	66.07	64.22
28	5	1	100	100	80.67	83.50	45.67	43.08
29	3	4.5	100	60	80.98	80.99	68.19	68.86
30	1	4.5	60	60	42.26	45.15	66.93	68.43

Table 5.7: ANOVA for respective response surface quadratic models

Source	Sum of squares (SS)	Degree of freedom (DF)	Mean square (MS)	F-value	p value Prob>F	Remarks
%Deposition of Zn(II)						
Model	10572.45	14	755.18	87.96	<0.0001	In this case A, B, C, AB, A^2, C^2 are significant model
A	3445.61	1	3445.61	401.33	<0.0001	
B	40.23	1	40.23	4.69	<0.0469	
C	3465.00	1	3465.00	403.58	<0.0001	
D	7.33	1	7.33	0.85	0.3700	
AB	39.53	1	39.53	4.60	0.0487	
AC	29.78	1	29.78	3.47	0.0822	
BC	9.17	1	9.17	1.07	0.3179	
BD	6.57	1	6.57	0.76	0.3956	
CD	31.00	1	31.00	3.61	0.0768	
A^2	691.46	1	691.46	80.54	<0.0001	
B^2	1.87	1	1.87	0.22	0.6478	
C^2	174.49	1	174.49	20.32	0.0004	
D^2	0.50	1	0.50	0.058	0.8129	
Residual	128.60	15	8.59			
Lack of fit	128.60	10	12.86	350.06	<0.0001	
Pure error	0.18	5	0.037			
R^2=0.9880, R^2_{adj}=0.9767, R^2_{pred}=0.9056, Adequate precision=29.201						
%Deposition of Ni(II)						
Model	12609.62	14	900.69	29.01	<0.0001	In this case B, D, BD, B^2, D^2 is significant model
A	0.53	1	0.53	0.071	0.8981	
B	2587.44	1	2587.44	83.33	<0.0001	
C	2.14	1	2.14	0.069	0.7964	
D	5676.45	1	5676.45	182.81	<0.0001	
AB	3.00	1	3.00	0.097	0.7601	
AC	3.25	1	3.25	0.10	0.7508	
AD	11.61	1	11.61	0.37	0.5500	
BC	0.24	1	0.24	0.007654	0.9314	
BD	154.57	1	154.57	4.98	0.0414	
CD	0.21	1	0.21	0.006741	0.9357	
A^2	42.25	1	42.25	1.36	0.2616	
B^2	954.81	1	954.81	30.75	<0.0001	
C^2	64.33	1	64.33	2.07	0.1706	
D^2	488.91	1	488.91	15.75	0.0012	
Residual	465.76	15	31.05			
Lack of fit	465.60	10	46.56	1425.74	<0.0001	
Pure error	0.16	5	0.033			
R^2=0.9644, R^2_{adj}=0.9311, R^2_{pred}=0.8436, Adequate precision=15.805						

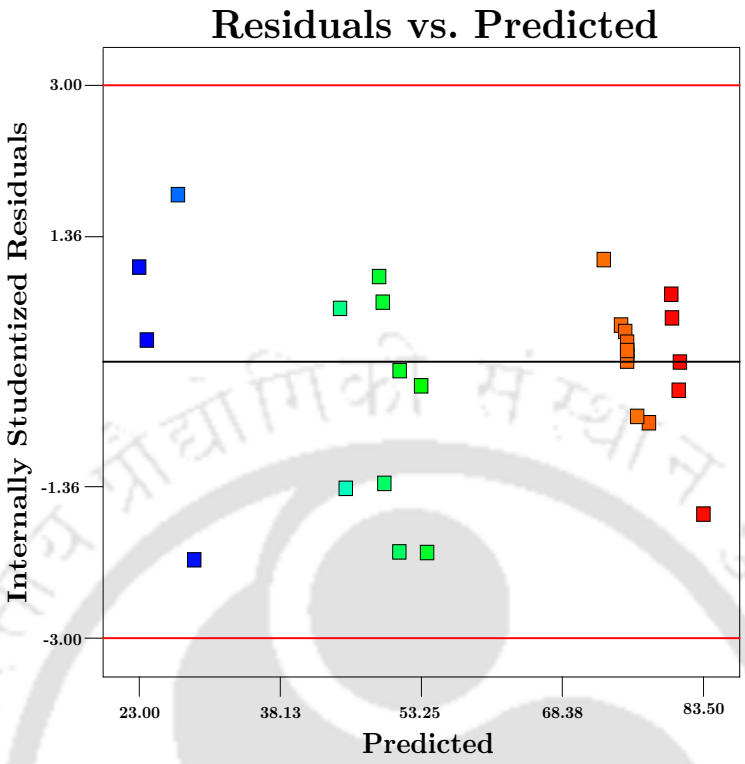

(a) %Deposition of Zn(II)

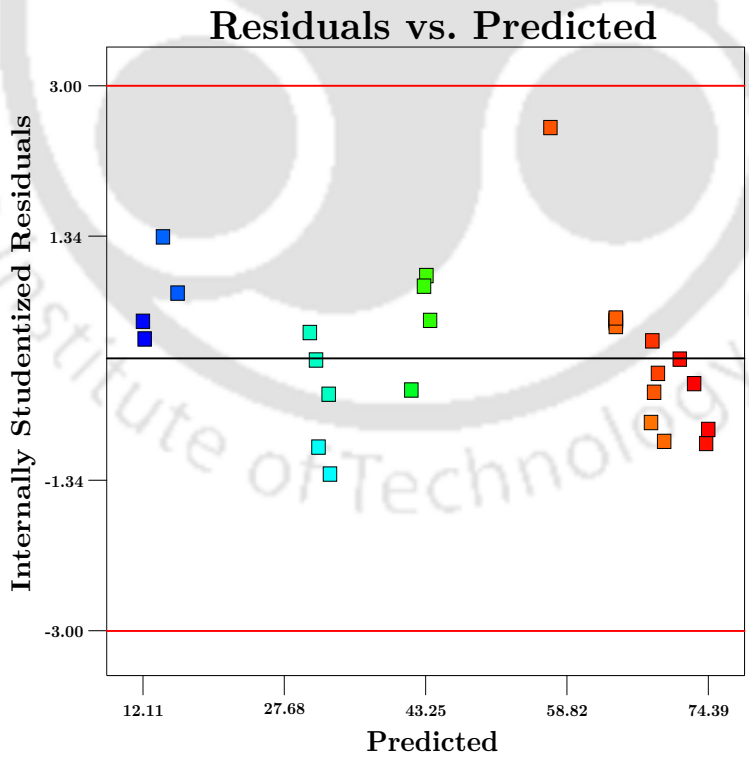

(b) %Deposition of Ni(II)

Figure 5.19: Residual versus predicted graphs.

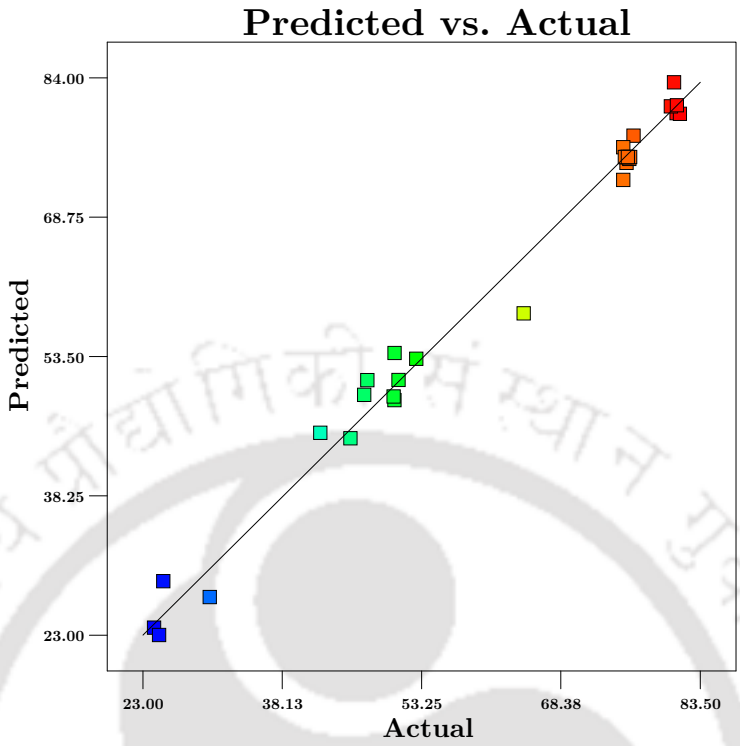

(a) %Deposition of Zn(II)

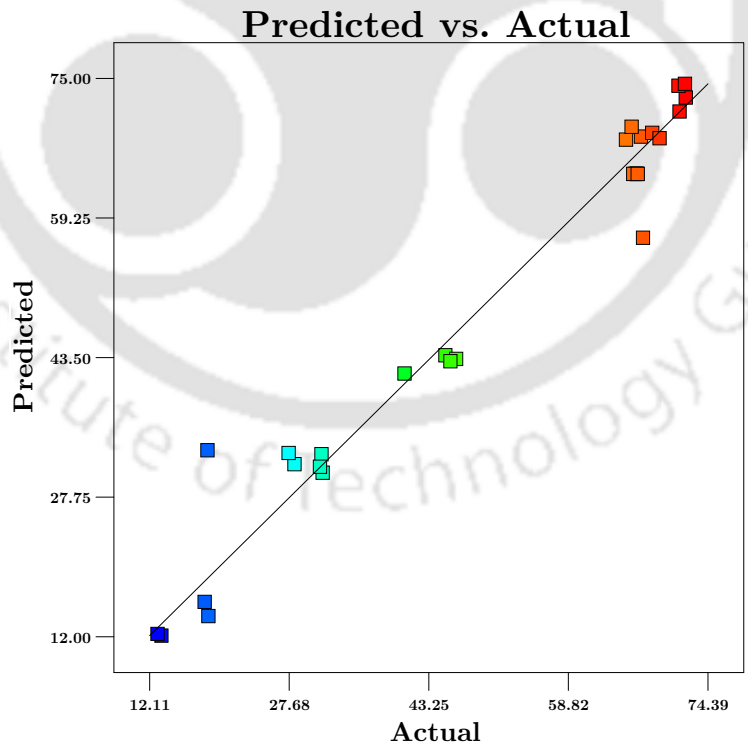

(b) %Deposition of Ni(II)

Figure 5.20: Predicted versus actual graphs.

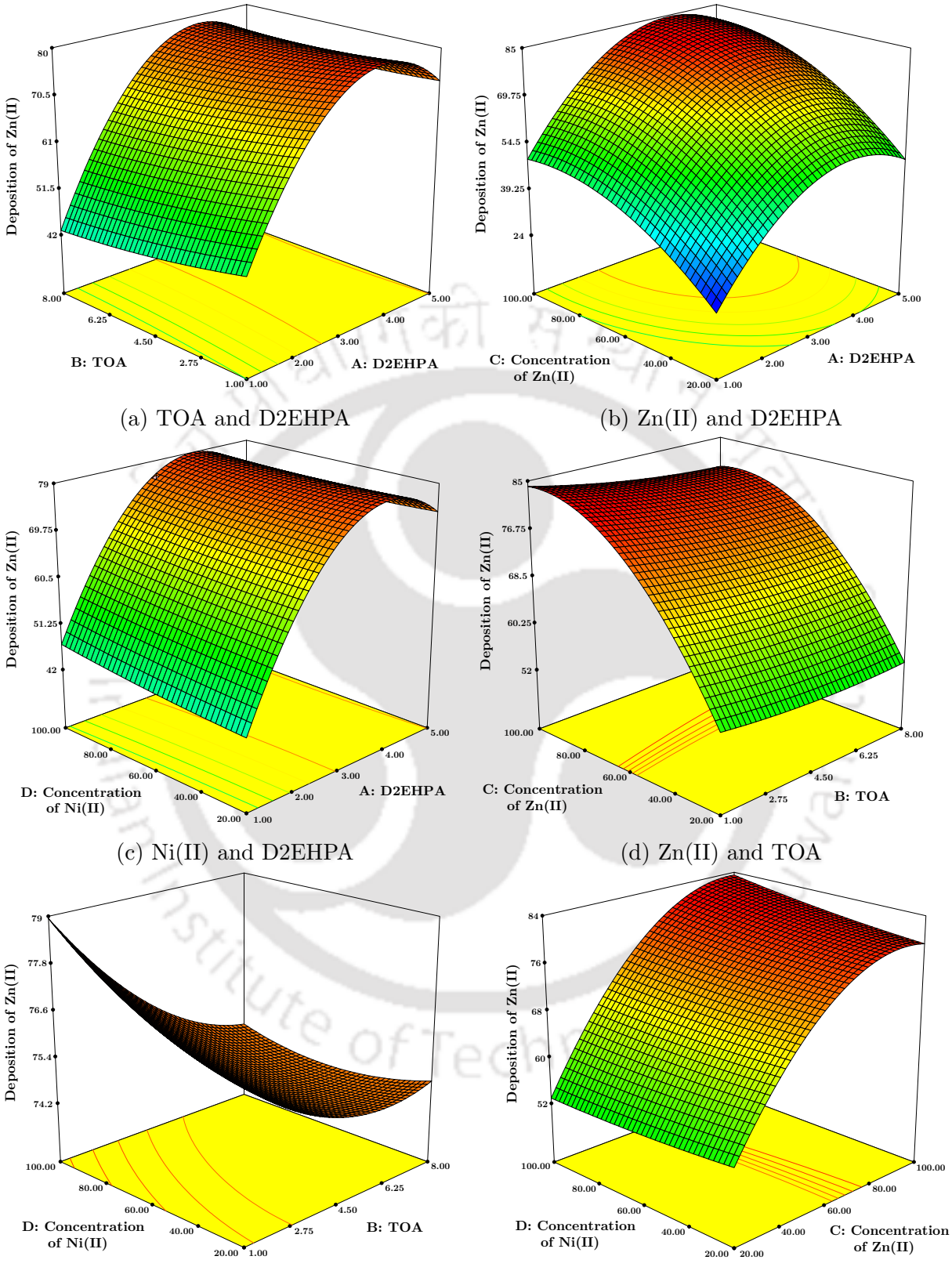

(a) TOA and D2EHPA

(b) Zn(II) and D2EHPA

(c) Ni(II) and D2EHPA

(d) Zn(II) and TOA

(e) Ni(II) and TOA

(f) Zn(II) and Ni(II)

Figure 5.21: Response surface plots of concentrations of binary components for optimum %deposition of Zn(II).

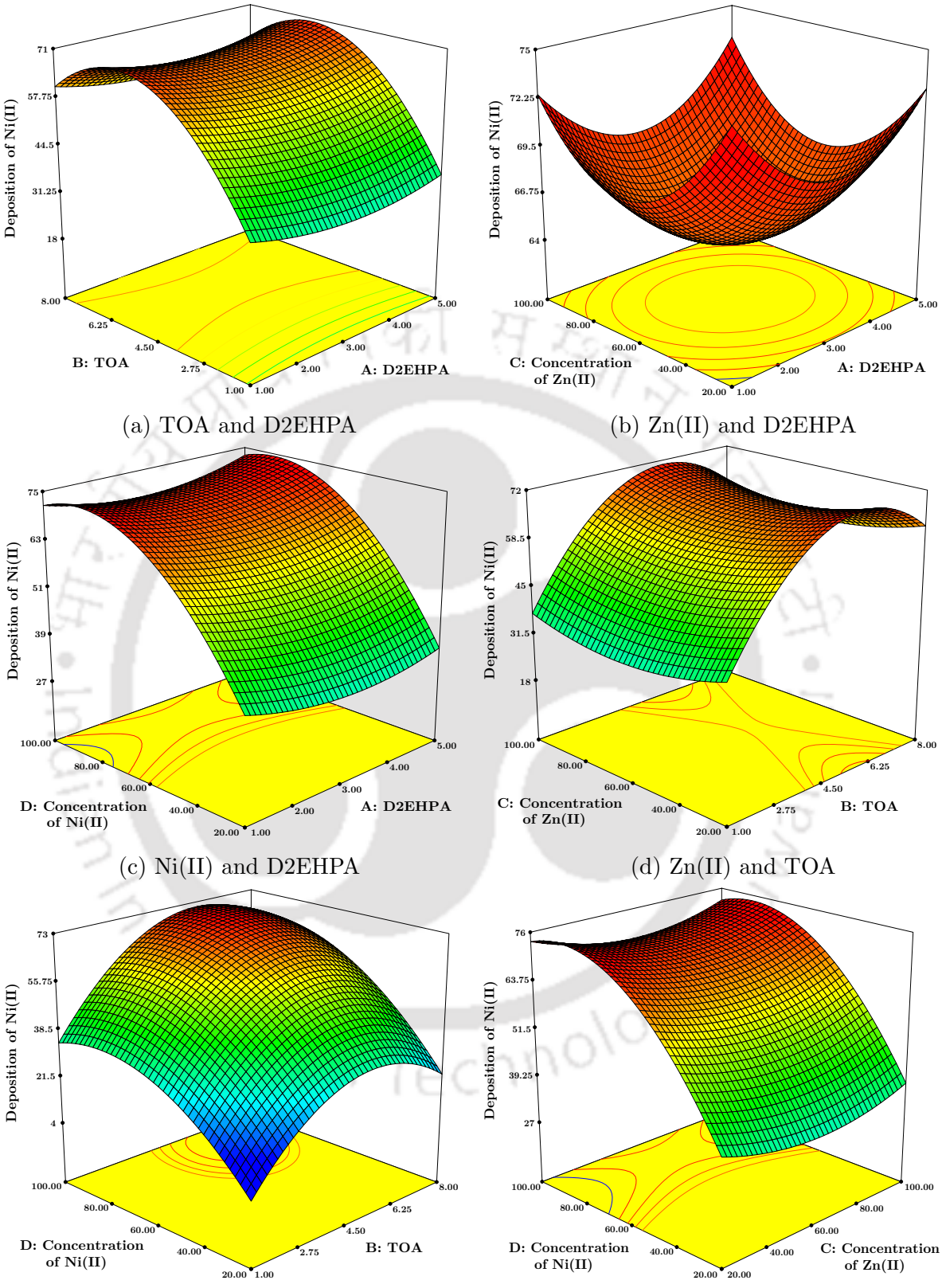

(a) TOA and D2EHPA

(b) Zn(II) and D2EHPA

(c) Ni(II) and D2EHPA

(d) Zn(II) and TOA

(e) Ni(II) and TOA

(f) Zn(II) and Ni(II)

Figure 5.22: Response surface plots of concentrations of binary components for optimum %deposition of Ni(II).

Table 5.8: Optimization constraints for %electrodeposition of Zn(II) and Ni(II)

Name	Goal	Lower limit	Upper limit	Lower weight	Upper weight	Importance
Concentration of D2EHPA	in range	1	5	1	1	3
Concentration of TOA	in range	1	8	1	1	3
Concentration of Zn(II)	in range	20	100	1	1	3
Concentration of Ni(II)	in range	20	100	1	1	3
%Deposition of Zn(II)	maximize	24.22	81.31	1	1	3
%Deposition of Ni(II)	maximize	13	71.93	1	1	3

Table 5.9: Optimization Results for %electrodeposition of Zn(II) and Ni(II)

Variable	Value
Concentration of D2EHPA (% vol/vol)	3.01
Concentration of TOA (% vol/vol)	4.87
Concentration of Zn(II) (mg L^{-1})	93.25
Concentration of Ni(II) (mg L^{-1})	88.27
Electrodeposition of Zn(II) (%)	82.45
Electrodeposition of Ni(II) (%)	74.29
Desirability	1

Table 5.10: Error analysis between predicted and experimental results

Responses	Predicted value	Experimental value	Error (%)
%Deposition of Zn(II)	82.45	80.22	2.69
%Deposition of Ni(II)	74.29	71.73	3.44

5.3 Summary of studies on electrodeposition of Ni(II) and Zn(II)

- ✓ A new type of design mechanism has been successfully implemented for extraction and recovery with deposition/electroplating of Ni(II) and Zn(II).
- ✓ The integration of the electrodeposition module in the strip phase of SLM not only helped to increase the separation efficiency but also proved to be a way to generate a value added product.
- ✓ The copper plate was found to be an ideal cathode.
- ✓ The optimum parameters of the two phase studies are 100 mg L^{-1} of Ni(II) as the initial concentration, pH of 5 in aqueous solution, 5% (v/v) of TOA as the carrier/extractant in the organic phase, stirring speed of 200 rpm, and run time of 12 h.
- ✓ In case of Ni(II), the optimum parameters of the three phase SLM studies are 100 mg L^{-1} of Ni(II) in the feed phase, pH 5 in the feed phase, 0.15 M of NH_4Cl in the strip phase, 5% (v/v) of TOA in the sunflower oil, 3 V DC electric potential in the strip phase, stirring speed of 120 rpm in both phases, and 8 h of run time.
- ✓ In case of Zn(II), the optimum parameters of the three phase SLM studies are 100 mg L^{-1} of Zn(II) in the feed phase, pH 5 in the feed phase, 0.2 M of NH_4Cl in the strip phase, 3% (v/v) of D2EHPA in the sunflower oil, 3 V DC electric potential in the strip phase, stirring speed of 120 rpm in both phases, and 8 h of run time.
- ✓ The maximum deposition of Ni(II) and Zn(II) were found over $\sim$ 93% for both the cases.

- ✓ In the case of binary pollutants, the mixture of Zn(II) and Ni(II) with a 1:4 ratio, yields a maximum total deposition at 85% with TOA as the carrier, whereas the mixture of Zn(II) and Ni(II) with a 4:1 ratio, yields a maximum total deposition at 75.98% with D2EHPA as the carrier.

- ✓ Experimental optimization with face centered CCD in RSM was done for the binary pollutants (i.e., Zn(II) and Ni(II)) with mixtures of binary carriers (i.e., TOA and D2EHPA) as parameters to optimize deposition of Zn(II) and Ni(II), which also showed good agreement with the experimental results.

Chapter 6

Conclusion and future scope

This chapter summarizes the inferences drawn from the present research work and provides recommendations towards future direction for separation of heavy metal from wastewater.

6.1 Conclusion

The performance of LM towards separation (*i.e.* extraction and recovery) of heavy metals from wastewater has been investigated in this thesis. The heavy metals *i.e.* Cr(VI), Ni(II) and Zn(II) were separated from their aqueous solution using different LM techniques. The experiments were accomplished using two-phase equilibrium study, three-phase BLM study and three-phase FS-SLM study. Various physico-chemical parameters have been optimized to maximize the transport of heavy metals. A series of experiments were carried out to find the efficiency of LM through various techniques. For easy waste management a novel technique has been implement where a separate module has been included in strip phase of FS-SLM system to precipitate/deposit the heavy metals to convert them as value added product. The prime physico-chemical parameters affecting the system performance were identified for experimental optimization through RSM using central composite design rule. A regression model along with ANOVA evaluates whether the chosen parameters were

of good agreement with experimental results. The major conclusions are summarized below:

- ✓ Among the various solvent sunflower oil come out as best green solvent in LM based separation process for heavy metals.
- ✓ BLM process is well suited for lab scale study. The up-gradation of BLM process to pilot/industrial scale is restricted due to much lower value of surface area to volume ratio of LM.
- ✓ In case of separation of Cr(VI), combination of sunflower oil and aliquat 336 was found best solvent-carrier combination.
- ✓ In FS-SLM study for separation of Cr(VI), combination of PVDF-sunflower oil-aliquat 336-Na_2-EDTA was found suitable.
- ✓ Na_2-EDTA was found to be best stripping agent and the yield of %extraction and %recovery of Cr(VI) were 80% and 73% respectively in FS-SLM study.
- ✓ Electrochemical reaction was successfully carried out for synthesis of chromium-iron oxide using FS-SLM technology where, the separation efficiency of Cr reached around 97%.
- ✓ FS-SLM with in situ electrochemical reaction helps to reduce hexavalent chromium (Cr(VI)) to trivalent chromium (Cr(III)) by forming chromium-iron complex which converts liquid waste to solid waste as a useful value added product for end user.
- ✓ In case of separation of Ni(II), combination of PVDF-sunflower oil-TOA-NH_4Cl was found suitable, whereas in case of separation of Zn(II), combination of PVDF-sunflower oil-D2EHPA-NH_4Cl was found suitable.
- ✓ NH_4Cl was found best stripping agent for electrodeposition of Ni(II) and Zn(II) on cathode plate.

- ✓ Application of electroplating technology on SLM system converts the liquid waste into an useful end product in the form of electroplated material.

- ✓ For each study the out come of optimized parameters using RSM technique have been used for experimentation and the error percentage were found with in 3.5%. The error percent between model and actual value proves that the chosen parameters were good agreement with experimental results using RSM technique with CCD and ANOVA.

6.2 Recommendations for future work

Separation of heavy metal using FS-SLM technology is still emerging area and there is huge scope for work in future. Some other topics related to the ones presented in this thesis that needs to be addressed in future are the following:

- ✓ Development of a mathematical model for simulating the solute-transport mechanism through LM, including process chemistry, speciation dynamics and metal recovery etc. would be an useful exercise.

- ✓ FS-SLM study was carried out with binary pollutant (*i.e.* Ni(II) and Zn(II)) condition. The work can be extended using more than two pollutants and using multiple carriers with their synergistic effect on the transportation efficiency can be evaluated.

- ✓ The FS-SLM configuration, used in the present work, yielded promising results for separation of heavy metals. Therefore, similar studies using other configurations such as hollow fiber SLM, spiral wound SLM and series of two or more SLMs can be carried out.

- ✓ Detailed stability criteria of SLMs may be studied.

- ✓ In the present work, chromium-iron oxide nanoparticle was synthesized as a recovery of metal towards value added product. The same technique can be used for other metals also.
- ✓ In the present research work, electroplating was done only for Ni(II) and Zn(II). However, the same electroplating technique can be used for separation of other metals also.
- ✓ All the experiments in this research work were carried out in batch and fed-batch mode. The efficacy of a continuous mode SLM can be studied in future.

References

[1] Heike B. Bradl. Preface. In H.B. Bradl, editor, *Heavy Metals in the Environment: Origin, Interaction and Remediation*, volume 6 of *Interface Science and Technology*. Elsevier, 2005.

[2] M J Udy. *Chromium*. New York : Reinhold, 1956.

[3] Mahdi Chiha, Mohamed H Samar, and Oualid Hamdaou. Extraction of chromium(VI) from sulphuric acid aqueous solutions by a liquid surfactant membrane(LSM). *Desalination*, 194(1):69 – 80, 2006.

[4] V. Coman, B. Robotin, and P. Ilea. Nickel recovery/removal from industrial wastes: A review. *Resources, Conservation and Recycling*, 73:229 – 238, 2013.

[5] Basudev Swain, Kadambini Sarangi, and Radhanatha Prasad Das. Effect of different anions on separation of copper and zinc by supported liquid membrane using TOPS-99 as mobile carrier. *Journal of Membrane Science*, 243(1):189 – 194, 2004.

[6] A D Dayan and A J Paine. Mechanisms of chromium toxicity, carcinogenicity and allergenicity: Review of the literature from 1985 to 2000. *Human & Experimental Toxicology*, 20(9):439–451, 2001.

[7] B. K. Sharma, P. C. Singhal, and K. S. Chugh. Intravascular haemolysis and acute renal failure following potassium dichromate poisoning. *Postgraduate Medical Journal*, 54(632):414–415, 1978.

[8] Michelle Science, Jennie Johnstone, Daniel E. Roth, Gordon Guyatt, and Mark Loeb. Zinc for the treatment of the common cold: a systematic review and meta-analysis of randomized controlled trials. *CMAJ*, 184(10):E551–E561, 2012.

[9] Patrick E McKinney, Jeffrey Brent, and Ken Kulig. Acute zinc chloride ingestion in a child: Local and systemic effects. *Annals of Emergency Medicine*, 23(6):1383 – 1387, 1994.

[10] Nelson Leonel Martnez-Rodrguez, Sara Tavrez, and Zaira Isabel Gonzlez-Snchez. In vitro toxicity assessment of zinc and nickel ferrite nanoparticles in human erythrocytes and peripheral blood mononuclear cell. *Toxicology in Vitro*, 57:54 – 61, 2019.

[11] J W Patterson. *Industrial Wastewater Treatment Technology*. Butterworth-Heinemann, London, second edition, 1985.

[12] S. Erdogan, Y. Onal, C. Akmil-Basar, S. Bilmez-Erdemoglu, C. Sarici-Ozdemir, E. Koseoglu, and G. Icduygu. Optimization of nickel adsorption from aqueous solution by using activated carbon prepared from waste apricot by chemical activation. *Applied Surface Science*, 252(5):1324 – 1331, 2005.

[13] P. Gomathi Priya, C. Ahmed Basha, V. Ramamurthi, and S. Nathira Begum. Recovery and reuse of Ni(II) from rinsewater of electroplating industries. *Journal of Hazardous Materials*, 163(2):899 – 909, 2009.

[14] Prakash Sarwa and Sanjay Kumar Verma. Recovery and recycling of Zn(II) from wastewater by Scenedesmus sp. MCC 26 isolated from a heavy metal contaminated site. *CLEAN Soil, Air, Water*, 42(9):1298–1303, 2014.

[15] Marta Rozenblat, Magdalena Regel-Rosocka, and Jan Szymanowski. Metal removal from spent pickling solutions of high zinc(II) concentration. *Physiochemical Problems of Mineral Processing*, 38(1):121–129, 2004.

[16] C. Ahmed Basha, N.S. Bhadrinarayana, N. Anantharaman, and K.M. Meera Sheriffa Begum. Heavy metal removal from copper smelting effluent using electrochemical cylindrical flow reactor. *Journal of Hazardous Materials*, 152(1):71 – 78, 2008.

[17] Loris Pietrelli, Sergio Ferro, and Marco Vocciante. Raw materials recovery from spent hydrochloric acid-based galvanizing wastewater. *Chemical Engineering Journal*, 341:539 – 546, 2018.

[18] World Health Organization. *Guidelines for Drinking-water Quality*. WHO, 2017.

[19] L. Cifuentes, G. Crisstomo, J.P. Ibez, J.M. Casas, F. Alvarez, and G. Cifuentes. On the electrodialysis of aqueous H_2SO_4-$CuSO_4$ electrolytes with metallic impurities. *Journal of Membrane Science*, 207(1):1 – 16, 2002.

[20] Jian-Jun Qin, Maung-Nyunt Wai, Maung-Htun Oo, and Fook-Sin Wong. A feasibility study on the treatment and recycling of a wastewater from metal plating. *Journal of Membrane Science*, 208(1):213 – 221, 2002.

[21] Ruey-Shin Juang, Yong-Yan Xu, and Ching-Liang Chen. Separation and removal of metal ions from dilute solutions using micellar-enhanced ultrafiltration. *Journal of Membrane Science*, 218(1):257 – 267, 2003.

[22] M. S. Hanra and V. Ramachandhran. Trace level separation of zinc sulfate and lead nitrate from toxic effluent streams by reverse osmosis modular systems. *Separation Science and Technology*, 31(1):49–61, 1996.

[23] John F. Scamehorn, Sherril D. Christian, Dawlat A. El-Sayed, Hirotaka Uchiyama, and Samia S. Younis. Removal of divalent metal cations and their mixtures from aqueous streams using micellar-enhanced ultrafiltration. *Separation Science and Technology*, 29(7):809–830, 1994.

[24] Grgorio Crini. Non-conventional low-cost adsorbents for dye removal: A review. *Bioresource Technology*, 97(9):1061 – 1085, 2006.

[25] A Dabrowski. Adsorption from theory to practice. *Advances in Colloid and Interface Science*, 93(1):135 – 224, 2001.

[26] Arshid Bashir, Lateef Ahmad Malik, Sozia Ahad, Taniya Manzoor, Mudasir Ahmad Bhat, G. N. Dar, and Altaf Hussain Pandith. Removal of heavy metal ions from aqueous system by ion-exchange and biosorption methods. *Environmental Chemistry Letters*, 17:729 – 754, 2019.

[27] Bilge Alyz and Sevil Veli. Kinetics and equilibrium studies for the removal of nickel and zinc from aqueous solutions by ion exchange resins. *Journal of Hazardous Materials*, 167(1):482 – 488, 2009.

[28] Yi-Chu Huang and S.Sefa Koseoglu. Separation of heavy metals from industrial waste streams by membrane separation technology. *Waste Management*, 13(5):481 – 501, 1993.

[29] Marcel Mulder. *Basic principles of membrane technology*. Springer, 1996.

[30] Vladimir S Kislik et al. *Liquid membranes: principles and applications in chemical separations and wastewater treatment*. Elsevier, 2009.

[31] T. Araki and H. Tsukube. *Liquid Membranes: Chemical Applications*. CRC Press, 1990.

[32] Aloke Kumar Ghoshal and Prabirkumar Saha. Chapter five - liquid membrane filters. In Steve Tarleton, editor, *Progress in Filtration and Separation*, pages 155 – 205. Academic Press, Oxford, 2015.

[33] Petr Vanysek and Richard P. Buck. New developments in liquid/liquid interface transport: A literature review. *Journal of Electroanalytical Chemistry and Interfacial Electrochemistry*, 163(1):1 – 9, 1984.

[34] Norman N. Li. Separation of hydrocarbons by liquid membrane permeation. *Industrial & Engineering Chemistry Process Design and Development*, 10(2):215–221, 1971.

[35] N.M. Kocherginsky, Qian Yang, and Lalitha Seelam. Recent advances in supported liquid membrane technology. *Separation and Purification Technology*, 53(2):171 – 177, 2007.

[36] J.G. Wijmans and R.W. Baker. The solution-diffusion model: a review. *Journal of Membrane Science*, 107(1):1 – 21, 1995.

[37] Toshio Shinbo, Kenzo Kurihara, Yonosuke Kobatke, and Naoki Kamo. Active transport of picrate anion through organic liquid membrane. *Nature*, 270:277–278, 1977.

[38] W. Kaminski and W. Kwapinski. Applicability of liquid membranes in environmental protection. *Polish Journal of Environmental Studies*, 9(1):37–43, 2000.

[39] Recep Ali Kumbasar. Extraction of chromium (VI) from multicomponent acidic solutions by emulsion liquid membranes using TOPO as extractant. *Journal of Hazardous Materials*, 167(1):1141 – 1147, 2009.

[40] K. Chakraborty. *Liquid membrane based technology for removal of pollutants from wastewater*. PhD thesis, Indian Institute of Technology Guwahati, 2010.

[41] Recep Ali Kumbasar and Osman Tutkun. Separation of cobalt and nickel from acidic leach solutions by emulsion liquid membranes using Alamine 300 (TOA) as a mobile carrier. *Desalination*, 224(1):201 – 208, 2008.

[42] A. I. Alonso, A. Irabien, and M. I. Ortiz. Nondispersive extraction of Cr(VI) with Aliquat 336: Influence of carrier concentration. *Separation Science and Technology*, 31(2):271–282, 1996.

[43] Kamal Kumar Bhatluri, Mriganka Sekhar Manna, Prabirkumar Saha, and Aloke Kumar Ghoshal. Separation of Cd(II) from its aqueous solution using environmentally benign vegetable oil as liquid membrane. *Asia-Pacific Journal of Chemical Engineering*, 8(5):775–785, 2013.

[44] Ali Jabbari, Haraj Chaldavi, and Mojtaba Shamsipur. Specific membrane transport of mercury as $[Hg(SCN)_4]^{2-}$ ion using K^+-Dibenzo-18-crown-6 as carrier. *Separation Science and Technology*, 34(12):2421–2430, 1999.

[45] F.F. Zha, A.G. Fane, C.J.D. Fell, and R.W. Schofield. Critical displacement pressure of a supported liquid membrane. *Journal of Membrane Science*, 75(1):69 – 80, 1992.

[46] Kabita Chakrabarty, Prabirkumar Saha, and Aloke Kumar Ghoshal. Separation of lignosulfonate from its aqueous solution using supported liquid membrane. *Journal of Membrane Science*, 340(1):84 – 91, 2009.

[47] R.M. Cespon-Romero, M.C. Yebra-Biurrun, and M.P. Bermejo-Barrera. Preconcentration and speciation of chromium by the determination of total chromium and chromium(III) in natural waters by flame atomic absorption spectrometry with a chelating ion-exchange flow injection system. *Analytica Chimica Acta*, 327(1):37 – 45, 1996.

[48] Deborah M. Proctor, Joanne M. Otani, Brent L. Finley, Dennis J. Paustenbach, Judith A. Bland, Ned Speizer, and Edward V. Sargent. Is hexavalent chromium carcinogenic via ingestion? a weight-of-evidence review. *Journal of Toxicology and Environmental Health, Part A*, 65(10):701–746, 2002.

[49] Anil Kumar, Avinash Thakur, and Parmjit Singh Panesar. Extraction of hexavalent chromium by environmentally benign green emulsion liquid membrane using tridodecyamine as an extractant. *Journal of Industrial and Engineering Chemistry*, 70:394 – 401, 2019.

[50] A. Bhowal, G. Bhattacharyya, B. Inturu, and S. Datta. Continuous removal of hexavalent chromium by emulsion liquid membrane in a modified spray column. *Separation and Purification Technology*, 99:69 – 76, 2012.

[51] Arunava Choudhury, Siddhartha Sengupta, Chiranjib Bhattacharjee, and Siddhartha Datta. Extraction of hexavalent chromium from aqueous stream by emulsion liquid membrane (ELM). *Separation Science and Technology*, 45(2):178–185, 2010.

[52] Eleni Sazakli, Cristina M. Villanueva, Manolis Kogevinas, Kyriakos Maltezis, Athanasia Mouzaki, and Michalis Leotsinidis. Chromium in drinking water: Association with biomarkers of exposure and effect. *International Journal of Environmental Research and Public Health*, 11(10):10125–10145, 2014.

[53] Cental Pollution Control Board India. The environment (protection) rules, 1986.

[54] Lynne T. Haber, Hudson K. Bates, Bruce C. Allen, Melissa J. Vincent, and Adriana R. Oller. Derivation of an oral toxicity reference value for nickel. *Regulatory Toxicology and Pharmacology*, 87:S1 – S18, 2017.

[55] Patrick H. Brown, Ross M. Welch, and Earle E. Cary. Nickel: A micronutrient essential for higher plants. *Plant Physiology*, 85(3):801–803, 1987.

[56] Claudio Buttice. *"Nickel Compounds". In Colditz, Graham A. (ed.). The SAGE Encyclopedia of Cancer and Society (Second ed.).* Thousand Oaks: SAGE Publications, 2015.

[57] Barbara K. Reck, Daniel B. Mller, Katherine Rostkowski, and T. E. Graedel. Anthropogenic nickel cycle: Insights into use, trade, and recycling. *Environmental Science & Technology*, 42(9):3394–3400, 2008.

[58] E. Denkhaus and K. Salnikow. Nickel essentiality, toxicity, and carcinogenicity. *Critical Reviews in Oncology/Hematology*, 42(1):35 – 56, 2002.

[59] Kazimierz S Kasprzak, F.William Sunderman, and Konstantin Salnikow. Nickel carcinogenesis. *Mutation Research/Fundamental and Molecular Mechanisms of Mutagenesis*, 533(1):67 – 97, 2003.

[60] ATSDR (Agency for Toxic Substances and Disease Registry). Toxicological profile for nickel. Atlanta, GA, USA: ATSDR/U.S. Public Health Service, ATSDR/TP-88/19, 1988.

[61] K. K. Das, S. N. Das, and S. A. Dhundasi. Nickel, its adverse health effects & oxidative stress. *Indian Journal of Medical Research*, 128:412 – 425, 2008.

[62] G J Fosmire. Zinc toxicity. *The American Journal of Clinical Nutrition*, 51(2):225–227, 1990.

[63] Samir Samman and David C.K. Roberts. The effect of zinc supplements on plasma zinc and copper levels and the reported symptoms in healthy volunteers. *Medical Journal of Australia*, 146(5):246–249, 1987.

[64] Richard D. Noble and J. Douglas Way. *Liquid Membranes*. American Chemical Society, Washington, DC, 1987.

[65] Ali Jabbari, Majid Esmaeili, and Mojtaba Shamsipur. Selective transport of mercury as $HgCl_4^{2-}$ through a bulk liquid membrane using K^+-dicyclohexyl-18-crown-6 as carrier. *Separation and Purification Technology*, 24(1):139 – 145, 2001.

[66] Maria D. Granado-Castro, Maria D. Galindo-Riano, and Manuel Garcia-Vargas. Model experiments to test the use of a liquid membrane for separation and preconcentration of copper from natural water. *Analytica Chimica Acta*, 506(1):81 – 86, 2004.

[67] M.D. Granado-Castro, M.J. Casanueva-Marenco, M.D. Galindo-Riano, H. El Mai, and M. Daz de Alba. A separation and preconcentration process for metal speciation using a liquid membrane: A case study for iron speciation in seawater. *Marine Chemistry*, 198:56 – 63, 2018.

[68] F.J. Alguacil, A.G. Coedo, and M.T. Dorado. Transport of chromium (VI) through a Cyanex 923-xylene flat-sheet supported liquid membrane. *Hydrometallurgy*, 57(1):51 – 56, 2000.

[69] M.D. Granado-Castro, M.D. Galindo-Riano, and Manuel Garcia-Vargas. Separation and preconcentration of cadmium ions in natural water using a liquid membrane system with 2-acetylpyridine benzoylhydrazone as carrier by flame atomic absorption spectrometry. *Spectrochimica Acta Part B: Atomic Spectroscopy*, 59(4):577 – 583, 2004.

[70] I. Van de Voorde, L. Pinoy, and R.F. De Ketelaere. Recovery of nickel ions by supported liquid membrane (SLM) extraction. *Journal of Membrane Science*, 234(1):11 – 21, 2004.

[71] Patthaveekongka Weerawat, Vijitchalermpong Nattaphol, and Pancharoen Ura. Selective recovery of palladium from used aqua regia by hollow fiber supported with liquid membrane. *Korean Journal of Chemical Engineering*, 20(6):1092–1096, 2003.

[72] B Zhang, G Gozzelino, and Y Dai. A non-steady state model for the transport of iron(III) across n-decanol supported liquid membrane facilitated by D2EHPA. *Journal of Membrane Science*, 210(1):103 – 111, 2002.

[73] M.E. Martinez Perez, J.A. Reyes-Aguilera, T.I. Saucedo, M.P. Gonzalez, R. Navarro, and M. Avila-Rodriguez. Study of As(V) transfer through a supported liquid membrane impregnated with trioctylphosphine oxide (Cyanex 921). *Journal of Membrane Science*, 302(1):119 – 126, 2007.

[74] Guillaume Zante, Maria Boltoeva, Abderrazak Masmoudi, Remi Barillon, and Dominique Trebouet. Lithium extraction from complex aqueous solutions using supported ionic liquid membranes. *Journal of Membrane Science*, 580:62 – 76, 2019.

[75] Larysse Caixeta Ferreira, Layse Caixeta Ferreira, Vicelma Luiz Cardoso, and Ubirajara Coutinho Filho. Mn(II) removal from water using emulsion liquid membrane composed of chelating agents and biosurfactant produced in loco. *Journal of Water Process Engineering*, 29:100792, 2019.

[76] Stella Dernini, Simona Palmas, Anna M. Polcaro, and Bruno Marongiu. Extraction and transport of sodium ion and potassium ion in a liquid membrane containing crown ethers: effect of the mixed solvent. *Journal of Chemical & Engineering Data*, 37(2):281–284, 1992.

[77] Bipan Bansal, Xiao Dong Chen, and Md. Monwar Hossain. Transport of lithium through a supported liquid membrane of LIX54 and TOPO in kerosene. *Chemical Engineering and Processing: Process Intensification*, 44(12):1327 – 1336, 2005.

[78] P. Kandwal, S.A. Ansari, and P.K. Mohapatra. Transport of cesium using hollow fiber supported liquid membrane containing calix[4]arene-bis(2,3-naphtho)crown-6 as the carrier extractant: Part II. Recovery from simulated high level waste and mass transfer modeling. *Journal of Membrane Science*, 384(1):37 – 43, 2011.

[79] P.K Mohapatra, D.S Lakshmi, D Mohan, and V.K Manchanda. Selective transport of cesium using a supported liquid membrane containing di-t-butyl benzo 18 crown 6 as the carrier. *Journal of Membrane Science*, 232(1):133 – 139, 2004.

[80] Ruey-Shin Juang and Yu-Yin Wang. Amino acid separation with D2EHPA

by solvent extraction and liquid surfactant membranes. *Journal of Membrane Science*, 207(2):241 – 252, 2002.

[81] Su-Hsia Lin, Chia-Nan Chen, and Ruey-Shin Juang. Kinetic analysis on reactive extraction of aspartic acid from water in hollow fiber membrane modules. *Journal of Membrane Science*, 281(1):186 – 194, 2006.

[82] Z. Lazarova, B. Syska, and K. Schgerl. Application of large-scale hollow fiber membrane contactors for simultaneous extractive removal and stripping of penicillin G. *Journal of Membrane Science*, 202(1):151 – 164, 2002.

[83] G.C Sahoo and N.N Dutta. Studies on emulsion liquid membrane extraction of cephalexin. *Journal of Membrane Science*, 145(1):15 – 26, 1998.

[84] Sang Cheol Lee. Comparison of extraction efficiencies of penicillin G at different w/o ratios in the emulsion liquid membrane systems with dilute polymer solutions. *Journal of Membrane Science*, 237(1):225 – 232, 2004.

[85] M. Teresa A. Reis, Ondina M.F. Freitas, Shiva Agarwal, Licnio M. Ferreira, M. Rosinda C. Ismael, Remgio Machado, and Jorge M.R. Carvalho. Removal of phenols from aqueous solutions by emulsion liquid membranes. *Journal of Hazardous Materials*, 192(3):986 – 994, 2011.

[86] Yonggyun Park, A.H.P. Skelland, Larry J. Forney, and Jae-Hong Kim. Removal of phenol and substituted phenols by newly developed emulsion liquid membrane process. *Water Research*, 40(9):1763 – 1772, 2006.

[87] Chiraz Zidi, Rafik Tayeb, and Mahmoud Dhahbi. Extraction of phenol from aqueous solutions by means of supported liquid membrane (MLS) containing tri-n-octyl phosphine oxide (TOPO). *Journal of Hazardous Materials*, 194:62 – 68, 2011.

[88] Chiraz Zidi, Rafik Tayeb, Mourad Ben Sik Ali, and Mahmoud Dhahbi. Liquid-liquid extraction and transport across supported liquid membrane of phenol using tributyl phosphate. *Journal of Membrane Science*, 360(1):334 – 340, 2010.

[89] Michiaki Matsumoto, Yasushi Inomoto, and Kazuo Kondo. Selective separation of aromatic hydrocarbons through supported liquid membranes based on ionic liquids. *Journal of Membrane Science*, 246(1):77 – 81, 2005.

[90] P.B. Warey. *New research on hazardous materials*. Nova Publishers, New York, 2007.

[91] P. Venkateswaran, A. Navaneetha Gopalakrishnan, and K. Palanivelu. Di(2-ethylhexyl)phosphoric acid-coconut oil supported liquid membrane for the separation of copper ions from copper plating wastewater. *Journal of Environmental Sciences*, 19(12):1446 – 1453, 2007.

[92] G. Muthuraman and K. Palanivelu. Transport of textile dye in vegetable oils based supported liquid membrane. *Dyes and Pigments*, 70(2):99 – 104, 2006.

[93] A. S. Mahmoud, A.E. Ghaly, and M.S. Brooks. Removal of dye from textile wastewater using plant oils under different pH and temperature conditions. *American Journal of Environmental Sciences*, 3(4):205 – 218, 2007.

[94] Moamer Ehtash, Marie-Christine Fournier-Salan, Krasimir Dimitrov, Philippe Salan, and Abdellah Saboni. Phenol removal from aqueous media by pertraction using vegetable oil as a liquid membrane. *Chemical Engineering Journal*, 250:42 – 47, 2014.

[95] Pezhman Kazemi, Mohammad Peydayesh, Alireza Bandegi, Toraj Mohammadi, and Omid Bakhtiari. Stability and extraction study of phenolic wastewater treatment by supported liquid membrane using tributyl phosphate and

sesame oil as liquid membrane. *Chemical Engineering Research and Design*, 92(2):375 – 383, 2014.

[96] Kabita Chakrabarty, Prabirkumar Saha, and Aloke Kumar Ghoshal. Separation of mercury from its aqueous solution through supported liquid membrane using environmentally benign diluent. *Journal of Membrane Science*, 350(1):395 – 401, 2010.

[97] Mriganka Sekhar Manna, Kamal Kumar Bhatluri, Prabirkumar Saha, and Aloke Kumar Ghoshal. Transportation of catechin (±C) using physiologically benign vegetable oil as liquid membrane. *Industrial & Engineering Chemistry Research*, 51(46):15207–15216, 2012.

[98] Kamal Kumar Bhatluri, Mriganka Sekhar Manna, Prabirkumar Saha, and Aloke Kumar Ghoshal. Supported liquid membrane-based simultaneous separation of cadmium and lead from wastewater. *Journal of Membrane Science*, 459:256–263, 2014.

[99] Kamal Kumar Bhatluri, Mriganka Sekhar Manna, Aloke Kumar Ghoshal, and Prabirkumar Saha. Supported liquid membrane based removal of lead(II) and cadmium(II) from mixed feed: Conversion to solid waste by precipitation. *Journal of Hazardous Materials*, 299:504 – 512, 2015.

[100] Kamal Kumar Bhatluri, Sushma Chakraborty, Mriganka Sekhar Manna, Aloke Kumar Ghoshal, and Prabirkumar Saha. Separation of toxic heavy metals from its aqueous solution using environmentally benign vegetable oil as liquid membrane. *RSC Adv.*, 5:88331–88338, 2015.

[101] Vikas Kumar, Raghubansh K. Singh, and Pradip Chowdhury. Efficient extraction and recovery of lignosulfonate using sunflower oil as green solvent in liquid membrane transport: Equilibrium and kinetic study. *Journal of Industrial and Engineering Chemistry*, 67:109 – 122, 2018.

[102] Kaiwei Dong, Feng Xie, Xingyu Kuang, and Wei Wang. Recovery of copper and cyanide through emulsion liquid membrane with quaternary amine salt as the mobile carrier. *Mineral Processing and Extractive Metallurgy Review*, 39:1–7, 2018.

[103] Parisa Daraei, Sina Zereshki, and Amin Shokri. Application of nontoxic green emulsion liquid membrane prepared by sunflower oil for water decolorization: Process optimization by response surface methodology. *Journal of Industrial and Engineering Chemistry*, 2019.

[104] Meryem Mesli and Nasr-Eddine Belkhouche. Emulsion ionic liquid membrane for recovery process of lead. comparative study of experimental and response surface design. *Chemical Engineering Research and Design*, 129:160 – 169, 2018.

[105] Abdelkader Benderrag, Boumediene Haddou, Mortada Daaou, Houaria Benkhedja, Boumedienne Bounaceur, and Mostefa Kameche. Experimental and modeling studies on Cd (II) ions extraction by emulsion liquid membrane using Triton X-100 as biodegradable surfactant. *Journal of Environmental Chemical Engineering*, 7(3):103166, 2019.

[106] Bahram Mokhtari and Kobra Pourabdollah. Emulsion liquid membrane for selective extraction of Bi(III). *Chinese Journal of Chemical Engineering*, 23(4):641 – 645, 2015.

[107] Panpan Zhao, Fan Yang, Zhigang Zhao, Qiuxiao Liao, Yang Zhang, Peng Chen, Wanghuan Guo, and Ruixi Bai. A simple preparation method for rare-earth phosphate nano materials using an ionic liquid-driven supported liquid membrane system. *Journal of Industrial and Engineering Chemistry*, 54:369 – 376, 2017.

[108] Gulcin Ozevci, Senol Sert, and Meral Eral. Optimization of lanthanum transport through supported liquid membranes based on ionic liquid. *Chemical Engineering Research and Design*, 140:1 – 11, 2018.

[109] Lichang Zhang, Qianlin Chen, Chao Kang, Xin Ma, and Zunliang Yang. Rare earth extraction from wet process phosphoric acid by emulsion liquid membrane. *Journal of Rare Earths*, 34(7):717 – 723, 2016.

[110] S. Pavon, A. Fortuny, M.T. Coll, and A.M. Sastre. Improved rare earth elements recovery from fluorescent lamp wastes applying supported liquid membranes to the leaching solutions. *Separation and Purification Technology*, 224:332 – 339, 2019.

[111] Sareh Ammari Allahyari, Abdolhamid Minuchehr, Seyyed Javad Ahmadi, and Amir Charkhi. Th(IV) transport from nitrate media through hollow fiber renewal liquid membrane. *Journal of Membrane Science*, 520:374 – 384, 2016.

[112] Parisa Zaheri and Reza Davarkhah. Rapid removal of uranium from aqueous solution by emulsion liquid membrane containing thenoyltrifluoroacetone. *Journal of Environmental Chemical Engineering*, 5(4):4064 – 4068, 2017.

[113] Bholanath Mahanty, Prasanta K. Mohapatra, Andrea Leoncini, Jurriaan Huskens, and Willem Verboom. Pertraction of americium(III) through supported liquid membranes containing benzene-centered tripodal diglycolamides (Bz-T-DGA) as an extractant/carrier. *Chemical Engineering Research and Design*, 141:84 – 92, 2019.

[114] Chandrakant S. Gholap, S. Panja, P.S. Dhami, J.S. Yadav, and Sunil K. Ghosh. Supported liquid membrane transport studies of Pu(IV) using OTDA, a novel diamide. *Journal of Environmental Chemical Engineering*, 7(1):102784, 2019.

[115] T Kitagawa, Y Nishikawa, J W Frankenfeld, and N N Li. Wastewater treatment

by liquid membrane process. *Environmental Science & Technology*, 11(6):602–605, 1977.

[116] A.K. Chakravarti, S.B. Chowdhury, S. Chakrabarty, T Chakrabarty, and D.C. Mukherjee. Liquid membrane multiple emulsion process of chromium(VI) separation from waste waters. *Colloids and Surfaces A: Physicochemical and Engineering Aspects*, 103(1):59 – 71, 1995.

[117] Recep Ali Kumbasar. Studies on extraction of chromium (VI) from acidic solutions containing various metal ions by emulsion liquid membrane using alamine 336 as extractant. *Journal of Membrane Science*, 325(1):460–466, 2008.

[118] Recep Ali Kumbasar. Selective extraction of chromium (VI) from multicomponent acidic solutions by emulsion liquid membranes using tributhylphosphate as carrier. *Journal of hazardous materials*, 178(1):875–882, 2010.

[119] D Bonam, G Bhattacharyya, A Bhowal, and S Datta. Liquid- liquid extraction in a rotating-spray column: Removal of Cr (VI) by Aliquat 336. *Industrial & Engineering Chemistry Research*, 48(16):7687–7693, 2009.

[120] Ting-Chia Huang, Chee-Chang Huang, and Dong-Hwang Chen. Transport of chromium (VI) through a supported liquid membrane containing tri-n-octylphosphine oxide. *Separation science and technology*, 33(13):1919–1935, 1998.

[121] Nii-Kotey Djane, Kuria Ndungu, Carin Johnsson, Helen Sartz, Tina Tornstrom, and Lennart Mathiasson. Chromium speciation in natural waters using serially connected supported liquid membranes. *Talanta*, 48(5):1121 – 1132, 1999.

[122] P. Venkateswaran and K. Palanivelu. Studies on recovery of hexavalent chromium from plating wastewater by supported liquid membrane using tri-n-butyl phosphate as carrier. *Hydrometallurgy*, 78(12):107 – 115, 2005.

[123] M. Ashraf Chaudry, Naheed Bukhari, M. Mazhar, and Wajiha Abbasi. Coupled transport of chromium(III) ions across triethanolamine/cyclohexanone based supported liquid membranes for tannery waste treatment. *Separation and Purification Technology*, 55(3):292 – 299, 2007.

[124] Dr Mohammad Waqar Ashraf and Atiq Mian. Selective separation and preconcentration studies of chromium(VI) with Alamine 336 supported liquid membrane. *Toxicological & Environmental Chemistry*, 88(2):187–196, 2006.

[125] Cezary A. Kozlowski and Wladyslaw Walkowiak. Applicability of liquid membranes in chromium(VI) transport with amines as ion carriers. *Journal of Membrane Science*, 266(12):143 – 150, 2005.

[126] Robila Nawaz, Khurshid Ali, Nauman Ali, and Alia Khaliq. Removal of chromium(VI) from industrial effluents through supported liquid membrane using trioctylphosphine oxide as a carrier. *Journal of the Brazilian Chemical Society*, 27(1):209–220, 2016.

[127] Omid Jahanmahin, Mohammad Mehdi Montazer Rahmati, Toraj Mohammadi, Jaber Babaee, and Arash Khosravi. Cr(VI) ion removal from artificial waste water using supported liquid membrane. *Chemical Papers*, 70(7):913–925, Jul 2016.

[128] Aijuan Han, Hongwei Zhang, Jiulong Sun, Gaik-Khuan Chuah, and Stephan Jaenicke. Investigation into bulk liquid membranes for removal of chromium(VI) from simulated wastewater. *Journal of Water Process Engineering*, 17:63 – 69, 2017.

[129] Canan Onac, Ahmet Kaya, Duygu Ataman, Nefise Ayhan Gunduz, and H. Korkmaz Alpoguz. The removal of Cr(VI) through polymeric supported liquid membrane by using calix[4]arene as a carrier. *Chinese Journal of Chemical Engineering*, 27(1):85 – 91, 2019.

[130] H. Yesil and A.E. Tugtas. Removal of heavy metals from leaching effluents of sewage sludge via supported liquid membranes. *Science of The Total Environment*, 693:133608, 2019.

[131] P.K. Parhi and K. Sarangi. Separation of copper, zinc, cobalt and nickel ions by supported liquid membrane technique using LIX 84I, TOPS-99 and Cyanex 272. *Separation and Purification Technology*, 59(2):169 – 174, 2008.

[132] Hengpan Duan, Ziyue Wang, Xiaohong Yuan, Shixiong Wang, Hong Guo, and Xiangjun Yang. A novel sandwich supported liquid membrane system for simultaneous separation of copper, nickel and cobalt in ammoniacal solution. *Separation and Purification Technology*, 173:323 – 329, 2017.

[133] Hengpan Duan, Shixiong Wang, Xiangjun Yang, Xiaohong Yuan, Qin Zhang, Zhangjie Huang, and Hong Guo. Simultaneous separation of copper from nickel in ammoniacal solutions using supported liquid membrane containing synergistic mixture of M5640 and TRPO. *Chemical Engineering Research and Design*, 117:460 – 471, 2017.

[134] Jerzy Gega, Wladyslaw Walkowiak, and Bernadeta Gajda. Separation of Co(II) and Ni(II) ions by supported and hybrid liquid membranes. *Separation and Purification Technology*, 22-23:551 – 558, 2001.

[135] Yasemin Yildiz, Aynur Manzak, and Osman Tutkun. Synergistic extraction of cobalt and nickel ions by supported liquid membranes with a mixture of TIOA and TBP. *Desalination and Water Treatment*, 53(5):1246–1253, 2015.

[136] Ahmet Surucu, Volkan Eyupoglu, and Osman Tutkun. Selective separation of cobalt and nickel by supported liquid membranes. *Desalination*, 250(3):1155 – 1156, 2010.

[137] Ranpreet Singh, Rajeev Mehta, and Vineet Kumar. Simultaneous removal of

copper, nickel and zinc metal ions using bulk liquid membrane system. *Desalination*, 272(1):170 – 173, 2011.

[138] W. Mickler, A. Reich, E. Uhlemann, and H.J. Bart. Liquid membrane permeation of zinc, cadmium and nickel with 4-acyl-5-pyrazolones and β-diketones. *Journal of Membrane Science*, 119(1):91 – 97, 1996.

[139] Raffaele Molinari, Teresa Poerio, and Pietro Argurio. Selective removal of Cu^{2+} versus Ni^{2+}, Zn^{2+} and Mn^{2+} by using a new carrier in a supported liquid membrane. *Journal of Membrane Science*, 280(1):470 – 477, 2006.

[140] Ting-Chia Huang and Ruey-Shin Juang. Transport of zinc through a supported liquid membrane using di(2-ethylhexyl) phosphoric acid as a mobile carrier. *Journal of Membrane Science*, 31(2):209 – 226, 1987.

[141] Takashi Saito. Transportation of Zinc(II) ion through a supported liquid membrane. *Separation Science and Technology*, 25(5):581–591, 1990.

[142] Basudev Swain, Kadambini Sarangi, and Radhanath Prasad Das. Effect of different anions on separation of cadmium and zinc by supported liquid membrane using TOPS-99 as mobile carrier. *Journal of Membrane Science*, 277(1):240 – 248, 2006.

[143] A. Urtiaga, E. Bringas, R. Mediavilla, and I. Ortiz. The role of liquid membranes in the selective separation and recovery of zinc for the regeneration of Cr(III) passivation baths. *Journal of Membrane Science*, 356(1):88 – 95, 2010.

[144] W. S. Winston Ho, Bing Wang, Travis E. Neumuller, and Justin Roller. Supported liquid membranes for removal and recovery of metals from waste waters and process streams. *Environmental Progress*, 20(2):117–121, 2001.

[145] Francisco Jos Alguacil and Manuel Alonso. Separation of zinc(II) from cobalt(II) solutions using supported liquid membrane with DP-8R (di(2-

ethylhexyl) phosphoric acid) as a carrier. *Separation and Purification Technology*, 41(2):179 – 184, 2005.

[146] Jose Marchese, Mercedes E. Campderrosa, and Adolfo Acosta. Mechanistic study of cobalt, nickel and copper transfer across a supported liquid membrane. *Journal of Chemical Technology & Biotechnology*, 57(1):37–42, 1993.

[147] Jose Marchese, Mercedes Campderrosa, and Adolfo Acosta. Transport and separation of cobalt, nickel and copper ions with alamine liquid membranes. *Journal of Chemical Technology & Biotechnology*, 64(3):293–297, 1995.

[148] Prashant S Kulkarni, Krishnakant K Tiwari, and Vijaykumar V Mahajani. Membrane stability and enrichment of nickel in the liquid emulsion membrane process. *Journal of Chemical Technology & Biotechnology*, 75(7):553–560, 2000.

[149] Khurshid Ali, Robila Nawaz, Nauman Ali, Alia Khaliq, and Rizwan Ullah. Selective removal of zinc using tri-ethanolamine-based supported liquid membrane. *Desalination and Water Treatment*, 57(18):8549–8560, 2016.

[150] F. Valenzuela, J. Cabrera, C. Basualto, J. Sapag, J. Romero, J. Snchez, and G. Rios. Separation of zinc ions from an acidic mine drainage using a stirred transfer celltype emulsion liquid membrane contactor. *Separation Science and Technology*, 42(2):363–377, 2007.

[151] Hao Ma, Ozan Kokkilic, Raymond Langlois, Xuejuan Song, Yong Qin, and Kristian E. Waters. Selective separation of copper and nickel ions from aqueous solutions containing calcium by emulsion liquid membranes using central composite design. *The Canadian Journal of Chemical Engineering*, 97:1881–1893, 2019.

[152] Raja Norimie Raja Sulaiman, Norasikin Othman, Norul Fatiha Mohamed Noah, and Norela Jusoh. Removal of nickel from industrial effluent using a

synergistic mixtures of acidic and solvating carriers in palm oil-based diluent via supported liquid membrane process. *Chemical Engineering Research and Design*, 137:360 – 375, 2018.

[153] Raja Norimie Raja Sulaiman, Norela Jusoh, Norasikin Othman, Norul Fatiha Mohamed Noah, Muhammad Bukhari Rosly, and Hilmi Abdul Rahman. Supported liquid membrane extraction of nickel using stable composite SPEEK/PVDF support impregnated with a sustainable liquid membrane. *Journal of Hazardous Materials*, 380:120895, 2019.

[154] Aziza Hachemaoui and Kamel Belhamel. Simultaneous extraction and separation of cobalt and nickel from chloride solution through emulsion liquid membrane using cyanex 301 as extractant. *International Journal of Mineral Processing*, 161:7 – 12, 2017.

[155] C. Vergel, C. Mendiguchia, and C. Moreno. Liquid membranes as a tool for chemical speciation of metals in natural waters: Organic and inorganic complexes of nickel. *Membranes (Basel)*, 8:19(1 – 10), 2018.

[156] Asim K. Guha, Sudipto Majumdar, and Kamalesh K. Sirkar. A larger-scale study of gas separation by hollow-fiber-contained liquid membrane permeator. *Journal of Membrane Science*, 62(3):293 – 307, 1991.

[157] Raffaele Molinari and Pietro Argurio. *Applications of Supported Liquid Membranes and Emulsion Liquid Membranes*, pages 1–21. American Cancer Society, 2013.

[158] A.L. Ahmad, A. Kusumastuti, C.J.C. Derek, and B.S. Ooi. Emulsion liquid membrane for heavy metal removal: An overview on emulsion stabilization and destabilization. *Chemical Engineering Journal*, 171(3):870 – 882, 2011.

[159] W S Winston Ho and K K Sirkar. *Membrane Handbook*. Van Nostrand Reinhold, 1992.

[160] Norasikin Othman, Masahiro Goto, and Hanapi Mat. Liquid membrane technology for precious metals recovery from industrial waste. In *Regional Symposium on Membrane Science and Technology*, Puteri Pan Pacific Hotel, Johor Bahru, Johor, Malaysia, 2004.

[161] J.B. Wright, D.N. Nilsen, G. Hundley, and G.J. Galvan. Field test of liquid emulsion membrane technique for copper recovery from mine solutions. *Minerals Engineering*, 8(4):549 – 556, 1995.

[162] Ana I. Alonso, Berta Galan, Manuel Gonzalez, and Inmaculada Ortiz. Experimental and theoretical analysis of a nondispersive solvent extraction pilot plant for the removal of cr(vi) from a galvanic process wastewaters. *Industrial & Engineering Chemistry Research*, 38(4):1666–1675, 1999.

[163] A. Frank Seibert and James R. Fair. Scale-up of hollow fiber extractors. *Separation Science and Technology*, 32(1-4):573–583, 1997.

[164] Steven R. Reiken and Daina M. Briedis. Scale-up of hollow fiber reactor systems. *Chemical Engineering Communications*, 94(1):1–7, 1990.

[165] Jianfeng Song, Xuhong Niu, Xue-Mei Li, and Tao He. Selective separation of copper and nickel by membrane extraction using hydrophilic nanoporous ion-exchange barrier membranes. *Process Safety and Environmental Protection*, 113:1 – 9, 2018.

[166] Douglas C Montgomery. *Design and analysis of experiments*. John Wiley & Sons, 2008.

[167] V.V. Guaracho, N.M.S. Kaminari, M.J.J.S. Ponte, and H.A. Ponte. Central composite experimental design applied to removal of lead and nickel from sand. *Journal of Hazardous Materials*, 172(23):1087 – 1092, 2009.

[168] Anna Witek-Krowiak, Katarzyna Chojnacka, Daria Podstawczyk, Anna Dawiec, and Karol Pokomeda. Application of response surface methodology and artificial neural network methods in modelling and optimization of biosorption process. *Bioresource Technology*, 160:150 – 160, 2014.

[169] P. Roy, N.K. Mondal, and K. Das. Modeling of the adsorptive removal of arsenic: A statistical approach. *Journal of Environmental Chemical Engineering*, 2(1):585 – 597, 2014.

[170] Muhammad Abdur Rehman, Ismail Yusoff, Rasel Ahmmad, and Yatimah Alias. Arsenic adsorption using palm oil waste clinker sand biotechnology: an experimental and optimization approach. *Water, Air, & Soil Pollution*, 226(5):149, 2015.

[171] Krirkratthawit Wongkaew, Thanaporn Wannachod, Vanee Mohdee, Ura Pancharoen, Amornchai Arpornwichanop, and Anchaleeporn W. Lothongkum. Mass transfer resistance and response surface methodology for separation of platinum(IV) across hollow fiber supported liquid membrane. *Journal of Industrial and Engineering Chemistry*, 42:23 – 35, 2016.

[172] Duradundi Sawant Badkar, Krishna Shankar Pandey, and G. Buvanashekaran. Development of rsm- and ann-based models to predict and analyze the effects of process parameters of laser-hardened commercially pure titanium on heat input and tensile strength. *The International Journal of Advanced Manufacturing Technology*, 65(9):1319–1338, 2013.

[173] James Ying Tong and Edward L King. A spectrophotometric investigation of the equilibria existing in acidic solutions of chromium(VI). *Journal of the American Chemical Society*, 75(24):6180–6186, 1953.

[174] Arup K Sengupta, Suresh Subramonian, and Dennis Clifford. More on mech-

anism and some important properties of chromate ion exchange. *Journal of Environmental Engineering*, 114(1):137–153, 1988.

[175] Debabrata Bera, Parimal Chattopadhyay, and Lalitagauri Ray. Continuous removal of chromium from tannery wastwwater using activated sludge process determination of kinetic parameters. *Indian Journal of Chemical Technology*, 19:32–36, 2012.

[176] E J Fuller and N N Li. Extraction of chromium and zinc from cooling tower blowdown by liquid membranes. *Journal of membrane science*, 18:251–271, 1984.

[177] Supriyo Kumar Mondal and Prabirkumar Saha. Separation of hexavalent chromium from industrial effluent through liquid membrane using environmentally benign solvent: A study of experimental optimization through response surface methodology. *Chemical Engineering Research and Design*, 132:564 – 583, 2018.

[178] Ping Gao, Xueming Chen, Feng Shen, and Guohua Chen. Removal of chromium(VI) from wastewater by combined electrocoagulationelectroflotation without a filter. *Separation and Purification Technology*, 43(2):117 – 123, 2005.

[179] Miriam G Rodriguez, Ricardo Aguilar, Gabriel Soto, and Sergio A Martinez. Modeling an electrochemical process to remove Cr(VI) from rinse-water in a stirred reactor. *Journal of Chemical Technology & Biotechnology*, 78(4):371–376, 2003.

[180] M.Yousuf A Mollah, Robert Schennach, Jose R Parga, and David L Cocke. Electrocoagulation (EC) - science and applications. *Journal of Hazardous Materials*, 84(1):29 – 41, 2001.

[181] Umran Tezcan Un, Suzan Eroglu Onpeker, and Emel Ozel. The treatment of chromium containing wastewater using electrocoagulation and the produc-

tion of ceramic pigments from the resulting sludge. *Journal of Environmental Management*, 200:196 – 203, 2017.

[182] Mriganka Sekhar Manna, Kamal Kumar Bhatluri, Prabirkumar Saha, and Aloke Kumar Ghoshal. Transportation of bioactive (+)catechin from its aqueous solution using flat sheet supported liquid membrane. *Journal of Membrane Science*, 447:325 – 334, 2013.

[183] B. Ramachandra Reddy, D. Neela Priya, and Kyung Ho Park. Separation and recovery of cadmium(II), cobalt(II) and nickel(II) from sulphate leach liquors of spent nicd batteries using phosphorus based extractants. *Separation and Purification Technology*, 50(2):161 – 166, 2006.

[184] Jin Young Lee, B. Raju, B. Nagaphani Kumar, J. Rajesh Kumar, Hyung Kyu Park, and B. Ramachandra Reddy. Solvent extraction separation and recovery of palladium and platinum from chloride leach liquors of spent automobile catalyst. *Separation and Purification Technology*, 73(2):213 – 218, 2010.

[185] Chen-Yu Peng and Teh-Hua Tsai. Solvent extraction of palladium(II) from acidic chloride solutions using tri-octyl/decyl ammonium chloride (Aliquat 336). *Desalination and Water Treatment*, 52(4-6):1101–1121, 2014.

[186] Young-Woo Choi and Seung-Hyeon Moon. A study on supported liquid membrane for selective separation of Cr(VI). *Separation Science and Technology*, 39(7):1663–1680, 2005.

[187] Ting-Chia Huang, Chee-Chang Huang, and Dong-Hwang Chen. Transport of chromium(VI) through a supported liquid membrane containing tri-n-octylphosphine oxide. *Separation Science and Technology*, 33(13):1919–1935, 1998.

[188] Rahul Kumar Goyal, N.S. Jayakumar, and M.A. Hashim. Chromium removal

by emulsion liquid membrane using $[BMIM]^+[NTf_2]^-$ as stabilizer and TOMAC as extractant. *Desalination*, 278(1):50 – 56, 2011.

[189] Anil Kumar, Avinash Thakur, and Parmjit Singh Panesar. Extraction of hexavalent chromium by environmentally benign green emulsion liquid membrane using tridodecyamine as an extractant. *Journal of Industrial and Engineering Chemistry*, 70:394 – 401, 2019.

[190] Hubdar Ali Maitlo, Ki-Hyun Kim, Joo Yang Park, and Jung Hwan Kim. Removal mechanism for chromium (VI) in groundwater with cost-effective iron-air fuel cell electrocoagulation. *Separation and Purification Technology*, 213:378 – 388, 2019.

[191] Tulin Kiyak and Melike Kabasakalodlu. Anodic behavior of cathodically pretreated aluminum electrode. *Applied Surface Science*, 140(1):33 – 45, 1999.

[192] A. Kolics, J.C. Polkinghorne, and A. Wieckowski. Adsorption of sulfate and chloride ions on aluminum. *Electrochimica Acta*, 43(18):2605 – 2618, 1998.

[193] Jung Hwan Kim, I Seul Park, and Joo Yang Park. Electricity generation and recovery of iron hydroxides using a single chamber fuel cell with iron anode and air-cathode for electrocoagulation. *Applied Energy*, 160:18 – 27, 2015.

[194] M.Ashraf Chaudry, S. Ahmad, and M.T. Malik. Supported liquid membrane technique applicability for removal of chromium from tannery wastes. *Waste Management*, 17(4):211 – 218, 1998.

[195] Curtis W. Mcdonald and Raghbir S. Bajwa. Removal of toxic metal ions from metal-finishing wastewater by solvent extraction. *Separation Science*, 12(4):435–445, 1977.

[196] Berta Galan, Ane M. Urtiaga, Ana I. Alonso, J. Angel Irabien, and M. Inmac-

ulada Ortiz. Extraction of anions with aliquat 336: Chemical equilibrium modeling. *Industrial & Engineering Chemistry Research*, 33(7):1765–1770, 1994.

[197] Avijit Bhowal and Siddhartha Datta. Studies on transport mechanism of Cr(VI) extraction from an acidic solution using liquid surfactant membranes. *Journal of Membrane Science*, 188(1):1 – 8, 2001.

[198] Mahmut Bayramoglu, Mehmet Kobya, Orhan Taner Can, and Mustafa Sozbir. Operating cost analysis of electrocoagulation of textile dye wastewater. *Separation and Purification Technology*, 37(2):117 – 125, 2004.

[199] N. Daneshvar, H. Ashassi Sorkhabi, and M.B. Kasiri. Decolorization of dye solution containing Acid Red 14 by electrocoagulation with a comparative investigation of different electrode connections. *Journal of Hazardous Materials*, 112(1):55 – 62, 2004.

[200] N. Daneshvar, A. Oladegaragoze, and N. Djafarzadeh. Decolorization of basic dye solutions by electrocoagulation: An investigation of the effect of operational parameters. *Journal of Hazardous Materials*, 129(1):116 – 122, 2006.

[201] Serkan Bayar, Yaln evki Yldz, Alper Erdem Ylmaz, and ahset rdemez. The effect of stirring speed and current density on removal efficiency of poultry slaughterhouse wastewater by electrocoagulation method. *Desalination*, 280(1):103 – 107, 2011.

[202] M. Gheju and A. Iovi. Kinetics of hexavalent chromium reduction by scrap iron. *Journal of Hazardous Materials*, 135(1):66 – 73, 2006.

[203] Minghui Zhu, Tulio C. R. Rocha, Thomas Lunkenbein, Axel Knop-Gericke, Robert Schlgl, and Israel E. Wachs. Promotion mechanisms of iron oxide-based high temperature watergas shift catalysts by chromium and copper. *ACS Catalysis*, 6(7):4455–4464, 2016.

[204] Mahmoud Goodarz Naseri, Halimah Mohamed Kamari, Arash Dehzangi, Ahmad Kamalianfar, and Elias B. Saion. Fabrication of a novel chromium-iron oxide ($Cr_2Fe_6O_{12}$) nanoparticles by thermal treatment method. *Journal of Magnetism and Magnetic Materials*, 389:113 – 119, 2015.

[205] J. I. Langford and A. J. C. Wilson. Scherrer after sixty years: A survey and some new results in the determination of crystallite size. *Journal of Applied Crystallography*, 11(2):102–113, 1978.

[206] M. M. Abdullah, Fahd M. Rajab, and Saleh M. Al-Abbas. Structural and optical characterization of Cr_2O_3 nanostructures: Evaluation of its dielectric properties. *AIP Advances*, 4(2):027121(1–10), 2014.

[207] Svetozar Musi, Miroslava Maljkovi, Stanko Popovi, and Rudolf Trojko. Formation of chromia from amorphous chromium hydroxide. *Croatica Chemica Acta*, 72(4):789–802, 1999.

[208] Ali Akbar Bazrafshan, Shaaker Hajati, Mehrorang Ghaedi, and Arash Asfaram. Synthesis and characterization of antibacterial chromium iron oxide nanoparticle-loaded activated carbon for ultrasound-assisted wastewater treatment. *Applied Organometallic Chemistry*, 32(1):e3981 (1–13), 2018.

[209] J.A. Gadsden. *Infrared Spectra of Minerals and Related Inorganic Compounds*. Butterworths, 1975.

[210] S. Basavaraja, D.S. Balaji, Mahesh D. Bedre, D. Raghunandan, Swamy P.M. Prithviraj, and A. Venkataraman. Solvothermal synthesis and characterization of a cicular α -Fe_2O_3 nanoparticles. *Bulletin of Materials Science*, 34(7):1313–1317, 2011.

[211] M. Olper and M. Maccagni. *Electrolytic Zinc Production from Crude Zinc Oxides with the Ezinex Process*, pages 379–396. John Wiley & Sons, Ltd, 2013.

[212] M. Olper and M. Maccagni. From C.Z.O. to zinc cathode without any pre treatmentThe EZINEX process. In *International Symposium on Lead and Zinc Processing Lead & Zinc*, pages 85–98, Johannesburg, Republic of South Africa, 2013. The Southern African Institute of Mining and Metallurgy.

[213] H. W. Foote. The mixed crystals of ammonium chloride with nickel , cobalt and copper chlorides. *Journal of the American Chemical Society*, 34(7):880–886, 1912.

[214] Recep Ali Kumbasar. Selective extraction of cobalt from strong acidic solutions containing cobalt and nickel through emulsion liquid membrane using TIOA as carrier. *Journal of Industrial and Engineering Chemistry*, 18(6):2076 – 2082, 2012.

[215] T.Zh. Sadyrbaeva. Separation of cobalt(II) from nickel(II) by a hybrid liquid membraneelectrodialysis process using anion exchange carriers. *Desalination*, 365:167 – 175, 2015.

[216] R R Pawar, V J Suryavanshi, M M Patil, S S Patil, and G N Mulik. Liquid-liquid extraction of zinc(II) from acid media with n-n-heptylaniline as an extractant: Analysis of pharmaceutical and commercial sample. *Biomedical Journal of Scientific & Technical Research*, 10(3):1 – 7, 2018.

[217] G S Bell. The stability of zinc in zinc-chloride/ammonium-chloride electrolytes. *Electrochimica Acta*, 13(12):2197 – 2202, 1968.

[218] Charles F Windisch. *Corrosion: Fundamentals, Testing, and Protection*, volume 13A of ASM Handbook. ASM International, October 2003.

[219] Roel Cruz-Gaona and David Dreisinger. Study of the cathodic processes during the nickel electrowinning from ammonia-ammonium chloride solutions. *Electrochemistry in mineral and metal processing VI. The Electrochemical Society, New Jersey*, 2003.

[220] Simon Clark, Arnulf Latz, and Birger Horstmann. Rational development of neutral aqueous electrolytes for zinc-air batteries. *ChemSusChem*, 10(23):4735–4747, 2017.

[221] F Valenzuela, J Auspont, C Basualto, C Tapia, and J Sapag. Use of a surfactant liquid membrane contactor for zinc uptake from an acid aqueous effluent. *Chemical Engineering Research and Design*, 83(3):247 – 255, 2005.

[222] Masahiro Goto, Hiroko Yamamoto, Kazuo Kondo, and Fumiyuki Nakashio. Effect of new surfactants on zinc extraction with liquid surfactant membranes. *Journal of Membrane Science*, 57(2):161 – 174, 1991.

[223] Nasser Kanani. *Electroplating: Basic Principles, Processes and Practice*. Elsevier, November 2004.

[224] Razika Djouani, Qian Xu, Qiushi Song, and Ying Chen. The separation of copper and nickel from Ni-Cu mixed ore simulated leaching solution using electrochemical methods. *Eurasian Journal of Analytical Chemistry*, 12(7):1015–1044, 2017.

[225] M Rostom Ali, Md. Ziaur Rahman, and S Sankar Saha. Electroless and electrolytic deposition of nickel from deep eutectic solvents based on choline chloride. *Indian Journal of Chemical Technology*, 21:127–133, 2014.

[226] Shaohui Xu, Yiping Zhu, Dayuan Xiong, Lianwei Wang, Pingxiong Yang, and Paul K. Chu. Zinc electrodeposition on polycrystalline copper: Electrochemical study of early-stage growth mechanism. *The Journal of Physical Chemistry C*, 121(7):3938–3946, 2017.

[227] David P. Trudgeon, Kaipei Qiu, Xiaohong Li, Tapas Mallick, Oluwadamilola O. Taiwo, Barun Chakrabarti, Vladimir Yufit, Nigel P. Brandon, David Crevillen-Garcia, and Akeel Shah. Screening of effective electrolyte additives for zinc-based redox flow battery systems. *Journal of Power Sources*, 412:44 – 54, 2019.

Appendix A

Analysis of concentration of Cr(VI), Ni(II) and Zn(II) using Atomic Absorption Spectrometer (AAS)

A.1 Working principle of AAS

The principle of AAS is based on Beer-Lamberts law. The electrons of the atoms of an element can be exited to higher orbitals by absorbing light of a given wavelength. This amount of energy (or wavelength) is specific to a particular electron transition in a particular element. As the quantity of energy put into the flame is known, and the quantity remaining at the other side (at the detector) can be measured, it is possible, from Beer-Lambert law, to calculate how many of these transitions took place [1].

To analyze a sample in AAS, the sample solution is atomized and transforming the metals present in the sample to unexcited ground state atoms, which absorbs light at specific wavelengths. A light beam from a hollow cathode lamp whose cathode

is made of the element to be detected is passed through these atoms. Radiation is absorbed, transforming the ground state atoms to an excited state. The amount of radiation absorbed depends on the amount of the sample element present [2]. Working principle of AAS can be represented by a block diagram as shown in Figure A.1.

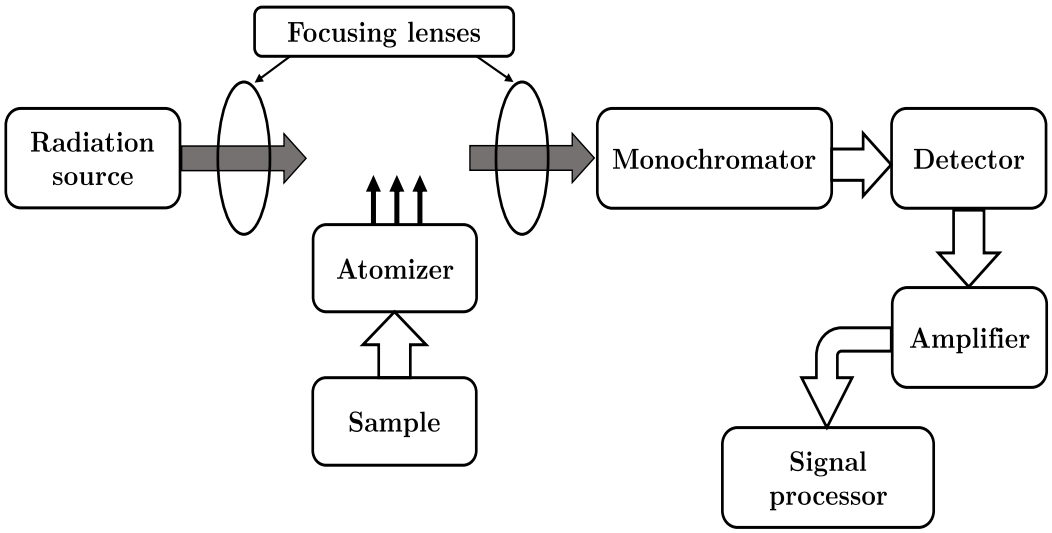

Figure A.1: Schematic diagram showing the working principle of AAS

A.2 Procedure for analysis of Cr(VI), Ni(II) and Zn(II) by AAS

Analysis of Cr(VI), Ni(II) and Zn(II) by AAS is done using flame atomic absorption mode. The following step by step procedures were followed for its analysis [3]:

A.2.1 Preparation of the sample

The collected samples from experimental runs were directly used for measurement of concentration in AAS without any further processing.

A.2.2 Preparation of standards

Standards were prepared freshly every time an analysis was made. A stock solution of 100 mg L^{-1} of Cr(VI), Ni(II) and Zn(II) were first prepared from the traceCERT® standard stock solution (1000 mg L^{-1}). To prepare this, 100 μl of traceCERT® standard stock solution was taken in a 100 ml volumetric flux and then diluted to 100 ml adding Milli-Q® deionized water. The standards of Cr(VI), Ni(II) and Zn(II) were then prepared from this stock solution by adding required amount of stock solution (*i.e.* Cr(VI) or Ni(II) or Zn(II)) in Milli-Q® deionized water.

A calibration curve was first prepared by injecting the standard samples (as prepared above) into the AAS. The standard samples of heavy metals (*i.e.* Cr(VI) or Ni(II) or Zn(II)) are evaporated by the desolvation process using flame atomiser where the solvent is completely evaporated. To attain the atomisation of samples, fuel and oxidants are used, for example, acetylene and air which produces at 2200-2300 °C. The concentration of Cr(VI), Ni(II) and Zn(II) were detected at 357.9 nm, 232 nm and 213.9 nm respectively. Unknown samples were injected after the calibration was over. The calibration curve was prepared each time an analysis was made from the fresh standards. The accuracy of the instrument is 0.1-0.8% in terms of RSD in mg L^{-1} level [3].

References

[1] G. H. Jeffery, J. Bassett, J. Mendham, and R. C. Denney. *Vogels text book of quantitative chemical analysis*. Longman Scientific and Technical (Harlow) publisher, 5^{th} edition, 1989.

[2] S . J. Haswell. *Atomic absorption spectrometry-theory, design and applications*. Elsevier, Amsterdam, 1991.

[3] Manual of atomic absorption spectrometer (Flame Atomic Absorption Spectrometry), Varian Australia, Model: AA240FS.

Appendix B

Composition of sunflower oil

Sunflower oil mainly contain high polyunsaturated fatty acid [1]. The typical fatty acid contents of sunflower oil is given in Table B.1 [2, 3].

Table B.1: Composition of fatty acids in sunflower oil.

Name of components	Quantity (%)
Palmitic acid (C16:0)	5.94
Palmitoleic acid (C16:1n7)	0.95
Stearic acid (C18:0)	2.53
Oleic acid (C18:1n9c)	68.88
Linoleic acid (C18:2n6)	21.58
Linolenic acid (C24:0)	0.31
Arachidic (C20:0)	0.28
Eicosenoic acid (C22:1n9)	0.23
Behenic acid (C24:0)	0.49

[0- saturated, 1- mono saturated, 2- poly saturated, n6- Omega-6, n7- Omega-7 and n9- Omega-9]

References

[1] U. S. Pal, R. K. Patra, N. R. Sahoo, C. K. Bakhara, and M. K. Panda. Effect of refining on quality and composition of sun ower oil. *Journal of food science and technology*, 52:4613 - 4618, 2015.

[2] Murat Akkaya. Fatty acid compositions of sunflowers (helianthus annuus l.) grown in east mediterranea region. *Rivista Italiana Delle Sostanze Grasse*, XCV:239 - 247, 2018.

[3] Dilsat Bozdogan Konuskan, Mehmet Arslan, and Abdullah Oksuz. Physico-chemical properties of cold pressed sunflower, peanut, rapeseed, mustard and olive oils grown in the eastern mediterranean region. *Saudi Journal of Biological Sciences*, 26(2):340 - 344, 2019.

Appendix C

Leakage test for BLM set-up

The BLM cell as described in Chapter-II was tested for leakage in the following manner.

- ✓ One compartment of the cell was filled with clear water and the other with a colored (crystal violet) solution.
- ✓ Both the aqueous phases were stirred continuously for 24 hours at a stirring speed of 500 rpm.
- ✓ The intensity of color in the aqueous phases was then measured with UV-vis spectrophotometer at a wave length of 584 nm.

The results of the leakage test are furnished in the Table C.1 below:

Table C.1: Result of leakage test of BLM set-up

Time (h)	Absorbance of clear water	Absorbance of colored water
0	0	0.0147
24	0	0.0145

Appendix D

Response surface methodology (RSM)

Response surface methodology (RSM) is a design of experiment (DOE) based method. RSM is an useful tool for developing, improving, and optimizing processes using statistical and mathematical techniques. The objective of RSM is to optimize response (or output variable) which influence by several independent variable (or input variables). RSM is based on fitting the mathematical models (linear, square polynomial functions and others) to the experimental results from the designed set of experiments and verification of the model obtained by the statistical techniques. The main objective of RSM is to obtain the optimum operational conditions for the system or to acquire a region that satisfies the operating specifications. The response can be represented graphically, either in the three-dimensional space or as contour plots that help visualize the shape of the response surface. The general approach of RSM for process optimization includes: conducting screening experiments; moving the experimental region near the optimal point [1, 2]. The simulation and optimization of physico-chemical processes using RSM consists of various steps which illustrated in the flow chart shown in Figure D.1.

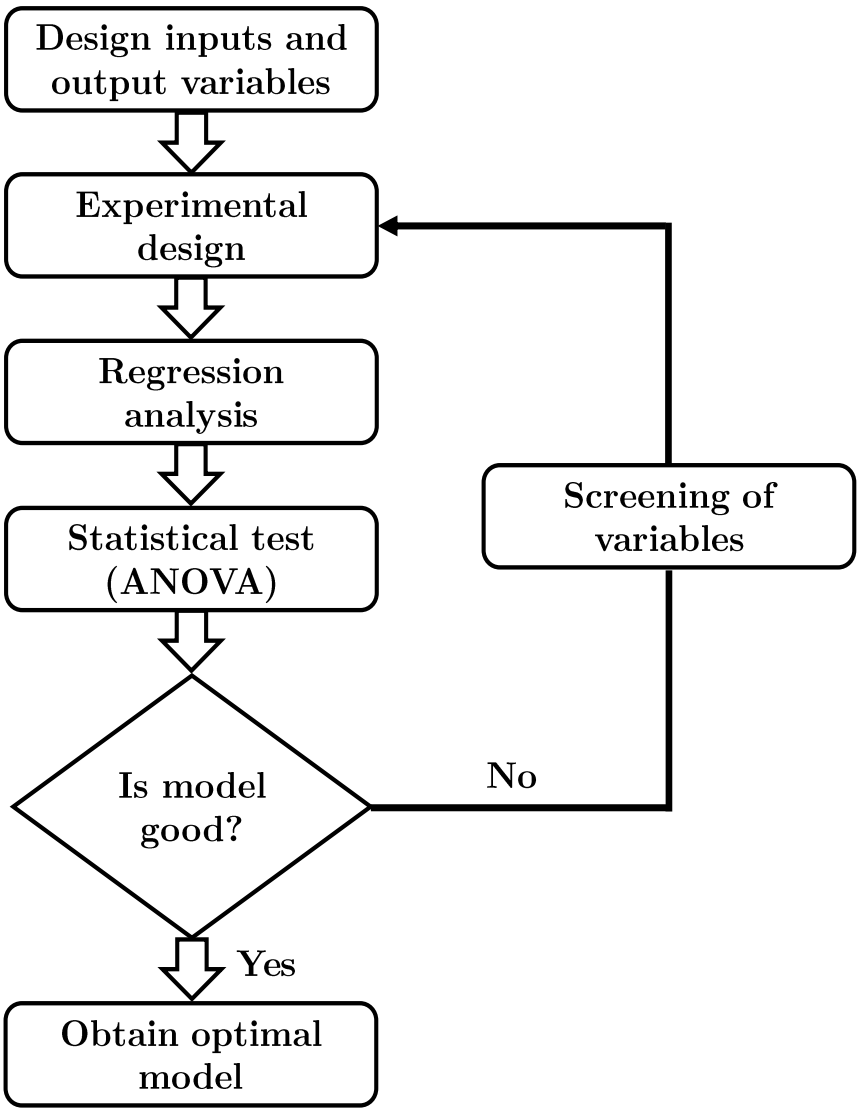

Figure D.1: The procedure of the model development with RSM

References

[1] R. H. Myers, and D. C. Montgomery. *Response Surface Methodology*. John Wiley & Sons, 1995.

[2] D. C. Montgomery. *Design and Analysis of Experiments: Response Surface Method and Designs*. John Wiley & Sons, 2008.

Visible outputs of the thesis

Peer-reviewed

1. Supriyo Kumar Mondal and Prabirkumar Saha. Removal of hexavalent chromium from wastewater using supported liquid membrane: Synthesis of chromium-iron complex through electrochemical reaction. *Water and Environment Journal*, doi: 10.1111/wej.12576.

2. Supriyo Kumar Mondal, Manoj Kumar Beriya and Prabirkumar Saha. Separation and recovery of nickel and zinc from synthetic wastewater using supported liquid membranes with *in Situ* Electrodeposition. *Industrial & Engineering Chemistry Research*, 58 (2019) 9970-9987.

3. Supriyo Kumar Mondal and Prabirkumar Saha. Separation of hexavalent chromium from industrial effluent through liquid membrane using environmentally benign solvent: A study of experimental optimization through response surface methodology. *Chemical Engineering Research and Design*, 132 (2018) 564 - 583.

Conference presentations

1. Supriyo Kumar Mondal, Manoj Kumar Beriya and Prabirkumar Saha. Separation of Zinc and Nickel from Industrial Wastewater through Supported Liquid Membrane Using Environmentally Benign Solvent. *AIChE annual meeting (AIChE-2018)*, October 28 - November 2, 2018, Pittsburgh, USA.

2. Supriyo Kumar Mondal and Prabirkumar Saha. Separation of zinc (II) through supported liquid membrane using environmentally benign solvent. *International conference on waste management (Recycle-2018)*, 22-24 February, 2018, Guwahati, India.

3. Supriyo Kumar Mondal and Prabirkumar Saha. Extraction of hexavalent chromium from wastewater using environmentally benign solvent. *DAE-BRNS Biennial Symposium on Emerging Trends in Separation Science and Technology (SESTEC-2016)*, 17-20 May, 2016, Guwahati, India.

4. Supriyo Kumar Mondal and Prabirkumar Saha. Comparative extraction study of environmentally benign solvent over traditional solvent. *Indian Chemical Engineering Congress (CHEMCON-2015)*, 27-30 December, 2015, Guwahati, India.